EVOLUTION OF TERRESTRIAL DEVELOPMENT IN ANURANS

Dissertation

in Partial Fulfilment of the Requirements for the Degree of

"Doctor rerum naturalium" (Dr. rer. nat.)

Submitted to the Council of the Faculty of Biological Sciences

of Friedrich Schiller University Jena

by Susan Schweiger

born on 05/11/1984 in Gera

Reviewer

Prof. Dr. Lennart Olsson[1]
PD Dr. Hendrik Müller[2]
Prof. Ryan Kerney (PhD)[3]

[1]Institut für Zoologie und Evolutionsforschung, Friedrich-Schiller-Universität, Jena, Germany

[2]Zentralmagazin Naturwissenschaftlicher Sammlungen, Martin-Luther-Universität Halle-Wittenberg, Halle, Germany

[3]Biology Department, Gettysburg College, Gettysburg, PA, USA

Date of defense

15/07/2022

Table of content

Introduction

Developmental diversity in amphibians

One of the key questions in evolutionary developmental biology is to understand the mechanisms that produced diverse reproductive strategies in amphibians, a clade of tetrapod vertebrates comprising living (Lissamphibia) and extinct taxa. In particular, the major evolutionary transition from biphasic development with an aquatic larval stage to a fully terrestrial development in which froglets hatch from the eggs have long captured the interest of biologists.

Lissamphibia currently include approximately 8407 described species (amphibiaweb.org, Nov 20, 2021) and are divided into three subgroups: Anura with 7426 species, Urodela with 766 species and Gymnophiona with 215 species. Lissamphibians can be found in all types of habitats except the Polar Regions and at very high altitudes (Wells 2007). The actual global geographical distribution of Lissamphibia varies among these three groups. Anurans have the broadest geographical distribution; urodeles are more restricted to the northern hemisphere and parts of Central and South America, while caecilians only inhabit tropical and subtropical regions (Wells 2007; Just et al. 1981; Wake 1976).

Within Amphibia, major evolutionary transitions from a fully aquatic to a complete terrestrial life history have taken place. The earliest forms of amphibians are known from the Devonian period, about 400 million years ago (mya) (Wells 2007; Clack 2002). There is a wide gap in the fossil record; however, between the late Devonian and the Carboniferous that complicates our understanding of relationships as well as reproductive strategies and development among early amphibians (Carroll 2007; Zhang et al. 2005; Ahlberg & Milner 1994; Fritzsch 1990). Temnospondyli, often considered as the ancestors of lissamphibians first appeared during the late Carboniferous and the early Permian (286 mya) and include fully aquatic, semiaquatic and terrestrial forms (Wells 2007; Schoch & Carroll 2003; Carroll 2000a; Laurin & Reisz 1997; Schoch 1995). Although different hypotheses exist, there is strong support for a monophyletic Lissamphibia and a sistergroup relationship between Urodela and Anura (consistent with the Batrachia hypothesis, Siu-Ting et al. 2019; Frost et al. 2006; Duellman & Trueb 1996) based on molecular phylogenies (Hime et al. 2021; Zhang et al. 2005).

For most Lissamphibia, reproduction is completely aquatic, with aquatic egg deposition and an aquatic larva that more or less metamorphoses into an adult-like individual (Gomez-Mestre et al. 2012; Wells 2007; Thibaudeau & Altig 1999; Duellman & Trueb 1986). However, a high number of alternative life history strategies as well as reproductive and developmental modes have evolved independently within all three taxa of Lissamphibia (Nunes-de-Almeida et al. 2021; Wells 2007; Haddad & Prado 2005; McDiarmid & Altig 1999; Altig & Johnston 1989; Salthe & Duellman 1973; Lutz

1947; Noble 1931). In particular, the biphasic, metamorphosing condition has been repeatedly modified. For instance, in many salamanders paedomorphosis (e.g. neoteny in *Ambystoma*), which is characterized by the presence of a sexually mature larva retaining larval characters and an aquatic life-style (Bonett et al. 2013; Chippindale 2000), has evolved as a way to bypass metamorphosis. In caecilians, the knowledge about life-cycles and metamorphosis is poor, but most taxa develop terrestrially without an aquatic larval stage (Wells 2007; Rose 1999).

One of the most derived forms of development is direct development, which is associated with terrestrial egg deposition and the loss of the aquatic larval stage. In urodeles, direct development is only seen in the family Plethodontidae, the lungless salamanders. Because Plethodontidae represent two thirds of all salamander species, direct development is the predominant reproductive mode in this taxon (Wake 2012; Chippindale et al. 2004; Mueller et al. 2004; Hanken 1999; Wake & Hanken 1996). In caecilians, both direct development and viviparity are common (San Mauro et al. 2014; Carroll 2007; Wake 1976). Also a wide range of intermediary forms of reproduction and development have evolved within Lissamphibia (Brink et al. 2020; Castroviejo-Fisher et al. 2015; Wells 2007; Hanken 1989; Lutz 1948; Lutz 1947; Noble 1931; Noble 1925). These 'intermediary' forms range from egg-deposition outside of water, but still with an aquatic larva (semi-aquatic development), up to development in a subterranean nest where non-feeding terrestrial tadpoles hatch (terrestrial larval development).

In anurans, biphasic development is associated with externally fertilized aquatic eggs. A free-living aquatic larva, commonly known as a 'tadpole', hatches from such an egg and later metamorphoses into a terrestrial adult-like juvenile. The availability of bodies of standing (lentic) or flowing (lotic) water is essential for biphasic developing species. In contrast to larvae of other lissamphibian groups, anuran tadpoles exhibit an astonishing diversity regarding their morphology and feeding behaviour (Sherratt et al. 2018; Roelants et al. 2011). Such a metamorphic transition from an aquatic tadpole to a terrestrial frog also includes rapid and drastic changes from larval to adult morphology (Reiss 2002; McDiarmid & Altig 1999; Hayes 1997; Duellman & Trueb 1986; Werner 1986).

Despite the evolutionary success of the anuran tadpole (measured in species numbers), a more terrestrial life style, where reproduction and development are independent from direct access to bodies of water, is found in many anuran taxa (McDiarmid & Altig 1999; Thibaudeau & Altig 1999; Duellman & Trueb 1986). For instance, several arboreal forms (e.g. some rhacophorids, hyperoliids, microhylids) have changed oviposition sites: Eggs are layed above water-filled cavities, in tree holes and in epiphytes (Wells 2007; Schiøtz 1999; Brown & Alcala 1983; Wassersug et al. 1981; Lamotte & Lescure 1977; Perret 1962; Noble 1929). The larvae that hatch from these eggs, however, typically complete development within water similar to those of species, in which the eggs are deposited directly in water.

As a complete terrestrial mode of development, direct development has evolved several times independently in different anuran lineages (Hanken 1992; Duellman & Trueb 1986). As mentioned above, direct development differs dramatically from the biphasic life-history mode as there is no free-living larval stage. In contrast, development is completed inside the terrestrially laid egg resulting in a hatching froglet (***Figure 1***). Most of the tadpole specific structures such as the lateral line system, larval mouth parts, the cement gland, a coiled intestine and a muscularized tail are reduced or entirely absent during development (Elinson 2001; Hanken et al. 1997; Elinson 1990). The embryos of most direct developing frogs share an enlarged membranous tail with a highly vascularized fin, the reduction of external gills, an early and nearly simultaneous development of front and hind limbs and a large yolk reserve (Anstis et al. 2007; Bahir et al. 2005; Townsend & Stewart 1985).

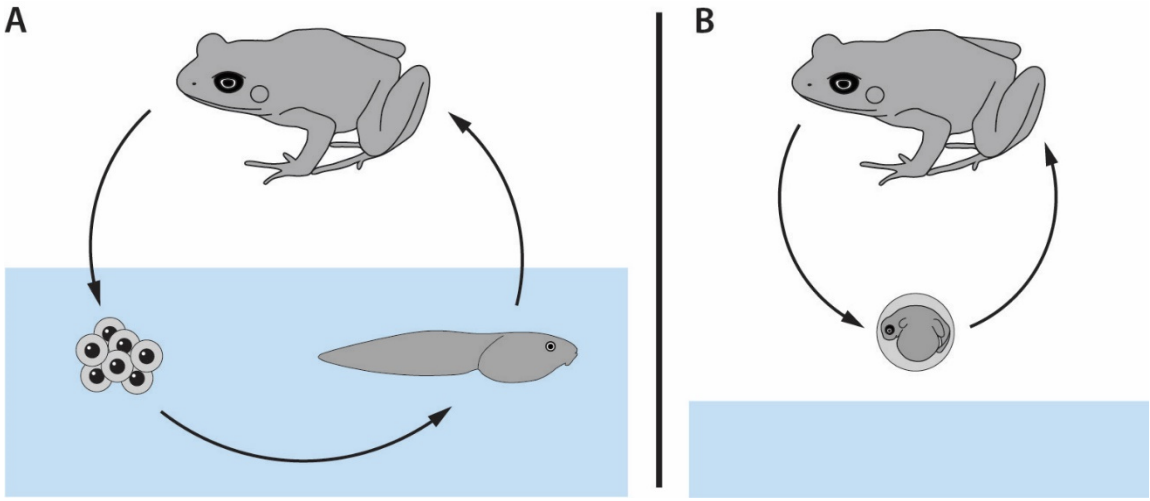

Figure 1: *Indirect (A) vs. direct development (B) in anurans.* ***A:*** *The plesiomorphic, biphasic condition: Aquatic eggs developing into a free swimming, aquatic larva (the tadpole) which transforms into a terrestrial adult.* ***B:*** *Complete terrestrial development: Direct development bypassing the aquatic larval stage. There is no free swimming aquatic larva and the embryo develops inside a terrestrially deposited egg. Most of the adult features form early in development and most of the typical larval features are absent during development.*

These observations have led to the hypothesis, that the evolution of direct development from a biphasic developmental mode is based on a large-scale repatterning of embryonic development ('repatterning hypothesis', Hanken et al.1997). Despite the broad phylogenetic distribution of direct development in frogs, detailed morphological data were mainly only available for the Puerto Rican coqui (*Eleutherodactylus coqui* THOMAS 1966) (Laslo et al. 2019; Kerney et. al. 2010; Olsson et al. 2002; Hanken et al. 2001; Callery et al. 2001; Callery & Elinson 2000; Schlosser et al. 1999; Elinson & Fang 1998; Jennings & Hanken 1998; Hanken et al. 1997; Fang & Elinson 1996; Schlosser & Roth 1997a,b; Townsend & Stewart 1985). Studies on other direct developing frogs are still limited to only a few species (and specimens per species) so far

(Goldberg et al. 2020, 2015, 2012; Narayan et al. 2010; Anstis 2008; Anstis et al. 2007; Kerney et al. 2007). In addition, a principal limitation is the lack of developmental data on direct developing species compared to closely related species with a biphasic, fully aquatic development.

Thus, the primary motivation for this study was to obtain detailed developmental data for direct developing species within Arthroleptidae (Afrobatrachia) and their close relatives. Perhaps unsurprisingly, these detailed comparative investigations show that direct development is not as uniform as it was previously assumed (**Chapter 1-3**).

Terrestrialization in Afrobatrachia (Anura): A Model Group

Terrestrialization, where reproduction and embryonic development is independent from bodies of water, has evolved in Afrobatrachia, a group of sub-Saharan African frogs containing four families – [(Hyperoliidae + Arthroleptidae) + (Brevicipitidae + Hemisotidae), ***Figure 2***] (Portik et al. 2019; Feng et al. 2017; Portik & Blackburn 2016; Pyron & Wiens 2011; Frost et al. 2006).

The colorful Hyperoliidae are diverse with respect to their habitat choices as well as reproduction sites (Drewes et al. 1984). Most species are arboreal, others inhabiting savannah and highland grasses as well as floating vegetation habitats. Both, aquatic egg deposition and a more terrestrial deposition of eggs, mostly on vegetation overhanging water and in phytotelma, are present in this group (Mercurio et al. 2009; Rödel 2000; Schiøtz 1999). The development is biphasic with a fully aquatic larva.

A more derived, terrestrial life-history is seen in the burrowing Hemisotidae and Brevicipitidae, in which reproduction is associated with large eggs deposited in a subterranean chamber (Mercurio et al. 2009; Müller et al. 2007; Minter 2004; Barbour & Loveridge 1928). The hemisotids breed close to bodies of water, where the female digs a tunnel towards the water, wherein the hatched tadpoles complete their development until metamorphosis (Kaminsky et al. 1999; Rödel et al. 1995; Wager 1952). Investigations in brevicipetids have shown that development is completely terrestrially. However, a free-living terrestrial larva is retained during development (Müller et al. 2007; Wager 1965; de Villiers 1929).

Within Arthroleptidae, fully aquatic, semi aquatic and completely terrestrial development in form of direct development have evolved (***Figure 2***). Although the diversity and relationships in Arthroleptidae are still in a state of flux, recent phylogenetic studies analyzed the genus-level relationships in this clade. Investigations of Portik & Blackburn (2016) revealed Arthroleptidae consisting of the clades *Leptopelis*, *Leptodactylodon*, a clade containing *Nyctibates*, *Scotobleps*, *Astylosternus* and *Trichobatrachus*, and a clade containing *Cardioglossa* and *Arthroleptis* (***Figure 2***).

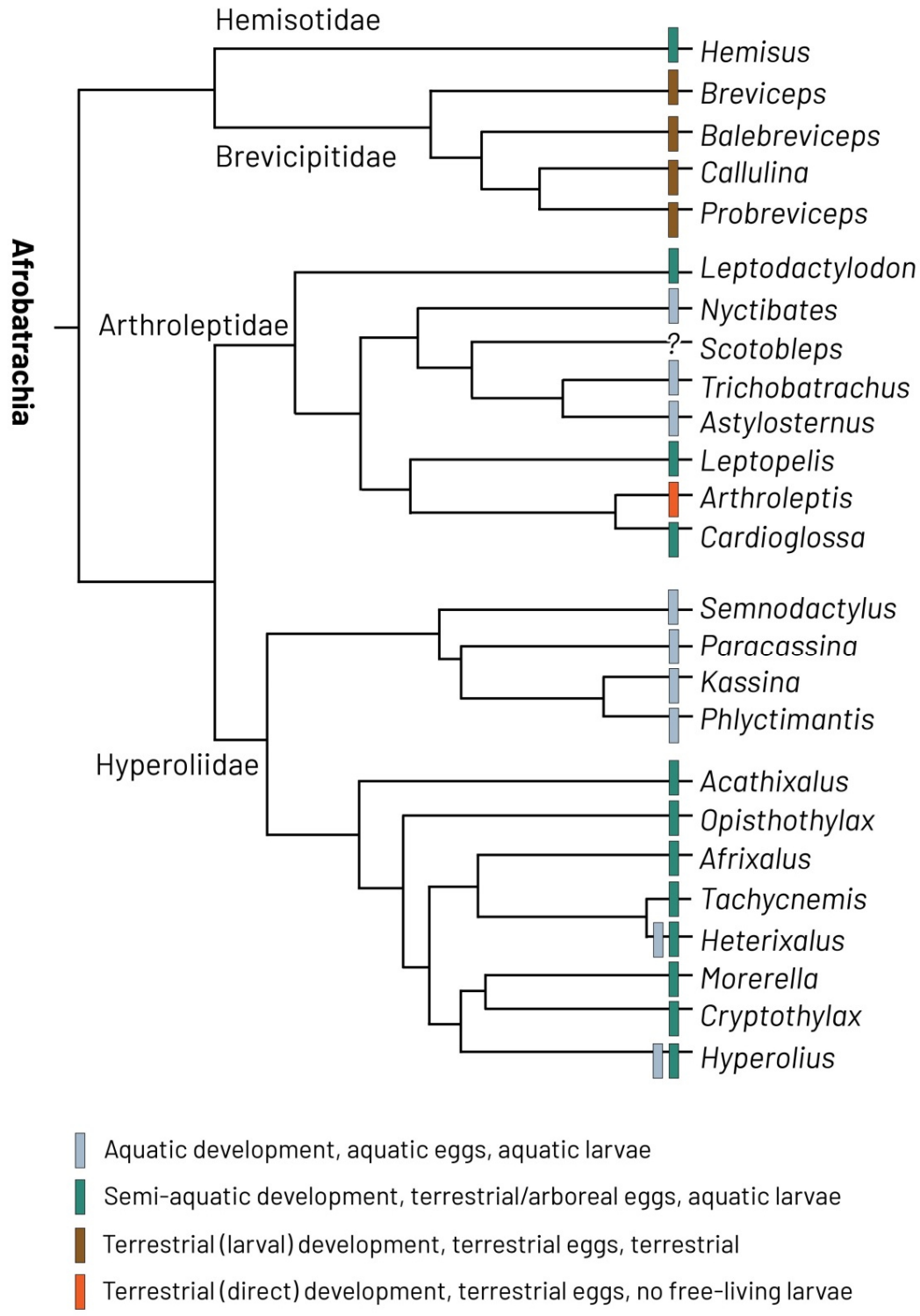

Figure 2: *Cladogramm showing the phylogeny of Afrobatrachia. Modes of reproduction were mapped on the branches. Cladogramm modified after Portik & Blackburn (2016).*

The largely arboreal genus *Leptopelis* exhibits a semi-aquatic life history with an aquatic larva (tadpole description of *L. natalensis* SMITH 1849 in **Chapter 5**). The eggs

are laid terrestrially, close to slow moving streams or small bodies of water and the hatched tadpoles actively move towards the water, where development continues until metamorphosis (Barej et al. 2015; Channing 2008; Rödel 2000; Oldham 1977; Wager 1930).

Several less diverse genera that are largely aquatic, including *Nyctibates, Trichobatrachus* and *Astylosternus*, have a typical biphasic life history with aquatic eggs and an aquatic larval stage (Griesbaum et al. 2019; Mapouyat et al. 2014; Ernst et al. 2014). Interestingly, these genera can be found close to fast moving streams (**Chapter 4**). Terrestrial breeding with direct development is only reported for *Arthroleptis*. The sistergroup *Cardioglossa* exhibits a semi-terrestrial development with terrestrial egg deposition, but the development of the tadpole is still aquatic (Portik & Blackburn 2016; Hirschfeld et al. 2012).

The high diversity of developmental modes in Arthroleptidae is ideal for investigating the developmental changes associated with the evolution of complete terrestrial direct development. In the present study, detailed data on external embryonic development (**Chapter 1**), and the development of the cranial musculoskeletal system (**Chapter 2**) as well as the skin (**Chapter 3**) of *Arthroleptis* were conducted. The data were compared to existing data on other direct developing species as well as close relatives of *Arthroleptis* with biphasic development. For the latter, the tadpoles of fully aquatic and semi-aquatic relatives (*Leptopelis, Astylosternus, Nyctibates, Trichobatrachus*) were comparatively described (**Chapter 4 and 5**). Collectively, these data shed light on possible evolutionary scenarios towards direct development in Afrobatrachia and anurans more broadly.

Consequently, this study focuses on the morphological and developmental differences between direct and biphasic development using different arthroleptid species as a model. The investigations address the central question of whether direct development is invariably linked to a complete loss of larval or tadpole-like features among different direct developing anurans. It is also pioneering by bridging the investigatory gap between direct developing and their closest related biphasic species. So far, most comparative approaches used *Xenopus laevis* DAUDIN 1802 and *Discoglossus pictus* OTTH 1837 as outgroup taxa for comparative developmental investigations (Ziermann & Diogo 2014; Schlosser & Roth 1997a, b).

Heterochrony, metamorphosis and the role of the larva in direct development

It is thought that the biphasic life-style with metamorphosis is the plesiomorphic condition in lissamphibians (Hanken 1999; Duellman 1989; Duellman & Trueb 1986; Noble 1925; Orton 1953), but there is no general consensus supporting this hypothesis due to missing data in the fossil record (Wells 2007; Harris 1999; Bogart 1981). Early amphibians may have passed through some form of metamorphosis, but the

evolutionary origin and the homology of amphibian larvae and metamorphosis in general is poorly understood (Schoch 2009; Schlosser 2005; Reiss 2002; Hanken 1999; Fritzsch 1990; Boy 1947; Szarski 1957). Some authors assume that the larvae of early anurans were comparatively similar to salamander larvae and that development has proceeded more gradually (Reiss 2002; Harris 1999; Elinson 1990; Fritzsch 1990; Wassersug & Hoff 1982). On the basis of molecular phylogenetic analyses, it has been hypothesized that aquatic larvae of anurans and salamanders may have re-evolved from an ancestor with a terrestrial, direct development (Wake & Hanken 1996; Duellman 1989; Duellman et al. 1988; Wassersug & Duellman 1984).

The complex life-cycle from an aquatic larva metamorphosing to an adult-like is found in many salamanders and frogs (Gomez-Mestre et al. 2012; Wells 2007; Hanken 2002; Hanken 1999; Rose 1999; Thibaudeau & Altig 1999). While metamorphosis is less dramatic in biphasic salamanders, it is associated with rapid morphological, biochemical, physiological and behavioral changes in anurans (Ziermann 2019; Reiss 2002; Altig & McDiarmid 1999; Harris 1999; Just et al. 1981; Wassersug 1975; Orton 1953). The tadpole differs substantially from the adult in terms of a highly specialized body plan with characters distinguishing it from all other lissamphibian larvae (Altig & McDiarmid 1999; Harris 1999). The radical transition by metamorphosis allows the adult structures to develop largely free of larval constraints (Fritzsch 1990; Hanken 1989). Morphological changes include a transformation of the cranium, where the typical tadpole cartilages of the chondrocranium (e.g. cartilagii labialis superior et inferior, cornua trabeculae, palatoquadrate, cartilago meckeli, hyobranchial skeleton) were considerably rebuilt (Wassersug 1975). Metamorphosis is triggered and controlled by the Thyroid hormone (TH) in all three groups of Lissamphibia (Denver 2013; Reiss 2002; Just et al. 1981; White & Nicoll 1981). Several experiments have shown that TH initiates processes leading to metamorphic climax and is needed to complete metamorphosis during anuran development (Denver 2013; Brown & Cai 2007; Tata 2006).

From an evolutionary point of view, several investigations focus on the loss of the free-living aquatic larva deducing hypotheses on the evolutionary origin of the amphibian larva in general (Ziermann & Diogo 2014; Schlosser 2005; Callery et al. 2001; Elinson 2001; Callery & Elinson 2000; Hanken 1999; Elinson 1990). Because direct development is associated with the loss of many typical larval features, it has been generally assumed that the tadpole was completely excised from the ontogeny of direct developing frogs ('tadpole module hypothesis', Callery et al. 2001; Elinson 2001; Callery & Elinson 2000; Elinson 1990). But does the loss of the free-living tadpole result in a more gradual development and do all direct developing anurans share similar or even the same developmental processes? Is the loss of the tadpole associated with the loss of the TH-dependent metamorphosis and if so, does this mean that the larva per se represents an evolutionary module?

The idea that the tadpole can be excised out of ontogeny resulting in a direct developing frog is controversial and has led to different views about the 'tadpole module hypothesis' (e.g. Schlosser 2005; Ziermann & Diogo 2014) that were also compared and discussed in this study. To appraise these hypotheses, this study provides a detailed description of the direct developing African Squeaker frogs (*Arthroleptis wahlbergii* SMITH 1849 and *A. xenodactyloides* HEWITT 1933, Arthroleptidae, Afrobatrachia) in comparison to closely related species exhibiting a more ancestral (e.g. biphasic) life history as well as to other direct developing species (**Chapter1-3**).

What mechanisms are involved in the evolution of direct development? Heterochrony has often been discussed as the most important mechanism of phenotypic changes in the ontogenetic pattern of direct development. This gains support by the observation that direct developing species show accelerated growth rates and develop faster in comparison to most biphasic species (Goldberg et al. 2012; Callery and Elinson 2000a,b; Hanken 1999; Hanken et al. 1992; Raff & Wray 1989; Lutz 1948). Heterochrony is associated with changes in timing of developmental events or features compared to the ancestral ontogeny (Callery & Elinson 2000a, b; Callery et al. 2001; Raff & Wray 1989; Hanken 1989; Lutz 1948; Haldane 1932).

Heterochrony not only leads to a highly derived development. Direct development is also characterized by the loss of typical tadpole specific features and at the same time, the formation of novel structures and the precocious formation of adult structures ('ontogenetic repatterning') as well as the 'recapitulation' of few larval characteristics (sensu Kerney et al. 2010; Hanken 2003; Hanken et al. 1997; Hanken et al. 1992). These complex processes indicate that the evolution of direct development might be more than just a simple deletion of the tadpole phase. The comparative approach of embryonic development in direct developing anurans used in this study offers the potential to clarify if the evolution of direct development is independently facilitated by heterochronic shifts (**Chapter 1-3**).

Chapter overview

Chapter 1: Direct development in African squeaker frogs (Anura: Arthroleptidae: *Arthroleptis*) reveals a mosaic of derived and plesiomorphic characters

Authors: **Schweiger, S.,** Naumann, B., Larson, J. G., Möckel, L., Müller, H.

Status: Published in Organisms Diversity & Evolution (2017) 17: 693-707

This paper provides the first detailed description of direct development in a family of African frogs, the Arthroleptidae. Egg deposition, clutch characteristics and embryonic development of direct developing squeaker frogs of the genus *Arthroleptis* are described. A developmental series of two species of *Arthroleptis, A .wahlbergii* and *A. xenodactyloides,* are investigated. The developmental series of *A. wahlbergii* were field collected at Eshowe and Entumeni Forest in KwaZulu-Natal, South Africa. Embryos of *A. xenodactyloides* were sampled at Kigogo and Luhota Forests, Mufindi District, Iringa Region, Tanzania. Data are compared with published information on other direct-developing anurans revealing higher disparity as expected. Several features previously thought to be characteristic for direct-developing anurans, such as an egg tooth, a greatly enlarged tail or only very rudimentary and transitory presence of an opercular fold, seem to be restricted to particular direct-developing taxa and are indeed rather variable among the different direct developing lineages. The idea proposed by some authors that the free-swimming tadpole larva represents some form of module that has been deleted from the ontogeny of direct developing frogs, conflicts with the available data and appears too simplistic. Variability in the developmental timing and pattern of the tail, which seems disconnected from the remaining tadpole characteristics, indicates a more complex, mosaic-like pattern of larval traits.

Chapter 2: The ghost of the tadpole - Embryonic development of the cranial musculoskeletal system in African squeaker frogs (*Arthroleptis*) reveals heterochronic shifts and parallel evolution of differential metamorphosis in direct developing frogs

Authors: **Schweiger, S.,** Naumann, B., Hammel, J. U., Müller, H.

Status: Drafted manuscript

This manuscript provides the first detailed description of the embryonic development of the cranial muscles, cartilages and bones in two species of African squeaker frogs of the genus *Arthroleptis, A. wahlbergii* and *A. xenodactyloides.* Until now, detailed developmental data on the muscoskeletal system are only available for the direct developing *Eleutherodactylus coqui* from Puerto Rico. Data on the skeletal development of the cranium are available for the Sri Lankan shrub frog *Pseudophilautus silus* MANAMENDRA-ARACHCHI & PETHIYAGODA 2005. A combination of histology (section series, cleared and stained specimens) with whole-mount fluorescent antibody staining, confocal laser scanning microscopy, micro-computed tomography and 3D-reconstruction were used to study and visualize the inner cranial development of *Arthroleptis* in great detail. Developmental ontogeny of *Arthroleptis* and non-related direct developing species (*E. coqui* and *P. silus*) are compared to investigate if the evolution of direct development is always facilitated by the same developmental changes and to uncover possible developmental constraints (or a release from it) governing this process. The investigation of the development of the cranial skeleton and associated muscles reveals a transient presence of tadpole-typical elements. This provides independent evidence for the concept of 'differential metamorphosis' stating that the tadpole consists of several developmental modules. These modules can change independently during evolution. Data on *Arthroleptis* are also compared to other species within the Arthroleptidae to reconstruct the evolutionary steps underlying the transition from a biphasic to a direct developing life style. The absence of some tadpole-typical mandibular muscles in con-familiar species of *Arthroleptis* suggests that this loss is not directly linked to the evolution of direct development.

Chapter 3: Parallel evolution of direct development in frogs – Skin and thyroid gland development in African Squeaker Frogs (Anura: Arthroleptidae: *Arthroleptis*)

Authors: Naumann, B., **Schweiger, S.,** Hammel, J. U., Müller, H.

Status: Published in Developmental Dynamics (2021) 250: 584-600

This study provides the first detailed data on skin development in direct developing frog species. The comparison of embryonic development of these direct developing frogs offers the possibility to identify how developmental constraints may have influenced the observed pattern of parallel evolution. In the few species examined, development is characterized by the condensed and transient formation of some tadpole-specific features and the early formation of adult-specific features during a 'cryptic' metamorphosis. In *Arthroleptis*, skin development can be divided into four major phases (embryonic, 'tadpole', metamorphic and adult) that are also typical for many biphasic species. As in biphasic species, skin development in *Arthroleptis* correlates with an increase in thyroid gland activity. Skin and thyroid gland histology is also investigated in a tadpole of *Cardioglossa,* the sister genus to *Arthroleptis.* Alterations of skin development in *Arthroleptis* seem to be correlated with the evolution of direct development. A comparison with fragmentary data from the Puerto Rican coqui (*Eleutherodactylus coqui*) reveals that direct development might have evolved in parallel via a heterochronic shift of thyroid gland activity. This suggests that the development of many adult features is still constrained by the ancestral dependency on thyroid hormone signaling.

Chapter 4: Don't go with the flow: Cranial morphology of fast-flowing stream tadpoles in the Afrobatrachian family Arthroleptidae

Authors: **Schweiger, S.**; Rödel, M.-O.; Hammel, J. U.; Müller, H.

Status: Drafted manuscript

This manuscript gives a detailed description of tadpole morphology of four species of the family Arthroleptidae. It provides insights in the cranium of *Leptopelis parkeri* BARBOUR & LOVERIDGE 1928, *Astylosternus occidentalis* PARKER 1931, *Trichobatrachus robustus* BOULENGER 1900 and *Nyctibates corrugatus* BOULENGER 1904. Interestingly, the tadpoles of these species all occur in medium to fast flowing water systems in hilly areas. This study investigates whether differences in the flow velocity of the microhabitat of each species are reflected in the muscoskeletal system of the tadpoles. Several methods including preparation, histology, clearing and staining as well as µ-CT scanning and three-dimensional reconstruction of the cranium of the tadpoles demonstrate that the muscolskeletal morphology of *A. occidentalis, N. corrugatus* and *T. robustus* is highly modified in comparison to the tadpole of *L. parkeri.* Modifications include a wide, robust and partly or fully fused cornua trabecular, a fused and strong chondrified cartilago labialis superior, as well as several modifications of the palatoquadrate, e.g. a broad commissura quadratocranialis anterior, a broad processus oticus, the presence of a processus ventralis and a wide and robust processus muscularis. The cranial muscles accompany the modifications of the robust chondrocranium, e.g. the far posterior origin of the Musculus (M.) levator mandibulae anterior and the massive muscles of the hyoid like the M. orbitohyoideus. Additionally, there is variation between the closely related *A. occidentalis, N. corrugatus* and *T. robustus.* The presence of a wide processus hyoquadratis is only seen in the tadpole of *N. corrugatus,* indicating a possible autapomorphy of the genus *Nyctiabtes.* These data support that the cranial morphology of the tadpoles is highly adaptive and associated the microhabitat the species occurs in.

Chapter 5: Meristic and morphometric characters of *Leptopelis natalensis* tadpoles (Amphibia: Anura: Arthroleptidae) from Entumeni Forest reveal variation and inconsistencies with previous descriptions

Authors: **Schweiger, S.**, Harvey, J., Otremba, T. S., Weber, J., Müller, H.

Status: Published in Acta Herpetologica (2017) 12(2): 125-132

This paper provides a detailed description of the tadpole of *Leptopelis natalensis* from Entumeni forest, KwaZulu Natal, South Africa. The treefrogs of the genus *Leptopelis* are known to deposit eggs terrestrially, outside of bodies of water, whereas the tadpole continues development in slow moving forest streams. Previous larval descriptions for the species are brief, lack morphometric data, or are based on specimens of imprecise origin. In this study, description, preparation and drawings with a stereomicroscope were used as techniques. For inspection of the buccopharyngeal morphology, one tadpole was dissected and investigated using scanning electron microscopy. The tadpole resembles other *Leptopelis* tadpoles, with some differences. Some of these differences seem to fall within the range of natural variation. Others, such as the presence of a fifth anterior row of keratodonts, might be indicative of variation at the population level.

CHAPTER 1

Direct development in African squeaker frogs (Anura: Arthroleptidae: Arthroleptis) reveals a mosaic of derived and plesiomorphic characters

Authors: **Schweiger, S.,** Naumann, B., Larson, J. G., Möckel. L., Müller, H.

Status: Published in Organisms Diversity & Evolution (2017) 17: 693-707

FORMULAR 1

Manuskript Nr.: 1

Titel des Manuskriptes: Direct development in African squeaker frogs (Anura: Arthroleptidae: *Arthroleptis*) reveals a mosaic of derived and plesiomorphic characters

Autoren: Schweiger, Susan; Naumann, Benjamin; Larson, Joanna G.; Möckel, Lars; Müller, Hendrik

Bibliographische Informationen: Published in Organisms Diversity & Evolution (2017) 17: 693-707

Der Kandidat / Die Kandidatin ist (bitte ankreuzen)

☒ Erstautor/-in, ☐ Ko-Erstautor/-in, ☐ Korresp. Autor/-in, ☐ Koautor/-in.

Anteile (in %) der Autoren / der Autorinnen an der Publikation (anzugeben ab 20%)

Autor/-in	Konzeptionell	Datenanalyse	Experimentell	Verfassen des Manuskriptes	Bereitstellung von Material
Schweiger, S.	80%	85%	95%	85%	20 %
Naumann, B.					20 %
Larson, J.G.					20 %
Möckel, L.					20 %
Müller, H.	20%				20 %

Org Divers Evol (2017) 17:693–707
DOI 10.1007/s13127-017-0335-5

ORIGINAL ARTICLE

ORGANISMS DIVERSITY & EVOLUTION

Direct development in African squeaker frogs (Anura: Arthroleptidae: *Arthroleptis*) reveals a mosaic of derived and plesiomorphic characters

Susan Schweiger[1] · **Benjamin Naumann**[1] · **Joanna G. Larson**[2,3] · **Lars Möckel**[1] · **Hendrik Müller**[1,2]

Received: 1 March 2017 / Accepted: 20 June 2017 / Published online: 18 July 2017

Abstract Direct development has evolved independently several times in anurans and direct-developing species are characterized by large-scale developmental repatterning and a complete, or near complete, absence of most tadpole-specific structures. Earlier studies stressed the similarities among different direct-developing species, but more recent studies have indicated differences in the reduction of tadpole-specific structures among different taxa. Here, we describe egg deposition, clutch characteristics and embryonic development of the direct-developing squeaker frogs of the genus *Arthroleptis*, providing the first detailed description of direct development in Arthroleptidae. Embryonic development in *Arthroleptis* is characterized by the presence of an opercular fold that still encloses the developing forelimbs, the absence of external gills and an only moderately extended tail. A comparison with published information on other direct-developing anurans reveals broad dissimilarities in the formation of an opercular fold and very different tail morphology among different taxa. An egg tooth, often considered characteristic of direct-developing anurans, seems to be restricted to New World Terrarana. The embryonic diversity seen in direct-developing anuran taxa argues against simplistic assumptions about the evolution of direct development.

✉ Hendrik Müller
hendrik.mueller@uni-jena.de

[1] Institut für Spezielle Zoologie und Evolutionsbiologie mit Phyletischem Museum, Friedrich Schiller Universität Jena, Erbertstrasse 1, 07743 Jena, Germany

[2] Museum of Comparative Zoology, Harvard University, Cambridge, MA 02138, USA

[3] Department of Ecology and Evolutionary Biology and Museum of Zoology, University of Michigan, Ann Arbor, MI 48109, USA

Keywords Breeding biology · Direct development · Afrobatrachia · Terrarana · Rhacophoridae · Myobatrachidae · Ceratobatrachidae · Eastern Arc Mountains · Tanzania · South Africa

Introduction

Direct development has evolved independently as a derived reproductive mode in many lineages of animals including molluscs, crustaceans, echinoderms and amphibians (e.g. Duellman and Trueb 1986; Raff 1992; Scholtz 2000; Collin 2004). In amphibians in particular, direct development is a surprisingly widespread reproductive strategy, as is witnessed by the large number of direct-developing species and its repeated, independent evolution in anurans, salamanders and caecilians (Wake and Hanken 1996; Thibaudeau and Altig 1999; San Mauro et al. 2014). In contrast to the biphasic ancestral state, the absence of an aquatic larval stage makes it possible to reproduce without any direct access to bodies of water and direct development might be favoured where environmental conditions do not provide any suitable aquatic larval habitats (Goin and Goin 1962; Müller et al. 2013; Liedtke et al. 2017). Biphasic aquatic reproduction has been lost in a number of other ways in various amphibians, including terrestrial, non-feeding tadpoles (e.g. Warren 1922; Wake 1980), viviparity (e.g. San Mauro et al. 2014; Sandberger-Loua et al. 2017) or incubating eggs in, e.g. dermal pouches or the male vocal sacs (see Wells 2007 for a comprehensive summary of amphibian reproduction), but direct development is by far the most common terrestrial reproductive strategy.

In all amphibians, direct-developing species are characterized by large scale developmental repatterning and in anurans in particular most tadpole-specific structures, such as the lateral line system, larval mouth parts, the cement gland or the

coiled intestine, are greatly reduced or entirely absent during development (Hanken et al. 1997a). In addition to the profound reduction of larval structures, embryos of most direct-developing frogs show similar modifications, such as an enlarged membranous tail with a highly vascularized fin, a reduction of external gills, an early and nearly simultaneous development of front- and hind limbs and a large yolk reserve (Townsend and Stewart 1985; Bahir et al. 2005; Anstis et al. 2007). The apparent similarity in embryonic development of the few studied direct-developing species has led to the idea that the anuran tadpole might represent a distinct developmental module that has been deleted from the ontogeny in direct-developing species (Callery and Elinson 2000a; Callery et al. 2001; Ziermann and Diogo 2014).

In anurans, direct development, in a strict sense in which development is completed within the egg, has been reported to occur in members of the Arthroleptidae, Bufonidae, Microhylidae, Myobatrachidae, Ranidae, Rhacophoridae, Sooglossidae and Terrarana (Brachycephaloidea sensu Frost 2016). In some of these taxa, all species are direct-developing (e.g. Terrarana), whereas in others, only some are (e.g. Myobatrachidae) and direct development may have even evolved several times independently within the group (e.g. Bufonidae). Although many species of frogs develop directly, developmental data are sparse or absent for many taxa that are known or presumed to develop directly (Thibaudeau and Altig 1999), a fact attributable to the often well-concealed breeding sites (Bahir et al. 2005). Direct development has been studied in detail for only a few species (Townsend and Stewart 1985; Hanken et al. 1992; Bahir et al. 2005; Kerney et al. 2007; Anstis et al. 2007), but short descriptions or cursory notes reporting direct development are available for a greater number of species (e.g. Alcala and Brown 1982; Bourne 1997; Jameson 1950; Krishnamurthy et al. 2002). The most well-known are those of the neotropical genus *Eleutherodactylus* and species formerly assigned to it (Terrarana; Hedges et al. 2008; Heinicke et al. 2009). Although direct development has been confirmed for a number of the ca. 1063 species of Terrarana (Frost 2016), detailed information on various aspects of development is only available for *Eleutherodactylus coqui*, a Puerto Rican species that is characterized by a nearly complete loss of larval characteristics (Townsend and Sewart 1985; Elinson 1990; Hanken et al. 1992). Primarily because of the paucity of information on other direct-developing frogs, especially non-terraranan anurans, *E. coqui* has come to be seen as representative of direct development in anurans in general. However, a recent study of development in *Oreobates barituensis*, a terraranan from northern Argentina, together with older reports (e.g. Lynn 1942; Gitlin 1944; Jameson 1950) indicates that development is not as uniform in Terrarana as previously thought (Goldberg et al. 2012). This, together with the limited amount of data available on other direct-developing species (e.g. Patil and Kanamadi 1997; Bahir et al. 2005; Anstis 2008; Anstis et al. 2007; Narayan et al. 2011), suggests that direct development is not as stereotypical as generally assumed.

Among African frogs, only species of the genus *Arthroleptis* appear to be true direct developers, although a number of related taxa show some degree of terrestrial reproduction (Müller et al. 2007). *Arthroleptis* currently comprises 47 moderately diverse species that are distributed throughout most of sub-Saharan Africa (Blackburn 2008; Frost 2016). All *Arthroleptis* species are assumed to be direct-developing, although only very limited developmental information is available for just two species (Lamotte and Perret 1963; Wager 1965). We investigated the embryonic development of the South African endemic *Arthroleptis wahlbergii* Smith 1849 and the East African dwarf squeaker *Arthroleptis xenodactyloides* Hewitt 1933 based on material collected in the field in South Africa and Tanzania. In this paper, we provide a detailed description of external development, clutch characteristics and egg deposition site. A comparison with published information on other direct-developing species shows that although both *Arthroleptis* species exhibit some general characteristics of direct-developing frogs, they also differ in a number of characters. This highlights the degree of developmental diversity that characterizes the different direct-developing anuran taxa and argues against simplistic assumptions about the evolution of direct development as being merely an excision of a 'tadpole developmental cassette' (Elinson 1990) from the ontogeny of direct-developing taxa.

Material and methods

Developmental series of two species of *Arthroleptis*, *A. wahlbergi* and *A. xenodactyloides* were available for investigation. Of *A. xenodactyloides*, a total of 47 embryos and hatchlings as well as two subadults and three adults were collected in December 2009 and March 2010 at Kigogo and Luhota Forests, Mufindi District, Iringa Region, Tanzania. The embryos were sampled from three field-collected clutches. The clutches were collected by systematically sifting through leaf litter on the forest floor (Fig. 1a), whereas adults and subadult frogs were collected opportunistically in the same general area where the clutches were found.

Of *A. wahlbergii*, a total of 80 embryos and hatchlings were sampled from four clutches of eggs collected in December 2015 at Eshowe and Entumeni Forest in KwaZulu-Natal, South Africa. In addition, several juvenile and adult specimens (Fig. 2) were available for comparison. One clutch was field-collected and the other three clutches were collected

Fig. 1 Habitat (**a**) and clutch (**b**) of *Arthroleptis xenodactyloides* at Luhota Forest, Mufindi, Southern Udzungwas, Tanzania. **c** Clutch of *A. wahlbergii* at Entumeni Forest, KwaZulu-Natal, South Africa. Clutches were photographed in situ after the removal of covering leaves and soil

from a temporary field enclosure. We constructed this using shade cloth to build a fence of ca. 40-cm height to enclose a space of approximately 1.5 m^2 in an area with thick, moist leaf litter and closed canopy where several adult *A. wahlbergii* had been found. We collected four gravid females and four males from the immediate surrounding area and maintained them in the enclosure for 2 weeks. At least once every 48 h we inspected the enclosure and moistened the leaf litter if no rain had occurred. Because no spontaneous egg deposition had occurred after 12 days, we gave all males and females a single injection of Amphiplex, consisting of des-Gly^{10}, D-Ala^{6}, Pro-LHRH (Bachem; 0.4 μg/g body weight; GnRH-A) and metoclopramide (Sigma; 10 μg/g body weight; MET), to induce oviposition (for details, see Trudeau et al. 2010). Two days after the hormonal stimulation, we dismantled the enclosure and found three clutches buried beneath the leaf litter in the relatively loose, uppermost layer of soil. No adults were found in attendance and the general clutch characteristics did not differ from the field-collected clutch.

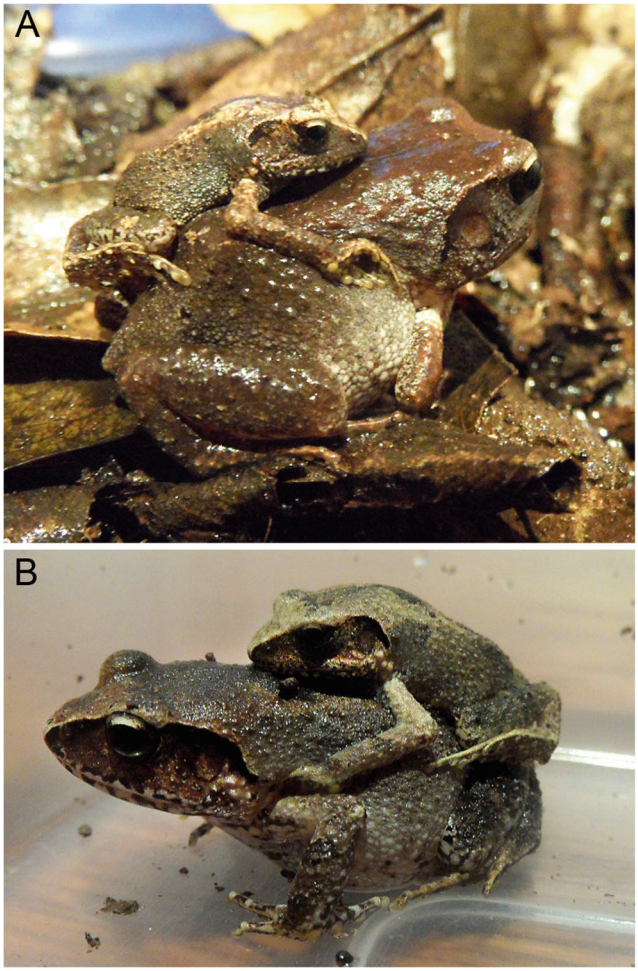

Fig. 2 Pair of *Arthroleptis wahlbergii* in amplexus. The male on top is slightly displaced to the side in **a**, showing the outward facing palm and elongated third finger. **b** Pair in full amplexus; note the disproportionately long forearm of the male

We transferred clutches to Petri dishes and maintained them under field conditions at ambient temperatures, sampling embryos at regular intervals (every 1–2 days). Specimens were euthanized using tricaine methanesulfonate (MS222; Fluka), fixed in 4% neutral-buffered formalin and subsequently stored in 70% ethanol. Voucher specimens of *A. xenodactyloides* have been deposited in the collections of the Museum of Comparative Zoology (MCZ A-149005-10). Conspecificity of the egg clutches was confirmed through raising individual eggs to hatching.

Descriptions of embryo and egg morphology are based on microscopic observations of live and preserved material. Drawings and photos were made using a Zeiss Discovery V12 stereomicroscope (Carl Zeiss) with an attached drawing mirror and an AxioCam digital camera. The description of embryonic development in *Arthroleptis* is based on the staging table for *E. coqui* (Townsend and Stewart 1985). Although different direct-developing species show considerable variation in external morphology and developmental timing (see 'Discussion'), we decided to follow the table by Townsend and Stewart (1985) because it has been widely used for the

description of direct-developing anurans (e.g. Bahir et al. 2005; Anstis et al. 2007; Anstis 2008; Goldberg et al. 2012) and is therefore the most suitable framework for comparing interspecific differences in development. Unless stated otherwise, reported observations refer to both *A. wahlbergii* and *A. xenodactyloides*.

Results

All three clutches of *A. xenodactyloides* were found hidden within moist leaf litter on the forest floor and consisted of 12, 16 and 19 eggs, respectively. The eggs were laid about 3 to 5 cm below the surface of the leaf litter, directly between leaves or inside curled leaves. A clutch consisted of single eggs (sensu Altig and McDiarmid 2007) that were more or less clustered, with some scattering of individual eggs or small groups of eggs (Fig. 1b). In the areas of the forest where the clutches were found, the leaf litter seemed considerably thicker, several layers deep, than in other parts of the forest and the ground had a gentle slope (Fig. 1a). The single clutch of *A. wahlbergii* found in a natural setting contained 23 eggs and was collected in a little *Macadamia* woodland on the outskirts of Eshowe. We collected it from a shallow mound of relatively compact earth, where it was buried about 3 cm deep inside the soil, underneath deep leaf litter. The three clutches obtained from the enclosure contained 19, 19 and 31 eggs. The two smaller clutches contained a number (four and nine) of unfertilized eggs. All clutches were found buried about 1–2 cm deep in the soil underneath leaf litter (Fig. 1c). In both *A. wahlbergii* and *A. xenodactyloides*, no adults were found attending the clutches.

The eggs of both species were non-pigmented and encased in a clear egg capsule. In *A. wahlbergii*, we observed five different layers of the egg capsule (Fig. 3a; no data available for *A. xenodactyloides*). The two outer layers were extremely thin, with the jelly of the first layer being more robust than in the second layer. Soil and other particles adhered to the outer surface of the eggs, but increasing wetness reduced the stickiness of the outer layer. The third and fourth layers were thicker and of a more rubbery consistency (Fig. 3a). The fifth layer was relatively thin again and surrounded the embryo (Fig. 3b, c). It tightly enveloped the embryo and was difficult to remove in preserved specimens. Apart from the unfertilized eggs of *A. wahlbergii*, all eggs developed normally and no fungal infections were observed. All clutches of *A. xenodactyloides* had already commenced development at the time of collection and the youngest embryos represented in our material are at Townsend and Stewart stage 3 (TS 3). We also could not observe a single clutch throughout the entire development, but from the material available, it took 30 days between TS 3 and hatching, and we therefore estimate the entire embryonic development to take around 32 to 33 days. For *A. wahlbergii*, almost the entire embryonic development could be observed in a single clutch and it took 30 days from gastrulation (TS 1) to hatching. Based on these data, we estimate the entire embryonic development to take not more than 31 to 32 days. Hatching in *A. xenodactyloides* occurred at an average size of SVL 3.7 mm (±0.2; n = 3) and hatchlings of *A. wahlbergii* had an average size of SVL 5.5 mm (±0.2; n = 5).

Embryonic morphology and development

Both species of *Arthroleptis* were very similar in their development and the following description pertains to both of them, except where stated otherwise.

Head Distinct cephalic areas were delimited by TS 4 and optic and otic regions were clearly differentiated (Fig. 4c). The large

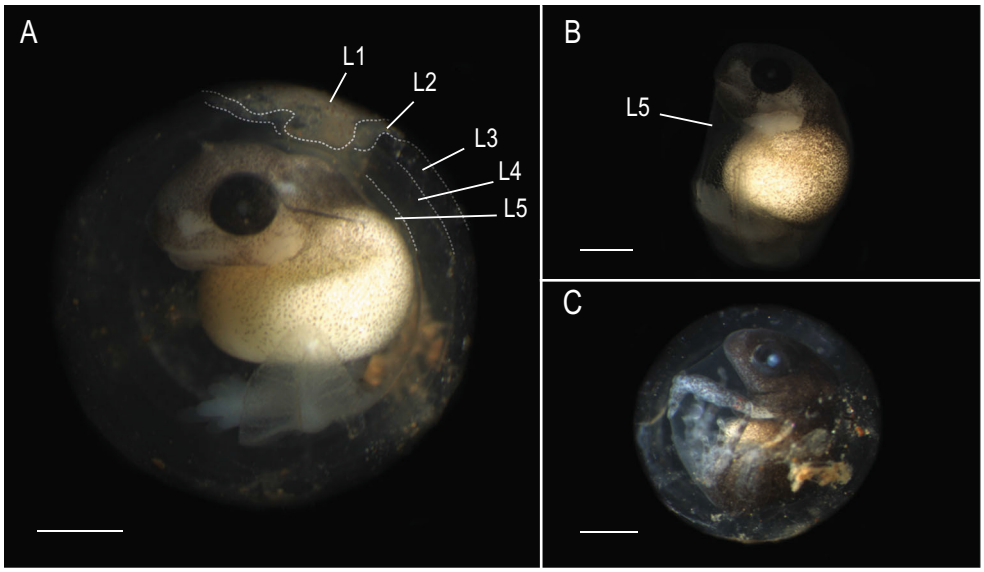

Fig. 3 Different stages of development inside the egg of *Arthroleptis wahlbergii*. **a** TS 9, different layers of the egg capsule are shown. Layers 1 and 2 (*L1* and *L2*) are partly removed. Layers 3 and 4 (*L3* and *L4*) are the thickest of all layers. Layer 5 (*L5*) closely surrounds the embryo. **b** In TS 10, all layers of the egg capsules have been removed except layer 5 (*L5*). **c** In TS 15, last stage inside the egg, hatching occurs at any time

eyes were initially evident as large, unpigmented optic vesicles. Pigmentation of the iris started at TS 6 (Fig. 4e) and the iris became increasingly dark during further embryonic development. The pupil remained clear throughout development. Eyelids were first evident relatively late in embryonic development at TS 15 (Fig. 4l). During TS 6, the mouth opened and the lower and upper jaws were differentiated. The mouth opening widened at TS 8 and the nostrils appeared at the same time (Fig. 4g). By TS 13, the mouth opening extended backwards to below the eye (Fig. 4k). The posterior extent of the mouth opening reached its final position at a level behind the eye during postembryonic development.

Gills At least two gill arch bulges were clearly visible during TS 4 in *A. xenodactyloides* (Fig. 5a). In *A. wahlbergii*, four gill arches were visible during TS 4 (Fig. 4c). The gill arches disappeared from external view at TS 5. External gills were not observed at any stage in the available specimens.

Body pigmentation and body wall Body pigmentation first appeared at TS 6 with the formation of melanophores on the head and in the vertebral region (Fig. 4e). During this stage, a few melanophores also appeared along the paravertebral region of the future body wall overlaying parts of the yolk (Fig. 4e, right). By TS 8, melanophores were widely spread over the head and body and the body wall had expanded laterally to enclose the yolk up to a narrow gap along the ventral side (Fig. 4g). The body wall completely enclosed the yolk ventrally by TS 10–11. In general, dorsal parts of the head and trunk as well as the outer sides of the fore- and hind limbs were more densely pigmented than the lower jaw and the inner sides of the fore- and hind limbs, which only showed slight pigmentation.

Limbs Overall, development was characterized by a very early appearance of the limb buds. Both fore- and hind limb buds first appeared as rounded swellings lateral to the neural tube. Hind limb buds were already distinct at TS 4, whereas the forelimb buds were only faintly indicated and less well defined at this stage (Fig. 4c). The hind limb buds were slightly larger than the forelimb buds and remained so during the differentiation stages. The limb buds increased in size, becoming more elongated and were joined to the trunk by TS 5 (Figs. 4d and 5c). The hind limbs continued to elongate, and by TS 6, slight constrictions of the knee joints appeared, while the forelimb buds were round to ovoid (Fig. 4e). The opercular fold started to overgrow the developing forelimbs at TS 6. At TS 7, the forelimbs were covered to about one third by the opercular fold and were completely covered by TS 9 (Fig. 5d–f). Differentiation of the hand and digits was completed under the opercular fold. Nubs of digits 1–3 and toes 1–4 first appeared at TS 8 (Fig. 5h), and all five toes were visible by TS 9. At TS 10, the forelimbs were fully erupted (Fig. 5g). The subarticular tubercles on hands and feet were first visible at TS 12 (Fig. 5j).

Tail A tail bud first appeared in TS 3 embryos. From the beginning of TS 4, the tail bud elongated and bent on the inside of the vitelline membrane of the embryo (Fig. 5b). There was no consistent orientation of the tail, and some embryos had the tail bent to the left, whereas in others, it was bent to the right. However, tail orientation in individual embryos seemed to remain constant throughout development. A small membranous fin developed at TS 5 (Fig. 5c). At this stage, the tail was about one third of its final length. The tail and its vascularized fin membrane continued to develop and elongate until TS 10, when it reached its full length at a size more or less equal to the body length of the embryo. The tail began to regress at TS 12. By TS 14 (Fig. 4k), the tail was reduced to a small stub and completely resorbed in hatchlings (Fig. 4l). The tail lacked pigmentation throughout development.

ECD Endolymphatic calcium deposits (ECD) first appeared at TS 6 as two small whitish dots, one on each side of the otic region (Fig. 4e). The ECD expanded during TS 7 (Fig. 4f) and developed extensions in the caudal direction that continued to grow until TS 11. By TS 12, the two ECD antimeres were joined in the midline. At the same stage, the ECD began to be obscured by the increasingly more dense pigmentation and were no longer visible from the beginning of TS 13.

Discussion

Reproduction in *Arthroleptis*

The males of many species of *Arthroleptis* are characterized by moderately to extremely elongated third fingers (Blackburn 2009). The function of this sexually dimorphic trait is unclear but is thought to perhaps be used in male to male combat or during amplexus (see Blackburn 2009 for details). We observed axillary amplexus in *A. wahlbergii* (Fig. 2) and the palms of the hands of the male were facing outward. We did not observe any special motion or posturing of the third finger and it does not seem to play a particular role in amplexus. However, given the large size difference between male and female, the elongated lower arm and third finger might overall improve the hold on the female.

The first observations on reproduction in *Arthroleptis* were made by Barbour and Loveridge (1928), who described three clutches of *A. stenodactylus* eggs (33, 40 and 54 eggs) collected from shallow burrows with some adults, plus an additional clutch of 80 eggs that they suspected to be a mix of at least two clutches. They pointed out the disproportionately large ova in gravid *A. xenodactylus* but did not explicitly infer a direct mode of development. The first explicit

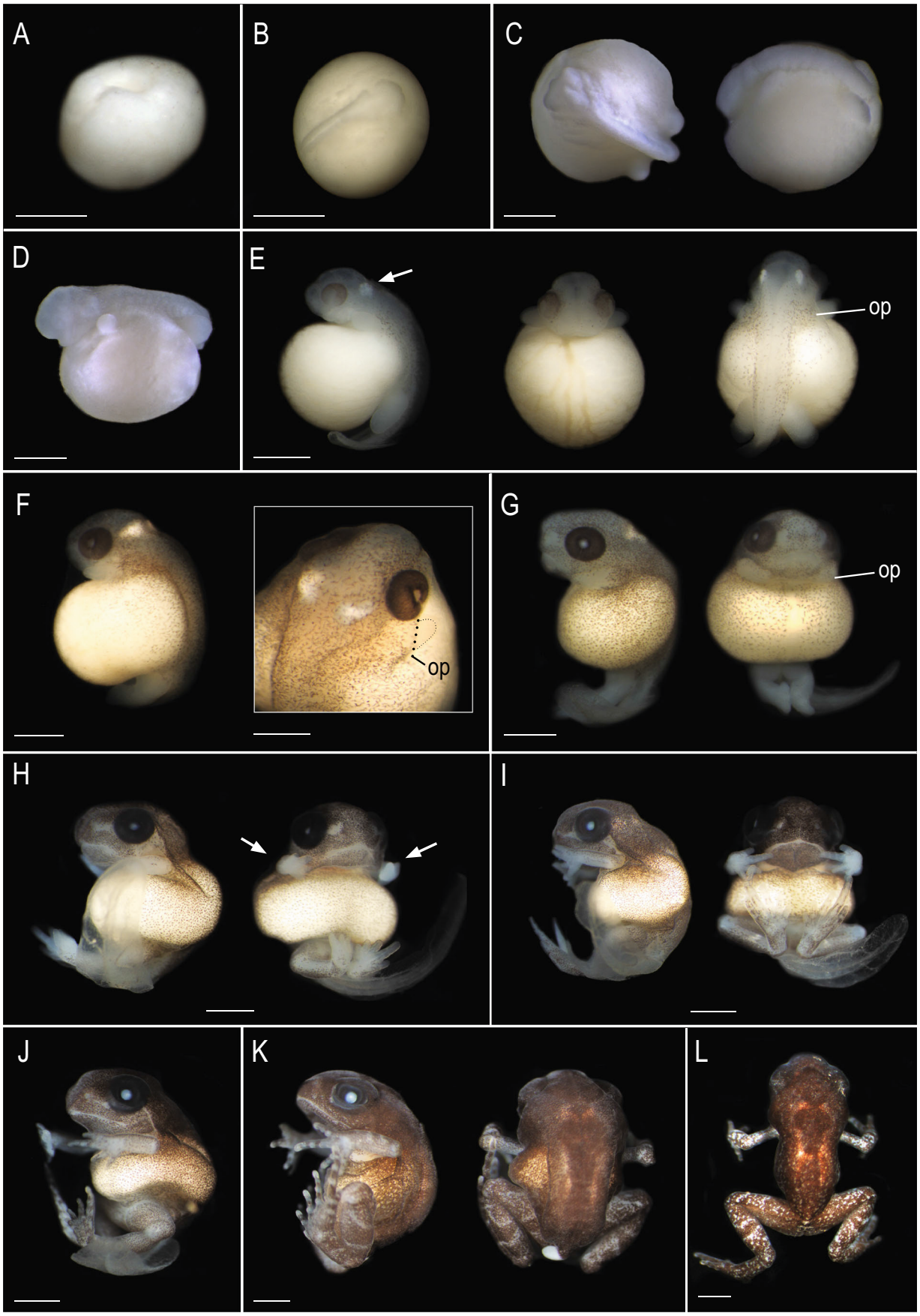
A
B
C
D
E
op
F
op
G
op
H
I
J
K
L

◀ **Fig. 4** External development in *Arthroleptis wahlbergii*. All embryos have been removed from the egg capsules. **a** TS 1. Formation of blastopore. **b** TS 3, dorsal view. Neural folds formed. **c** TS 4, dorsal and frontal view. Early limb bud stage, neural tube formed, gill arches apparent. **d** TS 5. Limb buds attached to trunk. **e** TS 6, *left*: lateral view (*arrow* indicates ECD), *middle*: frontal view, *right*: dorsal view. Opercular fold (*op*) begins to grow over developing forelimb. **f** TS 8, *left*: lateral view, *right*: close-up of head region, with edge of opercular fold and outline of limb bud indicated by *dotted lines*. Opercular fold covers two thirds of the forelimb bud. **g** TS 9, *left*: lateral view, right: ventral view. Opercular fold completely covers forelimbs. **h** TS 10, both forelimbs erupted (*arrow*), tail fin begins to decrease, pigmentation denser. **i** TS 11/12, *left*: lateral view, *right*: ventral view. Toes are much longer, tail begins to decrease in size. **j** TS 13, fingers longer, tubercles visible. **k** TS 14, *left*: lateral view, *right*: dorsal view. Distinct eyelids visible, toes full length, banding patterns on legs evident. **l** TS 15, hatchling. *Scale bars* = 1 mm

statement of direct development in *Arthroleptis* seems to have been made by Loveridge (1953), who reported that *A. stenodactylus* lay their eggs in a burrow and that metamorphosis is completed inside the egg. Guibé and Lamotte (1958) reported direct development for the West African *A. crusculum* and a clutch size of 15 eggs. The eggs were deposited in a spherical chamber of about 1–2 cm in diameter, a few centimetre below the surface of the soil. The wall of the chamber was reported to be rather regular and seemingly lined with mucus (Guibé and Lamotte 1958). Channing (2001) reported a clutch of *A. xenodactyloides* consisting of 20 eggs that he found 20 cm beneath leaf litter accumulated next to a wet rock face on Mt. Zomba, Malawi. Channing and Howell (2006) reported clutches of *A. xenochirus* to consist of about nine eggs that were laid in shallow nests in leaf litter and provided a photograph of a clutch. They also published a photograph of *A. adolfifriederici* eggs at approximately TS 6, and Altig and McDiarmid (2007) published a photograph of a clump of eggs of *A. schubotzi* found in leaf litter, confirming terrestrial reproduction for two additional species.

Lamotte and Perret (1963) provided a brief description of reproduction and development of the West African *A. poecilonotus* from material collected in Cameroon, where clutches were found in the soil in gardens planted with peanut and cassava. Clutch size averaged 20 to 25 eggs and the large eggs were surrounded by a thick gelatinous capsule that consisted of two to three concentric, spherical layers plus an outer and an inner membrane (Lamotte and Perret 1963). They illustrated five different developmental stages and provided some information on embryonic development, including that the tail was always bent to the left and the forelimbs were hidden under a membrane (presumably the opercular fold) for some unspecified time during development. Interestingly, Lamotte and Perret (1963) reported hatching to occur after 15 to 20 days at a seemingly less advanced stage compared to *A. wahlbergii* and *A. xenodactyloides*. Upon hatching, *A. poecilonotus* still possessed a tail remnant of about half the snout-vent length and eyelids were not yet differentiated. Lamotte and Perret (1963) reported raising their clutches inside a crystallizer at constant temperature (27 °C) and humidity. A constant 27 °C appears to be higher than normal soil temperatures and might explain the comparatively short developmental time reported. Whether hatching generally occurs at an earlier stage in *A. poecilonotus* or might be an artefact of higher-than-average incubation temperatures remains unclear at present. Tapley (2009) reported hatching to occur after about 1 month in captive-breeding *A. stenodactylus*. Some data on reproduction and development in *A. wahlbergii* were provided by Wager (1965), who described discovering eggs in a large pile of leaves, about 3 cm or more below the surface. He reported five clutches that consisted of 11, 18, 20, 26 and 30 eggs, respectively, with the eggs in the individual clutches being somewhat scattered over an area of about 8 cm in diameter. Wager (1965) very briefly summarized embryonic development and also illustrated six stages, but his drawings are very schematic and depict proportions incorrectly. However, he reported that the forelimbs are covered by skin and that hatching occurs at the end of the fourth week of development when the young are fully formed and about 6 mm long, which match our own observations presented here.

Although data on aspects of egg laying or development are only available for nine species of *Arthroleptis* (out of 47), these species do show a similar pattern of reproduction in that eggs are laid terrestrially in a moist, secluded place and develop directly into fully developed young. Egg deposition varies slightly in that eggs are either laid among leaf litter or buried in the soil beneath leaf litter. This is likely a function of the ability to burrow—better in species with a well-developed metatarsal tubercle like *A. stenodactylus* and *A. wahlbergii* and less so in small species with weakly developed metatarsal tubercles like *A. xenodactyloides*—and the local conditions (wetness, shade, thickness of leaf litter, etc.). The spherical breeding chamber described by Guibé and Lamotte (1958) for *A. crusculum* seems unusual and resembles the nesting chamber of *Anhydrophryne rattrayi* as described by Wager (1965). The number of eggs per clutch and size at hatching vary among species and seem to correlate with adult size, with smaller species having fewer eggs and smaller hatchlings and larger species having more eggs and larger hatchlings. The average hatching size of 3.7 mm in *A. xenodactyloides* is among the smallest hatchling sizes reported for any direct-developing anuran, except *Sooglossus* (Callery et al. 2001). Hatching at a somewhat earlier stage in *A. poecilonotus*, as reported by Lamotte and Perret (1963), might possibly be a result of suboptimal rearing and would require confirmation. In captive *A. stenodactylus*, Tapley (2009) observed occasional male egg-guarding behaviour but did not provide further details. In all other investigated species, no adults were found attending the clutches and it seems that dedicated egg-guarding does not occur in *Arthroleptis*. Interestingly, the eggs

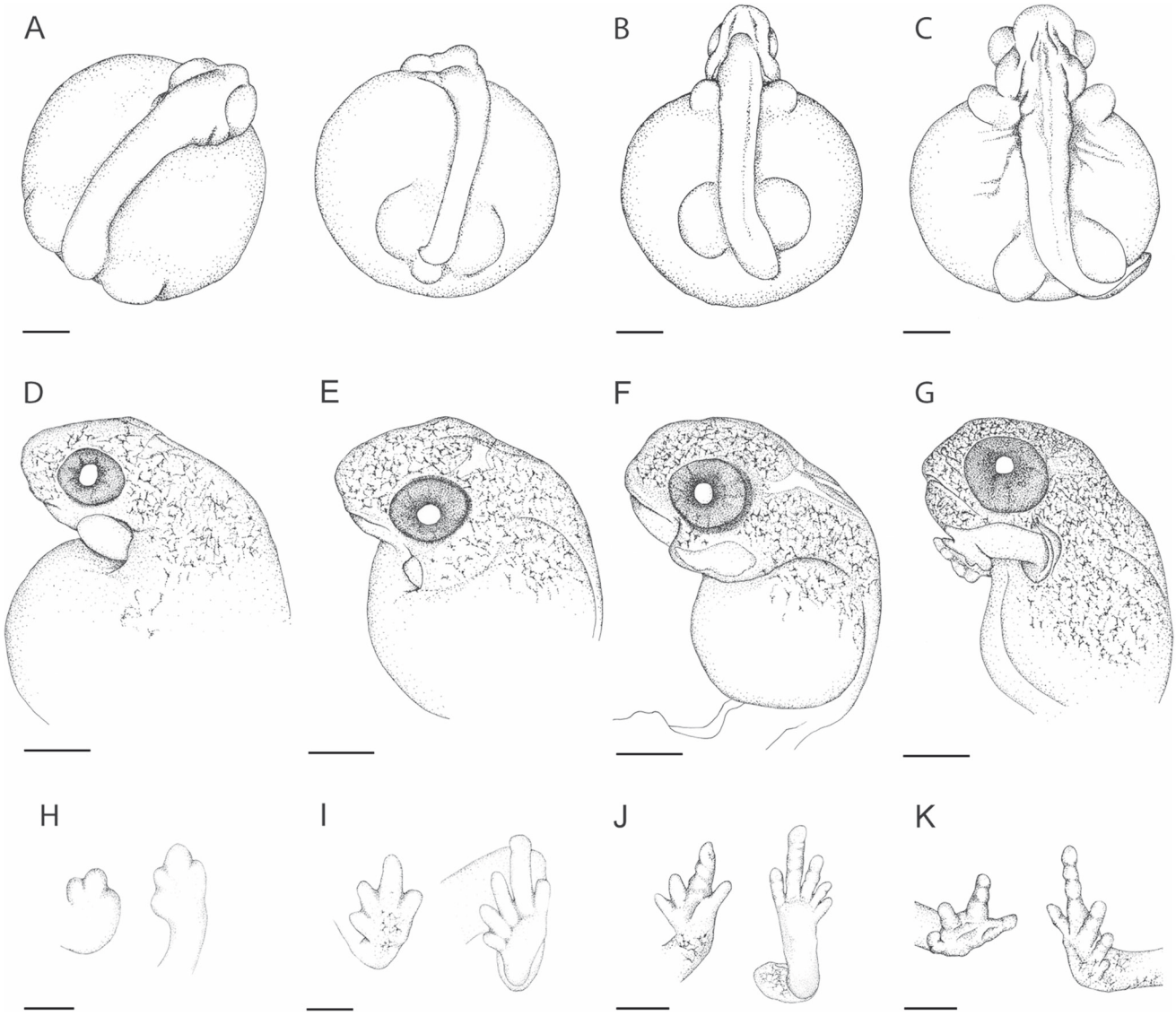

Fig. 5 Details of development of *Arthroleptis xenodactyloides*. **a** TS 3, *left*: dorsal view, *right*: caudal view. **b** TS 4, caudal view. **c** TS 5, dorsal view. **d–g** Development of the opercular fold. **d** TS 7, lateral view. Opercular fold covers one third of the forelimb buds. **e** TS 8, lateral view. Forelimbs almost covered beneath opercular fold. **f** TS 9, lateral view. *Arrow* indicates that forelimbs completely covered by opercular fold. **g** TS 10, lateral view. Forelimbs fully erupted. **h–k** Development of toes and digits. **h** TS 8, dorsal aspect, nubs of three digits and four toes visible. **i** TS 10, dorsal aspect of hand, ventral aspect of foot. Tips of toes and digits enlarged. At this stage, forelimbs are fully erupted and no longer covered by the opercular fold. **j** TS 12. Lateral aspect of hand, ventral aspect of foot. Digits enlarged, tubercles visible. **k** TS 15, ventrolateral aspect. Limbs fully developed. Hatching occurs at any time. *Scale bars*: **a–g** 0.5 mm; **h–k** 0.25 mm

we raised seemed resilient and we lost none to fungal infections. Although little information is available for anurans, in direct-developing salamanders, eggs are more likely to succumb to fungal infections if the attending parent is removed (Wells 2007). *Arthroleptis* eggs might possess some antimycotic properties.

Both species of *Arthroleptis* investigated here showed a remarkably similar embryonic development. The few details reported in earlier studies (Lamotte and Perret 1963; Wager 1965) are also in agreement with the observations reported here (with the exception of *A. poecilonotus* discussed earlier). *Arthroleptis wahlbergii* and *A. xenodactyloides* are not closely related (Blackburn 2008), and the near identical embryonic development observed in both species and available data on other species suggest that similar patterns of development might likely be characteristic for *Arthroleptis* in general.

Direct development in anurans

Direct development has evolved independently several times in all three orders of amphibians and represents a derived developmental mode in which the aquatic larval stage has

been eliminated as a functionally distinct life-history stage from the ontogeny (Hanken 1989; Wake and Hanken 1996; Hanken et al. 1997a; Wake 2003). The development of direct-developing anurans differs considerably from that of species with a biphasic life cycle in that most adult features, which typically form at metamorphosis in biphasic taxa, already appear during embryogenesis (Wake 1989; Hanken et al. 1997a). Heterochrony is considered a likely reason for these evolutionary changes in the timing of developmental events (Raff 1987; Hanken et al. 1992; Goldberg et al. 2012). Direct-developing species show accelerated growth rates and develop faster in comparison to most tadpoles (Lutz 1948; Callery and Elinson 2000a, b). Less clear is the extent to which larval features are expressed in different direct-developing taxa. Earlier studies focused on the neotropical terraranan *E. coqui*, which shows a near complete loss of larval characteristics (Townsend and Stewart 1985; Callery et al. 2001). This dramatic loss of larval characteristics paired with the scant availability of data on other direct-developing taxa led some authors to suggest that the free-swimming tadpole larva might represent a developmental cassette or module that has been excised from the ontogeny of direct-developing species (Elinson 1990; Callery and Elinson 2000a, b; Ziermann and Diogo 2014). This idea could potentially provide a more mechanistic explanation for the repeated evolution of direct development in anurans. The generality of this assumption however is contingent on the overall similarity of direct-developing anurans. In *E. coqui*, several studies have demonstrated large-scale, ontogenetic repatterning (e.g. Hanken et al. 1992, 1997b). These complex patterns of ontogenetic rearrangements suggest that the evolution of direct development in *E. coqui* might be more than just a simple deletion of the larval phase (Callery et al. 2001). A number of recent investigations have revealed different patterns of reduction of tadpole-specific characters in direct-developing species (e.g. Anstis et al. 2007; Goldberg et al. 2012), which indicates that the effects of direct development on embryogenesis are perhaps not consistent across different lineages that evolved this form of reproduction.

Comparability of TS staging The staging table of Townsend and Stewart (1985) has been used as a basic framework for describing development of terraranan and also non-terraranan species (e.g. Bahir et al. 2005; Anstis 2008; Goldberg et al. 2012). This staging table was originally devised to help assess embryonic age under field conditions and focused on features visible to the naked eye or with the aid of a 10× hand lens (Townsend and Stewart 1985). As such, it is a relatively coarse description of development and condenses developmental events into relatively few stages compared to other staging tables (Gosner 1960; Nieuwkoop and Faber 1967). This is especially the case for the early stages of development; Townsend and Stewart (1985) condensed the early development into three stages, beginning with the fertilized egg to the appearance of the limb and tail buds. As a consequence, embryos at different stages of development can still fall into the same TS stage. This complicates comparison of early development in direct-developing anurans based on stage descriptions derived from Townsend and Stewart's (1985) table. Some authors also employed modified stage definitions, which accounts for a lack of correspondence of the early stages between Townsend and Stewart (1985) and other staging tables (e.g. Bahir et al. 2005; Narayan et al. 2011). To compensate for the broad divisions of early development into stages, Moury and Hanken (1995) subdivided TS 3 into three substages defined by the degree of neural fold closure. In *Arthroleptis*, we also found several discrete stages of development that fit into single TS stages (Table 1). For instance, during the early TS 4, the neural tube is formed, the head is outlined and a tailbud is visible (Fig. 6a). This is followed by the beginning differentiation of the eyes, gill arches and the elongation of the tailbud (Fig. 6b). The late TS 4 comprises distinct eye anlagen and clearly defined forelimb buds (Fig. 6c). To document these, we described all discrete stages in Table 1 but did not alter the numbering of Townsend and Stewart (1985) to retain correspondence with later stages to facilitate comparison of different direct-developing species. We also indicated characters used by Townsend and Stewart (1985) to define stages and employed these to demarcate corresponding stages in *Arthroleptis*.

External gills Small, external gills are present during early embryonic development in some direct-developing species, but their presence seems rather variable, even among closely related species. Although small gill arches occur transitorily in *Arthroleptis*, as in other species, no external gills are present during embryonic development. External gills were also not observed in the myobatrachids *Arenophryne rotunda*, *Myobatrachus gouldii* (Anstis et al. 2007), *Metacrinia nichollsi* (Anstis 2008), the rhacophorids *Philautus viridis* and *Philautus silus* (Bahir et al. 2005) and the craugastorid *Haddadus binotatus* (Goldberg and Candioti 2015). External gills are present for less than one-fourth of the developmental period in *Philautus variabilis* (Patil and Kanamadi 1997). In *Philautus glandulosus*, they appear as lamellae and are also only present for a short period (Krishnamurthy et al. 2002). External gills have further been reported in the ceratobatrachid *Platymantis vitiana* (Narayan et al. 2011). In Terrarana, external gills have been reported in some species but seem to be absent in others. In *E. coqui,* external gills first appear at TS 5 and disappear by TS 9 (Townsend and Stewart 1985). A pair of small, external gills is present as short, stubby ectodermal projections off the third gill arch in *Eleutherodactylus portoricensis* for about 5 days of the 19-day developmental period (Gitlin 1944). No external gills were observed in *Craugastor augusti* (as *Eleutherodactylus latrans*, Jameson

Table 1 Synopsis of external characteristics in developmental stages of *Arthroleptis* embryos. Features in bold indicate diagnostic features of the developmental stages of *Eleutherodactylus coqui* (Townsend and Stewart 1985)

TS stage	*Arthroleptis* development
1	**Oviposition**
1	Late-Gastrula, **blastopore** visible
2	Early neurulation stage, **neural folds** forming neural groove
3	- Mid- to late neurulation stage - **Neural groove formed**, not yet closed to a neural tube
4	- **Neural tube formed** - Head outlined - **Forelimb buds** feebly defined, **hind limb buds** evident - Somites slightly visible - **Tail bud** evident
4	- **Eye bulges** visible - **Gill arches** distinct caudal to the eyes - Somites clearly visible - Tail bud elongated
4	- Head more prominent and separated into distinct areas: optic region, mouth and auditory region differentiable - Gill arches disappeared, no gill buds visible
4	- Eye bulges distinct but unpigmented - Forelimb buds round and clearly defined, hindlimb buds round to ovoid - **Limb buds separated from trunk** - Tail bud elongated and slightly curved to one side
5	- **Eyes distinct but unpigmented** - **Limb buds attached to trunk**, forelimb buds clearly defined and smaller than hind limb buds, hind limbs round to ovoid - **Tail elongated with small thin fin**, bends to one side
6	- **Iris** with light brown **pigment** - Forelimbs round to ovoid, **slight knee constrictions** on hind limbs - Opercular fold appears and begins to grow over forelimb buds - **Tail one third of its final length, small fin** - **ECD** (endolymphatic calcium deposits) **first visible** as small white points - **Light pigment over head and trunk**
7	- Iris darker on outer and inner border, colour of iris light brown - Opercular fold covers two thirds of forelimbs - **Knee joints more evident, foot paddles** - **ECD quadrangular patches** - **Tail with vascularized fin** - Pigment denser over head and trunk, spreads over yolk
8	- Opercular fold covers two thirds of forelimbs - **Nubs of digits and toes** - **ECD triangular** with forward **extensions** to eye
9	- Opercular fold closed - **Toes 1–5 demarcated** - Hind limbs have slight pigmentation except on inner sides and on ventral sides of feet - **Tail to two thirds of its final length** with well-vascularized fin - **ECD expand** to one third over trunk
10	- **Iris dark pigment, pupil light grey** - Nares distinct - Forelimbs erupted - Elbows distinct, fingers differentiable, hands ventrally orientated - Knees distinct, Toes 1–5 separated
	- **Tail at full size**, remains unpigmented - Slight pigment over forelimbs except inner sides - Yolk enclosed in body wall
11	- **Iris dark, pupil light grey** - Fingers and toes much longer - Forelimbs with light pigment on outer sides, hind limbs darker pigment on outer sides and light pigment on inner sides - **Tail at full size** - **ECD expanded backwards** toward the trunk - Pigment over dorsum darker
12	- Iris dark, pupil light grey - Fore and hind limbs darker pigment on outer sides, hind limbs light pigment on inner sides and on ventral side of feet - Tubercles slightly visible - **Toes two thirds of their length at hatching** - Tail begins to regress in size
13	- Tubercles distinct on hand and feet, darker pigment on palms of hand and feet - **Tail** further **regressed in size** - **Body heavily pigmented**, light pigment on abdomen - ECD joined in the midline, large longitudinal extensions
14	- Eyelids visible - **Limbs and toes fully developed** - Banding patterns on legs visible - **Tail regressing** - Pigment denser over ventral sides of body
15	- Tail reduced to a small stub - Minimal yolk reserves - **Hatching possible at any time**

1950), *Eleutherodactylus nubicola* (Lynn 1942), *Ischnocnema guentheri* (Lynn and Lutz 1946), *Ischnocnema nasutus* (Lynn and Lutz 1947) and *O. barituensis* (Goldberg et al. 2012).

Opercular fold In free-living tadpoles, the opercular fold covers the external gills and developing forelimbs and forms a gill chamber that opens via a paired or single spiracle (Altig and McDiarmid 1999). In *E. coqui*, epidermal folds briefly develop to cover the gills and the base of the limb buds but disappear rapidly, even before the digits start developing on the forelimbs (Callery and Elinson 2000b). Although present for only a few hours during development in *E. coqui*, these epidermal folds are considered to be homologous with the opercular fold of metamorphosing anurans (Callery and Elinson 2001). As such, the opercular fold is a useful character when comparing direct-developing frogs with respect to their deviation from the ancestral morphology. In *O. barituensis* (Goldberg et al. 2012) and *H. binotatus* (Goldberg and Candioti 2015), the opercular fold encloses the proximal half of the forelimbs and, as in *E coqui*, the opercular fold never completely covers the forelimbs, although it seems to persist

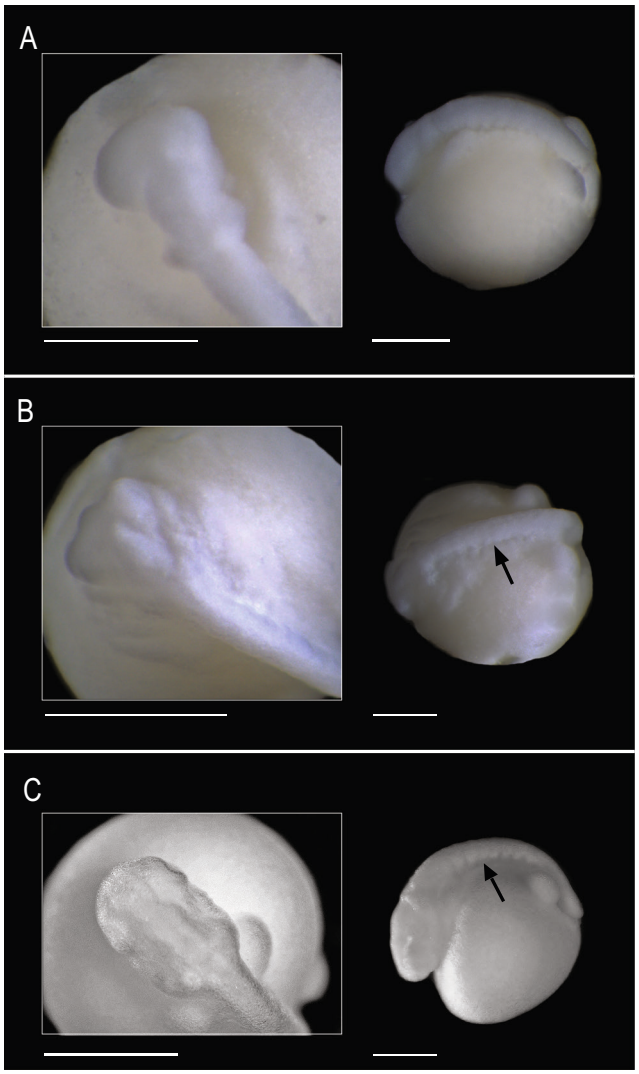

Fig. 6 Different discrete developmental events subsumed within TS 4 in *Arthroleptis*. **a** Early TS 4 of *A. wahlbergii*, *left*: close-up of head region, *right*: lateral view with head facing left. **b** Mid-TS 4 of *A. wahlbergii*, *left*: close-up of head region; *right*: lateral view, *arrow* indicates somites. **c** Late TS 4 of *A. xenodactyloides*, *left*: close-up of head region, forelimb buds clearly defined, *right*: lateral view, *arrow* indicates somites. *Scale bars* = 1 mm

for a somewhat longer period of development. This is substantially different from *Arthroleptis* and all other non-terraranan direct-developing species described so far, in which the developing forelimbs are partially or completely covered by the opercular fold for a comparatively long period of development, although the timing of appearance and disappearance of the opercular fold varies among the different taxa. In *Arthroleptis* and *A. rotunda*, the opercular fold persists for a period of five stages (Anstis et al. 2007), for six stages in *M. gouldii* (Anstis et al. 2007) and *M. nichollsi* (Anstis 2008) and up to eight stages in *P. viridis* (Bahir et al. 2005). Also, the period of complete enclosure of the forelimbs by the opercular folds ranges from a maximum of two stages in *Arthroleptis*, *P. viridis* (Bahir et al. 2005) and *Philautus surdus* (as *Philautus lissobrachius*, Alcala and Brown 1982), to up to six stages of development in myobatrachids (Anstis et al. 2007; Anstis 2008).

Limbs Simultaneous appearance of the fore- and hind limb buds very early in development is one of the most striking features of direct development (Townsend and Stewart 1985; Elinson 1994; Anstis et al. 2007). In all species investigated so far, fore- and hind limb buds appear more or less simultaneously and develop at a similar rate. At their first appearance during early embryonic development (about TS 4), hind limb buds are usually somewhat more distinct, whereas forelimb buds are smaller and slightly less well defined. The limb buds lengthen during subsequent stages and developing digits are first seen during TS 9 or 10 on the hands and feet. Subarticular tubercles first appear during TS 12, 13, and 14 or during postembryonic development, depending on the species.

Tail Many previous investigators have commented on the highly derived tail morphology of embryos of direct-developing frogs. In general, the tail of direct-developing frogs is usually enlarged with well-vascularized tailfins that are broadly expanded and envelop the embryo to varying degrees (e.g. Townsend and Stewart 1985; Bahir et al. 2005; Goldberg et al. 2012; Goldberg and Candioti 2015). In *O. barituensis* for example, the extensively developed tail envelops nearly the entire embryo (Goldberg et al. 2012). In *H. binotatus*, it forms a sac-like structure wrapped around the hind limbs for a relatively long period (Goldberg and Candioti 2015). This is not seen in either *Arthroleptis* species, where the tail is extended to its full length with a well-vascularized fin but never envelops the embryo. Instead, tail development in *Arthroleptis* is more similar to *E. coqui* (Townsend and Stewart 1985). In most species, including *E. coqui*, the expanded parts of the tail seem homologous to the dorsal and ventral tailfins of tadpole larvae. However, in the terraranans *O. barituensis* (Goldberg et al. 2012), *H. binotatus* (Goldberg and Candioti 2015) and *Pristimantis urichi* (Nokhbatolfoghahai et al. 2010), the expanded part does not correspond to the dorsal and ventral tailfin but represents lateral, fin-like expansions. This particular configuration might be apomorphic for Pristimantinae.

Because of its enlargement and apparently high degree of vascularization, the tail is usually assumed to function mainly as a respiratory organ in embryos of direct-developing anurans (Lutz 1948; Townsend and Stewart 1985; Bahir et al. 2005). A relationship between the presence or absence of gills and tail size has frequently been discussed (Townsend and Stewart 1985; Patil and Kanamadi 1997; Bahir et al. 2005; Goldberg et al. 2012) and it seems plausible that the tail has a potential role as the main respiratory organ, especially when considering that it has lost its locomotory function (Lutz 1948).

However, embryos of direct-developing ceratobatrachids (Alcala 1962; Narayan et al. 2011) and myobatrachids (Anstis et al. 2007; Anstis 2008) show little to no enlargement of the tail or tailfins. In the ceratobatrachid *P. vitiana* (Narayan et al. 2011), the tail is furthermore comparatively short and has only shallow fins. Interestingly, in both ceratobatrachids and myobatrachids, embryonic development is characterized by the reported absence of external gills (Anstis 2008; Narayan et al. 2011). In *P. vitiana*, highly vascularized abdominal sacs are thought to have a respiratory function (Narayan et al. 2011), whereas no specialized respiratory structures have so far been reported for myobatrachids. It seems clear that the tail of ceratobatrachids and myobatrachids has only a limited function as a respiratory organ. The co-option of the larval tail for a respiratory function is therefore not a general characteristic of direct-developing anurans.

The development of the tail in different direct-developing taxa also varies substantially regarding timing and growth rate. For instance, in the myobatrachids *A. rotunda* and *M. nichollsi*, the tail bud forms before the appearance of the limb buds (Anstis et al. 2007; Anstis 2008), whereas in *E. coqui*, it appears after limb buds have formed. In *O. barituensis*, tail development is apparently accelerated and by TS 6, only two stages after the tail bud has appeared, the tail envelops nearly the entire embryo (Goldberg et al. 2012).

Egg tooth An egg tooth has been reported for nearly every investigated species of *Eleutherodactylus* and those formerly referred to this genus (Lynn 1942; Lynn and Lutz 1946; Jameson 1950; Wake 1978; Bourne 1997; Goldberg et al. 2012). Jameson (1950) even considered the development of an egg tooth as a typical feature of terrestrially (i.e. direct-) developing species. Embryos of non-terraranan direct-developing species, however, have all been reported to lack an egg tooth (e.g. this study, Anstis et al. 2007; Bahir et al. 2005; Krishnamurthy et al. 2002). Based on available data, the presence of an egg tooth appears to be restricted to species of the New World direct-developing Terrarana (Hedges et al. 2008) and is presumably apomorphic for this group.

Evolution of direct development

Although direct development evolved independently in several different anuran taxa and generated early interest as an evolutionary phenomenon (e.g. Bavay 1873; Noble 1931), we still have only an incomplete understanding of its exact developmental basis and evolution. At first glance, direct-developing embryos show a high degree of overall similarity in their external development, such as early and nearly simultaneous appearance of limb buds and a more adult-like head morphology. A more detailed comparison however reveals differences in tempo and/or sequence of development of some features, such as an early enlargement of the tail or the presence and extent of an opercular fold (present study; Bahir et al. 2005; Anstis et al. 2007; Anstis 2008; Goldberg et al. 2012) among different direct-developing taxa. There is also variation among direct-developing anurans in the presence or absence of external gills, although no clear pattern is discernible and an often-suspected link between the absence of gills and an elaboration of the tail (Lutz 1948) is not without exceptions. Some taxa like the rhacophorid *Philautus* furthermore express a cement gland and a coiled gut (Bahir et al. 2005), characters more typically associated with tadpole larvae. Several features previously thought to be characteristic for direct-developing anurans, such as an egg tooth, a greatly enlarged tail or only very rudimentary and transitory presence of an opercular fold, seem to be restricted to particular direct-developing taxa and are indeed rather variable among the different direct-developing lineages. The scarce available data on patterns of internal development also present a more heterogeneous picture of the effects of direct development on, e.g. skeletal development (Lynn 1942; Hanken et al. 1992; Kerney et al. 2007).

Even though these differences in developmental morphology and timing suggest that there is no single developmental pattern among direct-developing species, we do not wish to discount the obvious similarities seen in the different direct-developing taxa. However, the idea of some authors (Elinson 1990; Ziermann and Diogo 2014) that the free-swimming tadpole larva represents some form of module that has been deleted from the ontogeny of direct-developing frogs conflicts with the available data and appears too simplistic. While the egg tooth seems to be an evolutionary novelty of Terrarana, most differences seen among direct-developing taxa concern the expression of typical larval features or their lack thereof. At present, it is unclear what accounts for these differences, but several reasons seem possible. The reduction of tadpole-specific features might be idiosyncratic and the similar phenotypes a function of the gradual accumulation of these reductions. Another alternative could be that the trajectory from larval to direct development follows a predictable sequence and the observed differences are the result of the various taxa being at different positions along that trajectory. However, the variability in the developmental timing and pattern of the tail, which seems disconnected from the remaining tadpole characteristics, indicates a more complex pattern of both integration and modularity of larval traits. More detailed studies including external and internal morphology of different direct-developing lineages are needed for a better and more comprehensive picture of the specific, evolutionary changes involved in the larval to direct development transition. More detailed morphological data might further provide valuable clues in the search for the underlying molecular mechanisms leading to the reduction of a free-swimming, feeding tadpole larva and the evolution of direct development.

Acknowledgements We thank Unilever Tea Tanzania, particularly Andrew Mitei, Amiri Kivambe, Sylvia Rutatina, and Charles Kumbemba, for permission to work on the estate and for providing invaluable help with logistics and accommodation. For help in the field, we are indebted to E. Mulungu. Permits to collect and export *A. xenodactyloides* were issued by the Tanzania Wildlife Research Institute (TAWIRI), the Tanzanian Commission of Science and Technology (COSTECH Permit No. 2009-306-NA-2009-201) and the Wildlife Division of the Tanzanian Ministry of Tourism and Natural Resources. We particularly thank Drs. V. Kakengi, J. Keyyu and K. Oola (TAWIRI) and M. Munshi (COSTECH) for their help and support. For help with logistics, we thank D. Moyer, K. Howell and D. Nkini (Tanzania Conservation Resource Centre). Permits to collect and export *A. wahlbergii* were issued by Ezemvelo KZN Wildlife (OP4507/2015). We especially thank Adrian Armstrong, Sharon Louw and James Harvey for facilitating fieldwork in KZN and Jane Chennells for permission to work on her property. We thank Lennart Olsson for commenting on an earlier version of the manuscript. Funding was provided through a Putnam Expedition Grant of the Museum of Comparative Zoology and a German Research Foundation grant (DFG MU2914/2-1) to HM and a Museum of Comparative Zoology Grant-in-Aid for Undergraduate Research and the Harvard College Research Program to JGL. Support by a Volkswagen Postdoctoral Fellowship in Evolutionary Biology to HM is gratefully acknowledged. Two anonymous reviewers provided valuable and insightful comments that helped to improve this manuscript.

References

Alcala, A. C. (1962). Breeding behaviour and early development of frogs of Negros, Philippine Islands. *Copeia, 1962*, 679–726.

Alcala, A. C., & Brown, W. C. (1982). Reproductive biology of some species of *Philautus* (Rhacophoridae) and other Philippine anurans. *Philippine Journal of Biology, 11*, 203–226.

Altig, R., & McDiarmid, R. W. (1999). Body plan, development and morphology. In R. W. McDiarmid & R. Altig (Eds.), *Tadpoles. The biology of anuran larvae* (pp. 24–51). Chicago: University of Chicago Press.

Altig, R., & McDiarmid, R. W. (2007). Morphological diversity and evolution of eggs and clutch structure in amphibians. *Herpetological Monographs, 21*, 1–32.

Anstis, M. (2008). Direct development in the Australian myobatrachid frog *Metacrinia nichollsi* from Western Australia. *Records of the Western Australian Museum, 24*, 133–150.

Anstis, M., Roberts, J. D., & Altig, R. (2007). Direct development in two myobatrachid frogs, *Arenophryne rotunda* Tyler and *Myobatrachus gouldii* Gray, from Western Australia. *Records of the Western Australian Museum, 23*, 259–271.

Bahir, M. M., Meegaskumbura, M., Manamendra-Arachchi, K., Schneider, C. J., & Pethiyagoda, R. (2005). Reproduction and terrestrial direct development in Sri Lankan shrub frogs (Ranidae: Rhacophorinae: *Philautus*). *The Raffles Bulletin of Zoology, Supplement, 12*, 339–350.

Barbour, T., & Loveridge, A. (1928). A comparative study of the herpetological faunae of the Uluguru and Usambara Mountains, Tanganyika Territory with description of new species. *Memoirs of the Museum of Comparative Zoology, 50*, 87–265.

Bavay, M. (1873). On *Hylodes martinicensis* and its metamorphoses. *Annals and Magazine of Natural History, 12*, 79–80.

Blackburn, D. C. (2008). Biogeography and evolution of body size and life history of African frogs: phylogeny of squeakers (*Arthroleptis*) and long-fingered frogs (*Cardioglossa*) estimated from mitochondrial data. *Molecular Phylogenetics and Evolution, 49*, 806–826.

Blackburn, D. C. (2009). Diversity and evolution of male secondary sexual characters in African squeakers and long-fingered frogs. *Biological Journal of the Linnean Society, 96*, 553–573.

Bourne, G. R. (1997). Reproductive behavior of terrestrial breeding frogs *Eleutherodactylus johnstonei* in Guyana. *Journal of Herpetology, 31*, 221–229.

Callery, E. M., & Elinson, R. P. (2000a). Thyroid hormone-dependent metamorphosis in a direct developing frog. *Proceedings of the National Academy of Sciences of the United States of America, 97*, 2615–2620.

Callery, E. M., & Elinson, R. P. (2000b). Opercular development and ontogenetic re-organization in a direct-developing frog. *Development, Genes and Evolution, 210*, 377–381.

Callery, E. M., Fang, H., & Elinson, R. P. (2001). Frogs without polliwogs: evolution of anuran direct development. *BioEssays, 23*, 233–241.

Channing, A. (2001). *Amphibians of Central and Southern Africa*. Ithaca: Cornell University Press.

Channing, A., & Howell, K. M. (2006). *Amphibians of East Africa*. Ithaca: Cornell University Press.

Collin, R. (2004). Phylogenetic effects, the loss of complex characters, and the evolution of development in calyptraeid gastropods. *Evolution, 58*, 1488–1502.

Duellman, W. E., & Trueb, L. (1986). *Biology of amphibians*. London: Johns Hopkins University Press.

Elinson, R. P. (1990). Direct development in frogs: wiping the recapitulationist state clean. *Seminars in Developmental Biology, 1*, 263–177.

Elinson, R. P. (1994). Leg development in a frog without a tadpole (*Eleutherodactylus coqui*). *Journal of Experimental Zoology, 270*, 202–210.

Elinson, R. P. (2001). Direct development: an alternative way to make a frog. *Genesis, 29*, 91–95.

Frost, D. R. (2016). *Amphibian species of the World: an online reference*, *Version 6.0*. New York: American Museum of Natural History http://research.amnh.org/herpetology/amphibia/index.html. Accessed 20 February 2017.

Gitlin, D. (1944). The development of *Eleutherodactylus portoricensis*. *Copeia, 1944*, 91–98.

Goin, O. B., & Goin, C. J. (1962). Amphibian eggs and montane environment. *Evolution, 16*, 364–371.

Goldberg, J., & Candioti, F. V. (2015). A tale of a tail: variation during the early ontogeny of *Haddadus binotatus* (Brachycephaloidea: Craugastoridae) as compared with other direct developers. *Journal of Herpetology, 49*, 479–484.

Goldberg, J., Candioti, F. V., & Akmentins, M. S. (2012). Direct-developing frogs: ontogeny of *Oreobates barituensis* (Anura: Terrarana) and the development of a novel trait. *Amphibia-Reptilia, 33*, 239–250.

Gosner, K. L. (1960). A simplified table for staging anuran embryos and larvae with notes on identification. *Herpetologica, 16*, 183–190.

Guibé, J., & Lamotte, M. (1958). Morphologie et reproduction par développement direct d'un anoure du Mont Nimba, *Arthroleptis crusculum* Angel. *Bulletin du Musée National d'Histoire Naturelle, 2*, 125–133.

Hanken, J. (1989). Development and evolution in amphibians. *American Scientist, 77*, 337–343.

Hanken, J., Klymkowsky, M. W., Summers, C. H., Seufert, D. W., & Ingebrigsten, N. (1992). Cranial ontogeny in the direct-developing frog, *Eleutherodactylus coqui* (Anura: Leptodactylidae), analyzed using whole-mount immunohistochemistry. *Journal of Morphology, 211*, 95–118.

Hanken, J., Jennings, D. H., & Olsson, L. (1997a). Mechanistic basis of life-history evolution in anuran amphibians: direct development. *American Zoologist, 37*, 160–171.

Hanken, J., Klymkowsky, M. W., Alley, K. E., & Jennings, D. H. (1997b). Jaw muscle development as evidence for embryonic repatterning in direct-developing frogs. *Proceedings of the Royal Society, Series B, 264*, 1349–1354.

Hedges, S. B., Duellman, W. E., & Heinicke, M. P. (2008). New World direct-developing frogs (Anura: Terrarana): molecular phylogeny, classification, biogeography, and conservation. *Zootaxa, 1737*, 1–182.

Heinicke, M. P., Duellman, W. E., Trueb, L., Means, D. B., MacCulloch, R. D., & Hedges, S. B. (2009). A new frog family (Anura: Terrarana) from South America and an expanded direct-developing clade revealed by molecular phylogeny. *Zootaxa, 2211*, 1–35.

Hewitt, J. (1933). Descriptions of some new reptiles and a frog from Rhodesia. *Occasional Papers of the National Museum of Southern Rhodesia, 2*, 45–50.

Jameson, D. L. (1950). The development of *Eleutherodactylus latrans*. *Copeia, 1950*, 44–46.

Kerney, R., Meegaskumbura, M., Manamendra-Arachchi, K., & Hanken, J. (2007). Cranial ontogeny in *Philautus silus* (Anura: Ranidae: Rhacophorinae) reveals few similarities with other direct-developing anurans. *Journal of Morphology, 268*, 715–725.

Krishnamurthy, S. V., Gururaja, K. V., & Reddy, A. H. M. (2002). Direct development in *Philautus glandulosus* (Anura: Rhacophoridae). *Herpetological Natural History, 9*, 97–102.

Lamotte, M., & Perret, J. L. (1963). Contribution à l'étude des batraciens de l'Ouest Africain XV. Le développement direct de l'espèce *Arthroleptis poecilonotus* Peters. *Bulletin de l'Institut fondamental d'Afrique noire A, 25*, 277–284.

Liedtke, H. C., Müller, H., Hafner, J., Penner, J., Gower, D. J., Mazuch, T., Rödel, M.-O., & Loader, S. P. (2017). Terrestrial reproduction as an adaptation to steep terrain in African toads. *Proceedings of the Royal Society, Series B, 284*, 20162598.

Loveridge, A. (1953). Zoological results of a fifth expedition to East Africa. IV. Amphibians from Nyassaland and Tete. *Bulletin of the Museum of Comparative Zoology, 110*, 323–406.

Lutz, B. (1948). Ontogenetic evolution in frogs. *Evolution, 2*, 29–39.

Lynn, W. G. (1942). The embryology of *Eleutherodactylus nubicola*, an anuran which has no tadpole stage. *Contributions to Embryology, 541*, 27–62.

Lynn, W. G., & Lutz, B. (1946). The development of *Eleutherodactylus guentheri* Stdnr. 1864. *Boletim do Museu Nacional Zoologia, 71*, 1–46.

Lynn, W. G., & Lutz, B. (1947). The development of *Eleutherodactylus nasutus* Lutz. *Boletim do Museu Nacional Zoologia, 79*, 1–30.

Moury, J. D., & Hanken, J. (1995). Early cranial neural crest migration in the direct-developing frog, *Eleutherodactylus coqui*. *Acta Anatomica, 153*, 243–253.

Müller, H., Loader, S. P., Ngalason, W., Howell, K. M., & Gower, D. J. (2007). Reproduction in brevicipitid frogs (Amphibia: Anura: Brevicipitidae)—evidence from *Probreviceps m. macrodactylus*. *Copeia, 2007*, 72–733.

Müller, H., Liedtke, H. C., Menegon, M., Beck, J., Balesteros, L., Nagel, P., & Loader, S. P. (2013). Forests as promoters of terrestrial life-history strategies in East African amphibians. *Biology Letters, 9*, 20121146.

Narayan, E. J., Hero, M. J., Christi, K. S., & Morley, C. G. (2011). Early developmental biology of *Platymantis vitiana* including supportive evidence of structural specialization unique to the Ceratobatrachidae. *Journal of Zoology, 284*, 68–75.

Nieuwkoop, P. D., & Faber, J. (1967). *Normal table of Xenopus laevis (Daudin)*. Amsterdam: North-Holland Publishing Company.

Noble, G. K. (1931). *The biology of the Amphibia*. New York: McGraw-Hill.

Nokhbatolfoghahai, M., Mitchell, N. J., & Downie, J. R. (2010). Surface ciliation and tail structure in direct-developing frog embryos: a comparison between *Myobatrachus gouldii* and *Pristimantis (= Eleutherodactylus) urichi*. *The Herpetological Journal, 20*, 59–68.

Patil, N. S., & Kanamadi, R. D. (1997). Direct development in the rhacophorid frog, *Philautus variabilis* (Gunther). *Current Science, 73*, 697–701.

Raff, R. A. (1987). Constraint, flexibility, and phylogenetic history in the evolution of direct development in sea urchins. *Developmental Biology, 119*, 6–19.

Raff, R. A. (1992). Direct-developing sea urchins and the evolutionary reorganization of early development. *BioEssays, 14*, 211–218.

San Mauro, D., Gower, D. J., Müller, H., Loader, S. P., Zardoya, R., Nussbaum, R. A., & Wilkinson, M. (2014). Life-history evolution and mitogenomic phylogeny of caecilian amphibians. *Molecular Phylogenetics and Evolution, 73*, 177–189.

Sandberger-Loua, L., Müller, H., & Rödel, M.-O. (2017). A review of the reproductive biology of the only known matrotrophic viviparous anuran, the West African Nimba toad, *Nimbaphrynoides occidentalis*. *Zoosystematics and Evolution, 93*, 105–133.

Scholtz, G. (2000). Evolution of the nauplius stage in malacostracan crustaceans. *Journal of Zoological Systematics and Evolutionary Research, 38*, 175–187.

Smith, A. (1849). Illustrations of the zoology of South Africa; consisting chiefly of figures and descriptions of the objects of natural history collected during an expedition into the interior of South Africa, in the years 1834, 1835, and 1836; fitted out by "The Cape Of Good Hope association for exploring Central Africa": together with a summary of African zoology, and an inquiry into the geographical ranges of species in that quarter of the globe. Vol. III. Reptilia. Appendix. London: Smith, Elder, & Co..

Tapley, B. (2009). Notes on the captive husbandry and breeding of the shovel-footed squeaker, *Arthroleptis stenodactylus* (Pfeffer 1893). *Herpetological Bulletin, 110*, 38–41.

Thibaudeau, G., & Altig, R. (1999). Endotrophic anurans, development and evolution. In R. W. McDiarmid & R. Altig (Eds.), *Tadpoles. The biology of anuran larvae* (pp. 170–188). Chicago: University of Chicago Press.

Townsend, D. S., & Stewart, M. M. (1985). Direct development in *Eleutherodactylus coqui* (Anura: Leptodactylidae): a staging table. *Copeia, 1985*, 423–436.

Trudeau, V. L., Somoza, G. M., Natale, G. S., Pauli, B., Wignall, J., Jackman, P., Doe, K., & Schueler, F. W. (2010). Hormonal induction of spawning in 4 species of frogs by coinjection with a gonadotropin-releasing hormone agonist and a dopamine antagonist. *Reproductive Biology and Endocrinology, 8*, 1–36.

Wager, V. A. (1965). *The frogs of South Africa*. Cape Town: Purnell and Sons.

Wake, M. H. (1978). The reproductive biology of *Eleutherodacytlus jasperi* (Amphibia, Anura; Leptodactylidae), with comments on the evolution of live-bearing systems. *Journal of Herpetology, 12*, 121–133.

Wake, M. H. (1980). The reproductive biology of *Nectophrynoides malcolmi* (Amphibia: Bufonidae), with comments on the evolution of reproductive modes in the genus *Nectophrynoides*. *Copeia, 1980*, 193–209.

Wake, M. H. (1989). Phylogenesis of direct development and viviparity. In D. B. Wake & G. Roth (Eds.), *Complex organismal functions: integration and evolution in vertebrates* (pp. 235–250). Chichester: Wiley.

Wake, M. H. (2003). Reproductive modes, ontogenies and the evolution of body form. *Animal Biology, 53*, 209–223.

Wake, D. B., & Hanken, J. (1996). Direct development in the lungless salamanders: what are the consequences for developmental biology, evolution and phylogenesis? *International Journal of Developmental Biology, 40*, 859–869.

Warren, E. (1922). Observations on the development of the non-aquatic tadpole of *Anhydrophryne rattrayi* Hewitt. *South African Journal of Science, 19*, 254–262.

Wells, K. D. (2007). *The ecology and behavior of amphibians*. Chicago: University of Chicago Press.
Ziermann, J. M., & Diogo, R. (2014). Development of fore- and hindlimb muscles in frogs: morphogenesis, homeotic transformations, digit reduction and the forelimb-hindlimb enigma. *Journal of Experimental Zoology (Molecular Development and Evolution), 322 B*, 86–105.

CHAPTER 2

The ghost of the tadpole - Embryonic development of the cranial musculoskeletal system in African squeaker frogs (*Arthroleptis*) reveals heterochronic shifts and parallel evolution of differential metamorphosis in direct developing frogs

Authors: **Schweiger, S.,** Naumann, B., Hammel, J. U.; Müller, H.

Status: Drafted manuscript

FORMULAR 1

Manuskript Nr.: 2

Titel des Manuskriptes: **The ghost of the tadpole - Embryonic development of the cranial musculoskeletal system in African squeaker frogs (*Arthroleptis*) reveals heterochronic shifts and parallel evolution of differential metamorphosis in direct developing frogs**

Autoren: Schweiger, Susan; Naumann, Benjamin; Hammel, Jörg U., Müller, Hendrik

Der Kandidat / Die Kandidatin ist (bitte ankreuzen):

☒ Erstautor/-in, ☐ Ko-Erstautor/-in, ☐ Korresp. Autor/-in, ☐ Koautor/-in.

Status (falls nicht publiziert; „zur Publikation eingereicht", „in Vorbereitung"): in Vorbereitung (drafted manuscript)

Anteile (in %) der Autoren / der Autorinnen an der Publikation (anzugeben ab 20%):

Autor/-in	Konzeptionell	Datenanalyse	Experimentell	Verfassen des Manuskriptes	Bereitstellung von Material
Schweiger, S.	90%	70%	75%	90%	33%
Naumann, B.		20%	20%		33%
Hammel, J. U.					
Müller, H.					33%

The ghost of the tadpole - Embryonic development of the cranial musculoskeletal system in African squeaker frogs (*Arthroleptis*) reveals heterochronic shifts and parallel evolution of differential metamorphosis in direct developing frogs

Susan Schweiger[1], Benjamin Naumann[2], Jörg U. Hammel[3], Hendrik Müller[4]

[1]Institut für Zoologie und Evolutionsforschung, Friedrich-Schiller-Universität Jena, Germany
[2]Institut für Biowissenschaften, Abteilung Allgemeine und Spezielle Zoologie, Universität Rostock, Germany
[3]Helmholtz-Zentrum Geesthacht, Zentrum für Material- und Küstenforschung, Röntgenbildgebung mit Synchrotronstrahlung, Hereon-Außenstelle am DESY, Hamburg, Germany
[4]Zentralmagazin Naturwissenschaftlicher Sammlungen, Martin-Luther-Universität Halle-Wittenberg, Halle, Germany

Correspondence: Susan Schweiger, Institut für Zoologie und Evolutionsfoschung, Friedrich-Schiller-Universität Jena, Erbertstrasse 1, 07743 Jena, Germany
Email: susan.schweiger@uni-jena.de

Abstract

Despite the evolutionary success of the anuran tadpole, direct development has evolved several times independently in different frog lineages. We compare the embryonic development of two species of *Arthroleptis* (*A. xenodacytloides* HEWITT 1933 and *A. wahlbergii* SMITH 1849), the only direct developing genus within Afrobatrachia. We questioned to what extent the ancestral larval development is repatterned during the evolution of direct development and if the tadpole represents a distinct developmental and evolutionary module. Therefore we present detailed data on the cranial ontogeny of *Arthroleptis* and compare it with available information on the direct developing Puerto Rican coqui (*Eleutherodactylus coqui* THOMAS 1966) and the Sri Lankan shrub frog *Pseudophilautus silus* (MANAMENDRA-ARACHCHI & PETHIYAGODA 2005). We found that the development of the cranial skeleton and associated muscles reveals a transient presence of tadpole-typical elements. This gives independent evidence for the concept of 'differential metamorphosis', which states that the frog larva consists of several developmental modules that can change during evolution instead of a so-called 'tadpole-cassette' concept, in which the tadpole is seen as a more or less single module that can either appear or disappear during development and evolution.

Key words (3-6): direct development; Afrobatrachia; cranial ontogeny; metamorphosis; tadpole hypothesis

Introduction

Alterations in an ancestral ontogenetic program, resulting in derived developmental modes, are key processes underlying evolutionary change. Direct development, as such a derived developmental mode, has evolved in many animal lineages independently including crustaceans, molluscs, echinoderms, fishes and amphibians (Collin 2004; Scholtz 2000; Raff 1992; Evans & Fernald 1990; Duellman & Trueb 1986).

In Lissamphibia (caecilians, salamanders and frogs) the ancestral life history is biphasic with an aquatic, free-swimming larval stage (Wake 1989; Duellman & Trueb 1986). Alternative reproductive strategies, where the ancestral requirement for aquatic reproduction is removed, have evolved several times independently and include terrestrial larval development and direct development (Gomez-Mestre et al. 2012; Schlosser & Roth 1997; Lynn 1961; Lutz 1948). Direct development occurs in all three lissamphibian groups and may have evolved in response to environmental conditions that do not provide suitable aquatic larval habitats promoting a more terrestrial reproductive mode (Liedtke et al. 2017; Müller et al. 2013; Goin and Goin 1962). In biphasic frogs, the larval stage is called tadpole. In contrast to larvae of other Lissamphibia, anuran tadpoles exhibit an astonishing diversity regarding their morphology and feeding behaviour (Altig & McDiarmid 1999). Despite the evolutionary success of the anuran tadpole, direct development has evolved several times independently in different frog lineages (Fig. 1).

Direct development is characterized by a complete or near complete loss of tadpole-specific features such as the larval jaw skeleton and its associated musculature, the cement glands, the lateral line system and the coiled intestine (Hanken et al. 1997b). These observations led to the hypothesis that the evolution of direct development from a biphasic developmental mode is based on a large-scale repatterning of embryonic development ('repatterning hypothesis'; Hanken, Jennings, and Olsson 1997a). However, detailed morphological studies adding evidence to this hypothesis are scarce and mainly based on only one species from the Caribbean island of Puerto Rico, the Puerto Rican coqui (*Eleutherodactylus coqui*) (Ziermann & Diogo 2014; Schlosser & Roth 1997; Hanken et al. 1992; Lynn 1942). Detailed developmental data from distantly related frog species, where direct development evolved independently from *E. coqui*, are needed to test this hypothesis. Studies on other direct developing frogs are still limited to only a few species (and specimens per species) so far (Goldberg et al. 2015, 2012; Narayan et al. 2010; Anstis 2008; Anstis et al. 2007; Kerney et al. 2007). We therefore investigate the embryonic and post-hatching development of the cranial skeleton and the associated musculature in two species of the African genus *Arthroleptis*, *A. xenodactyloides* and *A. wahlbergi*, belonging to Afrobatrachia.

Afrobatrachia are a taxon of sub-Saharan frogs containing four families – Hyperoliidiae and the sister Arthroleptidae, and Brevicipitidae and the sister Hemisotidae

(Feng et al. 2017; Portik & Blackburn 2016; Pyron & Wiens 2011; Frost et al. 2006). Within this group, direct development occurs only in *Arthroleptis*, but most Afrobatrachians show some degree of developmental terrestrialization (e.g. eggs attached to vegetation outside of water or eggs buried in the soil near water) (Portik & Blackburn 2016). This high diversity of developmental modes in Afrobatrachia is ideal for investigating the developmental changes associated with the evolution of complete terrestrial direct development from the ancestral biphasic mode. The tadpole larva has been proposed to represent a distinct developmental and evolutionary module in anurans (Ziermann & Diogo 2014; Gould 1977); however, this idea is controversial and data of species that independently evolved apparently similar modes of reproduction are needed to further evaluate the aforementioned 'tadpole module hypothesis'.

Materials and Methods

Specimens

Embryos of *A. wahlbergii*, collected in South Africa, and *A. xenodactyloides*, collected in Tanzania, were euthanized using tricaine methanesulfonate (MS222; Fluka), fixed in 4% buffered formalin, and subsequently stored in 70% ethanol. Staging of embryos follows Townsend & Stewart (1985); TS stages hereafter. See Schweiger et al. (2017) for further details on specimen collection and staging. The usage of the examined species is described in the following (see Tab. 1 for listed usage of specimen).

Histological sectioning

Early embryos were dehydrated in ethanol series (70%, 90%, 2 x 96%; 5 min each) sectioned and subsequently rehydrated (2 x 96%, 90%, 70% ethanol, distilled water; 5 min each) prior to staining. Then embryos were embedded in Technovit 8100, sectioned at 3µm and stained with a mixture of basophilic Methylene blue and acidic Fuchsin red (Böck 1989). Late embryos were embedded in Histoplast, sectioned at 8 µm and stained with Heidenhain's Azan (Romeis 2010). Sections were made using a Zeiss Microm HM 360 and investigated and photographed using a Zeiss Axioplan microscope with an attached Zeiss camera.

Whole-Mounts

Clearing and Staining

Whole-mounts were prepared using standard methods for clearing and staining (Dingerkurs & Uhler 1977, modified by Taylor & van Dyke 1985). Before staining, the yolk was manually removed from specimens younger than TS 14 using Dumont watchmaker's forceps. Specimens were photographed with a Zeiss Axiocam ICc1-camera and images were processed using Adobe Photoshop CS6.

Fluorescent antibody staining

Specimens were fixed in Dent's fixative and bleached in Dent's bleach (10% hydrogen peroxide in Dent's fixative). Specimens were incubated at room temperature (21–25°C). Antibody staining was conducted on whole mounts according to standard protocols (Klymkowsky & Hanken 1991). After bleaching, specimens were washed three times in PBS 1 0,1% TritonX-100 for 20 min each and then blocked for 2 hours in DAKO antibody diluent. The 12/101 antibody (against newt skeletal muscle, 1:100, DSHB) was applied and incubated overnight. The day after, specimens were washed again three times in PBS 1 0,1 % TritonX-100 for 20 min each and blocked in DAKO antibody diluent for 2 hours. Afterwards, Alexa488-anti-mouse (Thermo Fisher Scientific, Product # R37120) and Alexa568-anti-rabbit (Thermo Fisher Scientific, Product # A-11011) were applied as secondary antibodies (1:500 in DAKO antibody diluent) and incubated overnight. Stained specimens were dehydrated two times in 100% methanol for 10 min each and cleared and stored in BABB (benzyl alcohol/benzyl benzoate, 1/2).

µ-CT Scanning and 3D reconstruction

Specimens were contrasted using a solution of 1% polymolybdenic acid in 70% Ethanol following Metscher (2009) and CT-scanned using a Phoenix Nanotom S µCT scanner (Phoenix X-Ray) at the Helmholtz-Zentrum Geesthacht (Deutsches Elektronen Synchrotron – DESY, Hamburg, Germany). Three-dimensional reconstructions of the cranial musculoskeletal system were prepared using Amira® 5.4.2 (FEI Visualization, Sciences Group,) and Maya®2015 (Autodesk).

Comparative analysis/regression models

Cranial ossification sequences of the two species of *Arthroleptis* were compared with biphasic and other direct developing species. Only regression lines of species staged according to a similar system (TS or Go) could be compared directly/absolutely. Ossification data of biphasic species originate from *Bombina orientalis* Boulenger 1890 (Maglia & Púgener 1998), *Spea bombifrons* Cope 1863 (Wiens 1989), *Xenopus laevis* (Trueb & Hanken 1992), *Ascaphus truei* Stejneger 1899 (Moore & Townsend Jr. 2003), *Bufo boreas* (Baird and Girard 1852) (Gaudin 1978) and *Hyla lancriformis* (Cope 1870) (De Sa 1988). Ossification data of other direct developing species examined so far include *Pseudophilautus silus* (Kerney et al. 2007), *Eleutherodacytlus coqui* (Hanken et al. 1992) and *Pipa pipa* Linnaeus 1758 (Trueb et al. 2000). Data were plotted and regression lines and the associated slopes were calculated.

Results

Cranial skeleton

The chondrocranium

In *A. wahlbergii* at TS 5/6, the space between the brain and the eye is filled with a loosely packed mesenchyme. This mesenchyme extends continuously from the dorsal aspect of the brain ventrally into the pharyngeal arches (Fig. 2A, black dotted line). We interpret this mesenchyme as the migrated neural crest cells and the head mesoderm that will give rise to the cartilaginous braincase and trabeculae in later developmental stages.

Ethmoidal region.— The nasal capsule forms the cartilaginous skeleton of the anterior head region. The trabeculae are first detectable at TS 8. In the laterodorsal region of the developing nasal capsule, the lamina orbitonasalis arises to separate the capsule from the orbit. Anteriorly, cranial trabeculae are separated, cornua trabeculae never form. Dorsally, each cranial trabecula bears a broad cartilaginous plate forming the lateral wall of the braincase (Fig. 3A). At TS 10/11 the septum nasi emerges to separate the nasal capsule anteromedially. The tectum nasi arises to form the roof of the nasal capsule. Ventrally, the solum nasi has formed. The lamina orbitonasalis has further developed into the planum antorbitale and is attached to the processus maxillaris on its anterolateral end. At TS 12, all nasal cartilages are distinct and resemble the adult shape (Fig. 3D-F). Mediolaterally, the cartilago obliquus runs across the dorsal and lateral part of the nasal capsule. The cartilago alaris, the crista subnasalis as well as the superior and inferior nasal cartilages are also formed at this stage of development.

Orbital region and the braincase.— Posterior to the trabeculae, the parachordal cartilage is formed and the parachordalia are fused to form the basal plate by TS 11. In the same stage, a thin cartilaginous wall above each trabecula forms the cartilago orbitalis. During TS 11 and 12, several cartilaginous elements of the braincase become visible (Fig. 3D-F). Anteriorly, the extensive preoptic root forms the anterior margin of the foramen opticum and is attached to the trabecula. At TS 12, the pila metoptica separates the much smaller foramen oculomotori from the foramen opticum (Fig. 3D). The pila antotica also arises and separates the small foramen oculomotori from the wide foramen prooticum. Both, in pre- and postembryonic stages, as well as in the adult, the braincase is open dorsally via the frontoparietal fenestra, bordered laterally by the taenia tecti marginalis. Posteriorly, the cartilago orbitalis is connected with the capsula auditiva. The taenia tecti transversalis forms a dorsal bridge over the braincase.

The capsula auditiva.— The capsula auditiva is first detectable at TS 5/6 as a large ovoid chondrification forming the posterior part of the early chondrocranium. At TS 10, the processus oticus of the palatoquadrate nearly reaches the anteroventral region of the capsula auditiva and is clearly attached to it at TS 11. In this stage, the

tectum synoticum connects each auditory capsule. At the beginning of TS 13, the prootic bone develops from several ossification centres within the capsula auditiva. At TS 15, the processus oticus is no longer visible.

The mandibular skeleton

Early organization of the mandibular arch.— In *A. wahlbergii* at TS 5/6, the mandibular arch (first pharyngeal arch) is located ventral to the eye (Fig. 2B). Five cell layers are recognizable in a proximal to distal orientation. The most-proximal cell layer is the pharyngeal endoderm, recognizable by a huge amount of intercellular yolk granules (Fig. 2B). The second layer is made up of cells with big somata, forming a loosely packed mesenchyme. The central layer is more densely packed, forming a slightly curved rod. After about three quarters of its length it shows a slight constriction (Fig. 2B, black arrow). The central cell mass is made up of small, basophilic, ovoid cells. These are typical characteristics for chondroblasts. We therefore interpret this central cell layer as the anlage of the palatoquadrate (dorsolateral part) and cartilago meckeli (ventromedian part) (Fig. 2B). The fourth layer is similar to the second in forming a more loosely packed mesenchyme. The fifth, most-proximal layer is the epidermis (Fig. 2B).

Palatoquadrate and suspensorium.— A commissura quadratocranialis, a typical feature of the cranium in anuran tadpoles, is not present in *Arthroleptis* embryos. At TS 8, a prominent -y-shaped, transversally orientated palatoquadrate is located medioventrally to the foramen opticum. The palatoquadrate bears somewhat of a processus muscularis (Fig. 3A). The processus oticus of the palatoquadrate approaches the anterior border of the capsula auditiva during TS 10, but still remains separated from it. At TS 11, the palatoquadrate reaches the capsula auditiva on its anteroventral side and articulates with it via the processus oticus. The palatoquadrate seems to be less horizontal and assumes a more upright position. At TS 12/13, the jaw articulation begins to assume the characteristic adult shape and position (Fig. 3D). The palatoquadrate is now formed as a nearly vertical cartilage, which is dorsally connected to the neurocranium and articulates with the lower jaw on its ventral side. Anteriorly, the processus pterygoideus of the palatoquadrate fuses with the processus maxillaris. At TS 14, the palatoquadrate assumes a vertical position and is largely covered laterally by the squamosal bone by TS 15 (Fig. 3G).

Lower jaw.— At TS 8, the cartilago meckeli is strongly curved medially, with the anterior third offset at an angle of about 60 degrees. Anteriorly, the cartilago labialis inferior articulate and is partly fused the cartilago meckeli at its posteriodorsal end (Fig. 3A-C). Dorsomedially and posteriorly, the cartilago meckeli articulates with the palatoquadrate. During TS 10 and 11, the anterior portion becomes proportionately shorter and the cartilago meckeli is increasingly less strongly curved in lateral view. At TS 11, the cartilago meckeli extends caudally to the level of the anterior part of the capsula auditiva. By TS 12, the cartilago labialis inferior starts to ossify as the

mentomeckelian but is otherwise no longer distinguishable as a separated part of the cartilago meckeli. During the following stages, the jaw articulation shifts below the level of the capsula auditiva (Fig. 3D, G).

The hyobranchial skeleton

Early organization of the hyoid arch and the posterior branchial arches.— In *A. wahlbergii* at TS 5/6, the hyoid arch (second pharyngeal arch) is located directly posterior to the eye (Fig. 2C). The hyoid arch appears slightly more differentiated compared to the mandibular arch. Similarly, five distinct cell layers are recognizable. The central layer of condensed chondroblasts is divided into two distinct cell masses by the hyoid arch mesenchyme (Fig. 2C). We interpret the dorsal cell mass as the anlage of the hyomandibular cartilage and the ventral cell mass as the anlage of the ceratohyal (Fig. 2C, both encircled in black dotted lines). The posterior branchial arches (pharyngeal arches three to six) are located ventral to the developing otic capsule (Fig. 2D). They appear more undifferentiated compared to the mandibular and hyoid arches. Only three distinct cell layers are recognizable in a proximal to distal orientation. The most proximal layer is a thick layer of pharyngeal endoderm (Fig. 2D). The central layer is made up by a homogenous, slightly condensed mesenchyme (Fig. 2D, red dotted line). No distinct, central population of chondroblasts is recognizable. The ectoderm represents the distal-most third layer (Fig. 2D).

At TS 8, the hyobranchial skeleton consists of a central cartilaginous mass, the planum hyobranchiale. To each side, five processes are present. The anterior process represents the ceratohyale, the following four the ceratobranchialia I-IV (Fig. 4A). At TS 12, the hyobranchial skeleton has profoundly changed and begins to resemble the adult form (Fig. 4B). The ceratohyale has changed into the hyale. It is more elongated and articulates with the palatoquadrate and the ventral part of the capsula auditiva (Fig. 3F). The ceratobranchial IV has changed into the processus posteromedialis, the ceratobranchialia I-III are no longer visible. In the hatchling, the planum hyobranchiale is wider and the processus posteromedialis is replaced by bone (Fig. 4C).

Cranial bones

Premaxilla.— The pars dentalis, one of the three rami of the paired premaxilla appears as a thin sheet of bone investing the anteromedial part of the snout at TS 12/13 (Figs. 5D, 6B) In *A. xenodactyloides*, the lateral extension of the premaxilla is first seen at TS 14, while it is first visible in TS 15 of *A. wahlbergii* embryos. At the same stage, the pars palatina of the premaxilla begins to form and a small dorsal, laterally curved processus alaris is visible. At TS 15, the premaxilla is laterally, dorsally and caudally extended and has nearly assumed its adult shape in both species (Figs. 5J-L, 6E, F).

Maxilla.— The maxilla is initially seen at TS 12/13 (Fig. 5D-F). In whole-mounts, the long pars dentalis of the maxilla emerges as an extremely thin bone beneath the foramen opticum. At TS 14, the pars dentalis of the maxilla is broader and the pars facialis appears to form the dorsolateral part of the maxilla. At TS 15, the pars facialis articulates with the processus maxillaris of the nasal capsule (Fig. 5K). The pars palatina is present at TS 15. In the adult, each maxilla bears distinct teeth on the pars dentalis, which are not present during embryonic development (Fig. 6J).

Quadratojugal.— The quadratojugal arises as a small v-shaped bone ventral to the posterior end of the processus pterygoideus of the palatoquadrate (Fig. 5H, I). At TS 15, the quadratojugal exhibits three extensions and nearly approaches the maxilla anteriorly (Figs. 5E, F, 6F). Posterodorsally, it articulates with the palatoquadrate and is connected to cartilago meckeli posteroventrally. After hatching, the quadratojugal is connected to the ventral ramus of the squamosal and is extended anteriorly to articulate with the maxilla (Figs. 5K, 6H).

Septomaxilla.— In whole-mounts, this tiny u-shaped bone is seen at TS 15 and is situated next to the ventral end of the cartilago obliquus (Figs. 5K, 6E, F).

Frontoparietal.— The frontoparietal is first visible at TS 13/14 as a thin sheet of bone investing the dorsolateral side of the braincase (Fig. 5G, H). At TS 14, the frontoparietal has markedly increased in size. It posterodorsally adjoins the capsula auditiva. Anterolaterally, it extends to the level of the foramen opticum. In whole mounts of *A. wahlbergii*, the frontoparietal bone is only faintly seen. At TS 15, the frontoparietal of *A. xenodactyloides* already reaches the planum antorbitale anterolaterally and is in close proximity to the septum nasi of the nasal capsule medially (Fig. 6F). In *A. xenodactyloides*, the frontoparietal of a hatchling forms a robust, homogeneous element, while it is formed as a porous, tessellated structure in a hatchling of *A. wahlbergii*.

Squamosal.— The squamosal is first present at TS 12 (Fig. 5E). At this stage, it is slightly curved and consists of a ramus ventralis and a ramus oticus. At TS 13/14, the squamosal is strongly curved and a short, anteriorly directed ramus zygomaticus is present (Figs. 5H, 6C, D).

Pterygoid.— The pterygoid forms alongside the cartilaginous processus pterygoideus of the palatoquadrate. In whole-mounts, it initially appears at TS 13 as a thin bone along the posterodorsal side of the processus pterygoideus. In hatchlings, the pterygoid is triangular with a long anterior ramus and two short posterior rami (Figs. 5N, 6H). The ramus anterior of the pterygoid articulates with the maxilla. Posteriorly, it is connected with the palatoquadrate and the ramus ventralis of the squamosal.

Parasphenoid.— In whole-mounts of *A. xenodactyloides*, this thin bone is not detectable until TS 13/14 (Fig. 5I). In ventral view, the parasphenoid consists of a single,

rectangular-shaped processus cultriformis. By TS 15, the parasphenoid is distinctly broader on its posterior end and forms short posterolateral alae, which nearly approach the anterior margin of each capsula auditiva in ventral view. At this stage, the processus cultriformis extends anteriorly to the level of the planum antorbitale and the parasphenoid alae extend laterally.

Dentary.— The dentary is initially seen in whole-mounts at TS 12/13 where it appears as a slender bone at the anterolateral margin of the cartilago meckeli (Figs. 5D, 6B). At TS 14, the dentary is broader anteriorly and closely approaches the mentomeckelian bone. At the time of hatching, the dentary overlaps the angulosplenial in lateral view (Fig. 5N).

Angulosplenial.— The angulosplenial is first visible at TS 12 (Fig. 5D, E). At TS 13, the angulosplenial has elongated anteriorly to the level of the processus maxillaris. During subsequent stages, the angulosplenial elongates rostrally, where it reaches the level of the cartilago obliquus by TS 15 (Figs. 5J-L, 6F). In the adult, the angulosplenial comprises the longest bone of the lower jaw and possesses a concave surface, where it articulates with the palatoquadrate (Fig. 6J).

Prootic.—The prootic is initially seen at TS 11 as an ossification center anteroventrally within the capsula auditiva (Figs. 5 A, B, 6A). Additional ossification centers belonging to the prootic are not visible before TS 14 (Fig. 6C). The development of the prootic bone is not completed during the embryonic stages but continues during postembryonic development.

Exoccipital.— The paired exoccipital is first present at TS 13, where it covers the dorsal part of the occipital arch as a thin sliver of perichondral bone. The occipital arch is completely ossified by TS 15 (Fig. 6F). At the time of hatching, the exoccipitals form the occipital condyles, the margin of the foramen magnum and the posteromedial part of the capsula auditiva, but remain separated medially. In the adult, the exoccipital fuses with the prootic posterolaterally.

Mentomeckelian.— The mentomeckelian bone replaces the anterior part of the cartilago meckeli resembling the larval cartilago labialis inferior by perichondral ossification. At TS 12, the mandibular symphysis is distinctly formed as a round-ovoid structure between the mentomeckelians. At TS 13, the mentomeckelian forms a tubular bone that completely encloses its cartilaginous precursor. At TS 15, the mentomeckelian is fully ossified and fused with the dentary (Figs. 5N, 6F).

Endolymphatic calcium deposits.— Calcium deposits appear very early in embryonic development. At TS 6, they are first visible as symmetric points and expand cranially during TS 7 to the level of the foramen opticum and enlarge into quadrangular patches by TS 10. At TS 12/13, the endolymphatic calcium deposits join at the mid-

line (Fig. 5D, F). During subsequent stages, the deposits extend caudally into the neural canal of the vertebral column.

Cranial muscles

Early embryonic development till TS 10
Early embryonic development is characterized by the presence of some larval muscles. Name, origin and insertion point of the muscles present up to TS 10 are listed in Tab. 2. The muscles were grouped into mandibular muscles, hyoid muscles, branchial muscles and hyobranchial muscles. Differences between *A. wahlbergii* and *A. xenodacytloides* are mentioned, where present. For illustration see Figures. 7-9.

During TS 7 – 9 two distinct, relatively strong levator muscles are visible (Figs. 7A, 8A, B). Based on its position, we interpret the dorsalmost as the musculus (m.) levator (l.) mandibulae longus. The second l. is interpreted as the m. l. mandibulae lateralis. In TS 7, all four l. arcus branchialis muscles are visible, but only three constrictor branchialis muscles are present. From TS 8, the l. constrictor branchialis muscles are no longer seen in their larval appearance. At TS 7/8, the m. hyoangluaris, the m. orbitohyoideus and the m. interhyoideus as well as the m. geniohyoideus have formed Fig. 7A, B). The m. suspensorioangularis et quadratoangularis are present as a coalesced angularis-complex (Fig. 8B). At TS 8, the m. mandibulolabialis (Fig. 7A) and the m. intermandibularis anterior et posterior are distinct (Fig. 7A, B).

Ontogenetic changes during TS 10 – TS 12 („differential metamorphosis")
During TS 10 and 11, the m. l. mandibulae longus and the m. l. mandibulae lateralis are in a more upright position caused by the elogation of the cartilago meckeli and the rotation of the palatoquadrate (Fig. 8C). In TS 11, the m. suspensorioangularis and the m. quadratoangularis are beginning to fuse with each other and with the m. hyoangularis (Fig. 8C, D).

Late embryonic development TS 12 – TS 15
From TS 12 on, nearly all cranial muscles resemble their adult form / are present in their adult configuration (Fig. 7 C, D). In TS 15 embryos, the last stage before hatching occurs, all cranial muscles are in their adult configuration (Figs. 7E, F, 8F). All of these muscles are listed and described in Tab. 3. From TS 12 on, the m. l. mandibulae longus originates on the anterolateral part of the capsula auditiva and inserts medio- to posterolaterally on the cartilago meckeli (Fig. 7C). In TS 12, the m. l. mandibulae externus originates posteriorly on the processus pterygoideus and broadly inserts medio- to posterolaterally on the cartilago meckeli, where it covers the insertion side of the m. l. mandibulae lateralis. In TS 15, the m. l. mandibulae externus originates along the ramus ventralis of the squamosal and inserts posterolaterally on the cartilago meckeli and partly on the angulosplenial bone (Fig. 7E). The m. intermandibularis lateralis is only seen in specimens of *A. xenodactyloides,* but not in *A.*

wahlbergii and first appears at TS 12. In TS 12, the m. suspensorioangularis, the m. quadratoangularis and the m. suspensorioangularis have coalesced to form the m. depressor mandibulae anterior. The position of the muscle fibres is in a more upright position, as a result of the changing lower jaw and suspensorium. In TS 12, the m. orbitohyoideus has been remodelled into the m. depressor mandibulae posterior (Fig. 7C). It originates on the mediolateral part of the capsula auditiva and inserts on the posteriormost part of the cartilago meckeli. From TS 12 on, the m. petrohyoideus I-IV are formed in an adult condition. From TS 12 on, the m. geniohyoideus has assumed its adult configuration and consists of two portions, a medial and a lateral portion (m. geniohyoideus medialis and m. geniohyoideus lateralis).

Discussion

Many aspects of the development are similar in *A. xenodactyloides* and *A. wahlbergi,* and are discussed together. Aspects (differences or parallels) of larval and direct development are compared to other direct developing species.

The development of the cranial skeleton reveals the transient presence of tadpole-typical elements and a 'differential metamorphosis' in *Arthroleptis*

The ontogeny of the cartilaginous cranial skeleton of *Arthroleptis* is characterized by (1) the short and incomplete development of few larval elements during early stages (*sensu* Hanken et al. 1992), (2) the appearance of most cartilaginous skeletal elements in an already mid-metamorphic state (*sensu* Hanken et al. 1992) and (3) a 'differential metamorphosis'.

(1) Tadpole-typical cartilages are present for a short period, until TS 10. These are the cartilago labialis inferior, the processus muscularis of the palatoquadrate, the processus oticus and the ceratobranchialia of the hyobranchial skeleton. These elements do not function as it is seen in a typical tadpole of biphasic anurans. However, larval elements that never develop comprise the commisura quadratocranialis and the processus ascendens of the palatoquadrate. A processus ascendens is also not present in the closest relatives of *Arthroleptis* showing a biphasic lifecycle (Schweiger et al., unpublished manuscript). This indicates that the loss of this structure is not necessarily connected to the evolution of direct development in *Arthroleptis*.

(2) The transiently present larval elements appear in a mid-metamorphic form before they disappear or undergo metamorphic reconstruction. The processus muscularis of the palatoquadrate is seen in embryos of TS 8, but is no longer present from TS 10 on. The cartilago labialis inferior is recognizable until TS 9/10. The palatoquadrate shortens and reorients, while the cartilago meckeli elongates and fuses with the cartilago labialis inferior. This is similar to metamorphosing tadpoles in which the palatoquadrate transforms and reorients, while the cartilago meckeli and the cartilago labialis inferior fuse together and form the elongated mandibulare. Changes are also occurring dur-

ing the development of the hyobranchial skeleton. As in anuran tadpoles, four ceratobranchialia are present during early development in *Arthroleptis.* At TS 12, the ceratohyale has changed into the hyale, the ceratobranchialia I-IV are no longer visible and the overall appearance of the hyobranchial skeleton resembles the adult condition. In TS 12, none of the larval elements are visible. The chondrocranium has reached its adult form.

(3) The early developmental period, just before the onset of 'metamorphosis', can be characterized as the 'larval period'. During TS 10 – 12, a short 'differential metamorphosis' takes place in embryonic development. Larval cartilages show only minor rearrangements to reach the adult condition during 'metamorphosis'. From TS 12 on, the chondrocranium is formed in its adult configuration.

The development of the cartilaginous cranial skeleton is strikingly similar in *Eleutherodactlyus coqui* (Hanken et al. 1992) and *Arthroleptis*. Both exhibit the so called mid-metamorphic shape of the palatoquadrate, the unjoined four ceratobranchialia of the hyobranchial skeleton and an anterior structure of the lower jaw corresponding to the larval cartilago labialis inferior (Hanken at al. 1992). However, both species show differences with regard to the derivation from the ancestral larval pattern. E.g. in *Arthroleptis,* a tadpole-typical processus muscularis appears transiently while it is totally absent in *E. coqui*.

By comparison, the Sri Lankan shrub frog *Pseudophilautus silus* retains far more larval characteristics than *E. coqui. Pseudophilautus silus* shows a processus muscularis of the palatoquadrate (also present in *Arthroleptis*) and the tadpole specific cartilago labialis superior of the upper jaw, which is not present during development of *E. coqui* and *Arthroleptis.* Kerney et al. (2010) however showed that the anlagen of the cartilago labialis superior are transiently detectable in *E. coqui* using gene expression techniques. This shows that this structure, respectively, is not completely reduced in *E. coqui* and may play a more conservative role during anuran development (Kerney et al. 2010).

Strikingly, *Arthroleptis, E. coqui* and *P. silus* are all developing a 'larval' hyobranchial skeleton during early embryonic development. As in biphasic anurans, the hyobranchial skeleton consists of a large ceratohyale and four ceratobranchialia. The ceratobranchiale IV rapidly elongates to form the processus posteromedialis during development. The presence of a 'larval' hyobranchial skeleton in all four direct developing species discussed here leads us to conclude that some larval traits are highly conserved whereas others, e.g. the presence or absence of a cartilago labialis superior or a processus muscularis, are variable during direct development.

However, the tadpole-specific processus oticus (present in *Arthroleptis*) and processus ascendens do not develop in *P. silus*. Kerney et al. (2007) suggest that the lack of these processes is not invariably linked to the evolution of direct development and

that they have been lost in some biphasic species, possessing an endotrophic tadpole.

The comparison of the development of the cartilaginous cranial skeleton between *Arthroleptis, E. coqui* and *P. silus* reveals different degrees of the loss of tadpole-features during the evolution of direct development. Many elements appear already at a mid-metamophic stage in embryos of *Arthroleptis* and *E. coqui* (Fig. 9B). In *P. silus*, the rearrangement of skeletal structures is more similar to the metamorphosis of tadpoles of biphasic frogs (compare Fig. 9A, B). Thus, all direct developing species reviewed in this study exhibit different degrees of derivation of the plesiomorphic condition.

The presence of tadpole-like structures during ontogeny confirms that the tadpole has not been eliminated during the evolution of direct development. This is in opposition to the hypothesis of Elinson (2001), in which direct development is linked to the removal of the tadpole in life-history. This also means that the reduction or the absence of larval features is not necessarily a requisite of a complete terrestrial development. In the evolution of direct development, the developmental differences of tadpole skeletal elements has been modified independently to different degrees ('differential metamorphosis') leading to similar results in different direct developing frogs.

The development of the cranial muscles follows the skeletal development in *Arthroleptis*

The development of the cranial muscles in *Arthroleptis* follows the mosaic pattern of the cartilaginous cranial skeleton: (1) A few larval-typical muscles appear during early development in a plesiomorphic condition in *Arthroleptis*, (2) most of the muscles already appear in a mid-metamorphic state, when first detectable, and (3) larval muscles change during a short and 'differential metamorphosis'.

(1) Three of the five larval hyoid muscles are developed in the tadpole-typical state (m. hyoangularis, m. orbitohyoideus and m. interhyoideus). The tadpole-typical m. l. arcus branchialis and m. l. constrictor branchialia are also detectable during early stages of development. The presence of these muscles is consistent with the existence of the ceratobranchialia I-IV of the hyobranchial skeleton. By contrast, none of the five larval-typical mandibular muscles are developed as a distinct muscle (m. l. mandibulae longus superficialis, m. l. mandibulae longus profundus, m. l. mandibulae anterior, m. l. mandibulae internus and m. l. mandibulae anterior articularis (Edgeworth 1935). Additionally, one of the five larval-typical hyoid muscles, the m. supensoriohyoideus, also never forms.

(2) The tadpole-typical five mandibular muscles appear as a complex of coalesced l. muscles with no distinct portions, typical for mid-metamorphosis. However, there is considerable variation in the mandibular muscles of tad-

poles of biphasic members within the afrobatrachid family Arthroleptidae. A larval m. l. mandibulae internus is not present in tadpoles of this family and a m. l. mandibulae internus and m. l. mandibulae anterior articularis is only present in tadpoles of *Nyctibates* (Schweiger et al., unpublished manuscript). The absence of these tadpole-typical mandibular muscles in con-familial species suggests that this loss is not directly linked to the evolution of direct development.

(3) During stages TS 10 – 12, larval muscles begin to change and shifting in dependence and relative to the posterior migration of the palatoquadrate and simultaneous elongation of the jaw. The m. hyoangularis and the m. orbitohyoideus start to form the m. depressor mandibuale anterior et posterior during 'metamorphosis'. At the end of TS 12, all cranial muscles begin to assume their adult configuration.

Only a small number of studies have investigated the ontogeny of the cranial muscles in direct developing anurans (Ziermann & Diogo 2014; Hanken et al. 1997b; Schlosser & Roth 1997). In *E. coqui,* cranial muscle development is characterized by the lack of many larval features (Hanken et al. 1997b; Schlosser & Roth 1997). Four of the larva-typical hyoid muscles are present and are formed in a mid-metamorphic stage of development. They are subsequently remodelled to form the adult m. depressor mandibulae complex before the onset of hatching. The development of the branchial muscles in biphasic anurans is described by Edgeworth (1935), and indicates that the m. petrohyoideus I-IV are forming during the ontogenetic changes of the m. l. constrictor branchialis and the m. l. arcus branchialis. Ziermann & Diogo (2014) described the development of the m. petrohyoidei forming out only of the m. l. arcus branchialia in *E. coqui*. Hanken et al. (1992) described the development of the hyobranchial apparatus in *E. coqui* and indicated the presence of three ceratobranchialia during TS 8-12, but none of the four m. l. constrictor branchialia could be detected by Ziermann & Diogo (2014). Unfortunately, no data on the cranial muscles of *P. silus* are available (Kerney et al. 2007).

A comparison with non-feeding, endotrophic tadpoles is also of interest because, as the embryos of direct developing species, these are freed from the constraints of a functioning larval feeding apparatus. However, the only non-feeding, endotrophic tadpole, from which cranial muscles are described, is *Eupsophus calcaratus* GÜNTHER 1881 (Candioti et al. 2005). Despite the non-use of the jaw-apparatus, it develops similar to that of free-swimming, feeding tadpoles. The only absent tadpole-typical muscles are the m. l. mandibulus externus superficialis and the m. subarcualis obliquus (Candioti et al. 2005).

In general, the overall pattern of cranial muscle development in tadpoles is relatively similar. However, the presence, absence or coalescence of single muscles or muscle groups varies between different taxa and different studies have demonstrated that embryonic development in anurans is not as conserved as has often been assumed. There is also inconsistency regarding the description of these muscles

among the literature. Haas (1997) discussed the hyobranchial muscles of *Ascaphus, Bombina,* and *Discoglossus* and pointed out that the m. supsensoriohyoideus is present in *Ascaphus,* while Pusey (1943) reported it as absent. The complexity of the m. l. arcus branchialia makes it difficult to homologize each muscle of this group within Anura (Cannatella 1999). Cannatella (1999) summarizes, that in some taxa, all levators or only some of them are fused (*Xenopus laevis,* Ziermann & Diogo 2004; *Pipa carvalhoi* MIRANDA-RIBEIRO 1937, Sokol 1977), while in others some of the m. l. arcus branchialia are lacking (*Hymenochirus boettgeri* TORNIER 1896, Sokol 1977). This implies that the absence or coalescence of some muscles in *Arthroleptis* is not invariably linked to direct development.

The ossification sequence of the cranial bones reveals heterochronic shifts in direct developing compared to biphasic frogs

In *Arthroleptis* most of the cranial bones ossify during the embryonic period, before hatching occurs. By contrast, the cranium in biphasic anurans starts to ossify after hatching, when all yolk resources are consumed (Weisbecker & Mitgutsch 2010). The first bones ossifying in most biphasic anurans, e.g. *Bombina orientalis* (Maglia & Púgener 1998), *Spea bombifrons* (Wiens 1989), *Xenopus laevis* (Trueb & Hanken 1992), *Ascaphus truei* (Moore & Townsend Jr. 2003), *Bufo boreas* (Gaudin 1978) and *Hyla lancriformis* (De Sa 1988), are the frontoparietal, parasphenoid and exoccipital, supporting the dorsal and ventral cranium (Fig. 9A). The cranial ossification sequences in the direct developing *Arthroleptis* (present study) and *E. coqui* (Hanken et al. 1992) differ substantially from the ancestral mode. In direct developing anurans, bones of the lower jaw and the suspensorium (angulosplenial and squamosal) ossify first (presentstudy, Hanken et al. 1992). This heterochronic shift of jaw ossification may be due to the need for a functioning musculoskeletal system, enabling an adult-like feeding mode for hatchlings (Hanken et al. 1992). In the direct developing *P. silus* (Kerney et al. 2007), the situation is similar to the ancestral mode present in anuran tadpoles (Fig. 9B). It has been suggested that anatomical repatterning, in form of *de novo* formation, is an important pre-requisite for the evolution of direct development (Hanken et al. 1992). The examination of the cranial ontogeny of *P. silus* (Kerney et al. 2007) revealed that direct development is not necessarily linked to dramatic changes to heterochronic shifts in the ossification sequence. This becomes particularly clear by comparing the slope of the regression lines of ossification sequences seen in Figure 9C-M. The lower the slope of the linear regression in each of the diagrams, the earlier the onset of ossification of bones used for feeding or support of the adult brain. Direct developers tend to have lower slopes (approx. <0.22 in *Pipa*) than biphasic species (approx. >0.23). This assumption is indicated by the slope of the regression line in *P. silus,* which is similar to biphasic species and development can be interpreted as ancestral relative to *E. coqui* and *Arthroleptis*. Surprisingly, the slopes of the regression lines of ossification events in *Arthroleptis* are nearly horizontal, revealing that ossification events are more derived from the ancestral development than in *E. coqui.*

The timing and sequence of development of early embryonic structures is extremely variable in frogs (Chipman 2002). Rank variation analysis suggests that the species-specific ossification sequences of anuran cranial bones are highly variable, possibly because tadpole and adult cranial morphology do not co-evolve, but are decoupled from each other (Weisbecker & Mitgutsch 2010). What is the reason for this decoupling, resulting in highly variable ossification sequences? One possible explanation focuses on the feeding biology and functional morphology of the tadpole.
In contrast to almost all other tetrapods, lissamphibian larvae exhibit a cartilaginous feeding apparatus that is completely functional. This feature might release lissamphibian larvae from the constraints opposed by dependence on bony elements in the feeding apparatus, opening up the opportunity for diverse heterochronic shifts in the cranial ossification sequence in frogs. In other tetrapods, gross ossification sequences are more invariable. For instance, ossification sequences in marsupial and placental mammals are relatively conserved and are mostly due to an overall delay of cranial ossification that is coupled to a delay of brain development (Sánchez-Villagra et al. 2008; Nunn & Smith 1998). In birds, cranial ossification sequences show some small differences, e.g. the timing of skull roof closure in precocical and altrical birds, but is thought to be relatively conserved in general (Mitgutsch et al. 2011; Maxwell 2008). In non-avian sauropsids, ossification sequences are more variable between higher taxonomic groups (e.g. between snakes and other squamates) while it is relatively conserved within these groups (Werneburg & Sánchez-Villagra 2015).

Differential metamorphosis and the role of developmental constraints in the evolution of direct development

The near complete loss of larval characters in the direct developing *E. coqui* has led to the suggestion that the tadpole larva of the ancestral biphasic life-history involves the deletion of a 'larval cassette' during ontogeny of direct development ('tadpole module hypothesis', Elinson & Del Pino 2012; Elinson 2001; Callery & Elinson 2000; Elinson 1990).

Several investigations suggest that *E. coqui*, whose development is similar to that of *Arthroleptis,* undergoes a 'cryptic' metamorphosis and show that neuroendocrine signalling is conserved between biphasic and direct developing frogs (Kulkarni et a. 2010; Callery et al. 2001; Callery & Elinson 2000). Here, we conclude that metamorphosis in *Arthroleptis* is shorter than and not as climactic as that of biphasic anurans. Based on metamorphic characters present during embryonic development in *Arthroleptis* and other direct developing species, we follow the more suitable term 'differential metamorphosis' (Wake & Hanken 1996) to characterize metamorphosis in direct development. Hanken et al. (1992) discussed the embryonic recapitulation and whether metamorphosis occurs during direct development or if there has been a repatterning of early ontogeny involving the loss of larval structures, heterochrony, and the presence of novelties in embryonic morphology. In *E. coqui*, the absence of some typical larval cartilages found in biphasic anurans is discussed as

evidence for repatterning and simultaneously implies the development of mid-metamorphic structures during early stages of development (Hanken et al. 1992). The development of the jaw, the jaw suspensorium, and the hyobranchial skeleton suggests that there is also partial recapitulation of few larval characteristics (Kerney et al. 2010; Hanken et al. 1992). Our data indicate that some tadpole specific structures differentiate during a short metamorphic phase. This phase appears between TS 9/10 and TS 12. During these stages, the opercular fold overgrows and breaks through the developing forelimbs (Schweiger et al.2017). Additionally, changes of larval cartilages (reorientation of the palatoquadrate, development of the hyobranchial skeleton) and cranial muscles are detectable and indicate that the embryo of *Arthroleptis* undergoes, at least in some aspects, a metamorphosis.

All direct developing species compared in this study share striking similarities in external morphology. Investigations of internal morphology, however, show that all four species develop a transient larval-like hyobranchial skeleton. Beside these similarities, the presence or absence of typical larval features of the jaw (e.g. cartilago labialis inferior, cartilago labialis superior, processus muscularis of the palatoquadrate) is more variable. Some of the direct developing species show more plesiomorphic features than others and the (transient) presence of larval characters reveals that direct development is not necessarily linked to a complete loss of the 'tadpole module'. Thus, the idea of a single 'tadpole module', that can either appear or disappear during development and evolution, is not supported. In addition, it seems that some larval traits are more conserved than others. The hyobranchial skeleton can be interpreted as a highly conserved module which is remarkably similar in direct developing species. Other larval modules have higher variation and are less conserved during evolution. The comparison of the presence of larval, 'tadpole', elements in different direct developing anurans is in accordance with the 'modular tadpole hypothesis' (Schlosser 2005) in which the tadpole stage represents a 'meta-module' composed of several morphological modules. These modules can change during development and evolution resulting in a more terrestrial life-history mode.

Tadpoles exhibit a high degree of diversity due to the evolution of peculiar morphological adaptations to their different environments. This tadpole diversity is based on a high degree of developmental variability (Chipman 2002). This leads to the question of the evolutionary origin of a completely terrestrial developmental mode such as direct development. We showed that direct development in *Arthroleptis* is built upon a mosaic of the presence, reduction and complete absence of tadpole-specific characters. Schlosser (2005) argued, that 'mosaic evolution' is directly linked to various changes or 'patterns of dissociation' affecting all phases in development, e.g. loss of one character but not the other, heterochrony, heterotopy and changes in size and shape. Developmental modularity might have been a pre-requisite for the evolution of derived developmental modes such as direct development. Possibly, environmental conditions have changed and effected specialization involving changes in a developmental mode. Direct developing anurans have multiple evolutionary origins but their embryos externally look relatively similar (Elinson & Del

Pino 2012) – a result of a more or less water independent life-history. In comparison to direct development, ontogeny of free-living anuran larvae is constrained to larval morphology throughout the larval period (Roelants et al. 2012). Developmental constraints occur when developmental characters are coupled to perform a function and often prevent characters from varying independently (Schlosser 2005). The developmental constraint in biphasic anurans is relaxed in direct developing species in that way that some characters can be less functional or change in function (e.g. development of an operculum, gill buds, a vascularized tail and the presence of some larval structure of the cranial musculoskeletal system).

Acknowledgements

Permits to collect and export *A. xenodactyloides* were issued by the Tanzania Wildlife Research Institute (TAWIRI), the Tanzanian Commission of Science and Technology (COSTECH Permit No. 2009-306-NA-2009-201) and the Wildlife Division of the Tanzanian Ministry of Tourism and Natural Resources. Permits to collect and export *A. wahlbergii* were issued by Ezemvelo KZN Wildlife (OP4507/2015). We especially thank Adrian Armstrong, Sharon Louw and James Harvey for facilitating fieldwork in KZN and Jane Chennells for permission to work on her property. We also thank Lars Möckel for the help during the field trips. We particularly thank Katja Felbel for valuable help in the laboratory. Funding was provided through a Putnam Expedition Grant of the Museum of Comparative Zoology and a German Research Foundation grant (DFG MU2914/2-1).

References

Altig, R., McDiarmid, R.W. (1999). Diversity, familial and generic characterizations. In: Tadpoles – the biology of anuran larvae. Edited by R. W. Mc Diarmid and R. Altig. Chicago University Press, USA, pp. 24–51.

Anstis, M. (2008). Direct development in the Australian myobatrachid frog Metacrinia nichollsi from Western Australia. Records of the Western Australian Muse-um 24: 133-150.

Anstis, M., Roberts, J.D., Altig, R. (2007). Direct development in two Myobatrachid Frogs, *Arenophryne rotunda* Tyler and *Myobatrachus gouldii* Gray, from Western Australia. Records of the Western Australian Museum 23: 259–271.

Bahir, M.M., Meegaskumbura, M., Manamendra-Arachchi, K., Schneider, C. J., Pethiyagoda, R. (2005). Reproduction and terrestrial direct development in Sri Lankan shrub frogs (Ranidae: Rhacophorinae: *Philautus*). The Raffles Bulletin of Zoology, Supplement 12: 339-350.

Böck, P. (1989). Romeis Mikroskopische Technik. Urban & Schwarzenberg, München.

Callery, E.M., Elinson, R.P. (2000). Opercular development and ontogenetic reorganization in a direct-developing frog. Development, Genes and Evolution 210: 377–381.

Callery, E.M., Fang, H., Elinson, R.P. (2001). Frogs without polliwogs: Evolution of anuran direct development. BioEssays 23: 233–241.

Candioti, M.F.V., Úbeda, C., Lavilla, E. (2005). Morphology and metamorphosis of *Eupsophus calcaratus* tadpoles (Anura: Leptodactylidae). Journal of Morphology 264 (2): 161-177.

Chipman, A.D. (2002). Variation, plasticity and modularity in anuran development. Zoology 105 (2):97-104.

Collin, R. (2004). Phylogenetic effects, the loss of complex characters, and the evolution of development in calyptraeid gastropods. Evolution 58: 1488–1502.

De Sa, R.O. (1988). Chondrocranium and ossification sequence of *Hyla lanciformis*. Journal of Morphology 195(3): 345-355.

Duellman, W.E., Trueb, L. (1986). Biology of Amphibians. London: Johns Hopkins University Press.

Edgeworth, F.H. (1935). The cranial muscles of vertebrates. Cambridge [Eng.]. The University Press.

Elinson, R.P. (1990). Direct development in frogs: wiping the recapitulationist slate clean. Seminars in Cell and Developmental Biology 1: 263-270.

Elinson, R. P. (2001). Direct development: an alternative way to make a frog. Genesis, 29: 91–95.

Elinson, R.P., Del Pino, E.M. (2012). Developmental diversity of amphibians. WIREs Developmental Biology 1: 345-369.

Evans, B.I., Fernald, R.D. (1990). Metamorphosis and fish vision. Journal of Neurobiology 21 (7):1037-1052.

Feng, Y.J., Blackburn, D.C., Liang, D., Hillis, D.M., Wake, D.B., Cannatella, D.C., Zhang, P. (2017). Phylogenomics reveals rapid, simultaneous diversification of three major clades of Gondwanan frogs at the Cretaceous–Paleogene boundary. Proceedings of the National Academy of Sciences 114: E5864–E5870.

Frost, D.R., Grant, T., Faivovich, Bain, R.H., Haas A., Haddad, C.F.B., De Sá, R.O., Channing, A. Wilkinson, M., Donnellan, S.C., Raxworthy, C.J., Campbell, J.A., Blotto, Moler, B.L. P., Drewes, R.C., Nussbaum, R.A., Lynch, J.D., Green D.M., Wheeler, W.C. (2006). The amphibian tree of life. Bulletin of the American Muse-um of National History 297:1–370.

Gaudin, A.J. (1978). The sequence of cranial ossification in the California toad, *Bufo boreas* (Amphibia, Anura, Bufonidae). Journal of Herpetology 12 (3): 309-318.

Gould, S.J. (1977). Ontogeny and phylogeny: Harvard University Press.

Goldberg, J., Candioti, M. F.V., Akmentins, M.S. (2012). Direct-developing frogs: ontogeny of *Oreobates barituensis* (Anura: Terrarana) and the development of a novel trait. Amphibia-Reptilia 33: 239–250.

Goldberg, J., Candioti, M. F. V. (2015). A tale of a tail: variation during the early ontogeny of *Haddadus binotatus* (Brachycephaloidea: Craugastoridae) as compared with other direct developers. *Journal of Herpetology* 49: 479–484.

Goin, O.B., Goin, C. J. (1962). Amphibian eggs and montane environment.

Evolution 16: 364–371.

Gomez-Mestre I, Pyron RA, Wiens JJ. (2012). Phylogenetic analyses reveal unexpected patterns in the evolution of reproductive modes in frogs. Evolution 66: 3687–3700.

Hanken, J., Klymkowsky, M.W., Summers, C.H., Seufert, D.W., Ingebrigsten, N. (1992). Cranial ontogeny in the direct-developing frog, *Eleutherodactylus coqui* (Anura: Leptodactylidae), analyzed using whole-mount immunohistochemistry. Journal of Morphology 211: 95–118.

Hanken, J., Carl, T.F., Richardson, M.K., Olsson, L., Schlosser, G., Osabutey, C.K., Klymkowsky, M. (2001). Limb development in a 'nonmodel' vertebrate, the direct-developing frog *Eleutherodactylus coqui*. Journal of Experimental Zoology (Molecular Development and Evolution) 291: 375–388.

Hanken, J., Jennings, D.H., Olsson, L. (1997a). Mechanistic basis of life-history evolution in anuran amphibians: Direct Development. American Zoologist 37: 160–171.

Hanken, J., Klymkowsky, M.W., Alley, K.E., Jennings, D.H. (1997b). Jaw muscle development as evidence for embryonic repatterning in direct-developing frogs. Proceedings of the Royal Society, Series B, 264: 1349–1354.

Haas, A. (1997). The larval hyobranchial apparatus of discoglossoid frogs: its structure and bearing on the systematics of the Anura (Amphibia: Anura). Journal of Zoological Systematics and Evolutionary Research 35: 179-197.

Kerney, R., Gross, J.B., Hanken, J. (2010). Early cranial patterning in the direct Eleutherodactylus coqui revealed through gene expression. Evolution & Development 12 (4): 373-382.

Kerney, R., Meegaskumbura, M., Manamendra-Arachchi, K., Hanken, J. (2007). Cranial ontogeny in *Philautus silus* (Anura: Ranidae: Rhacophorinae) reveals few similarities with other direct-developing anurans. Journal of Morphology 268: 715–725.

Liedtke, H. C., Müller, H., Hafner, J., Penner, J., Gower, D. J., Mazuch, T., Rödel, M.-O., Loader, S.P. (2017). Terrestrial Reproduction as an Adaptation to Steep Terrain in African Toads. Proceedings of the Royal Society, Series B, 284: 20162598.

Lutz, B. (1948). Ontogenetic evolution in frogs. Evolution 2: 29–39.

Lynn, W.G. (1942). The embryology of *Eleutherodactylus nubicola*, an anuran which has no tadpole stage. Contributions to Embryology 541: 27–62.

Lynn, W.G. (1961). Types of amphibian metamorphosis. American Zoologist 1: 151–161.

Maglia, A.M., Púgener, L.A. (1998). Skeletal development and adult osteology of *Bombina orientalis* (Anura: Bombinatoridae). Herpetologica 344-363.

Maxwell, E.E. (2008). Ossification sequence of the avian order Anseriformes, with comparison to other precocial birds. Journal of Morphology 269 (9):1095-1113.

Mitgutsch, C., Wimmer, C., Sánchez-Villagra, M.R., Hahnloser, R., Schneider, R.A. (2011). Timing of ossification in duck, quail, and zebra finch: intraspecific variation, heterochronies, and life history evolution. Zoological science 28 (7):491-500.

Moore, M.K., & Townsend Jr, V.R. (2003). Intraspecific variation in cranial ossification in the tailed frog, *Ascaphus truei*. Journal of Herpetology 37(4): 714-717.

Müller, H., Liedtke, H.C., Menegon, M., Beck, J., Balesteros, L., Nagel, P., Loader, S.P. (2013). Forests as promoters of terrestrial life-history strategies in East African amphibians. Biology Letters 9: 20121146.

Narayan, E.J., Hero, J.-M., Christi, K.S., Morley, C.G. (2011). Early developmental biology of Platymantis vitiana including supportive evidence of structural specialization unique to the Ceratobatrachidae. Journal of Zoology 284: 68–75.

Nunn, C.L., Smith, K. K. (1998). Statistical analyses of developmental sequences: the craniofacial region in marsupial and placental mammals. The American Naturalist 152 (1):82-101.

Portik, D.M., Blackburn, D.C. (2016). The evolution of reproductive diversity in Afrobatrachia: A phylogenetic comparative analysis of an extensive radiation of African frogs. Evolution 70-9: 2017-2032.

Pusey, H.K. (1943). On the head of the liopelmid frog, *Ascaphus truei*. I. The chondrocranium, jaws, arches, and muscles of a partly-grown larva. The Quarterly journal of microscopical science, 84: 105-185.

Pyron, R.A., Wiens, J.J. (2011). A large-scale phylogeny of Amphibia including over 2,800 species, and a revised classification of extant frogs, salamanders, and caecilians. Molecular Phylogenetics and Evolution 61: 543–583.

Raff, R.A. (1992). Direct-developing sea urchins and the evolutionary reorganization of early development. BioEssays 14: 211–218.

Sánchez-Villagra, M.R., Goswami, A., Weisbecker, V., Mock, O., Kuratani, S. (2008). Conserved relative timing of cranial ossification patterns in early mammalian evolution. Evolution & Development 10 (5):519-530.

Schlosser, G. (2005). Amphibian Variations: The Role of Modules in Mosaic Evolution. In: Modularity: Understanding the Development and Evolution of Natural Complex Systems. Edited by W. Callebaut and D. Rasskin–Gutman. The Vienna Series in Theoretical Biology, pp. 143-179.

Schlosser, G., Roth, G. (1997). Evolution of nerve development in frogs. II. Modified development of the peripheral nervous system in the direct-developing frog *Eleutherodactylus coqui* (Leptodactylidae). Brain, Behavior and Evolution 50 (2): 94-128.

Scholtz, G. (2000). Evolution of the nauplius stage in malacostracan crustaceans. Journal of Zoological Systematics and Evolutionary Research 38: 175–187.

Schweiger, S. (2012). Entwicklung des Kopfskeletts und assoziierter Muskulatur beim direkt entwickelnden Frosch *Arthroleptis* cf. *xenodactyloides*. Unpublished diploma thesis.

Schweiger, S., Naumann, B., Larson, J. G., Möckel, L., Müller, H. (2017). Direct development in African squeaker frogs (Anura: Arthroleptidae: *Arthroleptis*) reveals a mosaic of derived and plesiomorphic characters. Organisms, Diversity and Evolution 17: 693–707.

Sokol, O.M. (1975). The phylogeny of anuran larvae: A new look. Copeia l-23.

Stephenson, E.M. (1955). The head of the frog, *Leiopelma hamiltoni* McCulloch. Proceedings of the Zoological Society of London 124: 797– 801.

Townsend, D.S., Stewart, M.M. (1985). Direct development in *Eleutherodactylus coqui* (Anura: Leptodactylidae): a staging table. Copeia 1985: 423–436.

Trueb, L., Hanken, J. (1992). Skeletal development in *Xenopus laevis* (Anura: Pipidae). Journal of Morphology 214(1): 1-41.

Trueb, L., Púgener, L.A., Maglia, A.M. (2000). Ontogeny of the bizarre: an osteological description of *Pipa pipa* (Anura: Pipidae), with an account of skeletal development in the species. Journal of Morphology 243(1): 75-104.

Wake,M.H.(1980).Thereproductivebiologyof *Nectophrynoidesmalcolmi* (Amphibia: Bufonidae), with comments on the evolution of reproductive modes in the genus *Nectophrynoides*. Copeia 1980: 193–209.

Wake, D.B., Hanken, J. (1996). Direct development in the lungless salamanders: what are the consequences for developmental biology, evolution and phylogenesis? International Journal of Developmental Biology 40: 859–869.

Wake, M.H. (1989). Phylogenesis of direct development and viviparity in vertebrates. Complex organismal functions: Integration and Evolution in Vertebrates: 235-250.

Weisbecker, V., Mitgutsch, C. (2010). A large-scale survey of heterochrony in anuran cranial ossification patterns. Journal of Zoological Systematics and Evolutionary Research 48 (4): 332-347.

Wiens, J.J. (1989). Ontogeny of the skeleton of *Spea bombifrons* (Anura: Pelobatidae). Journal of Morphology 202(1): 29-51.

Wiens, J.J., Kuczynski, C.A., Duellman, W.E., Reeder, T.W. (2007). Loss and re-evolution of complex life cycles in marsupial frogs: Does ancestral trait reconstrucion mislead? The Society for the Study of Evolution. Evolution 61-8: 1886-1899.

Ziermann, J.M., Diogo, R. (2014). Cranial muscle development in frogs with different developmental modes: direct development versus biphasic development. Journal of Morphology, 275: 398–413.

Tables

Table 1: Specimen list. ab, Antibody; PMA, polymolybdenic acid; µCT, micro-computed tomography.

Nr.	TS Stage	Species	Technique	Staining
1	5/6	*A. wahlbergii*	histology	Azan
2	6	*A. xenodactyloides*	histology	Azan
3	7/8	*A. wahlbergii*	fluorescent antibody staining	12/101 ab
4	8	*A. wahlbergii*	µCT	1% PMA
5	9	*A. xenodactyloides*	histology	Azan
6	10	*A. wahlbergii*	fluorescent antibody staining	12/101 ab
7	10/11	*A. wahlbergii*	fluorescent antibody staining	12/101 ab
8	11	*A. wahlbergii*	clearing & staining	Alcian/Alizarin
9	11	*A. wahlbergii*	fluorescent antibody staining	12/101 ab
10	11/12	*A. wahlbergii*	fluorescent antibody staining	12/101 ab
11	12	*A. wahlbergii*	fluorescent antibody staining	12/101 ab
12	12	*A. xenodactyloides*	µCT	1% PMA
13	12/13	*A. wahlbergii*	clearing & staining	Alcian/Alizarin
14	13	*A. wahlbergii*	fluorescent antibody staining	12/101 ab
15	13	*A. wahlbergii*	fluorescent antibody staining	12/101 ab
16	13/14	*A. xenodactyloides*	clearing & staining	Alcian/Alizarin
17	14	*A. wahlbergii*	fluorescent antibody staining	12/101 ab
18	14	*A. wahlbergii*	clearing & staining	Alcian/Alizarin
19	15	*A. xenodactyloides*	µCT	1% PMA
20	15	*A. wahlbergii*	fluorescent antibody staining	12/101 ab
21	15	*A. wahlbergii*	fluorescent antibody staining	12/101 ab
22	15	*A. wahlbergii*	clearing & staining	Alcian/Alizarin
23	hatchling	*A. wahlbergii*	fluorescent antibody staining	12/101 ab
24	hatchling	*A. xenodactyloides*	clearing & staining	Alcian/Alizarin
25	adult	*A. xenodactyloides*	clearing & staining	Alcian/Alizarin
26	adult	*A. xenodactyloides*	Illustration	—

Table 2: Muscles of the "larval phase" in *Arthroleptis* till TS 10.

Group	Name	Origin	Insertion	Stage first appearance	Stage adult configuration	Comments
Mandibular group	M. l. mandibulae longus	Palatoquadrate	Cartilago meckeli	TS 7	TS 12	changes origin during TS 10/11 to capsula auditiva
	M. l. mandibulae lateralis	Palatoquadrate?	Cartilago meckeli	TS 7	TS 12	changes during TS 10/11
	M. l. mandibulae externus	Proc. pterygoideus	Cartilago meckeli			
	M. mandibulolabialis			TS 8	TS 12	runs along cartilago labialis inferior
	M. intermandibularis anterior (=M. submentalis)	Median raphe	anteroventrally on cartilago meckeli	TS 5/6 ?	TS 12	
	M. intermandibularis posterior	Median raphe	posteroventrally on Cartilago meckeli	TS 5/6 ?	TS 12	
	M. intermandibularis lateralis	Palatoquadrate	Cartilago meckeli	TS 12	TS 15	only in *A. xenodactyloides*
Hyoid group	M. hyoangularis	Ceratohyale	Cartilago meckeli	TS 7/8		fuses with m. orbitohyoideus (TS11) to form anterior part of m. depr. mandibulae
	M. suspensorionagularis	Palatoquadrate	Cartilago meckeli	TS 7/8		fusing with each other and with Hyoangularis at TS 11, from TS 12 on forming the m. depressor mandibulae anterior
	M. quadratoangularis	Palatoquadrate	Cartilago meckeli	TS 7/8		
	M. orbitohyoideus	posterolateral on Palatoquadrate	Ceratohyale	TS 7/8		changing during TS 11
	M. interhyoideus	Ceratohyale	Median raphe	TS 7	TS 15	
Branchial group	M. l. arc branchialis I-IV	Capsula auditiva	corresponding Ceratobranchiale	TS 7		change into m. petrohyoidei I-IV
	M. l. con. branchialis I-III	?	?	TS 7		no longer seen from TS 8 on
	M. cucullaris	capsula auditiva	scapula		?	
Hyobr. group	M. geniohyoideus	hyobranchial plate	cartilago meckeli	TS 7/8	TS 12	two portions from TS 12 on

Table 3: Muscles of *Arthroleptis* from TS 12 on.

Group	Name	Origin	Insertion	Fig.
Mandibular group	M. l. mandibulae longus	lateral part of capsula auditiva	medio- to posterolaterally on angulosplenial	Fig. 7E, 7F
	M. l. mandibulae lateralis	ventral ramus of squamosal	mediolaterally on angulosplenial and cartilago meckeli	
	M. l. mandibulae externus	ramus ventralis of the squamosal (TS 15)	posterolaterally on cartilago meckeli (TS 15)	Fig. 7E
	M. intermandibularis anterior (= M. submentalis)	Median raphe	anteroventral part of cartilago meckeli	Fig. 7D
	M. intermandibularis posterior	Median raphe	ventrally alongside cartilago meckeli	
	M. intermandibularis lateralis	lateromedially on palatoquadrate (TS 12), quadrate, partly on quadratojugal (TS 15)	medio- to posterolaterally on cartilago meckeli (TS 12)	Fig. 7C
Hyoid group	M. depressor mandibuale anterior	posterior part of ramus ventralis of squamosal	posterior end of cartilago meckeli.	Fig. 7C
	M. depressor mandibuale posterior	broad area on capsula auditiva	posterior end of cartilago meckeli	Fig. 7C
	M. interhyoideus	Median raphe	posterolaterally on hyale	Fig. 7F
Branchial group	M. petrohyoideus I-IV	capsula auditiva	ventrolaterally on hyoid plate (m. petrohyoidei I-III), ventrolaterally on processus posteromedialis (m. petrohyoideus IV)	
	M. cucullaris	dorsal occipital fascia	anteror margin of scapula	
Hyobr. group	M. geniogyoideus medialis	posterior end of planum hyobranchiale	anteriorly on mentomeckelian	Fig. 7D
	M. geniohyoideus lateralis	anterior on processus posteromedialis	anteromedial part of cartilago meckeli and angulosplenial	Fig. 7D

Figures

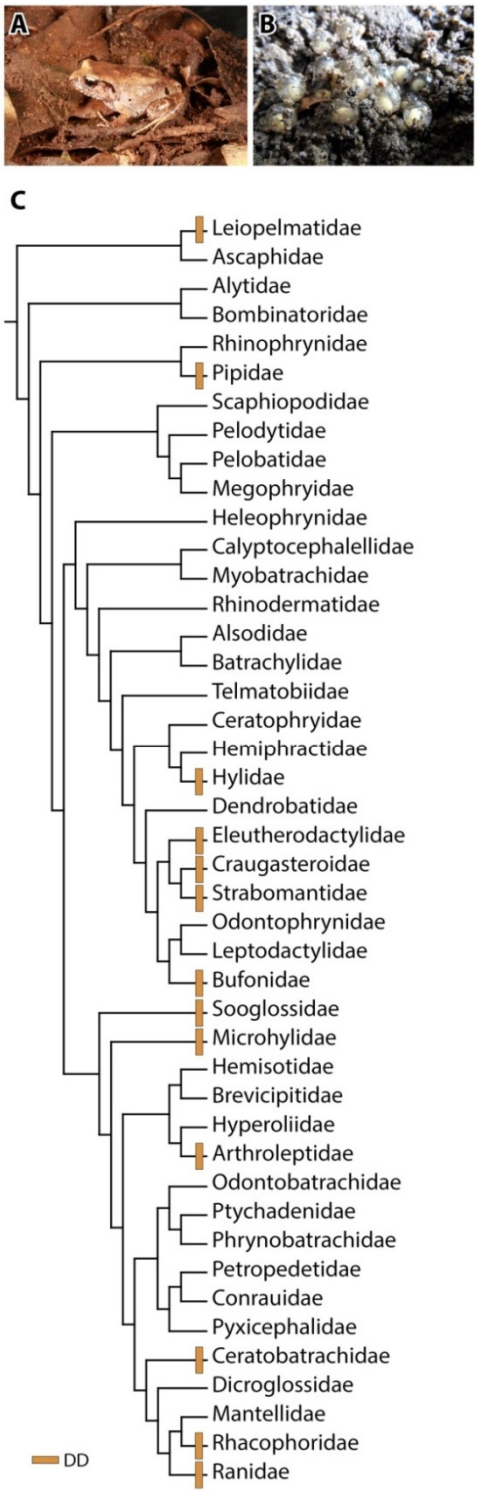

Figure 1: Cladogramm showing the distribution of direct development in anuran taxa and photographs of adult frog and egg clutch of the direct developing *Arthroleptis wahlbergii*. **A:** Adult female of *A. wahlbergii* at Entumeni Forest, KwaZulu-Natal, South Africa. **B:** Clutch of *A. wahlbergii* at Entumeni Forest, KwaZulu-Natal, South Africa. Clutch was photographed in situ after the removal of covering leaves and soil. **C:** Phylogeny from Feng et al. (2017). Plotted data on direct development from Müller et al. (2005), Wake & Hanken (1996), Stephenson (1955), Trueb et al. (2000), Wiens et al. (2007), Townsend & Stewart (1985), Goldberg et al. (2015), Goldberg et al. (2012), Wake (1980), Callery et al (2001), Anstis et al (2007), Schweiger et al. (2017), Narayan et al. 2010, Kerney et al. (2007), Bahir et al. (2005).

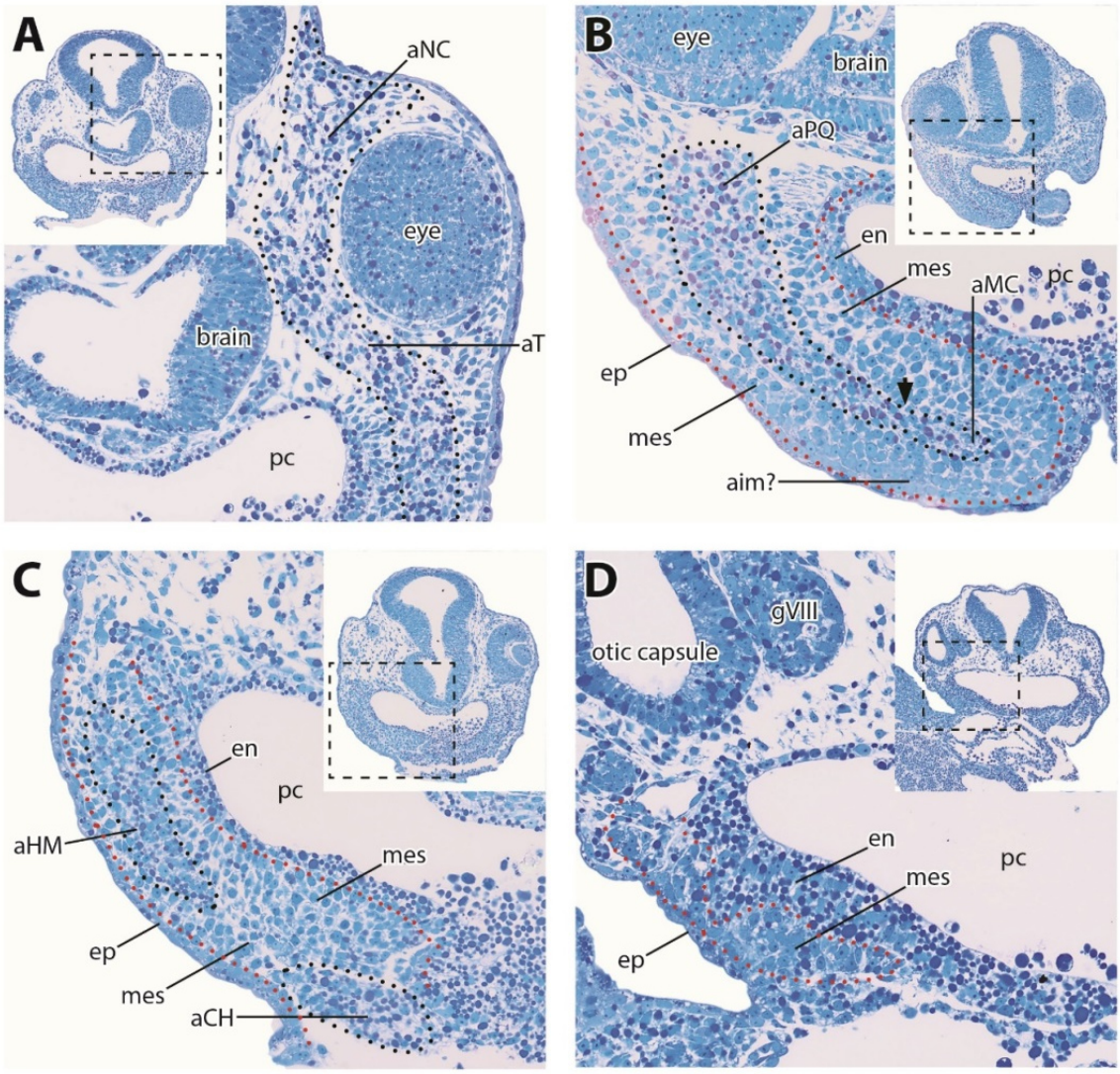

Figure 2: Cross sections through an embryo of *A. wahlbergii* at late TS 5/early TS6 (thickness 3 µm). A small overview image of the section is shown in the upper left or right corner. **A**: section through the anterior head region. The head mesenchyme is marked by a dotted black line. **B**: Section through the mandibular arch region. The anlage of the palatoquadrate and the cartilago meckeli (layer three) are marked by a dotted black line. The mesenchyme (layer two and four) are marked by a dotted red line. **C**: Section through the hyoid arch region. The anlagen of the hyomandibula and ceratohyale (layer three) are marked by two dotted black line. The mesenchyme (layer two and four) are marked by a dotted red line. **D:** Section through the branchial arch region at the anterior limb bud level. The central mesenchyme (layer three) is marked by a dotted red line. Abbreviations: **aCH** anlage of the ceratohyale, **aHM** anlage of the hyomandibula, **aim?** anlage of the intermandibularis muscle?, **aMC** anlage of the cartilago meckleli, **aNC** anlage of the neurocranium, **aPQ** anlage of the palatoquadrate, **aT** anlage of the trabeculae, **en** endoderm, **ep** epidermis, **gVIII** vestibulocochlear ganglion, **mes** mesenchyme, **pc** pharyngeal cavity.

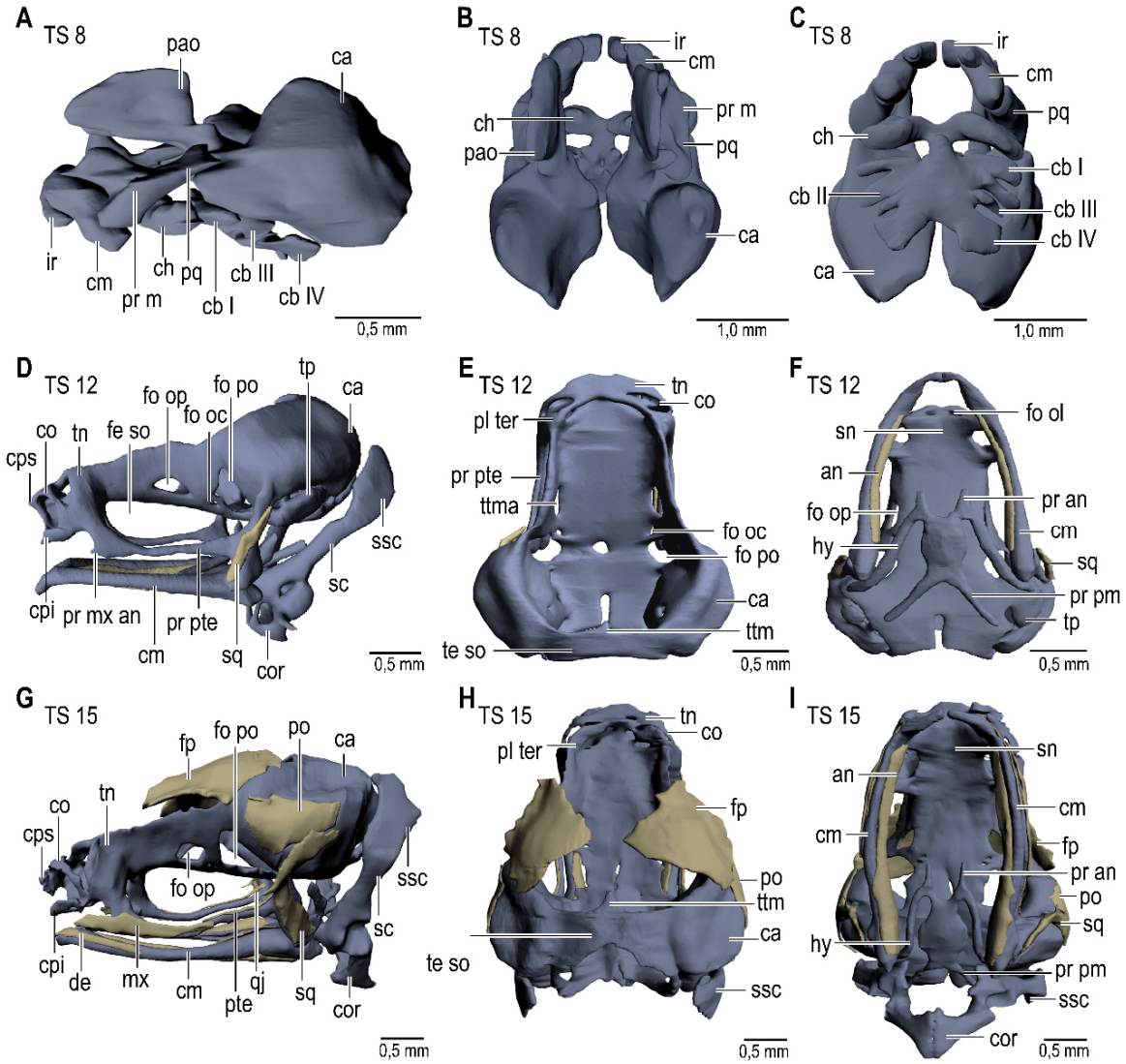

Figure 3: 3D reconstruction of µCT scans of embryos of *Arthroleptis* showing the development of the chondrocranium. The different structures have been coloured as follows: cartilage, blue; bones, ochre. **A-C:** *A. wahlbergii*. **A:** Lateral view, TS 8. **B:** Dorsal view, TS 8. **C:** Ventral view, TS 8. **D-I:** *A. xenodactyloides*. **D:** Lateral view, TS 12. **E:** Dorsal view, TS 12. **F:** Ventral view, TS 12. **G:** Lateral view, TS 15. **H:** Dorsal view, TS 15. **I:** Ventral view, TS 15. Abbreviations: **an** angulosplenial, **ca** capsula auditiva, **cb I-IV** ceratobranchialia I-IV**, ch** ceratohyale, **cm** cartilago meckeli, **co** cartilago obliquus, **cor** coracoid, **cpi** cartilago praenasalis inferior, **cps** cartilago praenasalis superior, **fe so** fenestra subocularis, **fo oc** foramen oculomotori, **fo ol** foramen olfactorium, **fo op** foramen opticum, **fo po** foramen prooticum, **hy** hyale, **ir** cartilago labialis inferior, **pao** pila antotica, **pl hyb** planum hyobranchiale, **pq** palatoquadrate, **pl ter** planum terminale, **pr an** processus anterior, **pr m** processus muscularis, **pr mx an** processus maxillaris anterior, **pr pm** processus posteromedialis, **pr pte** processus pterygoideus, **qu** quadrate, **sc** scapula, **ssc** suprascapula, **sn** solum nasi, **sq** squamosal, **te so** tectum synoticum, **tn** tectum nasi, **tp** tympanicum, **ttma** taenia tecti marginalis, **ttm** taenia tecti medialis.

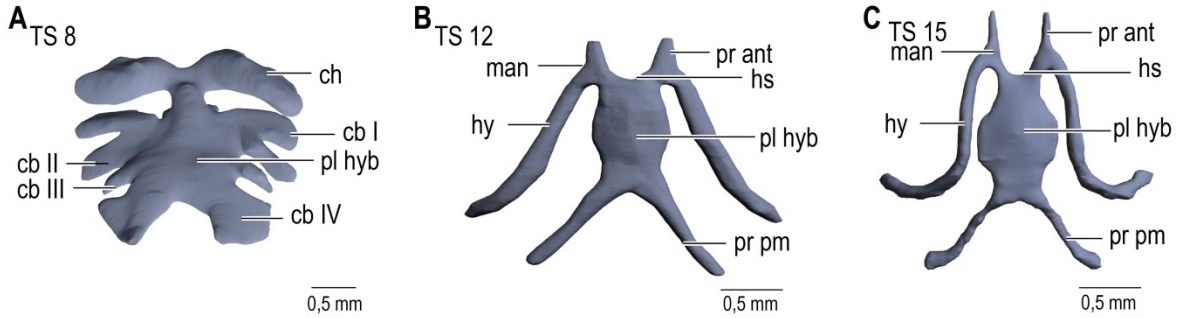

Figure 4: 3D reconstruction of µCT scans showing the development of the hyobranchial skeleton in *A. wahlbergii*. **A:** TS 8. **B:** TS 12. **C:** TS 15. Abbreviations: **ch** ceratohyale, **cb I** ceratobranchiale I, **cb II** ceratobranchiale II, **cb III** ceratobranchiale III, **cb IV** ceratobranchiale IV, **hs** hyoglossal sinus, **hy** hyale, **man** manubrium, **pl hyp** planum hyobranchiale, **pr ant** processus anterior, **pr pm** processus posteromedialis.

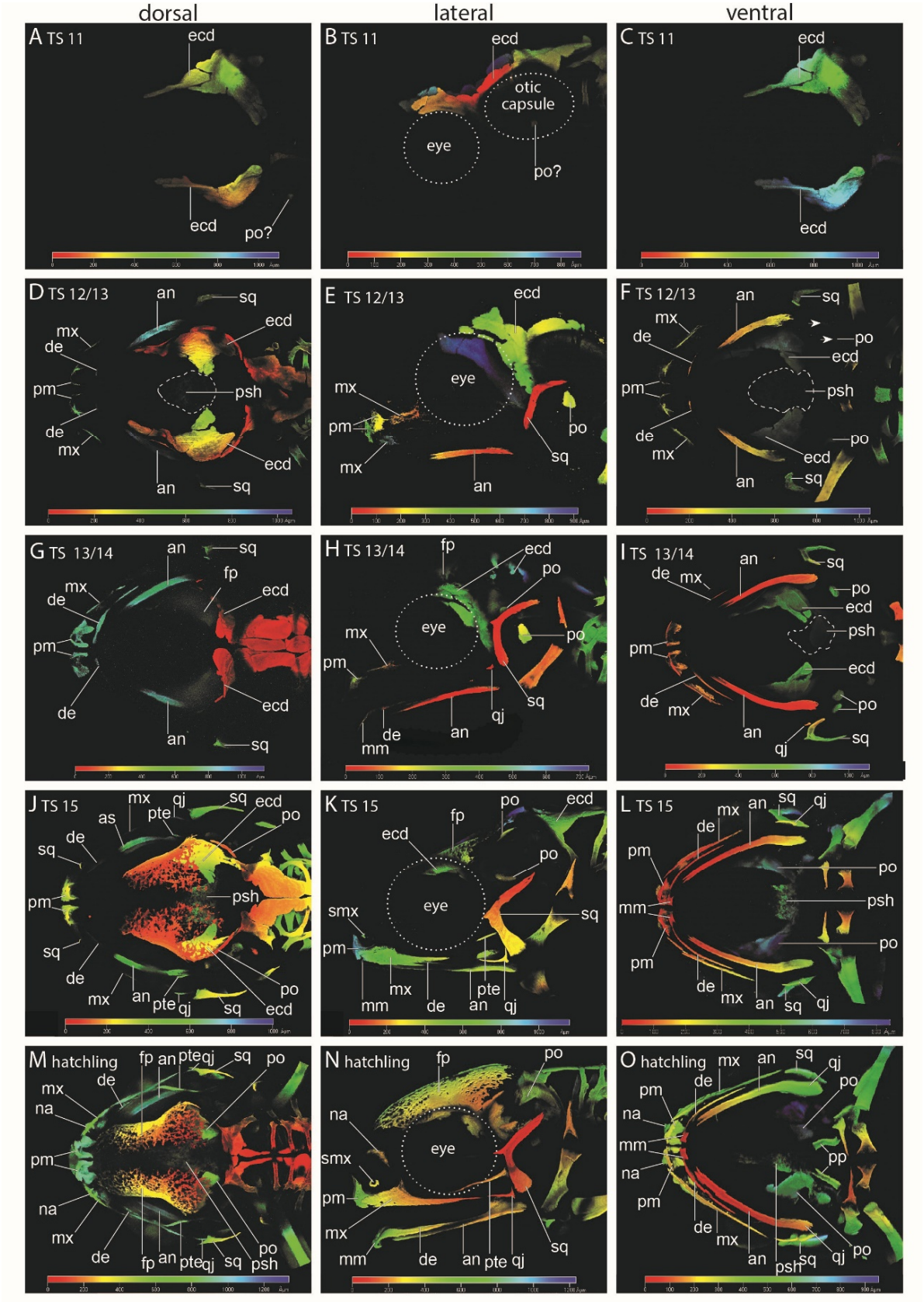

Figure 5: Maximum intensity projections of whole-mount antibody staining of *A. wahlbergii* showing the development of bones from TS 11-hatchling. Abbreviations: **an** angulosplenial, **de** dental, **ecd** endolymphatic calcium deposits**, ex** exoccipital, **mm** mentomeckelian, **mx** maxilla, **na** nasal, **pmx** praemaxilla, **po** prootic, **psh** parasphenoid, **pte** pterygoid, **qj** quadratojugal, **smx** septomaxilla, **sq** squamosal.

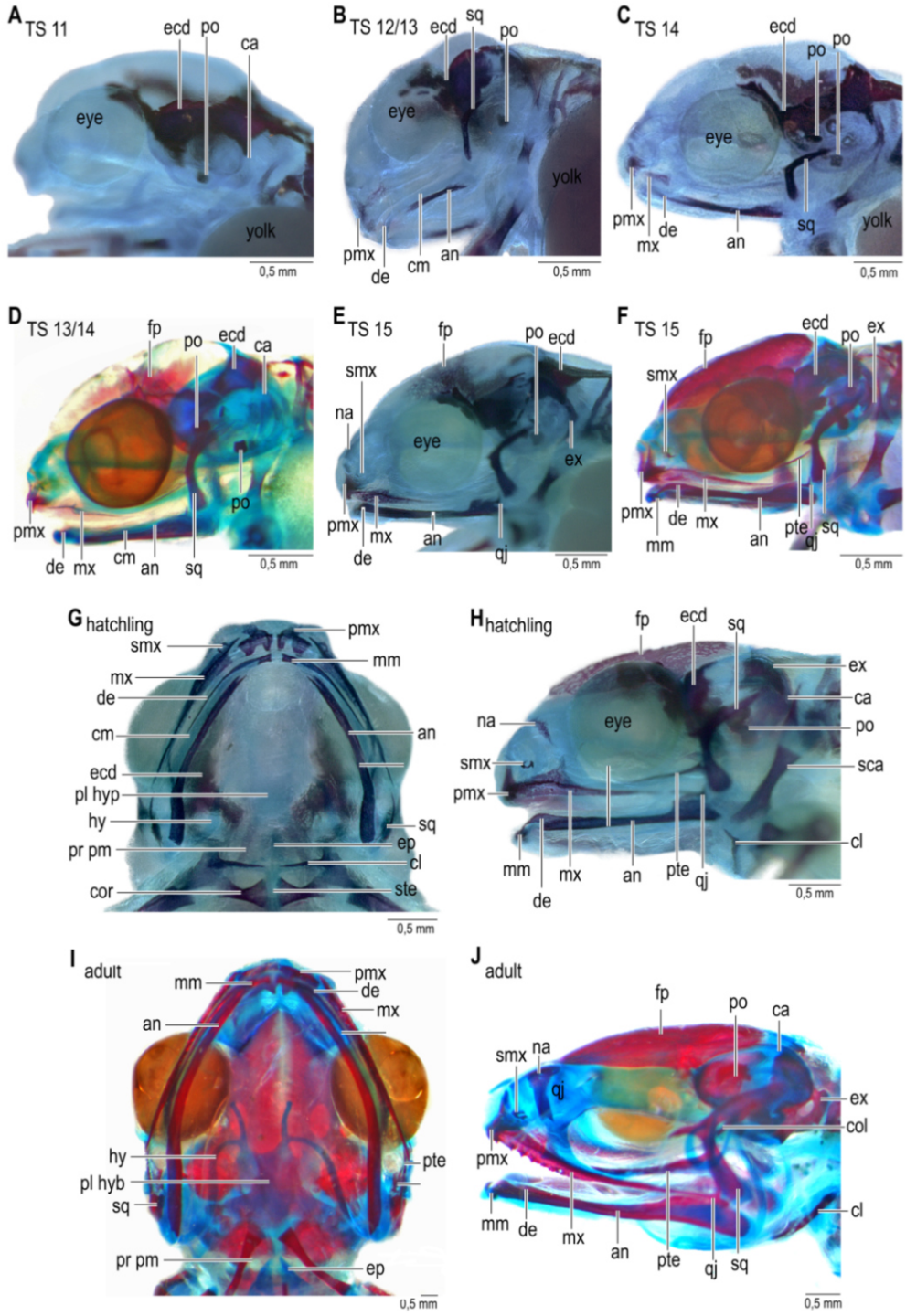

Figure 6: Cleared and stained whole-mounts of *Arthroleptis* showing the development of bones from TS 11-adult. **A:** *A. wahlbergii*, TS 11, lateral view. **B:** *A. wahlbergii*, TS 12/13, lateral view. **C:** *A.wahlbergii*, TS 14, lateral view. Bones of the upper and lower jaw are more prominent, the squamosal assumes a vertical position. **D:** *A. xenodacytloides*, TS13/14, lateral view. **E:** *A. wahlbergii*, TS 15, lateral view. Most of the adult bones nearly assumed their adult shape, the frontoparietal begins to extend in cranial and caudal direction. **F:** *A. xenodacytloides*, TS 15, lateral view. The frontoparietal is more significant than in TS 15 of *A. wahlbergii*. **G** and **H**: Ventral and lateral view, hatchling of *A. wahlbergii*. **I** and **J:** Ventral and lateral view, adult male of *A. xenodacyloides*. **an** angulosplenial, **ca** capsula auditiva, **cl** clavicular, **cm** cartilago meckeli, **cor** coracoid, **de** dental, **ecd** endolymphatic calcium deposits**, ex** exoccipital, **mx** maxilla, **na** nasal, **pl hyb** planum hyobranchiale, **pmx** praemaxilla, **po** prootic, **pr pm** processus posteromedialis, **po** prootic, **pte** pterygoid, **qj** quadratojugal, **sca** scapula, **smx** septomaxilla, **sq** squamosal. D, I, J modified from unpublished diploma thesis (Schweiger, 2012).

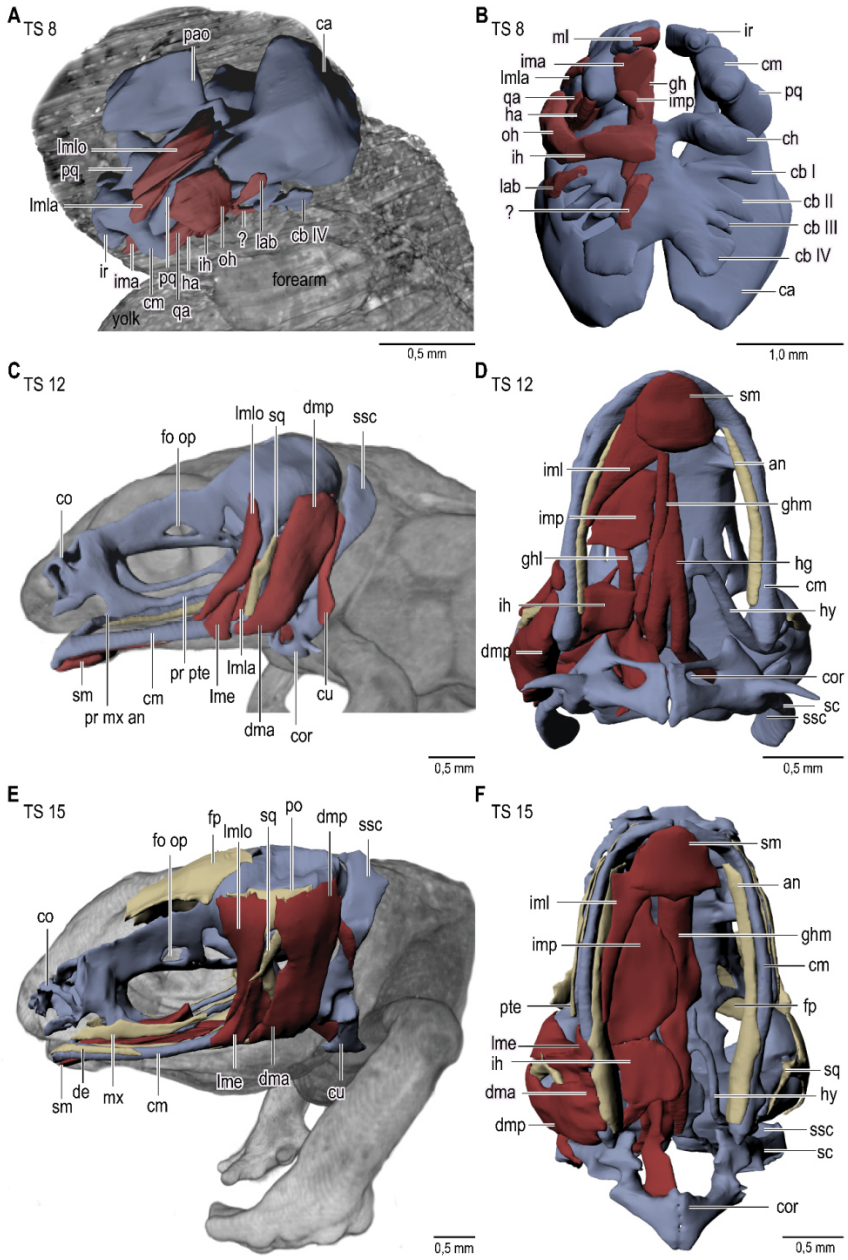

Figure 7: 3D reconstruction of µCT scans of embryos of *Arthroleptis* showing the development of the cranial muscles. The different structures have been coloured as follows: cartilage, blue; bones, ochre; muscles, red. **A-B:** *A. wahlbergii*. **C-F:** *A. xenodactyloides*. **A: TS 8,** lateral view. **B:** TS 8, ventral view. **C:** TS 12, lateral view. **D:** TS 12, ventral view. **E:** TS 15, lateral view. **F:** TS 15, ventral view. Abbreviations: **an** angulosplenial, **ch** ceratohyale, **cb** I-IV ceratobranchiale I-IV, **cm** cartilago meckeli, **co** cartilago obliquus, **cor** coracoid, **cu** musculus cucullaris, **dma** musculus depressor mandibulae anterior, **dmp** musculus mandibulae posterior, **fo op** foramen opticum, **fp** frontoparietal, **ghl** musculus geniohyoideus lateralis, **ghm** musculus geniohyoideus medialis **ha** musculus hyoangularis, **hg** musculus hyoglossus, **hy** hyale, **ih** musculus interhyoideus, **ima** musculus intermandibularis anterior**, iml** musculus intermandibularis lateralis, **imp** musculus intermandibularis posterior, **ir** cartilago labialis inferior, **lab** musculus levator arcus branchialis**, lme** musculus levator mandibulae externus, **lmlo** musculus levator mandibulae longus, **lmla** musculus levator mandibulae lateralis, **ml** musculus mandibulolabialis, **oh** musculus orbitohyoideus, **pao** pila antotica, **pq** palatoquadrate, **pr mx an** processus maxillaris anterior, **pr pte** processus pterygoideus, **qa** musculus quadratoangularis, **sc** scapula, **sm** musculus submentalis, **sq** squamosal, **ssc** suprascapula.

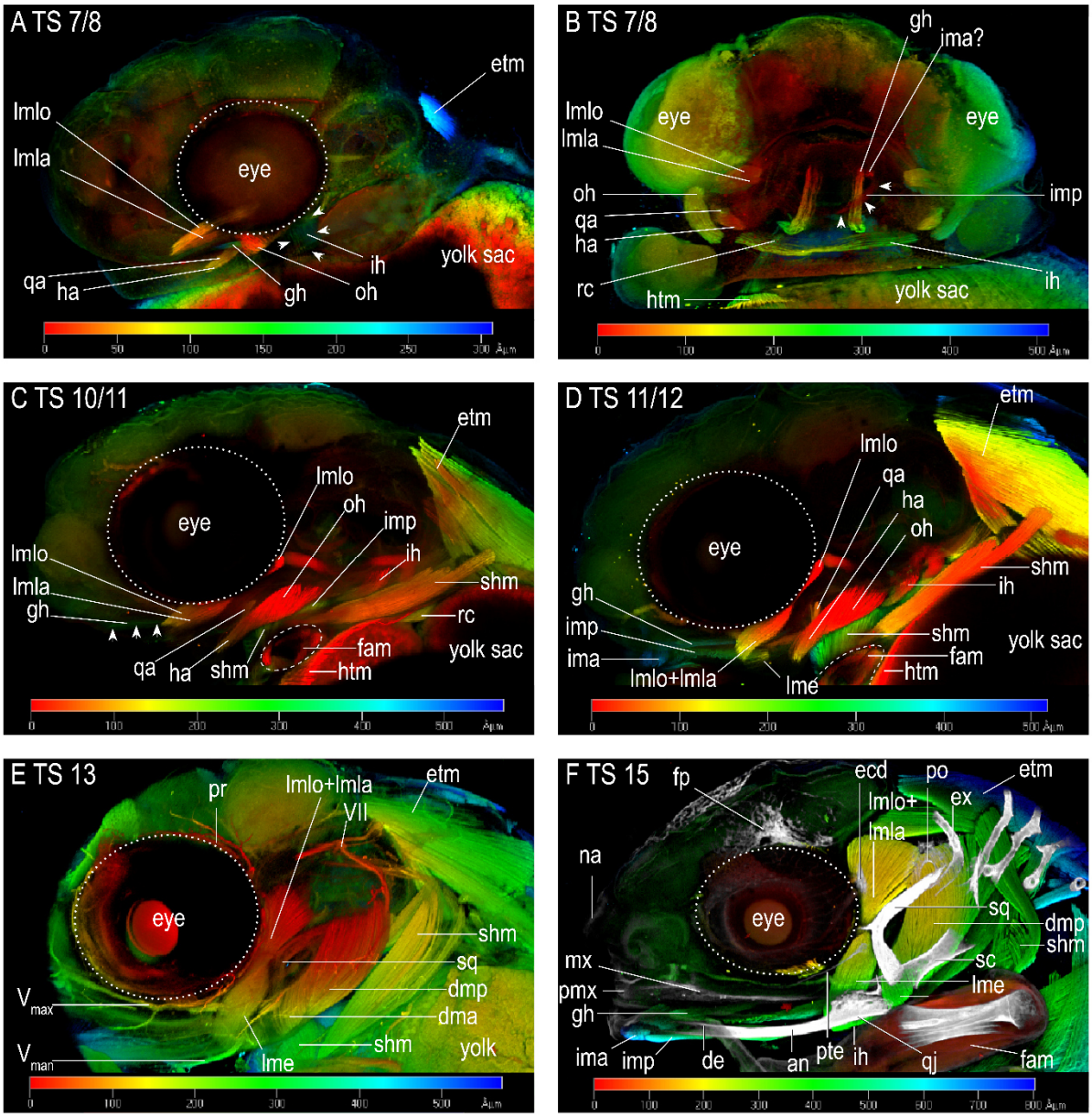

Figure 8: Maximum intensity projections of whole-mount antibody staining, showing the development of the cranial muscles in *A. wahlbergii* embryos from TS 7/8 – TS 15. **A:** TS 7/8, lateral view. **B:** TS 7/8, ventral view. **C:** TS 10/11, lateral view. Muscles are beginning to fuse and change their orientation. **D:** TS 11/12, lateral view. **E:** TS 13, lateral view. **F:** TS 15, lateral view. **D:** TS 15, lateral view. All cranial muscles are formed in their adult shape before hatching occurs. Abbreviations: **an** angulosplenial, **de** dental, **dma** musculus depressor mandibulae anterior, **dmp** musculus mandibulae posterior, **ecd** endolymphatic calcium deposits, **ex** exoccipital, **fp** frontoparietal, **gh** musculus geniohyoideus, **ha** musculus hyoangularis, **ih** musculus interhyoideus, **ima** musculus intermandibularis anterior, imp musculus intermandibularis posterior, **lmla** musculus levator mandibulae lateralis **lme** musculus levator mandibulae externus, **lmlo** musculus levator mandibulae longus, **mx** maxilla, **na** nasal, **oh** musculus orbitohyoideus, **pmx** praemaxilla, **po** prootic, **pte** pterygoid, **qa** musculus quadratoangularis, **qj** quadratojugal, **sc** scapula, **sm** musculus submentalis, **sq** squamosal.

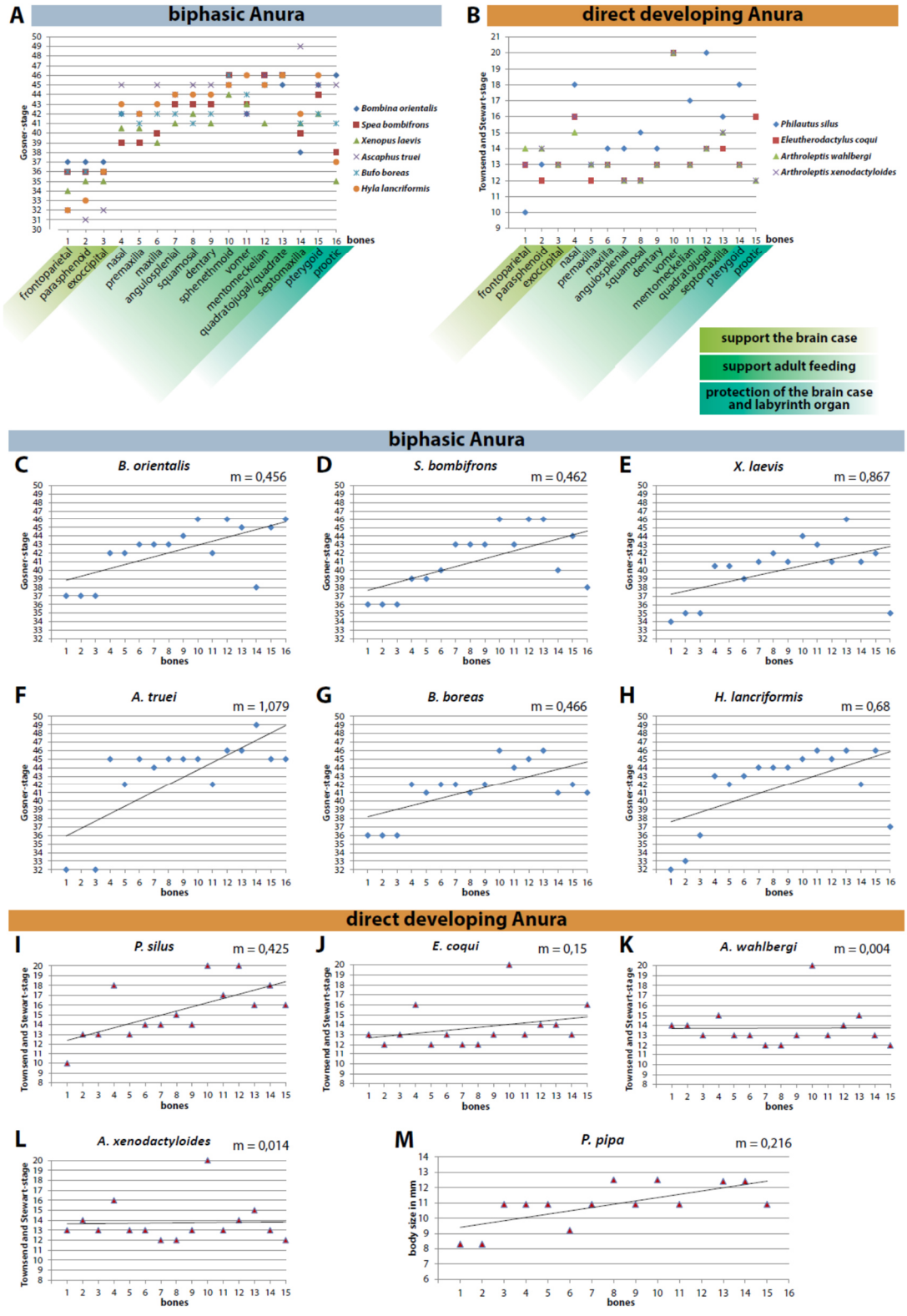

Figure 9: Cranial ossification sequence in biphasic and direct developing species. Only regression lines of species staged according to a similar system (TS or Go) can be compared directly/absolutely. Data references: *Bombina orientalis* (Maglia & Púgener 1998), *Spea bombifrons*, (Wiens 1989), *Xenopus laevis* (Trueb & Hanken 1992), *Ascaphus truei* (Moore & Townsend Jr. 2003), *Bufo boreas* (Gaudin 1978) and *Hyla lancriformis* (De Sa 1988), Pseudophilatus *silus* (Kerney et al. 2007), *Eleutherodacytlus coqui* (Hanken et al. 1992), *Arthroleptis wahlbergi* and *Arthroleptis xenodactyloides* (present study), *Pipa pipa* (Trueb et al. 2000).

CHAPTER 3

Parallel evolution of direct development in frogs – Skin and thyroid gland development in African Squeaker Frogs (Anura: Arthroleptidae: *Arthroleptis*)

Authors: Naumann, B., **Schweiger, S.,** Hammel, J. U., Müller, H.

Status: Published in Developmental Dynamics (2021) 250: 584-600

FORMULAR 1

Manuskript Nr.: 3

Titel des Manuskriptes: Parallel evolution of direct development in frogs – Skin and thyroid gland development in African Squeaker Frogs (Anura: Arthroleptidae: *Arthroleptis*)

Autoren: Naumann, Benjamin; **Schweiger, Susan**; Hammel, Jörg U.; Müller, Hendrik

Bibliographische Informationen: Published in Developmental Dynamics (2021) 250: 584-600

Der Kandidat / Die Kandidatin ist (bitte ankreuzen):

☐ Erstautor/-in, ☐ Ko-Erstautor/-in, ☐ Korresp. Autor/-in, ☒ Koautor/-in.

Anteile (in %) der Autoren / der Autorinnen an der Publikation (anzugeben ab 20%):

Autor/-in	Konzeptionell	Datenanalyse	Experimentell	Verfassen des Manuskriptes	Bereitstellung von Material
Naumann, B.	60%	70%	65%	70%	33%
Schweiger, S.	35%	30%	30%	20%	33%
Hammel, J. U.					
Müller, H					33%

Received: 21 September 2020 | Revised: 1 December 2020 | Accepted: 2 December 2020

DOI: 10.1002/dvdy.275

Developmental Dynamics WILEY

Parallel evolution of direct development in frogs - Skin and thyroid gland development in African Squeaker Frogs (Anura: Arthroleptidae: *Arthroleptis*)

Benjamin Naumann[1] | **Susan Schweiger**[1] | **Jörg U. Hammel**[2] | **Hendrik Müller**[1,3,4]

[1]Institut für Zoologie und Evolutionsforschung, Jena, Germany

[2]Helmholtz-Zentrum Geesthacht, Zentrum für Material- und Küstenforschung, Außenstelle am DESY, Hamburg, Germany

[3]Zentralmagazin Naturwissenschaftlicher Sammlungen, Martin-Luther-Universität Halle-Wittenberg, Halle (Saale), Germany

[4]Department of Life Sciences, The Natural History Museum, London, UK

Correspondence
Benjamin Naumann and Hendrik Müller, Institut für Zoologie und Evolutionsforschung, Erbertstraße 1, 07743 Jena, Germany.
Email: benjamin.naumann@uni-jena.de (B. N.) and hendrik.mueller@zns.uni-halle.de (H. M.)

Funding information
Deutsche Forschungsgemeinschaft, Grant/Award Number: DFG MU2914/2-1

Abstract

Background: Cases of parallel evolution offer the possibility to identify adaptive traits and to uncover developmental constraints on the evolutionary trajectories of these traits. The independent evolution of direct development from the ancestral biphasic life history in frogs is such a case of parallel evolution. In frogs, aquatic larvae (tadpoles) differ profoundly from their adult forms and exhibit a stunning diversity regarding their habitats, morphology and feeding behaviors. The transition from the tadpole to the adult is a climactic, thyroid hormone (TH)-dependent process of profound and fast morphological rearrangement called metamorphosis. One of the organ systems that experiences the most comprehensive metamorphic rearrangements is the skin. Direct-developing frogs lack a free-swimming tadpole and hatch from terrestrial eggs as fully formed froglets. In the few species examined, development is characterized by the condensed and transient formation of some tadpole-specific features and the early formation of adult-specific features during a "cryptic" metamorphosis.

Results: We show that skin in direct-developing African squeaker frogs (*Arthroleptis*) is also repatterned from a tadpole-like to an adult-like histology during a cryptic metamorphosis. This repatterning correlates with histological thyroid gland maturation. A comparison with data from the Puerto Rican coqui (*Eleutherodactylus coqui*) reveals that the evolution of direct development in these frogs is associated with a comparable heterochronic shift of thyroid gland maturation.

Conclusion: This suggests that the development of many adult-features is still dependent on, and possibly constrained by, the ancestral dependency on thyroid hormone signaling.

KEYWORDS

Cardioglossa, developmental constraints, heterochrony, tadpole, terrestrialization

1 | INTRODUCTION

How do developmental constraints influence phenotypic evolution? A promising way to approach this question is studying cases of parallel evolution.[1] Parallel evolution can be defined as the independent origin of similar (derived) traits in two or more taxa sharing a common ancestry and bauplan.[2,3] Investigating patterns of parallel evolution allows to identify adaptive traits and to uncover developmental constraints on the evolutionary trajectories of these traits.[1] A potential case of parallel evolution is the repeated, independent origin of direct development within frogs (Anura) and other amphibians.[4-7] Direct development is characterized by the loss of an aquatic larval phase[8] and may have evolved in response to environmental conditions that restricted the availability of suitable habitats for aquatic development.[9-12]

In frogs, direct development evolved several times independently (Figure 1(A)), making them a suitable model system to unravel developmental constraints that underlay patterns of parallel evolution.[13,14] The ancestral biphasic life history of frogs includes a free-swimming larval stage called tadpole.[15] In contrast to other amphibian larvae, tadpoles differ extremely from their adult forms and exhibit a stunning diversity regarding their habitats, morphology and feeding behaviors.[16] In biphasic anurans, embryonic development from a fertilized egg to a tadpole happens more or less gradually, similar to other vertebrate groups. In contrast, the transition from the tadpole to the adult is a climactic, thyroid hormone (TH)-dependent process of profound and fast morphological rearrangement called metamorphosis (Figure 1(B)).[17] In direct-developing species, development from the embryo to the adult frog appears more gradual without an obvious climactic phase (Figure 1(B)).[18] Tadpole-specific traits such as the larval skeleton and its associated musculature, the cement glands, the lateral line system and the coiled intestine are nearly or completely reduced.[18,19] However, morphological studies on the embryonic development of direct-developing frogs are limited to only a few species.[6,13,20-22] The only species in which direct development has been investigated in greater detail is the Puerto Rican coqui, *Eleutherodactylus coqui* Thomas, 1966.[19,23-34]

Although direct-developing frogs have departed profoundly from their ancestral ontogeny[6,19,35], studies in *E. coqui* have shown that several developmental events are still under the control of TH[23,36] and that it undergoes a cryptic metamorphosis.[23,37] Ontogenetic repatterning seen in direct-developing frogs is thought to be the result of changes in the expression of TH, which leads to changes in timing of TH-dependent events during development ("heterochronic shift" hypothesis). At least some developmental events are thought to have become decoupled from TH-regulation ("loss of constraint" hypothesis), but so far data are only available for *E. coqui* and the general influence of TH during the ontogeny of other direct-developing frogs remains unclear.

An interesting system to study putative developmental constraints on the evolution of direct development is the skin. The frog skin hosts a complex microbiome and plays major roles in immune response, pathogen defense, respiration, osmoregulation, camouflage and even reproduction.[38-42] Among all tissues that remodel during metamorphosis the skin exhibits the most extreme changes regarding histology and gene expression.[43] It is exposed to completely different environments (aquatic vs. terrestrial) depending on life history phases and often exhibits tadpole- and adult-specific adaptations.[44] The skin of pre-metamorphic tadpoles is a mostly two-layered epithelium with unicellular glands and an outer mucus layer.[45] The underlying dermis consists of a stratum compactum and some melanophores in the mesenchyme beneath (Figure 1(C)). During pro-metamorphosis, the cells of the epidermis degenerate except for cells attached to the basal lamina. These basal cells start to proliferate during metamorphic climax and build up the post-metamorphic five- to seven-layered adult frog epidermis with an outer keratinized cell layer (stratum corneum) and different multicellular gland types. The underlying dermis contains an outer (exterior to the stratum compactum) and an inner (interior to the stratum compactum) melanophore layer (Figure 1(C)).[46-48] Metamorphic changes in biphasic species are initiated by TH production.[49-51] Thyroid hormone is also involved in several developmental processes in *E. coqui* indicating the presence of a cryptic metamorphosis in direct-developing species.[20,23,35,51]

In this study, we provide detailed data on skin development in direct-developing African Squeaker frogs (*Arthroleptis*) using histological and immunohistochemical techniques. To evaluate if potential changes in the skin and thyroid gland histology of *Arthroleptis* are due to direct development or instead shared by biphasic Arthroleptidae, we investigated the same tissues in a *Cardioglossa* tadpole, the sister genus of *Arthroleptis*. Additionally, we describe thyroid gland development in *Arthroleptis* and infer its maturity and activity based on morphology and morphometric measurements.

2 | RESULTS

Many aspects of the development of the embryonic pigmentation pattern, skin and thyroid glands are similar in

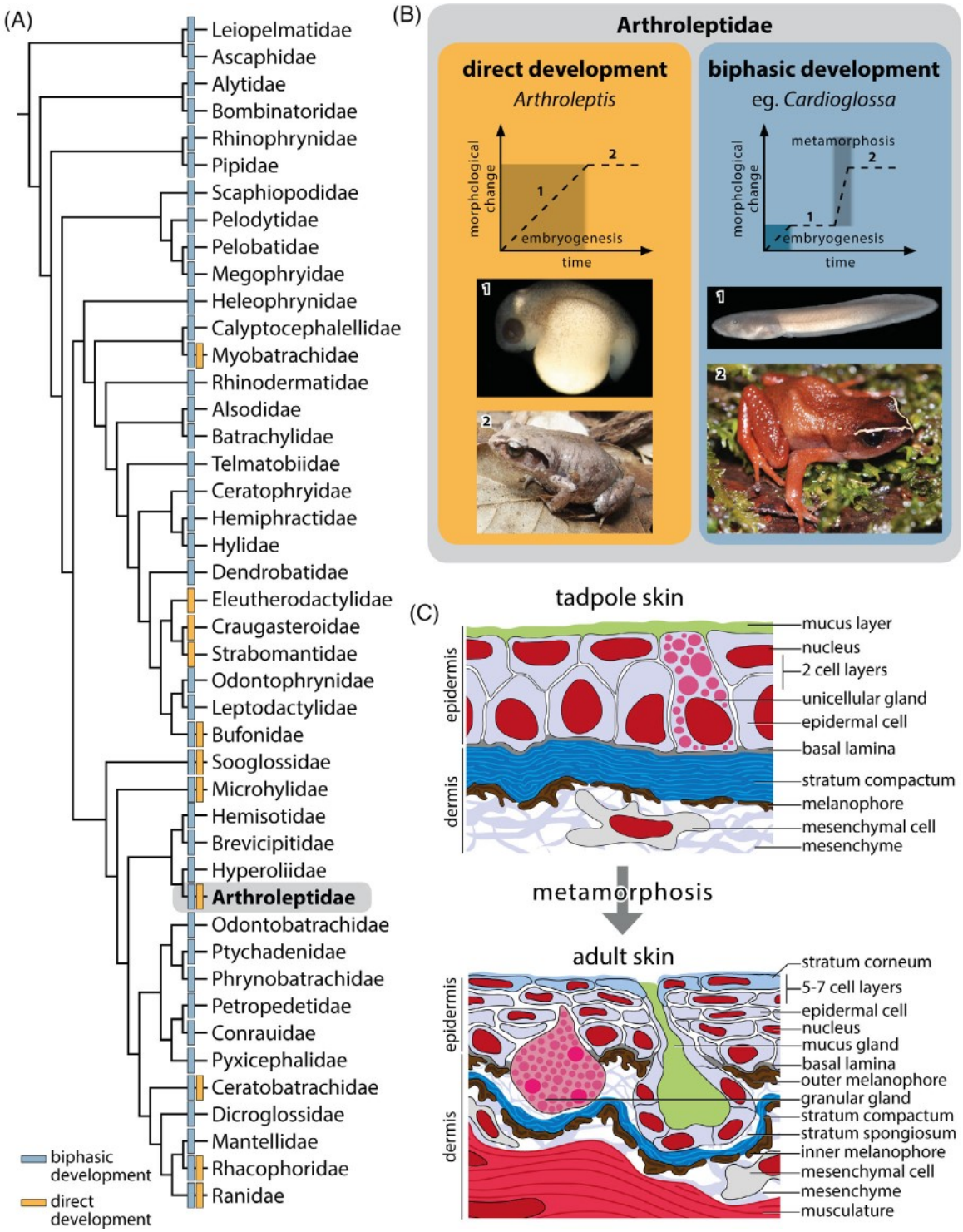

FIGURE 1 (A) A family-level phylogeny of recent frogs based on Feng et al., 2017 [86]. Blue boxes indicate the presence of an ancestral biphasic live history while orange boxes indicate direct development. (B) A schematic graph showing the gradual morphological change during ontogeny of the direct developing *Arthroleptis* (*A. wahlbergii*; 1, embryo; 2, adult frog) and the more climactic metamorphic change in its biphasic sister genus *Cardioglossa* (*C. manengouba*; 1, tadpole; 2, adult frog). Photographs are not to scale. (C) Schematic diagrams of the organization of the tadpole and adult frog skin

A. wahlbergii and *A. xenodactyloides*. Differences between the two species are mentioned where present.

2.1 | Development of the pigmentation pattern in *Arthroleptis* embryos

Embryos until mid Townsend and Stewart-stage (TS) 5 lack any obvious, externally visible pigmentation and have a white-yellowish color (Figure 2(A)). However, very few melanophores were found in the epidermal layer in histological sections of an embryo at TS4 (see Figure 3 (A4)). At late TS5/early TS6 melanophores are recognizable, extending ventrally until the ventral border of the eye in the head region and until the dorsal-most quarter of the lateral body wall in the trunk region (Figure 2(B)). Melanophores at this stage are spindle-shaped with long, thin extensions (Figure 2(B′)). From late TS7 to TS8, melanophores continue to extend ventrad in the head and the trunk regions (Figure 2(C), (D)) until they completely cover the lateral body wall from TS9 on (Figure 2(E),(F)). At this stage, the body wall has completely enclosed the yolk (Figure 2 (E3)). At TS11, the density of melanocytes of the head region starts to increase resulting in a darkening of the skin (Figure 2 (G)). Additionally, another type of melanophores becomes visible all over the body. These melanophores are smaller, with a more spherical shape and with only a few short or no extensions (Figure 2(G′)). At TS12, melanocyte density continues to increase dorso-ventrad until the whole lateral body wall is heavily pigmented at TS15 (Figure 2(H)-(K)).

In summary, pigmentation development is characterized by a first dorso-ventrad wave of melanophore development starting at late TS5 and a second wave made up by a morphologically different type of melanophores starting at TS11.

2.2 | Skin development in *Arthroleptis*

TS4 (Figure 3(A)) - The epidermis is single-layered with a sometimes indistinct border between the underlying cells and tissues. In the dorsal body region, cells are large and cuboid with spherical nuclei. Ventrally, cells are flattened and nuclei are ovoid to spindle-shaped. The cells possess

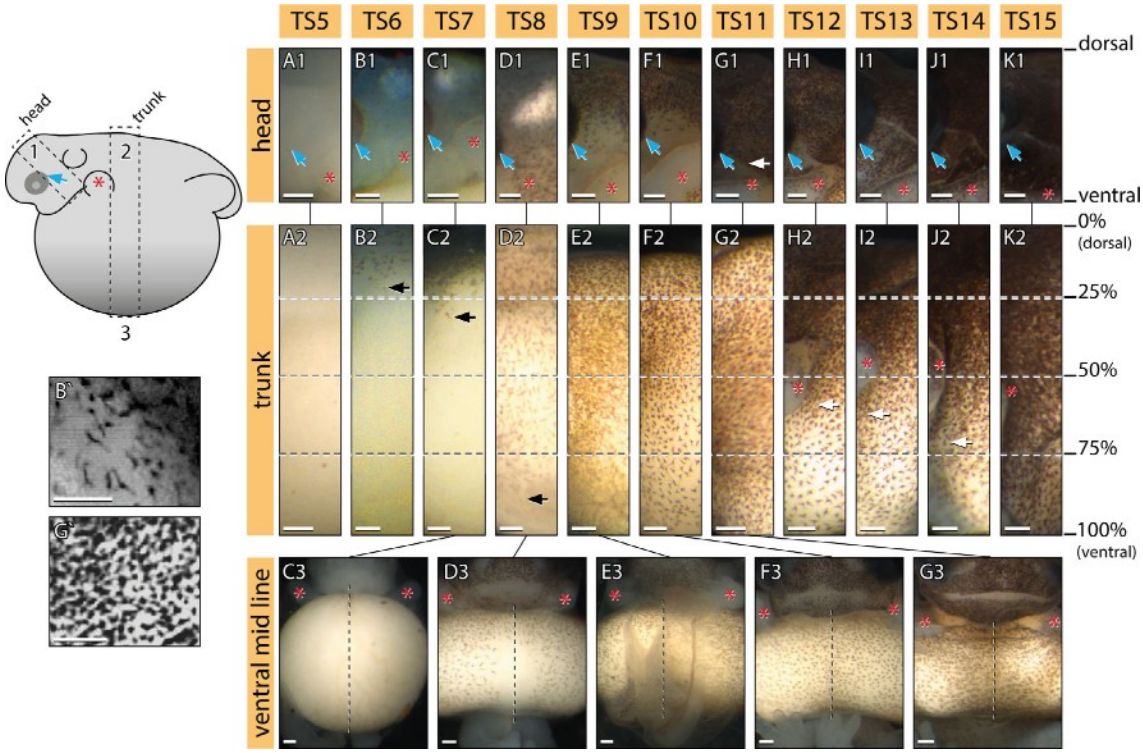

FIGURE 2 (A-G) Photographs of the skin pigmentation of different developmental stages of *Arthroleptis wahlbergii*. The schematic embryo on the left illustrates the photographed regions (1–3, and). Blue arrows indicate the position of the eye, red asterisks the position of the forelimb. The dotted grey lines and percentage number indicate the distance between the back (dorsal, 0%) and ventral midline (ventral, 100%). The black arrow in A2-D2 indicates the migration distance of the first melanophore type (shown in B′). The white arrow in H2-J2 indicates the migration distance of the second melanophore type (shown in G′). The black dotted line in C3-G3 indicates the ventral midline. Scale bar is 200 μm

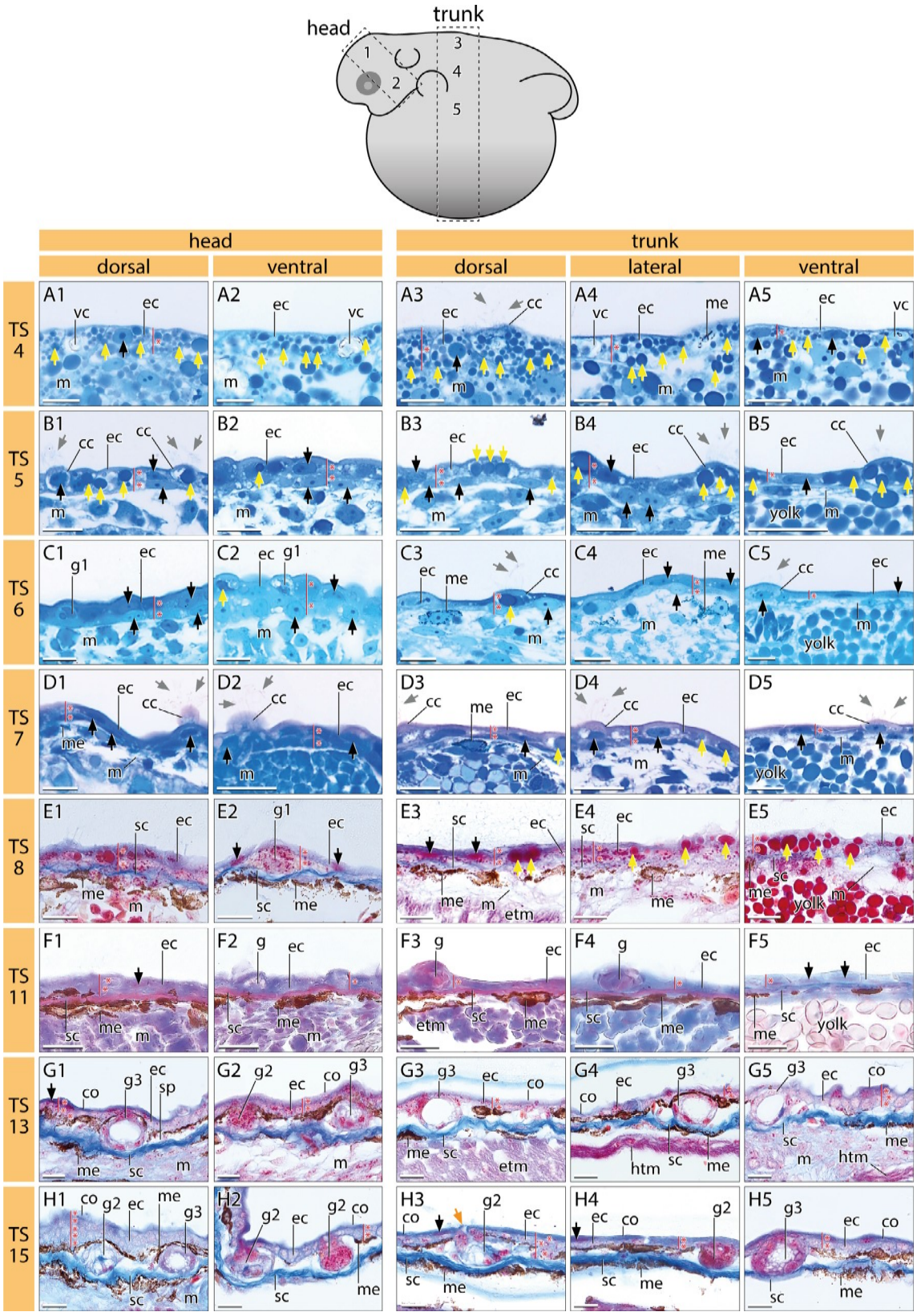

FIGURE 3 Histological cross sections of the skin of *Arthroleptis wahlbergii* at different developmental stages. The schematic embryo on top illustrates the photographed regions (1–5). Grey arrows indicate the epidermal cilia. Orange arrows indicate intracellular yolk droplets. Black arrows indicate epidermal nuclei. The yellow arrow in H3 indicates the glandular duct. The number of epidermal cellular layers is indicated by a red line and asterisks. Scale bar is 20 μm. cc, ciliated cell; co, stratum corneum; ec, epithel cell; etm, epaxonic trunk muscles; g, multicellular gland progenitor; g1, unicellular gland; g2, multicellular granular gland; g3, multicellular mucus gland; htm, hypaxonic trunk muscles; m, mesenchyme; me, melanophore; sc, stratum compactum; sp, stratum spongiosum; vc, vacuole

high amounts of intracellular yolk granules and some seem to have large vacuoles with dark pigments. Ciliated cells are found in a scattered pattern all over the embryo. Very few melanophores can be found intercalating between epidermal cells. A dense, undifferentiated mesenchyme lies beneath the epidermis.

TS5 (Figure 3(B)) - The dorsal epidermis of the head as well as of the dorso-lateral trunk is two-layered while the ventral epidermis of the trunk, covering the yolk sac, is single-layered. Most cells are slightly flattened with ovoid nuclei. The amount of intracellular yolk granules has decreased compared to TS4 but is still high. The number of ciliated cells has increased compared to TS4. A sharp border between epidermal cells and the underlying mesenchyme is recognizable.

TS6 and TS7 (Figure 3(C), (D)) - The number of epidermal layers has not changed compared to TS5. Some unicellular mucus glands are recognizable. The amount of intracellular yolk granules has further decreased compared to previous stages. A higher number of melanophores with long cytoplasmic extensions are present in the mesenchyme directly beneath the epidermis.

TS8 (Figure 3(E)) - The number of epithelial layers is similar to previous stages. Epidermal cells in both layers are flattened and show spindle-shaped nuclei. Some hypertrophied cells with a granular content that might represent unicellular glands are present in the skin of the head. Intracellular yolk granules are only detectable in the trunk epidermis. In the head, a distinct stratum compactum is present beneath the epidermis with a dense layer of inner melanophores interior to it. In the trunk, the stratum compactum is most distinct in the dorsal region and becomes gradually less obvious in lateral and ventral areas. This pattern is mirrored by the density of associated inner melanophores.

TS11 (Figure 3(F)) -The epidermis has become single-layered again in the head and dorsolateral trunk region and epidermal cells exhibit extremely flattened nuclei. In some scattered areas of the dorsal head, the epidermis is still two-layered. Intracellular yolk granules and ciliated cells are completely absent. Multicellular gland primordia, consisting of several compact cells, can be found all over the body. In the head, a few outer melanocytes are present between the stratum compactum and basal epidermal cells. In the trunk, the stratum compactum appears denser compared to the previous stage and the density of inner melanophores has increased. It is still lowest in the ventral trunk region.

TS13 (Figure 3(G)) - The skin exhibits many features of an adult frog skin. The epidermis is two- to three-layered. The majority of the basal epidermal cells are cuboid. The apical cell layer is flattened and is stained dark-blue in Azan-stained section, indicating an increased keratinization and the presence of a stratum corneum. The stratum corneum is more obvious in the head compared to the trunk epidermis. Multicellular mucus and granular glands can be found in various regions of the body. They are localized within a thin stratum spongiosum beneath the basal epidermal cell layer. Mucus glands are outlined by a single cell layer with an inner lumen. Granular glands are recognizable as large sacs filled with many granulated cells. The density of outer melanophores within the now developed stratum spongiosum has increased compared to previous stages.

TS15 (Figure 3(H)) - Hatching occurs at this stage and the skin of the froglet is similar to the skin of an adult *Arthroleptis* (see Figure 4). The thickness of the epidermis varies from two to five cell layers but is three-layered in most areas. In the trunk region, the dark blue-stained stratum corneum is now also recognizable as a distinct cellular layer. Multicellular glands in the whole skin are more numerous and melanophore density has increased in the ventral trunk region compared to TS13.

In summary, the embryonic ectoderm and underlying mesenchyme at TS4 are differentiated into a skin consisting of an epidermis and an underlying dermis. Both exhibiting pre-metamorphic tadpole-typical features at TS8. By TS11 the apical epidermal layers seem to degenerate to a certain degree while multicellular gland progenitors appear all over the body. The skin of embryos at TS13 and TS15 exhibit many features typical for the post-metamorphic frog skin.

2.3 | PCNA expression during epidermal development in *Arthroleptis*

Metamorphic skin remodeling is characterized by the degeneration of apical epidermal cells and the proliferation of remaining basal cells building the adult epidermis.[43] We therefore investigated the epidermal proliferation pattern in embryonic stages of *A. wahlbergii* using two different antibodies against proliferating cell nuclear antigen (PCNA). Signals from both antibodies were detected in the same tissues of two adjacent serial sections verifying antibody specificity. However, the signal from PCNA-1 antibody was always stronger than from the PCNA-2 antibody.

At TS8, scattered signals of the PCNA-1 antibody are detectable in nuclei of both epidermal cell layers as well as some mesenchymal cells (Figure 5(A),(A')). Only a few PCNA-2 positive cells are detectable at this stage (Figure 5(B),(B')). At TS11, PCNA-1 and PCNA-2 signals are detectable in the majority of epidermal cells, indicating a strong increase in the proliferation rate of the epidermis (Figure 5(C),(D)). A few PCNA-1 and PCNA-2

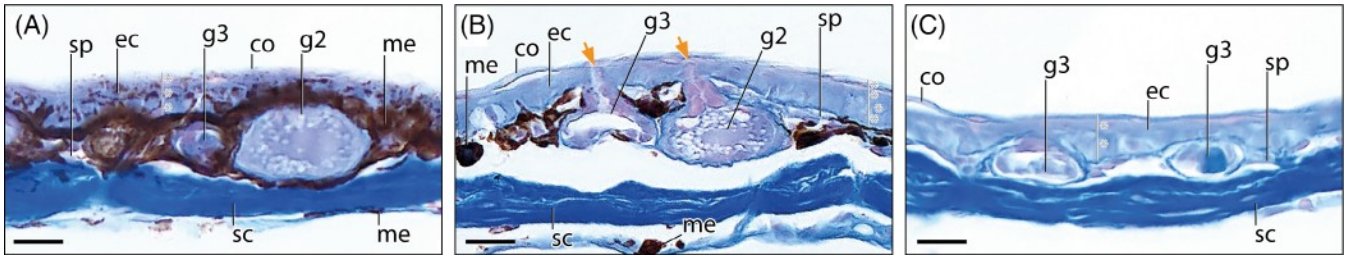

FIGURE 4 Adult skin histology. Histological cross sections of the skin of an adult (1.3 cm) *Arthroleptis wahlbergi*. (A) Dorsal head region. (B) Lateral head region. The orange arrow indicates the glandular duct. (C) Ventral head region. The number of epidermal cellular layers is indicated by a red line and asterisks. Scale bar is 20 µm. co, stratum corneum; ec, epithel cell; g2, multicellular granular gland; g3, multicellular mucus gland; me, melanophore; sc, stratum compactum; sp, stratum spongiosum

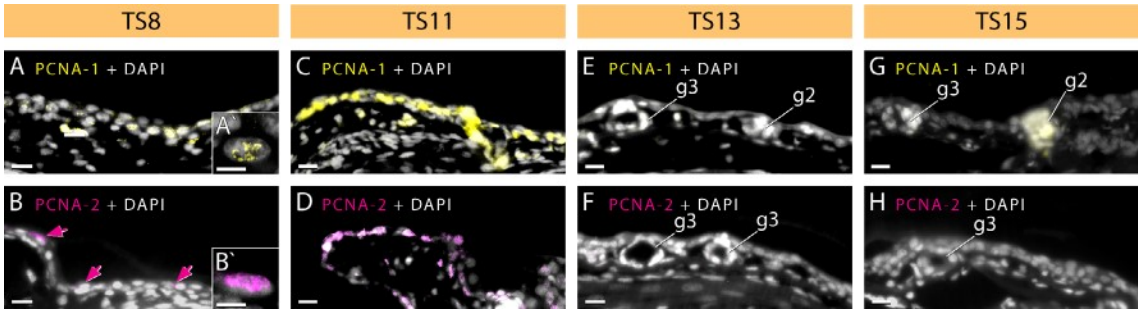

FIGURE 5 Fluorescent PCNA antibody staining in cross sections through the skin of *Arthroleptis wahlbergii* embryos at different developmental stages. Two different antibodies against PCNA have been used. PCNA-1 is colored in yellow and shown in A, C, E and G. PCNA-2 is colored in magenta and shown in B, D, F and H. Nuclei are stained with DAPI and colored in grey. A' and B' Show a close up of the PCNA signal within the nucleus. Magenta arrows in B indicate the scattered antibody signal. Scale bar for A-H is 20 µm. Scale bar for A' and B' is 10 µm. g2, multicellular granular gland; g3, multicellular mucus gland

positive mesenchymal cells are also present. No antibody signals are detectable in the epidermis at TS13 and TS15, indicating a low proliferation rate (Figure 5(E)-(G)). In some multicellular glands however, PCNA-1 positive cells can be detected (Figure 5(G)).

In summary, PCNA reactivity (and therefore cell proliferation rate) of the skin is detectable in a scattered pattern at TS8, has increased tremendously at TS11 and is low or absent at TS13 and TS15.

2.4 | Thyroid gland development in *Arthroleptis* embryos

The thyroid glands are paired, ovoid structures located at the lateral edges of the hyoid plate (Figure 6(A)-(C)). Primordia are first detectable at TS8. They appear as spherical, condensed cell masses including scattered lumina which lack an epithelial lining. The primordia are located on the left and right side ventrally to the lateral edges of the developing hyoid plate (Figure 6(A),(D)). First developing follicles are recognizable at TS10/11. The cells of the follicular epithelium are cuboid with little cytoplasm and large spherical nuclei (Figure 6(E)). At later TS11, thyroid glands have elongated, adopting a mature, adult-like morphology (Figure 6(B)). The follicles have increased in size and number and the follicular epithelium is now organized in a columnar pattern. Nuclei of follicular epithelial cells are spherical to ovoid-shaped. Some colloid, recognizable as a bluish substance in Azan-stained sections, is present within follicular lumina (Figure 6(F)). At TS13 the follicles have further increased in size and number. The cells of the follicular epithelium appear slightly flattened compared to the previous stage. No colloid is detectable in the investigated specimen (Figure 6(G)). At TS15 the thyroid glands have continued to elongate and are almost spindle-shaped (Figure 6(C)). The size and number of follicles have further increased and the follicular lumina are filled with colloid in the investigated specimen. Erythrocytes are recognizable around and in between follicles indicating a continuous vascularization of the thyroid gland (Figure 6(H)).

We measured the cell height of the follicular epithelium as well as the number and diameter of follicles (Figure 7(B)-(D)) from sections from the central region of the thyroid gland.[52] In *A. wahlbergi* we observed a huge increase in the follicle cell height from TS8 to TS10/11, followed by a gradual decrease in TS13 and TS15. In the two examined stages of *A. xenodactyloides* cells were smaller compared to

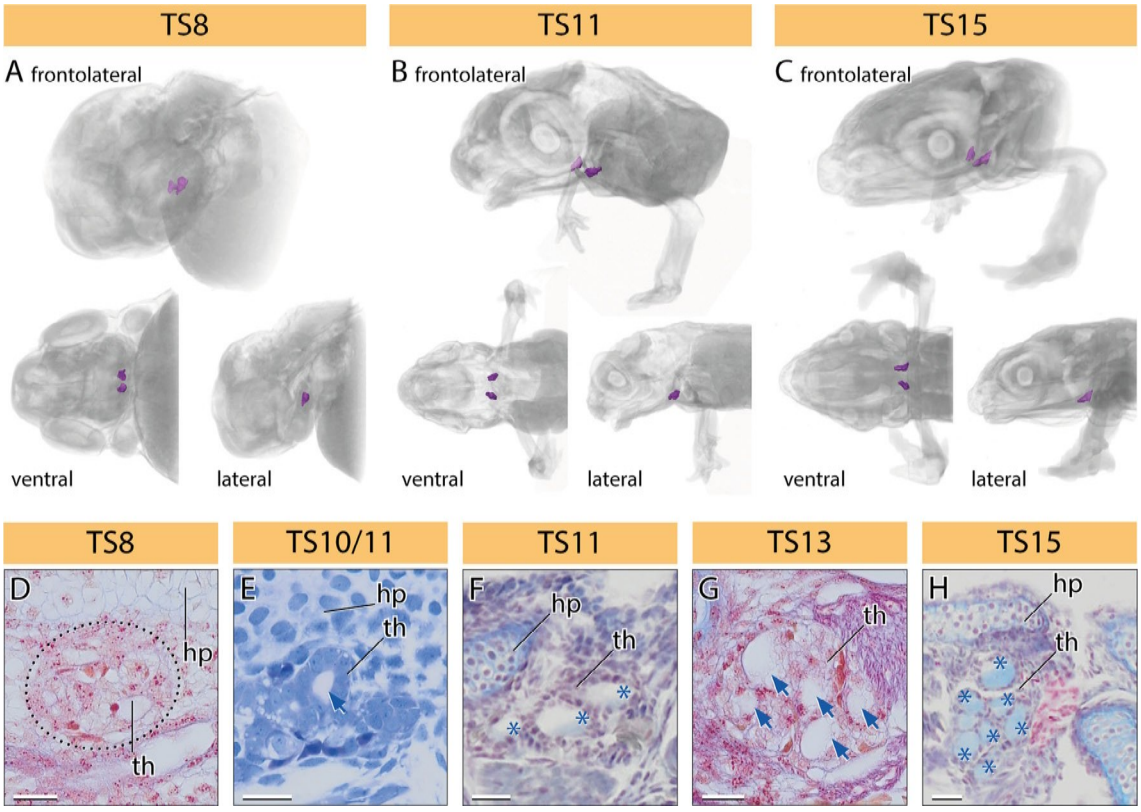

FIGURE 6 (A-C) Volume renderings of μCT scans of different developmental stages of *Arthroleptis xenodactyloides*. The thyroid glands are colored in lilac. Renderings are not to scale. (D-H) Histological cross-sections of the ventral head region of *A. wahlbergii* embryos at different developmental stages. Blue arrows indicate absence of colloid within follicles. Blue asterisks indicate the presence of colloid within follicles. Scale bar is 25 μm. hp, hyoid plate; th, thyroid gland

A. wahlbergii. However, a similar but lower decrease in cell height from TS11 to TS15 is also recognizable (Figure 7(B)). Follicle numbers and follicle diameter are more or less similar in *A. wahlbergii* and *A. xenodactyloides* (Figure 7(C),(D)). In *A. wahlbergi*, follicle number and diameter decrease from TS8 to TS10/11 and then increases gradually from TS10/11 to TS15. In the two specimens of *A. xenodactyloides*, an increase in follicle number and diameter can also be observed.

In summary, our data indicate that thyroid glands differentiate histologically between TS8 and TS10/11, become highly active at TS11 (follicle cell height, first detected colloid) and develop and adult-like morphology between TS13 and TS15 (increasing follicle diameter and number, decreasing cell height).

2.5 | Skin and thyroid gland histology in a *Cardioglossa* tadpole

The skin of *Cardioglossa* sp. at Gosner-stage 27[53] exhibits a pattern typical for most tadpoles.[15] The epidermis is two-layered. The basal layer consists of cuboid cells with spherical nuclei while the apical layer is slightly flattened in the head but not in the trunk region (Figure 8(A1)-(A5)). A dark-blue stained extracellular layer resembling the keratinized apical cell layer present in late *Arthroleptis* embryos can be found. Some unicellular gland cells are present in between basal and apical cells (Figure 8(A1),(A3)). A thick stratum compactum is present beneath the basal epidermal layer. Melanophores are associated with the stratum compactum. Their density decreases dorso-ventrad in the head as well as the trunk region (Figure 8(A1)-(A5)).

The thyroid glands exhibit a more elongated olive-shape and are localized in the same position as described for *Arthroleptis* embryos (Figure 8(B)). At this developmental stage, well developed follicle outlined by slightly flattened epithelial cells can be recognized. No colloid or vascularization was detected in the examined specimen. The flattened follicular epithelial cells and the absence of colloid and vascularization indicate a low activity of TH-production.

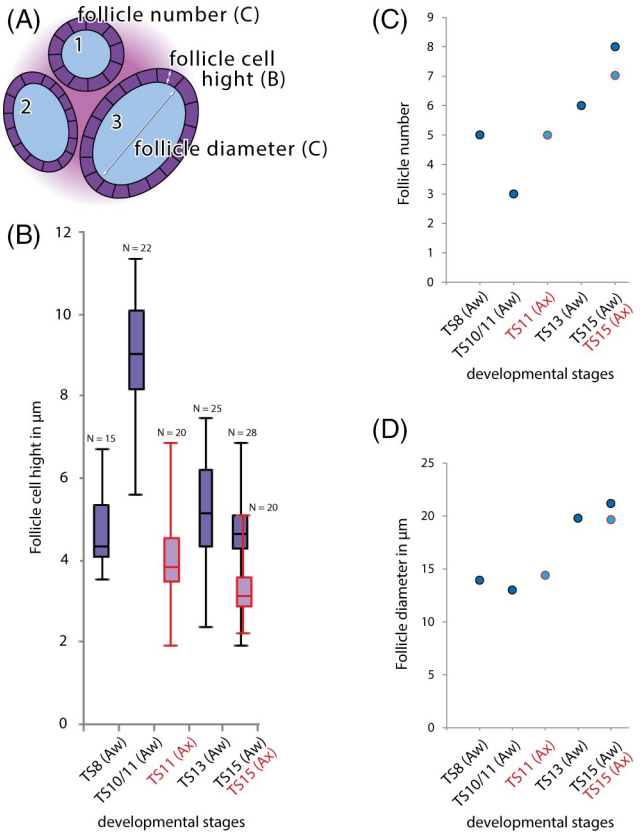

FIGURE 7 (A) Schematic illustration of thyroid gland follicels and the measured parameters. (B) Box plot of the follicle cell height in *Arthroleptis* at different developmental stages. (C) Diagram of the follicle number in *Arthroleptis* at different developmental stages. (D) Diagram of the average follicle diameter in *Arthroleptis* at different developmental stages. Aw, *A. wahlbergi* (black outline); Ax, *A. xenodactyloides* (red outline)

3 | DISCUSSION

3.1 | *Arthroleptis* exhibits accelerated body wall fusion and a phase of metamorphic skin pigmentation repatterning that correlates with increased thyroid gland activity

The skin of frogs harbors a variety of chromatophores.[45] In this study however we focus on the pattern of melanophores only. Different types of melanophores are present in the adult frog skin.[54] This adult pigmentation pattern is established via metamorphic changes in the dermal pigmentation, chromophore morphology, and biochemistry of the tadpole skin.[54] This indicates a correlation of TH production and metamorphic skin pigmentation repatterning in biphasic anurans.[55]

In direct developing species, pigmentation patterning has only been described in *E. coqui*.[33] At TS7, melanophores first appear in the trunk region and pigmentation increases slowly until it becomes heavy at TS10. Pigmentation of the head is delayed, becoming heavy at TS12. This general process of melanophore patterning is also seen in *Arthroleptis* [6] and we here provide the first detailed data on the morphology of different melanophore types during skin development in a direct developing frog species. In *Arthroleptis*, the first type of melanophore is spindle-shaped with long thin extensions. This type is typical of embryonic melanophores in biphasic species.[54,55] A second type of melanophore with a smaller, more circular-shape with a few short or no extensions appears at around TS11. This melanophore type resembles melanophores appearing during TH-mediated metamorphosis in biphasic species.[54,55] It is generally accepted that follicular cell height, follicle diameter and number (see Figure 7(A)) roughly reflect thyroid gland activity and TH production.[56,57] The appearance of this second melanophore type in *Arthroleptis* correlates with a histologically inferred, increased thyroid activity. The timing of pigmentation repatterning and melanophore type appearance in *Arthroleptis* is therefore very similar to the TH-mediated metamorphic transitions seen in the skin of biphasic species.[54,55]

Experimental studies on the pigmentation pattern[24] and histological investigation of thyroid gland activity[27]

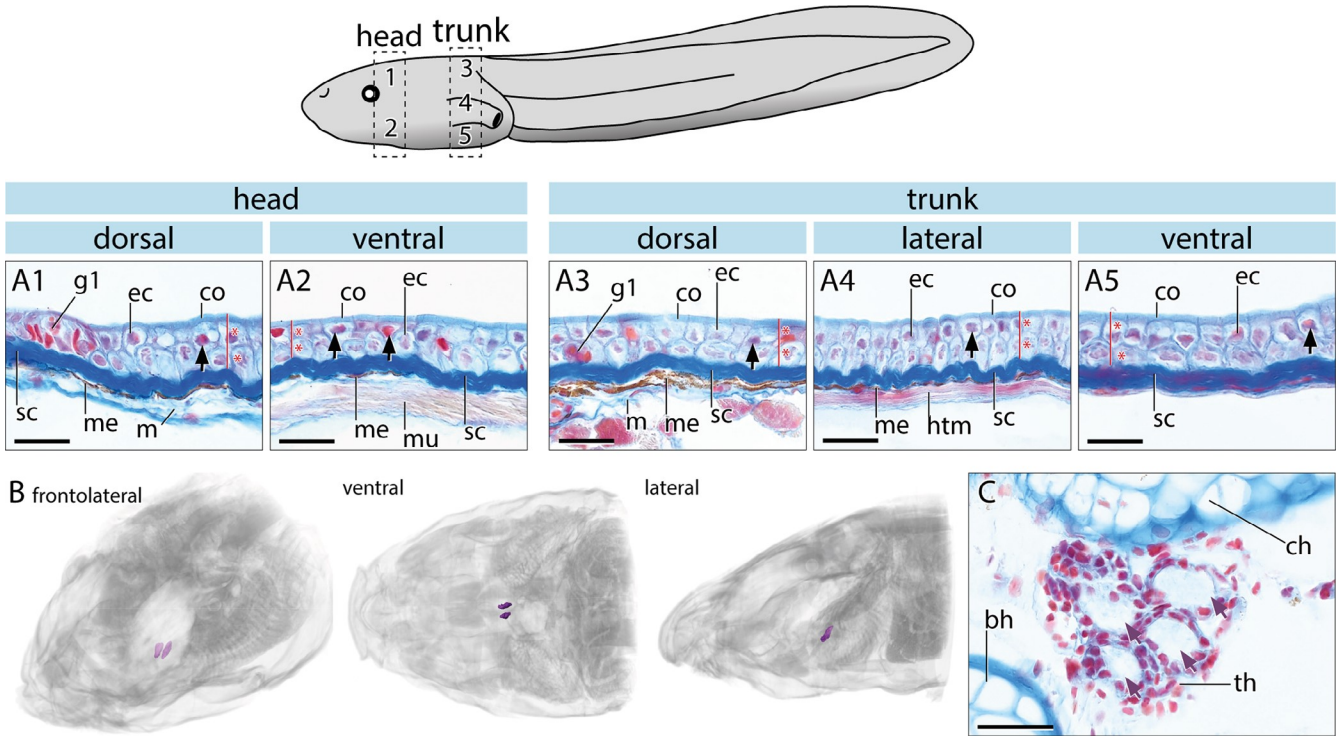

FIGURE 8 (A) Histological cross sections of the skin of a *Cardioglossa manengouba* tadpole at Gosner-stage 27. The schematic tadpole on top illustrates the photographed regions (1–5). Black arrows indicate epidermal nuclei. The number of epidermal cellular layers is indicated by a red line and asterisks. (B) Volume renderings of a synchrotron scan of a *C. manengouba* tadpole at Gosner-stage 27. The thyroid glands are colored in lilac. Renderings are not to scale. (C) Histological cross sections of the ventral head region of the same tadpole as in A. Lilac arrows indicate absence of colloid within follicles. Scale bar is 20 μm. bh, basihyal; ch, ceratohyal; co, keratinized layer; ec, epithel cell; g1, unicellular gland; htm, hypaxonic trunk muscles; m, mesenchyme; me, melanophore; mu, muscle; sc, stratum compactum; th, thyroid gland

in *E. coqui* suggest that TH is also involved in the closure of the pigmented body surface.[23,24] While the overall melanophore patterning and subsequent darkening of the skin are similar in *Arthroleptis* and *E. coqui,* there is a difference in the timing of the ventral fusion of the pigmented lateral body walls. This fusion appears much earlier in *Arthroleptis* (TS9, Figure 2) compared to *E. coqui* at TS12.[24] In *E. coqui* this event correlates with a peak in thyroid gland activity[29] and has experimentally been shown to be TH dependent.[23] In *Arthroleptis*, the thyroid gland appears histologically mature at TS10/11, and the morphology of the thyroid gland of *Arthroleptis* at this TS stage is comparable to histological and hormonal data from *Eleutherodactylus*.[27] Based on this histological comparison and available data from *Eleutherodactylus* we speculate that thyroid gland activity in *Arthroleptis* peaks at between TS11 and TS12. Therefore fusion of the lateral body walls seems slightly accelerated. This could be due to a higher TH-sensitivity of the lateral body wall tissue or a not detected earlier expression of TH due to a weaker correlation of histological maturity and actual TH production in *Arthroleptis* compared to *E. coqui*. Experimental and molecular/immuno-histochemical or mass spectroscopic data from *Arthroleptis* are needed to clarify this.

3.2 | Skin histology in *Arthroleptis* exhibits a phase of metamorphic repatterning that correlates with histologically inferred thyroid gland maturity

Skin and thyroid gland histology of the *Cardioglossa* tadpole are similar to many other tadpoles at a comparable developmental stage.[52] Alterations in skin development in *Arthroleptis* therefore seem to be correlated with the evolution of direct development. However, an apical extracellular layer resembling the stratum corneum in adult frog skin is present in the *C. manengouba* tadpole. Tadpoles of various species of *Cardioglossa*, including *C. manengouba*, have been frequently found buried in

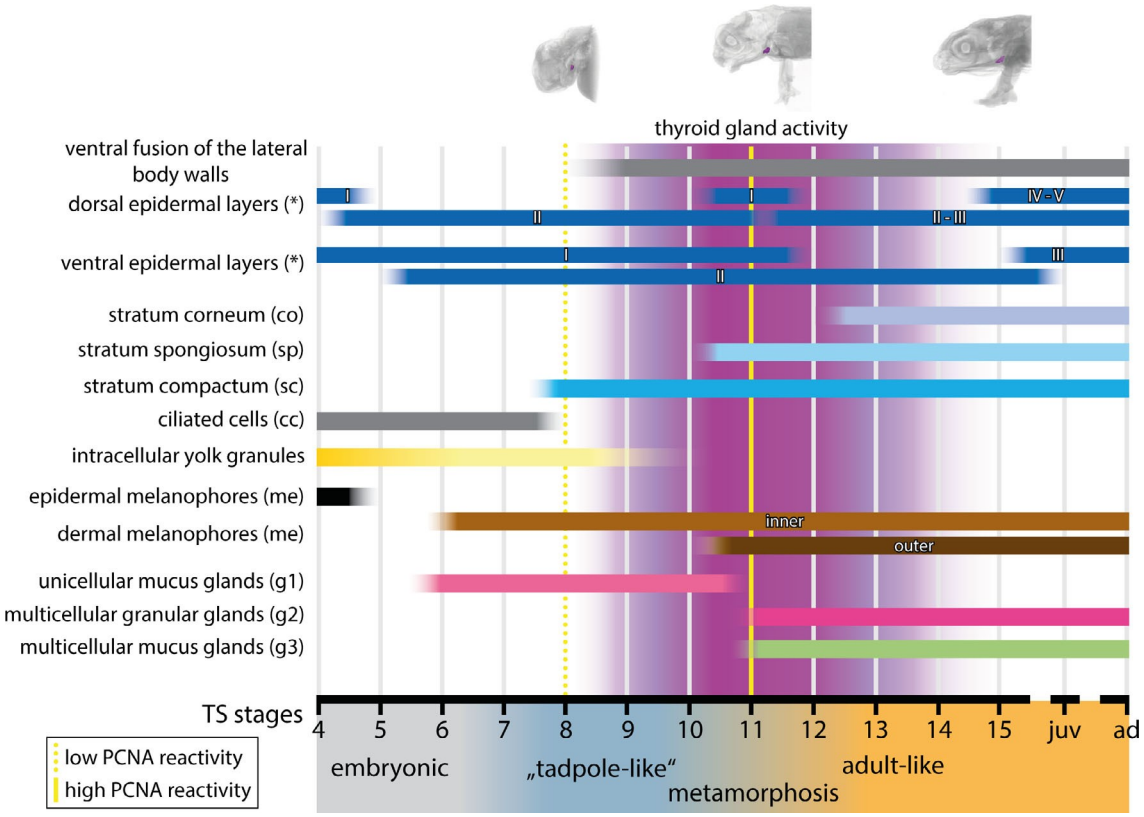

FIGURE 9 Schematic summary of the skin composition of *Arthroleptis* at different developmental stages. Presumptive thyroid gland activity inferred from histological measurements is indicated in lilac

the sediment of streams[58,59] and this putative stratum corneum could be an adaptation to their fossorial life style.

As reported for *E. coqui*[25,31], major tadpole characters such as cement glands, neuromasts and skein cells[48] were not observed in *Arthroleptis*. Data for *Ischnocnema henselii* are not available.[21] In *Arthroleptis*, skin development can be divided into four major phases (embryonic, "tadpole", metamorphic and adult; Figure 9) that are also typical for many biphasic species.[60,61] At TS4 embryonic ectoderm is a single-cell layered epithelium not yet differentiated into an epidermis. At around TS7 the ectodermal cells have differentiated into a tadpole-like epidermis (two-layered, unicellular glands, inner melanophores). However, the epidermis still exhibits some embryonic features (intracellular yolk granules, low melanophore density, ciliated cells and the lack of a stratum compactum; Figure 9). At TS8, the skin exhibits more mature tadpole-like features such as fewer intracellular yolk granules and ciliated cells, a higher melanophore density, many unicellular glands and a stratum compactum. At TS11, degeneration of the apical epidermal layer and unicellular glands together with the appearance of multicellular gland progenitors and an additional outer melanophore layer (Figure 9) resembles skin repatterning during the metamorphic climax of biphasic species.[46,62,63] In biphasic species, shortly before metamorphic climax, apical cells in the tadpole epidermis undergo apoptosis except for the single layer of basal cells. The remaining basal cells proliferate extensively during metamorphic climax building up the adult epidermis and gland cells.[43,47,64] In *Arthroleptis*, metamorphic skin repatterning is seen at TS11, when the "tadpole" apical epidermal layer degenerates and cells in the remaining basal layer start to proliferate (Figure 9; strong PCNA signal). This patterning of the tadpole-like skin and increased PCNA activity correlate with an increase of histologically inferred thyroid gland activity at TS10/11 (see Figure 7). From TS13 on, the skin of *Arthroleptis* exhibits major features of an adult frog skin, such as a multilayered (three to five layers dorsally) epidermis with an apical stratum corneum, large multicellular glands embedded into a stratum spongiosum and a layer of outer and inner melanophores bordering the thick stratum compactum (Figure 9). This in term correlates with a decreased thyroid gland activity, as inferred from histology, and the absence of a PCNA signal in epidermal cells.

Regarding other direct-developing species, detailed histological data are only available for two developmental stages of *I. henselii*.[21] At TS6, the epidermis of this species

is a single-layered epithelium overlaying an undifferentiated mesenchymal dermis.[21] This is very similar to *Arthroleptis* embryos except that the epidermis is two-layered in most body regions at this developmental stage. In *I. henselii* embryos at TS14, epidermal cells start to proliferate forming a two-layered epidermis. Ciliated cells are still present in many body areas, progenitors of multicellular glands are detectable and melanocyte density has increased compared to TS6. The dermis has also differentiated and a stratum compactum is present.[21] This is different to *Arthroleptis,* where the features described for *I. henselii* at TS14 are already present at TS11 (Figure 9). In contrast to *I. henselii*, the short description of a stage likely corresponding to TS9 in *Eleutherodactylus* that exhibits a two-layered epidermis[65], implies an earlier pattern of skin differentiation more similar to *Arthroleptis*. This is very interesting since a histologically differentiated thyroid gland is already present at TS6 in *I. henselii*. This is much earlier compared to *Arthroleptis* (TS8; this study) and *E. coqui* (TS10)[27] and skin development does therefore not seem to correlate with thyroid gland maturation in *I. henselii*.

This mismatch between very early thyroid gland maturation and very late skin remodeling in *I. henselli* could be indicative of a loss of TH-dependency of skin remodeling and hence a loss of constraint. Alternatively, skin maturation might still be dependent on TH-signaling, but TH-production of the thyroid gland could be very low and a concentration necessary to induce skin repatterning is reached very late. Another possibility is that TH-levels are normal but the sensitivity of the skin tissue is decreased, requiring higher TH concentrations to induce repatterning. Both of these TH-dependent scenarios would explain the late onset (ie, heterochronic shift) of skin remodeling.

3.3 | Thyroid gland development and maturation in direct developing frogs

It has been shown that metamorphic changes in anurans, and amphibians in general, are under a complex hormonal control with TH as a major regulator.[17] There are two hypotheses how the ancestral thyroid axis has influenced the evolution of direct development (see Jennings & Hanken, 1998 and references therein). (1) Thyroid gland activity and TH production are activated early in development leading to a precocious formation of adult features. Direct development is still constrained by the ancestral dependency on TH for adult development. Consequently, direct development evolved by a heterochronic shift[66] of ancestral developmental mechanisms rather than the loss of constraints from it ("heterochronic shift" hypothesis). (2) Metamorphosing tissues lost their ancestral TH-dependency. In this case, the loss of constraints would have been more important in the evolution of direct development than heterochronic shifts of ancestral mechanisms ("loss of constraint" hypothesis). Experimental studies on *E. coqui* have shown that this species exhibits a mosaic pattern of heterochronic shifts and loss of constraints for different morphological features.[19,23,27,33,67-70]

There are many similarities between *E. coqui* and *Arthroleptis* regarding metamorphic repatterning processes that correlate with histological thyroid gland maturation, such as tail regression, remodeling of the "larval" into the adult hyobranchial apparatus, and cranial muscle repatterning.[6,19,27,33,71] Most of these processes start slightly earlier in *Arthroleptis*, which correlates with an earlier appearance of the thyroid glands compared to *E. coqui* (Jennings & Hanken, 1998; this study). Assuming that histologically inferred thyroid gland maturity roughly correlates with its activity and the production of TH, *Ischnocnema henselii* might be another example where some features of skin development might have lost their dependency on TH. However, the interpretation of the data for *I. henselii* is hampered by the lack of a detailed investigation of thyroid gland and skin development over several developmental stages.

Our data indicate that many tadpole specific structures appear, differentiate, and are repatterned to the adult configuration during a short metamorphic phase that correlates with the histological thyroid gland maturation is in many biphasic taxa undergoing a metamorphosis. Although this cryptic metamorphosis appears to be not as climactic as it is in biphasic frogs.

3.4 | Developmental constraints, heterochrony and the parallel evolution of direct development

Direct development has evolved in parallel in different groups of frogs. The comparison of embryonic development of these direct developing frogs offers the possibility to identify how developmental constraints may have influenced the observed pattern of parallel evolution. Many developmental mechanisms are governed by major regulators such as TH. In case of a heterochronic shift of this regulator (eg, embryonic thyroid maturity and its inferred activity in direct developing frogs), traits that are under the control of this regulator have to follow this shift (they are constrained). Other traits not dependent on TH are not constrained by this hormone and do not follow the heterochronic shift of this regulator. This may lead to a decoupling of ancestrally synchronous processes

such as, for example, growth and differentiation of the retinotectal system in *E. coqui*.[35]

Further investigations of the developmental timing and experiments testing the TH-dependency of anatomical features of *Eleutherodactylus*, *Arthroleptis*, *Ischnocnema* and other direct developing frogs are needed to test the inferences made in this study. These investigations will clarify if repatterning of different tissues like the skin, muscles, cartilaginous and bony skeleton are generally under the control of TH and therefore constrained by thyroid gland activity. Studies on direct development in frogs, or amphibians in general, and various other cases such as the classic example of the evolution of similar morphotypes in African cichlids[72,73] or the recently "re-discovered" dispersion/re-aggregation and diapause phases in early killifish development[74,75] will help to better understand how developmental processes constrain the evolution of adaptive traits and further clarify mechanisms and identify major regulators underlying parallel evolution.

4 | EXPERIMENTAL PROCEDURES

4.1 | Specimens

Embryos of *Arthroleptis wahlbergii* Smith, 1849, collected in South Africa, and *A. xenodactyloides* Hewitt, 1933, collected in Tanzania, were euthanized using 0.1% tricaine methanesulfonate (MS222, Fluka), fixed in 4% phosphate buffered formalin and stored in 70% ethanol.[6] Staging of embryos follows Townsend and Stewart (1985); TS stages hereafter. One tadpole of *Cardioglossa manengouba* Blackburn, 2008 was available for investigation. For a complete list of specimen see Table 1.

4.2 | Histological sectioning and staining

For sectioning, embryos were dehydrated in an ethanol series (70%, 90%, 2 x 96%; 5 minutes each), sectioned and subsequently rehydrated (2 x 96%, 90%, 70% ethanol, distilled water; 5 minutes each) prior to staining. Embryos up to TS8 were embedded in Technovit 8100 (Kulzer, R0010022), sectioned at 3 μm and stained with a mixture of basophilic Methylene blue and acidic Fuchsin.[76] Embryos from TS10/11 on were decalcified for up to three days (Osteomoll, Merck), embedded in Paraplast (Roth, X881.1), sectioned at 8 μm and stained with Heidenhain's Azan.[76] All sections were made using a Microm HM 360 (Zeiss) and photographs were taken using an Olympus Dotslide BX51 microscope.

4.3 | Fluorescent antibody staining

Paraffin sections were rehydrated as described before. For antigen retrieval, slides were transferred to a plastic cuvette with citrate buffer (recipe see Schlosser, 2008) and heated in a microwave (Bosch HMT 72 M 420) for 10 minutes at 180 W. Subsequently, slides were placed at room temperature (RT, 21-25°C) to cool down for at least 5 minutes and then rinsed in distilled water for 1 minute. Afterwards, slides were rinsed with PBS (3 x 5 minutes), placed into a wet chamber and blocked with antibody diluent (DAKO) for 1 hour at RT. Primary antibodies against proliferating cell nuclear antigen (PCNA-1, 1/200, sc-7907, Santa Cruz; PCNA-2, 1/200, M087901, Dako) were applied overnight at 4°C. On the next day, slides were rinsed in PBS (3 x 5 minutes), blocked and incubated with secondary antibodies (Alexa-488 anti-mouse, #A28175, Thermo Fisher Scientific and Alexa-568 anti-rabbit, #A-11011, Thermo Fisher Scientific) for 1 hour at RT. Afterwards, slides were rinsed with PBS (3 x 5 minutes), quickly washed with distilled water and cover-slipped with Fluoroshield with DAPI (Sigma, F6057). Slides were photographed using a Zeiss Axioplan Microscope equipped with a Spot camera and the Zeiss Axioplan software.

4.4 | Micro-CT scanning and 3D reconstruction

Specimens were contrasted using a solution of 1% polymolybdenic acid in 70% ethanol.[77] *Arthroleptis* specimens were CT-scanned using a Nanotom S μCT scanner (Phoenix X-Ray) and the *Cardioglossa* tadpole was studied using synchrotron radiation based x-ray micro-CT. Imaging was performed at the Imaging Beamline P05 (IBL)[78-80] operated by the Helmholtz-Zentrum-Geesthacht at the storage ring PETRA III (Deutsches Elektronen Synchrotron - DESY, Hamburg, Germany) using a photon energy of 24 keV. Projections were recorded using a CCD camera system (MicroLine ML09000 - Finger Lake Instruments) with an effective pixel size of 2.42 μm. For each tomographic scan 1801 projections at equal intervals between 0 and π have been recorded. Tomographic reconstruction has been done by applying a filtered back projection algorithm (FBP) implemented in a custom reconstruction pipeline [81] using Matlab (Math-Works) and the Astra Toolbox.[82-84] For the tomographic reconstruction, raw projections

TABLE 1 Specimen list

ID	TS stage	Species	Technique	Staining
#01	3	*A. wahlbergi*	photo	-
#02	4	*A. wahlbergi*	histology/photo	MB-aF/ -
#03	5	*A. wahlbergi*	histology/photo	MB-aF/ -
#04	5/6	*A. wahlbergi*	photo	-
#05	5/6	*A. wahlbergi*	photo	-
#06	6	*A. wahlbergi*	histology/photo	MB-aF/ -
#07	6/7	*A. wahlbergi*	photo	-
#08	7	*A. xenodactyloides*	histology	MB-aF
#09	7	*A. wahlbergi*	photo	-
#10	8	*A. xenodactyloides*	µCT	1% PMA
#11	8	*A. wahlbergi*	histology/ICH	MB-aF/anti-PCNA
#12	8	*A. wahlbergi*	photo	-
#13	8	*A. wahlbergi*	photo	-
#14	9	*A. xenodactyloides*	histology	MB-aF
#15	9	*A. wahlbergi*	photo	-
#16	10	*A. wahlbergi*	photo	-
#17	10	*A. wahlbergi*	photo	-
#18	11	*A. xenodactyloides*	µCT	1% PMA
#19	11	*A. xenodactyloides*	histology	Azan
#20	11	*A. wahlbergi*	histology/ICH	Azan/anti-PCNA
#21	11	*A. wahlbergi*	photo	-
#22	11	*A. wahlbergi*	photo	-
#23	11/12	*A. wahlbergi*	photo	-
#24	12	*A. wahlbergi*	photo	-
#25	12	*A. wahlbergi*	photo	-
#26	12/13	*A. wahlbergi*	photo	-
#27	13	*A. xenodactyloides*	histology	Azan
#28	13	*A. wahlbergi*	histology/ICH	Azan/anti-PCNA
#29	13	*A. wahlbergi*	photo	-
#30	13	*A. wahlbergi*	photo	-
#31	14	*A. wahlbergi*	photo	-
#32	14/15	*A. wahlbergi*	photo	-
#33	15	*A. xenodactyloides*	µCT	1% PMA
#34	15	*A. xenodactyloides*	histology	Azan
#35	15	*A. wahlbergi*	histology/ICH	Azan/anti-PCNA
#36	15	*A. wahlbergi*	photo	-
#37	15	*A. wahlbergi*	photo	-
#38	15	*A. wahlbergi*	photo	-
#39	adut, 1.3 cm	*A. wahlbergi*	histology	Azan
#40	adult, 2 cm	*A. wahlbergi*	histology	Azan
#41	tadpole	*Cardioglossa* sp.	histology	Azan

Abbreviations: ICH, immune-histochemistry; MB-aF, Methylene blue acidic Fuchsin; PMC, polymolybdenic acid; µCT, micro-computed tomography.

were binned two times resulting in an effective pixel size of the reconstructed volume of 4.83 µm. Thyroid glands are easily recognizable as ovoid organs, with dense epithelial cells (light grey) surrounding follicular lumina (black), ventrally on both sides of the hypobranchial plate. Three-dimensional reconstructions and mixed surface-volume renderings of the thyroid gland were prepared using AMIRA 5.4.2 (FEI Visualization, Science Group, Bordeaux, France).

4.5 | Follicle cell height and follicle diameter measurements

Qualitative and quantitative descriptions of thyroid glands are based on sections from the middle region of the paired thyroid lobes according to Cruz and Fabrezi (2020). Measurements of follicle cell heights and follicle diameter were obtained from digitalized sections using ImageJ.[85] A box and whisker plot of follicle cell heights was prepared using Microsoft Excel 2010. Numbers of follicles were counted and mean values of the measured follicle diameters were calculated for each specimen investigated.

4.6 | Photographs and Image processing

Photographs of whole embryos were taken using a Zeiss Discovery V12 stereomicroscope with an attached Zeiss AxioCam digital camera. Brightness and Contrast of Images was adjusted using either ImageJ or Adobe Photoshop CS6. Channel colors of fluorescent antibody staining were assigned in ImageJ. In some images the "CLAHE" filter implemented in ImageJ was applied to enhance local contrast.

ACKNOWLEDGEMENTS

We would like to thank Katja Felbel for valuable help in the laboratory. We thank Mark-Oliver Rödel for critical reading of the manuscript and a photograph of an adult *C. manengouba* and Mareike Hirschfeld for a photograph of a *C. manengouba* tadpole. We thank Lennart Olsson for critical reading of the manuscript. We thank Paul Lukas for help with the Dot Slide Microscope. We would also like to thank Christoph Englert, Birgit Perner and Dagmar Kruspe for the kind gift of the two PCNA antibodies.

ORCID

Benjamin Naumann https://orcid.org/0000-0003-0970-2431

Hendrik Müller https://orcid.org/0000-0001-6764-7376

REFERENCES

1. Schluter D, Clifford EA, Nemethy M, McKinnon JS. Parallel evolution and inheritance of quantitative traits. *Am Nat*. 2004; 163(6):809-822.
2. Simpson GG. *Principles of Animal Taxonomy*. New York: Columbia University Press; 1961.
3. Futuyma D, Kirkpatrick M. *Evolution*. Sunderland, MA: Sinauer; 2017.
4. Wake D, Hanken J. Direct development in the lungless salamanders: what are the consequences for developmental biology, evolution and phylogenesis? *Int J Develop Biol*. 1996;40(4): 859-869.
5. San Mauro D, Gower DJ, Müller H, et al. Life-history evolution and mitogenomic phylogeny of caecilian amphibians. *Mol Phylogenet Evol*. 2014;73:177-189.
6. Schweiger S, Naumann B, Larson JG, Möckel L, Müller H. Direct development in African squeaker frogs (Anura: Arthroleptidae: *Arthroleptis*) reveals a mosaic of derived and plesiomorphic characters. *Organ Divers Evol*. 2017;17(3): 693-707.
7. Thibaudeau G, Altig R. Endotrophic anurans: development and evolution. In: McDiarmid R W, Altig R, eds. *Tadpoles: The Biology of Anuran Larvae*. 1st ed. Chicago and London: The University of Chicago Press; 1999;170-188.
8. Hall BK, Olson WM. *Keywords and Concepts in Evolutionary Developmental Biology*. Cambridge: Harvard University Press; 2003.
9. Goin OB, Goin CJ. Amphibian eggs and the montane environment. *Evolution*. 1962;16:364-371.
10. Müller H, Liedtke HC, Menegon M, et al. Forests as promoters of terrestrial life-history strategies in east African amphibians. *Biol Lett*. 2013;9(3):20121146.
11. Liedtke HC, Müller H, Hafner J, et al. Terrestrial reproduction as an adaptation to steep terrain in African toads. *Proc R Soc B*. 2017;284(1851):20162598.
12. Brink Ht ORE, de Roos AM. Habitat deterioration promotes the evolution of direct development in metamorphosing species. *Evolution*. 2020.74(8):1826-1850.
13. Goldberg J, Candioti FV, Akmentins MS. Direct-developing frogs: ontogeny of *Oreobates barituensis* (Anura: Terrarana) and the development of a novel trait. *Amphibia-Reptilia*. 2012; 33(2):239-250.
14. Heinicke MP, Duellman WE, Trueb L, Means DB, MacCulloch RD, Hedges SB. A new frog family (Anura: Terrarana) from South America and an expanded direct-developing clade revealed by molecular phylogeny. *Zootaxa*. 2009;2211(1):1-35.
15. McDiarmid RW, Altig R. *Tadpoles: the Biology of Anuran Larvae*. 1st ed. Chicago and London: University of Chicago Press; 1999.
16. Altig R, McDiarmid RW. Diversity: Familial and Generic Characterizations. In: McDiarmid RW, Altig R, eds. *Tadpoles: The Biology of Anuran Larvae*. 1st ed. Chicago and London: The University of Chicago Press; 1999;295-338.
17. Shi Y-B. *Amphibian Metamorphosis: from Morphology to Molecular Biology*. 1st ed. New York: John Wiley & Sons, Inc; 1999.
18. Callery EM, Fang H, Elinson RP. Frogs without polliwogs: evolution of anuran direct development. *Bioessays*. 2001;23(3): 233-241.

19. Hanken J, Klymkowsky MW, Alley KE, Jennings DH. Jaw muscle development as evidence for embryonic repatterning in direct-developing frogs. *Proc Biol Sci*. 1997;264:1349-1354.
20. Hanken J, Klymkowsky MW, Summers CH, Seufert DW, Ingebrigtsen N. Cranial ontogeny in the direct-developing frog, *Eleutherodactylus coqui* (Anura: Leptodactylidae), analyzed using whole-mount immunohistochemistry. *J Morphol*. 1992;211(1):95-118.
21. Goldberg J, Taucce PP, Quinzio SI, Haddad CF, Candioti FV. Increasing our knowledge on direct-developing frogs: the ontogeny of *Ischnocnema henselii* (Anura: Brachycephalidae). *Zool Anz*. 2020;284:78-87.
22. Kerney R, Meegaskumbura M, Manamendra-Arachchi K, Hanken J. Cranial ontogeny in *Philautus silus* (Anura: Ranidae: Rhacophorinae) reveals few similarities with other direct-developing anurans. *J Morphol*. 2007;268(8):715-725.
23. Callery EM, Elinson RP. Thyroid hormone-dependent metamorphosis in a direct developing frog. *Proc Natl Acad Sci*. 2000; 97(6):2615-2620.
24. Elinson R, Fang H. Secondary coverage of the yolk by the body wall in the direct developing frog, *Eleutherodactylus coqui*: an unusual process for amphibian embryos. *Dev Genes Evol*. 1998; 208(8):457-466.
25. Fang H, Elinson RP. Patterns of distal-less gene expression and inductive interactions in the head of the direct developing frog *Eleutherodactylus coqui*. *Dev Biol*. 1996;179(1):160-172.
26. Hanken J, Carl TF, Richardson MK, et al. Limb development in a "nonmodel" vertebrate, the direct-developing frog *Eleutherodactylus coqui*. *J Exp Zool*. 2001;291(4):375-388.
27. Jennings DH, Hanken J. Mechanistic basis of life history evolution in anuran amphibians: thyroid gland development in the direct-developing frog, *Eleutherodactylus coqui*. *Gen Comp Endocrinol*. 1998;111(2):225-232.
28. Kerney R, Gross JB, Hanken J. Early cranial patterning in the direct-developing frog *Eleutherodactylus coqui* revealed through gene expression. *Evol Dev*. 2010;12(4):373-382.
29. Laslo M, Denver RJ, Hanken J. Evolutionary conservation of thyroid hormone receptor and deiodinase expression dynamics in ovo in a direct-developing frog, *Eleutherodactylus coqui*. *Front Endocrinol*. 2019;10:307.
30. Olsson L, Moury DJ, Carl TF, Håstad O, Hanken J. Cranial neural crest-cell migration in the direct-developing frog, *Eleutherodactylus coqui*: molecular heterogeneity within and among migratory streams. *Fortschr Zool*. 2002;105(1):3-13.
31. Schlosser G, Kintner C, Northcutt RG. Loss of ectodermal competence for lateral line placode formation in the direct developing frog *Eleutherodactylus coqui*. *Dev Biol*. 1999;213(2):354-369.
32. Schlosser G, Roth G. Evolution of nerve development in frogs; pp. 94–112. *Brain Behav Evol*. 1997;50(2):94-112.
33. Townsend DS, Stewart MM. Direct development in *Eleutherodactylus coqui* (Anura: Leptodactylidae): a staging table. *Copeia*. 1985;1985:423-436.
34. Thomas R. New species of antillean *Eleutherodactylus*. *Q J Florida Acad Sci*. 1966;28(4):375-391.
35. Schlosser G. Development of the retinotectal system in the direct-developing frog *Eleutherodactylus coqui* in comparison with other anurans. *Front Zool*. 2008;5(1):9.
36. Hanken J, Summers CH. Skull development during anuran metamorphosis: III. Role of thyroid hormone in chondrogenesis. *J Exp Zool*. 1988;246(2):156-170.
37. Ziermann JM, Diogo R. Cranial muscle development in frogs with different developmental modes: direct development versus biphasic development. *J Morphol*. 2014;275(4):398-413.
38. Varga JF, Bui-Marinos MP, Katzenback BA. Frog skin innate immune defences: sensing and surviving pathogens. *Front Immunol*. 2019;9:3128.
39. Fernandes TL, Antoniazzi MM, Sasso-Cerri E, et al. Carrying progeny on the back: reproduction in the Brazilian aquatic frog *Pipa carvalhoi*. *S Am J Herpetol*. 2011;6(3):161-176.
40. Huang L, Li J, Anboukaria H, Luo Z, Zhao M, Wu H. Comparative transcriptome analyses of seven anurans reveal functions and adaptations of amphibian skin. *Sci Rep*. 2016;6(1):1-11.
41. Douglas AJ, Hug LA, Katzenback BA. Composition of the north American wood frog (*Rana sylvatica*) skin microbiome and seasonal variation in community structure. *bioRxiv*; 2020.
42. Katz U. The role of amphibian epidermis in osmoregulation and its adaptive response to changing environment. *Biology of the Integument*. Berlin, Heidelberg: Springer; 1986:472-498.
43. Yoshizato K. Death and transformation of larval cells during metamorphosis of anura. *Develop Growth Different*. 1992;34(6): 607-612.
44. Quinzio SI, Goldberg J. Transient integumentary structures in *Boana riojana* (Anura, Hylidae) tadpoles. *Amphibia-Reptilia*. 2019;40(4):543-549.
45. Duellman WE, Trueb L. *Biology of Amphibians*. 1st ed. Baltimore: Johns Hopkins University Press; 1994.
46. Fox H. Changes in amphibian skin during larval development and metamorphosis. In: M Balls MB, ed. *Metamorphosis*. Clarendon Press, Oxford; 1985.
47. Kinoshita T, Sasaki F. Body-specific proliferation of adult precursor cells in *Xenopus* larval epidermis. *Histochemistry*. 1994; 101(6):397-404.
48. Tamakoshi T, Oofusa K, Yoshizato K. Visualization of the initiation and sequential expansion of the metamorphic conversion of anuran larval skin into the precursor of adult type. *Dev Growth Differ*. 1998;40(1):105-112.
49. Brown DD, Cai L. Amphibian metamorphosis. *Dev Biol*. 2007; 306(1):20-33.
50. Tata JR. Amphibian metamorphosis as a model for the developmental actions of thyroid hormone. *Mol Cell Endocrinol*. 2006;246(1–2):10-20.
51. Kulkarni SS, Singamsetty S, Buchholz DR. Corticotropin-releasing factor regulates the development in the direct developing frog, *Eleutherodactylus coqui*. *Gen Comp Endocrinol*. 2010;169(3):225-230.
52. Cruz JC, Fabrezi M. Histology and microscopic anatomy of the thyroid gland during the larval development of *Pseudis platensis* (Anura, Hylidae). *J Morphol*. 2020;281(1):122-134.
53. Gosner KL. A simplified table for staging anuran embryos and larvae with notes on identification. *Herpetologica*. 1960;16(3):183-190.
54. Yasutomi M. Migration of epidermal melanophores to the dermis through the basement membrane during metamorphosis in the frog, *Rana japonica*. *Pigment Cell Res*. 1987;1(3):181-187.
55. Smith-Gill SJ, Carver V. Biochemical characterization of organ differentiation and maturation. *Metamorphosis*. Boston: Springer; 1981:491-544.
56. Coleman R, Evennett P, Dodd J. Ultrastructural observations on the thyroid gland of *Xenopus laevis* Daudin throughout metamorphosis. *Gen Comp Endocrinol*. 1968;10(1):34-46.

57. Grim KC, Wolfe M, Braunbeck T, et al. Thyroid histopathology assessments for the amphibian metamorphosis assay to detect thyroid-active substances. *Toxicol Pathol*. 2009;37(4):415-424.
58. Blackburn DC. A new species of *Cardioglossa* (Amphibia: Anura: Arthroleptidae) endemic to mount Manengouba in the Republic of Cameroon, with an analysis of morphological diversity in the genus. *Zool J Linn Soc*. 2008;154(3):611-630.
59. Hirschfeld M, Barej MF, Gonwouo NL, Rödel M-O. Tadpole descriptions of three *Cardioglossa* species from southwestern Cameroon (Amphibia: Anura: Arthroleptidae). *Salamandra*. 2012;48(3):147-156.
60. Fox H. The skin of amphibia. *Biol Integument Vertebrates*. 1986; 2:78-148.
61. Robinson DH, Heintzelman MB. Morphology of ventral epidermis of *Rana catesbeiana* during metamorphosis. *Anat Rec*. 1987;217(3):305-317.
62. Verma K. Regional differences in skin gland differentiation in *Rana pipiens*. *J Morphol*. 1965;117(1):73-85.
63. Gaupp E, Ecker AA. *Ecker's und R. Wiedersheim's Anatomie des Frosches. 3. Lehre von den Eingeweiden, dem Integument und den Sinnesorganen*. Wiesbaden: Vieweg; 1904.
64. Schreiber AM, Brown DD. Tadpole skin dies autonomously in response to thyroid hormone at metamorphosis. *Proc Natl Acad Sci*. 2003;100(4):1769-1774.
65. Adamson L, Harrison R, Bayley I. The development of the whistling frog *Eleutherodactylus martinicensis* of Barbados. *Proc Zool Soc London*. 1960;133(3):453-469.
66. Gould SJ. *Ontogeny and Phylogeny*. Cambridge: Harvard University Press; 1977.
67. Hughes A. The thyroid and the development of the nervous system in *Eleutherodactylus martinicensis*: an experimental study. *Development*. 1966;16(3):401-430.
68. Hughes A, Reier P. A preliminary study on the effects of bovine prolactin on embryos of *Eleutherodactylus ricordii*. *Gen Comp Endocrinol*. 1972;19(2):304-312.
69. Lynn WG. The effects of thiourea and phenylthiourea upon the development of *Eleutherodactylus ricordii*. *Biol Bull*. 1948;94(1):1-15.
70. Lynn WG, Peadon AM. The role of the thyroid gland in direct development in the anuran, *Eleutherodactylus martinicensis*. *Growth*. 1955;19(4):263-285.
71. Schweiger S, Naumann B, Müller H. The ghost of the tadpole - Embryonic development of the cranial musuloskeletal system in African squeaker frogs (Arthroleptis) reveals heterochronic shifts and parallel evolution of differential metamorphosis in direct developing frogs. in prep.
72. Elmer KR, Fan S, Kusche H, et al. Parallel evolution of Nicaraguan crater lake cichlid fishes via non-parallel routes. *Nat Commun*. 2014;5(1):1-8.
73. Meier JI, Marques DA, Wagner CE, Excoffier L, Seehausen O. Genomics of parallel ecological speciation in Lake Victoria cichlids. *Mol Biol Evol*. 2018;35(6):1489-1506.
74. Furness AI, Reznick DN, Springer MS, Meredith RW. Convergent evolution of alternative developmental trajectories associated with diapause in African and south American killifish. *Proc R Soc B*. 2015;282(1802):20142189.
75. Naumann B, Englert C. Dispersion/reaggregation in early development of annual killifishes: phylogenetic distribution and evolutionary significance of a unique feature. *Dev Biol*. 2018;442(1):69-79.
76. Mulisch M, Welsch U. *Romeis Mikroskopische Technik*. 8th ed. Heidelberg: Spektrum Akademischer Verlag; 2010.
77. Metscher BD. MicroCT for comparative morphology: simple staining methods allow high-contrast 3D imaging of diverse non-mineralized animal tissues. *BMC Physiol*. 2009;9(1):11.
78. Greving I, Wilde F, Ogurreck M, et al. P05 imaging beamline at PETRA III: first results. Paper presented at: Proceedings of SPIE - Developments in X-Ray Tomography IX; August 17, 2014 2014; San Diego, California, United States.
79. Haibel A, Ogurreck M, Beckmann F, et al. Micro- and nano-tomography at the GKSS imaging beamline at PETRA III. *Proc SPIE*. 2010;7804:78040B.
80. Wilde F, Ogurreck M, Greving I, et al. Micro-CT at the imaging beamline P05 at PETRA III. *AIP Conf Proc*. 2016;1741(1): 030035. https://doi.org/10.1063/1.4952858.
81. Moosmann J, Ershov A, Weinhardt V, et al. Time-lapse X-ray phase-contrast microtomography for in vivo imaging and analysis of morphogenesis. *Nat Protoc*. 2014;9(2):294-304. https://doi.org/10.1038/nprot.2014.033.
82. Palenstijn WJ, Batenburg KJ, Sijbers J. Performance improvements for iterative electron tomography reconstruction using graphics processing units (GPUs). *J Struct Biol Nov*. 2011;176 (2):250-253. https://doi.org/10.1016/j.jsb.2011.07.017.
83. van Aarle W, Palenstijn WJ, De Beenhouwer J, et al. The ASTRA toolbox: a platform for advanced algorithm development in electron tomography. *Ultramicroscopy*. 2015;157:35-47. https://doi.org/10.1016/j.ultramic.2015.05.002.
84. van Aarle W, Palenstijn WJ, Cant J, et al. Fast and flexible X-ray tomography using the ASTRA toolbox. *Opt Express*. 2016;24 (22):25129-25147. https://doi.org/10.1364/Oe.24.025129.
85. Schneider CA, Rasband WS, Eliceiri KW. NIH image to ImageJ: 25 years of image analysis. *Nat Methods*. 2012;9(7): 671-675.
86. Feng Y-J, Blackburn DC, Liang D, et al. Phylogenomics reveals rapid, simultaneous diversification of three major clades of Gondwanan frogs at the cretaceous–Paleogene boundary. *Proc Natl Acad Sci*. 2017;114(29):E5864-E5870.

How to cite this article: Naumann B, Schweiger S, Hammel JU, Müller H. Parallel evolution of direct development in frogs - Skin and thyroid gland development in African Squeaker Frogs (Anura: Arthroleptidae: *Arthroleptis*). *Developmental Dynamics*. 2021;1–17. https://doi.org/10.1002/dvdy.275

CHAPTER 4

Don't go with the flow: Cranial morphology of fast-flowing stream tadpoles in the Afrobatrachian family Arthroleptidae

Authors: **Schweiger, S.**; Rödel, M.O.; Hammel, J. U.; Müller, H.

Status: Drafted manuscript

FORMULAR 1

Manuskript Nr.: 4

Titel des Manuskriptes: Don't go with the flow: Cranial morphology of fast-flowing stream tadpoles in the Afrobatrachian family Arthroleptidae

Autoren: Schweiger, Susan; Rödel, Mark-Oliver; Hammel, Jörg U.; Müller, Hendrik

Der Kandidat / Die Kandidatin ist (bitte ankreuzen)

☒ Erstautor/-in, ☐ Ko-Erstautor/-in, ☐ Korresp. Autor/-in, ☐ Koautor/-in.

Status (falls nicht publiziert; „zur Publikation eingereicht", „in Vorbereitung"): In Vorbereitung (drafted manuscript)

Anteile (in %) der Autoren / der Autorinnen an der Publikation (anzugeben ab 20%):

Autor/-in	Konzeptionell	Datenanalyse	Experimentell	Verfassen des Manuskriptes	Bereitstellung von Material
Schweiger, S.	95%	95%	90%	90%	
Rödel, M.-O.					40%
Hammel, J. U.					
Müller, H.					60%

Don't go with the flow: Cranial morphology of fast-flowing stream tadpoles in the Afrobatrachian family Arthroleptidae

Susan Schweiger[1], Mark-Oliver Rödel[2], Jörg. U. Hammel[3], Hendrik Müller[4]

[1]Institut für Zoologie und Evolutionsforschung, Friedrich-Schiller-University Jena, Germany
[2]Museum für Naturkunde, Leibniz-Institut für Evolutions- und Biodiversitätsforschung, Berlin, Germany
[3]Helmholtz-Zentrum Geesthacht, Zentrum für Material- und Küstenforschung, Hereon-Außenstelle am DESY, Hamburg, Germany
[4]Zentralmagazin Naturwissenschaftlicher Sammlungen, Martin-Luther-Universität Halle-Wittenberg, Halle (Saale), Germany

Correspondence: Susan Schweiger, Institut für Zoologie und Evolutionsforschung, Friedrich-Schiller-Universität Jena, Erbertstraße 1, 07743 Jena, Germany
Email: susan.schweiger@uni-jena.de

Abstract

Within Arthroleptidae, a taxon of sub-Saharan frogs of the clade Afrobatrachia, a high ecological and reproductive diversity has evolved. Arthroleptid tadpoles predominately occur in flowing water systems of montane or hilly areas. Tadpole skeletal morphology, associated musculature and the relationship between tadpole morphology and lifestyle are poorly understood. To examine this question we investigated the cranial morphology of four arthroleptid tadpoles — *Leptopelis parkeri* BARBOUR & LOVERIDGE 1928, *Astylosternus occidentalis* PARKER 1931, *Trichobatrachus robustus* BOULENGER 1900 and *Nyctibates corrugatus* BOULENGER 1904. All live in streams of lowland or montane forests, but the microhabitat of each of these species differs regarding water flow velocity. We found that the muscolskeletal systems of the tadpoles of *A. occidentalis, N. corrugatus* and *T. robustus* are highly modified relative to *L. parkeri.* Modifications include wide, robust and partly or completely fused cornua trabeculae, a fused and strongly chondrified cartilago labialis superior as well as several modifications of the palatoquadrate. The cranial muscles accompany the modifications of the robust chondrocranium. Beside these common modifications there is also variation among the closely reated *A. occidentalis, N. corrugatus* and *T. robustus.* The presence of a big processus hyoquadratis is only seen in the tadpole of *N. corrugatus,* indicating a possible autapomorphy of the genus *Nyctibates* that may have evolved as an adaptation to its microhabitat. Collectively, our data reveal modifications of cranial morphology in arthroleptid tadpoles that are associated with the different microhabitats they inhabit.

Key words

Afrobatrachia, Arthroleptidae, mountain stream tadpoles, cranial morphology, habitat ecology

Introduction

There is high diversity in anuran larval morphology that results from adaptions to different habitats. In Afrobatrachia, a clade of endemic sub-Saharan frogs, a high degree of ecological and reproductive diversity has evolved primarily in lowland and montane forests (Portik & Blackburn 2016). Within the family Arthroleptidae (Afrobatrachia), fully aquatic, semi aquatic and completely terrestrial development in the form of direct development have evolved. Portik & Blackburn (2016) proposed that Arthroleptidae comprises the clades *Leptopelis*, *Leptodactylodon*, a clade containing *Nyctibates*, *Scotobleps*, *Astylosternus* and *Trichobatrachus*, and a clade containing *Cardioglossa* and *Arthroleptis*.

The skeletal morphology and associated musculature in arthroleptid tadpoles are poorly understood. We here present a detailed description of tadpole cranial morphology of four arthroleptids - *Leptopelis parkeri*, *Astylosternus occidentalis*, *Trichobatrachus robustus* and *Nyctibates corrugatus.* The tadpoles of all four species inhabit streams in lowland or montane forests, which differ in water flow velocity. While *L. parkeri* and *A. occidentalis* inhabit more slowly flowing stream sections, *T. robustus* and *N. corrugatus* occur in more fast flowing, rocky stream sections. Tadpoles that inhabit fast flowing water systems (lotic tadpoles) share several anatomical adaptations to prevent being swept away. These adaptations include the presence of a modified oral sucker and/or an abdominal sucker, low caudal tail fins and massive caudal tail muscles (De Oliveira et al. 2017; Baldo et al. 2014; Haad et al. 2014; Oberhummer et al. 2014; Raj et al. 2012; Haad et al. 2011; Haas et al. 2009; Aguayo et al. 2009, Lavilla & De Sá 2001, Altig & McDiarmid 1999, Haas & Richards 1998; Inger 1992; Cadle & Altig 1991). Because tadpoles show a variety of adaptive strategies, the architecture of the cranium with its highly specialized structures can give relevant insights to uncover evolutionary modifications as an adaptation to environmental factors. Inger (1992) discussed that not body shape but variations in head morphology (e.g. the oral discs) might be the features affected by water flow. Therefore head morphology should be regarded as the target of adaptation to varying water flow velocities. Therefore, the aim of this study is to compare the cranial morphology of lotic tadpoles of closely related species within Arthroleptidae and relate them to their favored microhabitats. We focus on the question, if differences in habitat choice of the arthroleptid tadpoles are reflected in the cranial muscoskeletal system.

Materials and methods

Because preserved material is rare, only one tadpole of *Leptopelis parkeri* (MTSN 7740, Tanzania, Uluguru North), three tadpoles of *Asytlosternus occidentalis* (MNHN uncatalogued, Collecion Lamotte), one tadpole of *Nyctibates corrugatus* (ZMB 79240, Cameroon, Ebo Forest) and one tadpole of *Trichobatrachus robustus* (MNHN uncatalogued, Collecion Lamotte) were available for examination. Specimens were measured, analyzed and partly dissected using a Zeiss Discovery V12 stereo

microscope. Photos were taken with a Zeiss Axiocam ICc1-camera and images were processed using Adobe Photoshop CS6. Developmental stages of the tadpoles were determined using Gosner (1960). For further details see Table 1.

Histology

Given the rarity of material, only one specimen of *Astylosternus occidentalis* was used for histological sectioning. The tadpole therefore was dehydrated in ethanol series (70%, 90%, 2 x 96%; 5 min each) and embedded in paraffin, sectioned at 8 µm in transverse orientation and stained after Heidenhain's Azan (Romeis 2010). Sections were made using a Zeiss Microm HM 360 and investigated and photographed using a Zeiss Axioplan microscope with an attached Zeiss camera. Histological sections were only used to compare them with the results of the µ-CT scans.

Clearing and Staining

One tadpole of *Astylosternus occidentalis* was prepared using standard methods for clearing and staining (Dingerkurs and Uhler 1977, modified by Taylor and van Dyke 1985). Specimens were photographed with a Zeiss Axiocam ICc1-camera and images were processed using Adobe Photoshop CS6. The cleared and stained specimen was then used for preparation and compared with the results of the µ-CT scan.

µ-CT Scanning and 3D reconstruction

One tadpole of each (*Leptopelis parkeri, Astylosternus occidentalis, Nyctibates corrugatus* and *Trichobatrachus robustus*) were contrasted with 1% polymolybdenic acid in 70% Ethanol following Metscher (2009). CT-scans were made using a Phoenix Nanotom at the Helmholtz-Zentrum Geesthacht (Deutsches Elektronen Synchrotron – DESY). Three-dimensional reconstructions of the cranial musculoskeletal system were prepared using Amira®5.4.2 (FEI Visualization, Sciences Group) and Maya®2015 (Autodesk). Muscles were only reconstructed on the right side of the head.

Results

The larval cranial skeleton and associated musculature are described *for Lepropelis parkeri, Astylosternus occidentalis, Nyctibates corrugatus* and *Trichobatrachus robustus*. Differences were mentioned when present. Origin and insertion of all cranial muscles of each species are listed in Table 2.

External morphology (Figure 2)

The tadpole of *L. parkeri* (Gosner stage 35) is slender, with a moderately elongated, slightly dorsoventrally flattened body and a relatively long tail with low dorsal and ventral fins.

The tadpole of *A. occidentalis* (Gosner stage 25/26) is robust and large with a long, muscular tail with low dorsal and ventral fins.

The tadpole of *Nyctibates corrugatus* (Gosner stage 26) is long and thick, exhibits an expanded oral disc and a heavily muscularized, thick tail. The tail is as thick as the body, and equipped with very low dorsal and ventral fins.

The tadpole of *T. robustus* (Gosner stage 36/37) is large and has an enlarged mouth modified into an oral sucker. The tail is long and heavily muscularized, the ventral fin is reduced.

Cranial skeleton

Leptopelis parkeri (Figure 3)

The cornua trabeculae are long and flat cartilages of the ethmoidal region extending to the anterior end of the head. Medially, they are separated by a wide gap and curve ventrally, articulating with the cartilago labialis superior each. Posteriorly, the cornua trabeculae are confluent with the planum ethmoidale. The cartilago orbitalis forms the lateral wall of the braincase and is joined to the floor of the cavuum cranii. The cartilago orbitalis consists of several pillars and exhibits several foramina. The anteriormost is the optic foramen. In posterior direction, the pila metoptica forms a cartilaginous wall between the optic foramen and the foramen oculomotori. The pila antotica separates the foramen oculomotori from the foramen prooticum. The foramen prooticum is large and has an ovoid-to triangulate shape. It is situated anterior to the capsula auditiva. The cavuum cranii opens dorsally via the fenestra frontoparietalis and ventrally via a large ovoid fenestra. Laterally, the taenia tecti marginalis forms the dorsal rim and is confluent with the cartilago orbitalis. Posteriorly, the tectum synoticum forms a thin cartilaginous bridge connecting the capsulae auditivae. There is no taenia tectum transversalis formed. A small taenia tecti medialis is seen anteromedially to the tectum synoticum. The capsula auditiva is large and ovoid in shape. A large foramen ovalis is located ventrolaterally and a foramen jugularis is present posteroventrally on each capsula auditiva.

The palatoquadrate appears as a long flat cartilaginous strip. At its anterior end, the palatoquadrate bears a prominent processus articularis anterior extending from the rectangle-shaped pars articularis quadrati. The most prominent part of the palatoquadrate is the anteriorly situated, broad and massive processus muscularis. Dorsally, the processus muscularis merges into a small strip of cartilage, the commissura quadrato-orbitalis and joins the anterolateral part of the cartilago orbitalis. Anteromedially, a thick commissura quadratocranialis anterior joins the

palatoquadrate to the floor of the cavuum cranii. Posteriorly, the palatoquadrate merges into the arcus subocularis. The arcus subocularis is less curved and relatively straight. It is separated from the neurocranium by the fenestra subocularis. A wide processus oticus connects the palatoquadrate to the capsula auditiva posteriorly. An ascending process is absent.

The cartilago labialis superior forms the massive upper jaw as a paired element. Each cartilago labialis superior consists of two distinct elements, the central corpus and the lateral ala, named the pars alaris. The pars alaris is short and slightly curved outwards, where it articulates with the cartilago meckeli. Dorsolaterally, the cartilago labialis superior is connected to the anterior end of the cornua trabeculae. The cartilago labialis inferior is a paired element of the lower jaw and is v-shaped in frontal view. Posteriorly, the cartilago labialis inferior articulates with the cartilago meckeli. The cartilago labialis inferior articulates with the dorsomedial process of the s-shaped cartilago meckeli. The cartilago meckeli bears two other processes, the ventromedial process and the processus retroarticularis, where it articulates with the pars articularis quadrati of the palatoquadrate.

At this developmental stage, the frontoparietal and the parasphenoid bones are ossified. The frontoparietals are not completely developed and form bony elements alongside the dorsal rim of the cartilago orbitalis and the taenia tecti marginalis. Medially, the frontoparietals are separated by a wide gap. The parasphenoid forms the bony protection of the ventral braincase. It is formed as an elongated element. Anteriorly, the parasphenoid is narrower, while it broadens posteriad.

Astylosternus occidentalis (Figure 4)

The cornuae trabeculae are about one third of the length of the chondrocranium and originate from the ethmoid. Each trabecula is transversely curved. Their tips are flat and rounded. Each trabecular horn is connected to the pars articularis quadrati of the palatoquadrate by a strong lateral circumoral ligament. The braincase opens dorsally via a frontoparietal fenestra and two parietal fenestrae; all of them fused together. A taenia tecti transversalis is absent. The taenia tecti medialis is reduced to a small protrusion and does not separate the parietal fenestra from each other; it is confluent with the tectum synoticum. The cranial floor is heavily chondrified. Posteriorly, at a level below the capsula auditiva, the prootic foramen is visible. The capsula auditiva is spheric and connected dorsally via the tectum synoticum. Posteriorly, the lateral rim of the tectum synoticum and the cranial floor form the foramen magnum.

The palatoquadrate is anteroventrally connected to the neurocranium via a broad commissura quadratocranialis anterior. Dorsally, the commissura quadrato-orbitalis is formed as a broad strip of cartilage. It is confluent with the processus muscularis of the palatoquadrate and connects the latter to the cartilago orbitalis. The processus muscularis is the most prominent process of the palatoquadrate. It is flattened and

heavily chondrified. The anteroventral situated pars articularis quadrati of the palatoquadrate is square-shaped and relatively short. It broadly articulates with the cartilago meckeli by the ventromedial process and the processus retroarticularis. Ventrolaterally, the palatoquadrate bears two ventrally angled processes, the short processus articularis anterior and the longer processus ventralis. In posterior direction, the palatoquadrate forms the dorsoventrally flattened arcus subocularis. The arcus subocularis merges into the processus oticus, connecting the palatoquadrate with the capsula auditiva. It is the only posterior connection with the neurocranium. An ascending process is reduced and has no contact to the neurocranium.

The upper jaw bears the cartilago labialis superior, a single massive element consisting of a central corpus, the pars corporis, and upwards and slightly outwards curved lateral alae, the pars alaris. The corpus is partially separated by a dorsomedial semicircular notch and forms a dorsolateral protrusion on each side. The dorsolateral surface on each side of the corpus is flattened forming a broad articulation with the cornu trabeculae. The cartilago labialis inferior is a paired element of the upper jaw and is v-shaped in frontal view. Posteriorly, it articulates with the cartilago meckeli. The latter appears s-shaped in lateral view and has a dorsomedial process, a ventromedial process and a processus retroarticularis. The cartilago meckeli articulates broadly with the pars articularis quadrati of the palatoquadrate by the ventromedial process and the processus retroarticularis.

The frontoparietal forms a relatively thin and narrow bone, which covers the dorsolateral part of the cavum cranii. Anteriorly it supports the posterolateral part of the ethmoid. On its posterior end, the frontoparietal covers the anterolateral part of the otic capsule and the tectum synoticum. The parasphenoid has a typical T-shape and covers the cranial floor ventrally. Posteriorly, it has two tapered, anteriorly angled alae. The exoccipital bone is a convex curved bone. It forms the bony lateral margin of the foramen magnum.

Nyctibates corrugatus (Figure 5)

The cornua trabeculae are fused together. They originate from the ethmoid and diverge laterad and curve slightly ventrad associating with the processus articularis anterior of the palatoquadrate by a lateral circumoral ligament. Laterally, the cornua trabeculae articulate with the cartilago labialis superior. Anteroventrally, the ethmoid bears a ventral, posteriad directed process on each side. The cavuum cranii is oval. Its lateral wall consists of a cartilago orbitalis, joined to the floor of the braincase. The floor of the braincase forms a huge fenestra. The braincase and the lateral wall of the cavuum cranii are well chondrified and bear several foramina. The anteriormost is the lateroventrally situated optic foramen, formed by the preoptic root. The pila metoptica separates the optic foramen from the foramen oculomotori. Mediodorsally, the lateral sidewall of the cavuum cranii bears a trochlear foramen. A spherical prootic foramen is formed between the capsula

auditiva and the pila antotica. The taenia tecti marginalis is located dorsolaterally to the cartilage orbitalis. A taenia tecti transversalis is absent, leading to the fusion of the frontoparietal fenestra with the parietal fenestra. A taenia tecti medialis is reduced to a small protuberance.

The palatoquadrate is a long cartilaginous strip. It is widest anteriorly and relatively thin and slender at its posterior end. The prominent processus muscularis of the palatoquadrate is flat and square-shaped. At the anteroventral part of the processus muscularis, a commissura quadratocranialis anterior connects the palatoquadrate to the ventral part of the neurocranium. The commissura quadrato-orbitalis forms a delicate, cartilaginous strip connecting the palatoquadrate to the trabecula cranii. Anteroventrally, the palatoquadrate forms the pars articularis quadrati bearing two short processes. The anterior process (processus articularis anterior) connects the palatoquadrate to the cornua trabeculae by a lateral circumoral ligament. At the medial part of the palatoquadrate, just anterior to the arcus subocularis, a long processus hyoquadratis is formed. It is thicker at its basis and tapers to its tip. The processus hyoquadratis articulates widely with the hypobranchial apparatus via the lateral part of the ceratohyale. There is a wide gap between this process and the processus muscularis. The ceratohyale fits into this gap, articulating with the palatoquadrate. Posteriorly, the palatoqudarate bears a processus ascendens and a processus oticus. The processus ascendens is reduced to a small stub and not connecting with the neurocranium. The processus oticus joins the ventrolateral part of the capsula auditiva connecting the posterior end of the palatoquadrate to the neurocranium.

The cartilago labialis superior is a massive, heavily chondrified, single element of the upper jaw. It bears lateral alae and each pars alaris is slightly curved dorsad where the cartilago labialis superior articulates with the cornua trabeculae. The lower jaw is formed by the cartilago labialis inferior and the cartilago meckeli. The cartilago labialis inferior is is v-shaped in frontal view and located medially to the cartilago meckeli and posterior to the cartilago labialis superior. The cartilago meckeli is robust and compact; it is concave on the dorsal side and convex on the ventral side. If forms three processes; a dorsomedial and ventromedial process articulating with the cartilago labialis inferior and a processus retroarticularis articulating with the anterior part of the palatoquadrate. It forms the insertion side of several muscles of the hyoid group.

The frontoparietal is a paired, thin and slender dermal bone supporting the cranium dorsolaterally. It is widest at its posterior end and narrows in anterior direction. Both frontoparietal bones are separated from each other by a wide gap. The parapshenoid is an extremely long bone and is present in typical T-shape. It supports the ventral side of the neurocranium over its nearly full length. Posteriorly, the parasphenoid bears strong lateral alae supporting the capsula auditiva ventrally. The parasphenoid broadens in medial direction covering the cavuum cranii ventrally. It continues anteriorly and narrows to a sharp tip at its anterior end where it supports the ventral side of the ethmoid and the ventral basis of the cornua

trabeculae. The prootic is a paired, round-ovoid dermal bone and lies in front of the capsula auditiva. The exoccipital is a c-shaped dermal bone forming the posterior end of the cranium and the lateral margin of the foramen magnum.

***Trichobatrachus robustus* (Figure 6)**

The cornu trabeculae are relatively long and heavily chondrified, representing one third of the length of the chondrocranium. They are flattened and triangular in shape. Anteriorly, each trabecular horn curves ventrad and slightly bends laterad articulating with the dorsolateral area of the cartilago labialis superior. Posteriorly, the trabecular horns merge at the level of the cartilago meckeli and fuse with the ethmoid. The cavuum cranii represents two thirds of the length of the chondrocranium. Anteriorly, the cavuum cranii is completed by the orbital cartilage and ventrally enclosed by the cranial floor. Posteriorly, the floor of the cavuum cranii is the planum basale which is confluent with the ventral area of the capsula auditiva. The cavuum cranii medially bears an optic foramen. The prootic foramen is formed between the posterior end of the lateral wall of the braincase and the capsula auditiva. The capsula auditiva is relatively small and in spherical shape. Dorsally, the otic capsules are connected by the tectum synoticum. Medially of this tectum synoticum is the taenia tecti medialis. It is formed as a rather reduced process. A taenia tecti transversalis is absent.

The palatoquadrate is anteroventrally connected to the neurocranium by a broad and heavily chondrified commissura quadratocranialis anterior. Anteriorly, the palatoquadrate forms a pronounced process (processus articularis anterior of the pars articularis quadrati) articulating with the cartilago meckeli. A second, upward and slightly backward curving process is distinct as processus ventralis. The prominent processus muscularis of the palatoquadrate is wide and squarish. Dorsally, the processus muscularis merges into the commissura quadrato-orbitalis connecting the palatoquadrate with the dorsal neurocranium. Posteriorly, the palatoquadrate narrows and forms the arcus subocularis. The latter is coincident with the processus oticus connecting the palatoquadrate with the capsula auditiva posteriodorsally. An ascending process is absent.

The upper jaw is composed of a single, heavily chondrified cartilago labialis superior. In dorsal view, the corpus is in triangular shape bearing a dorsolaterad protuberance on each side that serve as attachment sites to the cornu trabeculae. The lower jaw consists of the cartilago meckeli and the cartilago labialis inferior. The cartilago labialis inferior is triangular in shape and, both cartilages are medially separated. On the dorsal surface, the cartilago labialis inferior articulates with the cartilago meckeli. The cartilago meckeli is a short and stout transversally oriented cartilage which is in L-shape in frontal view. It bears three processes, the dorsomedial and ventromedial processes and the processus retroarticularis. Proximal, the cartilago meckeli articulates with the cartilago labialis inferior on its

medial surface. On its distal end, it is saddle-shaped and articulates with the pars articularis quadrati of the palatoquadrate.

The frontoparietal bone supports the dorsolateral part of the neurocranium and covers the cavuum crani. Each frontoparietal bone is tapering anteriorly. At its posterior end it covers one half of the capsula auditiva dorsally. The parasphenoid appears in typical T-shape and supports the braincase ventrally. It is comparatively long and runs from the ventral part of the capsula auditiva to the ventral part of the ethmoid, where it covers both cornu trabeculae. Posterially, the parasphenoid shows broad and strong alae. In anterior direction, the parasphenoid narrows and then widens mediad to a level of the ventromedial part of the chondrocranium. The anterior tip of the parasphenoid splits into two cusps. The prootic bone is small and rounded. Ventrolaterally, it partially covers the foramen jugulare of the capsula auditiva. The exoccipital is a, in longitudinal direction, convex curved bone. It supports the posterior part of the cranium enclosing the margin of the foramen magnum on each side.

Hyobranchial skeleton (Figure 7)

The hyobranchial apparatus of each tadpole examined is composed of the prominent ceratohyalia and the branchial basket, consisting of the ceratobranchialia I-IV. Each ceratohyale is situated anterior to the branchial basket. In *L. parkeri, A. occidentalis* and *T. robustus,* the ceratohyale is transversely oriented. Laterally, it is flattened dorsoventrally. Anteriorly, the ceratohyale forms a processus anterior. Posteriorly, the ceratohyale is connected to the planum hyobranchiale via the processus posterior hyalis. The processus anterior is much more prominent in *L. parkeri* than in the other species examined. A basibranchiale is formed in all four species and is connected to the ceratohyale and the planum hyobranchiale. A basihyale is only seen in *N. corrugatus* and is located anterior to the pars reuniens. The pars reuniens is also present in *T. robustus,* but is absent in *L. parkeri* and *A. occidentalis.*

The branchial basket is located posterior to the ceratohyalia and is composed of a planum hyobranchiale and the ceratobranchialia I-IV. The morphology of the branchial basket differs among the examined tadpoles. In *L. parkeri, A. occidentalis and N. corrugatus,* the planum hyobranchiale is anterolaterally connected to the ceratohyale via the processus anterior branchialis. Posteriorly, the planum hyobranchiale forms a processus posterior. In *L. parkeri,* the processus posterior is wide and square-shaped, whereas it is narrow and tapering in *A. occidentalis, N. corrugatus and T. robustus. A. occidentalis* and *N. corrugatus* show four separated ceratobranchialia. In *L. parkeri,* Ceratobranchiale I is anteriorly free-ending and the Ceratobranchialia II-IV are proximally fused to the planum hyobranchiale. The ceratobranchialia I-III are fused distally by the commissurae terminalis. Ceratobranchiale IV shows a free distal end. In *T. robstus,* the ceratobranchiale I and II are joined together while the ceratobranchiale III and IV are separated. In *A.*

occidentalis, N. corrugatus and *T. robustus,* all four ceratobranchialia are fused proximally to the planum hyobranchiale. Only three spiculae are formed in *L. parkeri* and *N. corrugatus.*

Cranial muscles

The origin and insertion of all cranial muscles of each species are shown in Table 2. The muscles are grouped into mandibular, hyoid, branchial and hypobranchial muscles. For each species, special configurations of particular muscles are described in detail hereafter (see Table 2 for comparison).

Leptopelis parkeri (Figure 8)

The musculus (M.) levator (l.) mandibulae posterior superficialis is the largest muscle of the levator complex. Posteriad and mediad, the M. l. mandibulae posterior superficialis is broad and wide. It narrows anteriad/craniad and is rounded at its anterior tip.

The M. l. mandibulae anterior lies ventrad/profound to the M. l. mandibulae posterior profundus. It is the deepest of the three muscles running along the orbit.

The M. orbitohyoideus is associated with the ceratohyale and is the largest cranial muscle.

The M. suspensoriohyoideus broadly originates on the surface of the processus muscularis of the palatoquadrate. The M. suspensoriohyoideus extends ventrad and anteriad and has insertion sides in both directions. Ventrally, muscle fibers insert on the ceratohyale. Anteriorly, the M. suspensoriohyoideus narrows and inserts on the ventrolateral surface of the cartilago meckeli.

The M. subarcularis rectus consists of four components. The dorsal head of the M. subarcularis rectus connects the ceratohyale with the branchial basket. The ventral head forms a coalescence of the M. subarcularis rectus II-IV. This muscle spans the branchial basket and is much longer than the M. subarcularis rectus I. It extends from the ceratohyale towards the ceratobranchiale IV.

Astylosternus occidentalis (Figure 9)

The M. l. mandibulae posterior superficialis runs posteroventrally from the capsula auditiva to the cartilago meckeli anteriorly. It partly overlaps the M. l. mandibulae longus profundus. The M. l. mandibulae longus superficialis originates from two heads: the posteromedial head originates on the inner side of the ventral part of the capsula auditiva, near the prootic foramen. The posterolateral head originates on the outer side of the capsula auditiva, directly behind the small processus ascendens of the palatoquadrate. The M. l. mandibulae longus superficialis is relatively broad

tapering on its anterior end. The muscle inserts on the dorsomedial process of the cartilago meckeli.

The M. hyoangularis is the second largest muscle of the hyoid group and is situated ventrolateral to the M. orbitohyoideus. It originates on the mediolateral part of the ceratohyale and inserts on the ventromedial process of the palatoquadrate.

The M. subarcularis rectus complex is present as a single muscle. It originates on the ventral side of the ceratohyale and inserts anteriorly on the ceratobranchiale III, next to the insertion side of the M. subarcularis obliquus. The latter is a short and triangular shaped muscle originating on the planum hyobranchiale anteriorly and inserting on the anterior part of the ceratobranchiale III.

The M. l. arcus branchialis group is represented by poorly developed thin muscles.

***Nyctibates corrugatus* (Figure 10)**

The M. intermandibularis posterior is a long muscle running along the ceratohyale.

The M. l. mandibulae longus profundus is situated below the M. l. mandibulae longus superficialis and is encased by the palatoquadrate and the sidewall of the cavuum cranii. Anteriorly, the muscle is narrow and originates on the dorsal part of the cartilago labialis inferior. The M. l. mandibulae longus profundus broadens and widens at a level of the palatoquadrate. Posteriorly, it inserts at the capsula auditiva.

The M. l. mandibulae anterior articularis consists of two incompletely separate portions. Both portions originate at the dorsolateral part of the inner side of the processus muscularis of the palatoquadrate. One portion inserts at the anterior part, the other portion inserts at the posterior part of the processus retroarticularis of the palatoquadrate.

The M. l. mandibulae lateralis is situated dorsal to the M. l. mandibulae anterior articularis. It originates at the medial part of the processus muscularis of the palatoquadrate and inserts medially on the cartilago meckeli.

The M. orbitohyoideus is a very long and strong muscle. It originates at the lateral part of the processus muscularis and the processus ventralis on the palatoquadrate. The M. orbitohyoideus inserts along the lateral part of the ceratohyale and on the processus hyoquadratis.

The M. subarcularis obliquus is a short triangular muscle. It originates on the hyobranchial plate of the hyobranchial apparatus and inserts on the anterior part of the ceratobranchiale III.

***Trichobatrachus robustus* (Figure 11)**

The M. l. mandibulae posterior superficialis is the most superficial muscle of the levator mandibulae complex. It originates dorsally on the lateral wall of the taenia

tecti marginalis and inserts between the dorsomedial process and the processus retroarticularis of the cartilago meckeli. The M. l. mandibulae longus superficialis is short compared to the other levator mandubulae muscles.

The M. l. mandibulae posterior profundus is the largest muscle of the levator mandibulae complex. Posteriorly, it originates on the ventromedial side of the capsula auditiva and the posterior end of the palatoquadrate. The M. l. mandibulae longus profundus is located between the lateral sidewall of the cavuum cranii and the arcus subocularis of the palatoquadrate. It inserts on the dorsomedial process of the cartilago meckeli.

The M. suspensorioangularis originates on the postolateral margin of the processus muscularis of the palatoquadrate and anterior part of arcus subocularis and inserts on the dorsal part of the processus lateralis hyalis of ceratohyale.

The M. subarcularis obliquus originates medially on the planum hyobranchiale and inserts on the anteromedial part of the ceratobtranchiale IV.

Discussion

Forest streams – Different microhabitats of arthroleptid tadpoles

A high diversity of tadpole-morphotypes has evolved in lotic habitats (Griesbaum et al. 2019; Candioti et al. 2016; Haad et al. 2014; Channing et al. 2012; Rödel et al. 2012; Haad et al. 2011; Lavilla & De Sá 2001; Saidapur 2001; Altig & McDiarmid 1999; Haas & Richards 1998; Inger 1992; Cadle & Altig 199). As mentioned above, Tadpoles of *Leptopelis parkeri, Astylosternus occidentalis, Nyctibates corrugatus* and *Trichobatrachus robustus* all inhabit streams of lowland or montane forests with different water flow velocities in each of the tadpoles (micro-)habitats.

The genus *Leptopelis* currently comprises 52 species (Frost 2020). The reproductive mode is semiaquatic and associated with water-independent egg-deposition in the moist soil. Tadpoles hatch with the beginning of the rainy season and move actively towards the water (Barej et al. 2015). The tadpole of *L. parkeri* is commonly found in slow moving streams of montane forest habitats of the Eastern Arc mountain chain of Tanzania. Within the stream, the tadpoles are mostly located where the water builds up in cavities (Fig. 1A) where in most cases water flow velocity is so low that these tadpoles do not suffer from drift.

The tadpole of *Astylosternus occidentalis* prefers slow moving streams in dense lowland forests (Fig. 1C) of Sierra Leone, Liberia, Guinea and the west of Ivory Coast (Griesbaum et al. 2019; Rödel et al. 2012; Channing et al. 2012). The reproductive mode is completely aquatic and eggs are attached on stones in deeper water regions (Rödel et al. 2012). The tadpole is large and robust with a long tail and low fins what might counteract drifting due to areas of higher water flow velocity (Griesbaum et al. 2019; Channing et al 2012).

Nyctibates corrugatus is the only species within the genus *Nyctibates* and occurs in the Oban Hills of Nigeria, Cameroon and mainland Equatorial Guinea. This species inhabits humid lowland forests with hilly areas and breeds in fast flowing and rocky streams with stony substrate and clear water (Fig. 1B). The species was re-described as *Astylosternus corrugatus* by Perret (1966), but Amiet (1971) resurrected *Nyctibates* on the basis of the tadpole morphology. Molecular data from Frost et al. (2006) also support the recognition of *Nyctibates*. The mouth field of the tadpole is big with large flattened lobes, but the species does not exhibit an oral sucker. To counteract drift, the tadpole of *N. corrugatus* has an 'eel-shaped body' (Channing et al. 2012).

Trichobatrachus robustus is the only described species within the genus *Trichobatrachus* and occurs from eastern Nigeria to the western Democratic Republic of Congo and inhabits shaded, fast flowing streams with mainly rocky substrate and occasional muddy areas (Fig. 1D). Little is known about the reproductive biology and about the morphology of the aquatic tadpole. However, the tadpole is recognized to be carnivorous. It has a large oral sucker preventing it from drifting in faster flowing water areas and is therefore ecomorphologically categorized as a suctorial tadpole (Channing et al. 2012; Altig & McDiarmid 1999).

Of these four species examined, the habitats of tadpoles of *N. corrugatus* and *T. robustus* can be characterized as the fastest flowing water systems in relation to the habitats of *L. parkeri* and *A. occidentalis*. One might expect that the more closely related *A. occidentalis* and *T. robustus* (Feng et al. 2017; Portik & Blackburn 2016) share similar craniomorphological features. Surprisingly, various differences exist further supporting that morphological structures in tadpoles are likely unsuitable for systematic analyses. Griesbaum et al. (2019) however reported only minor morphological variability among tadpoles of *Astylosternus, Nyctibates* and *Scotobleps.* This hints to an adaptation to fast flowing streams in humid montane forests exerting similar selection pressures (Lamotte & Lescure 1988, 1989a,b). Only *Nyctibates* differs in having a very elongated and muscular body.

Cranial morphology of the arthroleptid tadpoles – a comparative approach

Cranial skeleton

Overall, the cranium of the tadpole of *Leptopelis parkeri* is less robust and less heavily chondrified compared to the tadpoles of *Astylosternus occidentalis, Nyctibates corrugatus* and *Trichobatrachus robustus*. Comparing the microhabitats of *A. occidentalis* and *T. robustus* with *N. corrugatus* (Fig. 1), there is difference in water flow velocitiy presumably affecting the cranial skeleton.

In tadpoles of *L. parkeri,* the cornua trabeculae, the ethmoid and the orbital region are more delicate while these structures are wider and more massive in the three other tadpoles examined. In tadpoles of *A. occidentalis* and *T. robustus,* the cornua trabeculae do not form a continuous plate but diverge craniad. In the tadpoles of *N. corrugatus*, the cornua trabeculae are fused to form a continuous plate giving a

characteristic shape to the chondrocranium, and the ethmoid is comparatively narrower and broadens when continuing into the cornua trabeculae (Fig. 12, dark green). We interpret the near complete or entire fusion of the cornua trabeculae as an adaptation to lotic habitats, because the fusion of the cornua trabeculae is also reported for suctorial larvae of the neobatrachian species *Heleophryne* spp., *Hyla armata* BOULENGER 1902, and *Nyctimystes dayi* (GÜNTHER 1987) (Haas & Richards 1998), *Heleophryne orientalis* FITZSIMONS 1946(Lukas 2021) and for the bromeliad tapoles of *Phyllodytes gyrinaethes* PEIXOTO, CARAMASCHI & FREIRE 2003 (Candioti et al. 2016). The presence of this feature in bromeliad tadpoles reveals that environmental factors other than flowing water can lead to modifications of the cornua trabeculae. These modifications also occur in microhabitats, where stabilization of the cranium is needed. This is the case in bromeliads, where the tadpoles adhere to the wall of the water filled leaves.

The processus muscularis of the palatoquadrate in tadpoles of *A. occidentalis* and *T. robustus* is a massive element and reaches the anterior part of the cartilago orbitalis and is confluent with the broad commissura quadrato-orbitalis (Fig. 12, orange). The presence of a robust and wide processus muscularis can be interpreted as adaptation to lotic habitats as it is also reported for several other species inhabiting lotic water systems (De Oliveira et al. 2017, Haas & Richards 1998, Haas 1996, Haas 1995, De Sá 1988, De Jongh 1968).

A processus ventralis of the palatoquadrate is present in tadpoles of *A. occidentalis, N. corrugatus* and *T. robustus,* but it is not seen in the tadpole of *L. parkeri* (Fig. 12). This processus ventralis is also reported as a common feature of the palatoquadrate in suctorial tadpoles of the genera *Litoria* and *Nyctimystes* (Haas & Richards 1998) and may be an adaption of the cranium to lotic ecosystems.

In the tadpole of *T. robustus,* the processus articularis anterior and the processus ventralis are longer and more heavily chondrified compared to other species examined. The commissura quadrato-orbitalis in tadpoles of *A. occidentais* and *T. robustus* is massive and blends into the dorsal part of the processus muscularis of the palatoqadrate. In the tadpole of *N. corrugatus,* the same commisura is developed as a filigree slender cartilaginous strip (Fig. 12, orange). Tadpoles of *A. occidentalis, N. corrugatus* and *T. robustus* all share a broad and massive commissura quadratocranialis anterior, although it is wider in tadpoles of *N. corrugatus* and *T. robustus* (Fig. 12). This condition is described as one of the most characteristic features of the palatoquadrate in lotic tadpoles (De Oliveira et al. 2017; Nogueira-Costa & Wachlevski 2015; Haas & Richards 1998; van der Westhuizen 1961).

An additional processus, forming a long cartilaginous element binding the ceratohyale to the palatoquadrate, is only seen in the tadpole of *N. corrugatus.* We named this processus the processus hyoquadratis. This character is absent in tadpoles of *A. occidentalis, T. robustus* and *L. parkeri*. We propose that a long and massive processus hyoquadratis in the tadpole of *N. corrugatus* has evolved as adaption to lotic habitats with strong currents (Fig. 12). The processus hyoquadratis,

together with the ceratohyal, comprises the insertion side for the long and strong M. orbitohyoideus. This strong muscle may function as additional support preventing drift in faster flowing water areas. *Nyctibates corrugatus* is placed as the sister group to a clade containing *Scotobleps, Astylosternus* and *Trichobatrachus* (Portik & Blackburn 2016) and it might be possible that the processus hyoquadratis is an autapomorphy of this species. An investigation of the tadpoles of *Leptodactylodon* and *Scotobleps* is needed to clarify the presence of a processus hyoquadratis in these species.

In contrast to the tadpole of *L. parkeri*, the arcus subocularis of the palatoquadrate of tadpoles in *A. occidentalis*, *N. corrugatus* and *T. robustus* is very broad and robust. A broad processus oticus is seen in all species examined. A processus ascendens is absent in all these species. We follow the interpretation of Haas & Richards (1998) that the processus oticus replaces the function of the processus ascendens as the origin side of some of the jaw adductor muscles of the mandibular group.

In the tadpole of *L. parkeri*, the cartilago labialis superior is medially separated by a symphysis. This is strikingly different in tadpoles of *A. occidentalis, T. robustus and N. corrugatus*, where the partes corpores of the cartilago superior are fused into a continuous wide and massive, transverse element (Fig. 12, light blue). A fused cartilago labialis superior is also described in the gastromyzophorous tadpole of *Atelopus tricolor* BOULENGER 1902 (Lavilla1 & De Sá 2001), in the bufonid lotic tadpoles of *Rhinella rumbolli* CARRIZO 1992 (Haad et al. 2014) and *R. quechua* GALLARDO 1961 (Aguayo et al. 2009), in suctorial tadpoles of the neobatrachian *Litoria nannotis* (ANDERSSON 1916), *L. rheocola* (LIEM 1974), and *N. dayi* (Haas & Richards 1998), in the hylid tadpole of *Corythomantis greeningi* BOULENGER 1896 (De Oliveira et al. 2017) as well as the bromeliad tapole of *P. gyrinaethes* (Candioti et al. 2016). Brucker (Master thesis 2016) reported that a fused and robust cartilago labialis superior is seen in the hyperoliid tadpoles of *Afrixalus uluguruensis* and *A. fornasini*, which are known to inhabit lentic, but also lotic habitats. The tadpoles of *A. uluguruensis* (investigated by Brucker, Master thesis 2016) are carnivorous and inhabit lotic habitats, like it is seen in tadpoles of *Trichobatrachus*. Müller et al. (2013) suggested that a carnivorous feeding strategy might be advantageous for aquatic larvae in montane, lotic systems. This supports that a robust, fused cartilago labialis superior can be interpreted as head stabilizing structure, especially when strong forces are working (waterflow, gravity, larval feeding strategies etc.).

In contrast to the tadpole of *L. parkeri*, the cranial bones are more massive in tadpoles of *A. occidentalis, N. corrugatus* and *T. robustus* (Fig. 12, ochre). The frontoparietal is distinctly longer and broader and covers much more area of the dorsal braincase. The parasphenoid is more massive and bears strong lateral alae in tadpoles of *A. occidentalis, N. corrugatus* and *T. robustus.* We interpret this configuration as a protective adaptation to water turbulences in lotic habitats.

Hyobranchial skeleton

In comparison to the tadpole of *L. parkeri*, the overall appearance of the hyobranchial skeleton in tadpoles of *A. occidentalis, T. robustus* and *N. corrugatus* is massive and heavily chondrified (Fig. 6). The ceratohyalia are strikingly larger than in the tadpole of *L. parkeri*, especially in tadpoles of *N. corrugatus* and *T. robustus*. A large and heavily chondrified ceratohyale is a typical feature of lotic tadpoles. It is also present in the Australian suctorial tadpoles of the genera *Litoria* and *Nyctimystes* (Haas & Richards 1998) and in lotic tadpoles in different bufonid species (*A. tricolor, Atelophryniscus chrysophorus* (McCRANIE, WILSON & WILLIAMS 1989) (Lavilla & De Sá 2001); *R. rumbolli* (Haad et al. 2014) and *R. quechua* (Aguayo et al. 2009)), in tadpoles of *Hylodes meridionalis* (MERTENS 1927) (Nogueira-Costa & Wachlevski 2015) and in bromeliad tapoles of *P. gyrinaethes* (Candioti et al. 2016) (see 'fused cartilago labialis superior').

Cranial muscles

Table 2 and 3 show similarities and differences of the cranial muscle systems of the species investigated in this study. Table 2 shows the description of origin and insertion of each cranial muscle. In Table 3, muscles interpreted as an adaptation to lotic habitats, are highlighted in blue. These muscles appear more massive or differ in shape compared to the tadpole of *L. parkeri*.

The overall cranial muscle morphology of the tadpole of *L. parkeri* resembles a 'normal tadpole' and does not appear hypertrophied as in tadpoles of *A. occidentalis, N. corrugatus* and *T. robustus* (see also Fig. 13 for comparison). The tadpole of *N. corrugatus* shows more muscles of the mandibular group compared to the other species investigated (Tab. 2).

The mandibular muscles

In tadpoles of *L. parkeri*, *A. occidentalis* and *T. robustus*, only some of the mandibular levator muscles seen in the tadpole of *N. corrugatus* are present (Tab. 3, coloured in orange).

In the tadpole of *N. corrugatus*, the M. intermandibularis posterior differs from the other species examined, by not inserting on a median raphe. Instead, muscle fibers insert along the broad and massive ceratohyale.

The M. l. mandibulae posterior superficialis is one of the longest cranial muscles in all examined species. However, its origin differs in tadpoles of *A. occidentalis* and *T. robustus* compared to tadpoles of *L. parkeri* and *N. corrugatus*. In the tadpole of *A. occidentalis*, the muscle has a two-headed origin at the capsula auditiva. In the tadpole of *T. robustus*, the M. l. mandibulae posterior superficialis originates along the sidewall of the braincase. The M. l. mandibulae posterior superficialis functions as a lower jaw adductor. The lower jaws of the tadpoles of *A. occidentalis*, *N.*

corrugatus and *T. robustus* are slightly more massive compared to the lower jaw of the tadpole of *L. parkeri*. Nevertheless, there is no indication that the M. l. mandibulae posterior superficialis is adapted to lotic habitats. In Table 3, changes of muscles interpreted as an adaptation to lotic habitats, are highlighted in blue. These muscles appear more massive or differ in shape compared to the tadpole of *L. parkeri*.

In the tadpole of *L. parkeri*, the M. l. mandibulae anterior originates anteroventrally on the capsula auditiva. In tadpoles of *A. occidentalis, N. corrugatus* and *T. robustus* the muscle originates far posteriorly at the capsula auditva and the lateral alae of the parasphenoid. An expanded origin of the M. l. mandibulae posterior superficialis is reported for suctorial tadpoles of the neobatrachian hylids *L. nannotis, L. rheocola* and *N. dayi* (Haas & Richards 1998) and it is assumed that this feature is 'causally linked to highly specialized suctorial habits'.

The M. l. mandibulae anterior articularis is only present in the tadpole of *N. corrugatus.* There is no indication that this muscle is an adaptation to lotic habitats.

The M. l. mandibulae externus is absent in *T. robustus*. It is relatively strong and similar in tadpoles of *L. parkeri, A. occidentalis* and *N. corrugatus.* Haas (1996) reported, that the M. levator mandibulae externus is absent in some anuran taxa. Due to its presence and comparable shape in *L. parkeri* there seems to be no correlation between the strong muscle and a (fast) flowing microhabitat.

In the species examined, the M. l. mandibulae lateralis is only present in the tadpole of *N. corrugatus*. Brucker (Master thesis 2016) also found that this muscle is absent in tadpoles of the hyperoliid *Afrixalus uluguruensis, A. fornasini* and *Kassina senegalensis*. Haas & Richards (1998) stated that the phylogenetic and functional significance of this muscle is unclear, as it is found in lotic- and pond-dwelling (lentic) tadpoles.

The hyoid muscles

In *A. occidentalis, N. corrugatus* and *T. robustus,* the M. hyoangularis, the M. orbitohyoideus, the M. suspensoriohyoideus and the M. interhyoideus are distinctly bigger and heavier muscularized compared to the tadpole of *L. parkeri.*

In all specimens examined, the M. orbitohyoideus is the strongest and biggest muscle of the cranium (Fig. 13). In tadpoles of *A. occidentalis, N. corrugatus* and *T. robustus,* its origin extends onto the processus ventralis of the palatoquadrate. This is not seen in the tadpole of *L. parkeri*. In *T. robustus,* the M. orbitohyoideus in fact consists of three muscular layers (Fig. 10A). A big and well developed M. orbitohyoideus is likewise seen in the carnivorous tadpole of *Afrixalus uluguruensis,* occurring in lotic habitats (Brucker, Master thesis 2016). Descriptive analyses suggest that a big M. orbitohyoideus and a massive ceratobranchial correlate with higher bite forces providing a mechanical advantage for lotic tadpoles (Haas & Richards 1998; Satel & Wassersug 1981; Wassersug & Hoff 1979).

The M. suspensoriohyoideus in tadpoles of *A. occidentalis, N. corrugatus* and *T. robustus* is located posterior to the M. orbitohyoideus (Fig. 13). In these three species, the muscle originates along the palatoquadrate and inserts laterally on the ceratohyale. In the tadpole of *L. parkeri,* the M. suspensoriohyoideus originates at the cartilago meckeli, broadens running along the processus muscluaris and inserts at the ceratohyale.

The branchial muscles

In tadpoles of *L. parkeri, A. occidentalis, N. corrugatus* and *T. robustus* the M. levator arcus branchialis I-IV and the M. constrictor branchialis I-IV are present showing only little interspecific variation. In tadpoles of *A. occidentalis* and *T. robustus*, the muscles appear slightly more massive compared to the two other species examined. There is no obvious correlation with a lotic habitat.

The hypobranchial muscles

A single M. geniohyiodeus is present in tadpoles of *L. parkeri, A. occidentalis* and *T. robustus.* In the tadpole of *N. corrugatus* it is divided into a M. geniohyoideus lateralis and M. geniohyoideus medialis (Fig. 13). The muscles of the hyobranchial group are stronger and thicker in the tadpole of *T. robustus*, correlating with its stout and robust hyobranchial skeleton.

The sucker – a typical feature of lotic tadpoles?

Lotic Tadpoles often share several anatomical adaptations. One of these adaptations is the presence of a modified oral or abdominal sucker (Altig & McDiarmid 1999). These structures enable tadpoles to adhere to the substrate in order to prevent drift in lotic habitats. Tadpoles were distinguished as 'suctorial larvae', implying the presence of an oral sucker and 'gastromyzophorous larvae' meaning that tadpoles exhibit a modified abdominal sucker.

The presence or absence of characters adapted to lotic water systems varies across taxa. Of the four arthroleptid tadpoles examined in this study, an oral sucker is present in *T. robustus. Astylosternus occidentali*s and *N. corrugatus* rather have large lobes and a prominent oral mouthpart. Like the tadpole of *T. robustus*, the tadpole of *N. corrugatus* also occurs in very fast flowing streams, but an oral sucker is not formed. By contrast, *N. corrugatus* has a large processus hyoquadratis, a structure that potentially compensates an oral sucker functionally by supporting the chondrocranium with stronger muscles to prevent the tadpole from drift in stronger flowing water systems. The inhabitation of lotic habitats is not necessarily linked to the presence of an oral or abdominal sucker. Lavilla and De Sá (2001) proposed that the presence of e.g. a large abdominal sucker in tadpoles may compensate a less massive chondrocranium. We found that both, a sucker as well as a heavy and compact chondrified chondrocranium are present in the tadpole of *T. robustus.*

It is assumed that forces of the M. rectus abnominis possibly act on the processus ventralis as the oral sucker is attached to the stream bottom or on rocks (Haas & Richards 1998; Gradwell 1973). We did not investigate the morphology of the rectus abdominis muscle, but a processus ventralis of the palatoquadrate is also present in the lotic tadpoles of *A. occidentalis, N. corrugatus* and *T. robustus.* In these species, the processus ventralis of the palatoquadrate is the origin of the massive M. orbitohyoideus. The processus ventralis of *T. robustus* is much longer compared to the two other species. Primarily, the processus ventralis functions as an origin attachment side of the broad M. orbitohyoideus in all three species. We assume that the presence of an oral sucker is not directly linked to the presence of a processus ventralis of the palatoquadrate. The presence of a much longer processus venralis in *T. robustus,* together with the presence of a large oral sucker let us agree with the assumption of Haas & Richards (1998) that this process may additionally function as an attachment side for the M. rectus abdominis. Its action may pull the body of the tadpole to the ground after the oral sucker has been attached to the substrate.

The tadpoles of *P. gyrinaethes* are also known for their large suckers (Candioti et al. 2016). However, these tadpoles do not occur in lotic water systems but live in the water-filled leaf axis of bromeliads and mainly move with their oral and abdominal suckers (Candioti et al. 2016). Candioti et al. (2016) stated that the strong and wide ceratohyale functions as skeletal support to the sucker. Many gastromyzophorous tadpoles have a large, robust ceratohyale which gives functional support for the attached strong muscular hyoid masses (Candioti et al. 2016). In this study, we also found that a large ceratohyale, together with strong hyoid muscles, especially the strong orbitohyoideus and the hyoangularis muscles, are formed in each of the lotic tadpoles. These characters are not associated with the presence of an oral sucker except in *T. robustus.* Therefore, selection pressures for oral suckers and stronger ceratohyale skeletons are similar for lotic tadpoles (streaming forces) and for tadpoles in bromeliads. But it may not be excluded that different selection pressures may have led to a similar adaptation in these tadpoles.

Big heads in fast flows?

In the present study we found that the musculoskeletal system of the tadpoles of *A. occidentalis, N. corrugatus* and *T. robustus* correlate with their habitat type and are highly modified compared to the configuration present in the tadpole of *L. parkeri.*

In tadpoles of *A. occidentalis, N. corrugatus* and *T. robustus,* the cranium is massive, strongly chondrified and heavily muscularized. This correlates with occupation of streams in rocky areas (Fig. 1). The presence of highly adapted cranial features is reported for several lotic species and has evolved several times independently (Griesbaum et al. 2019; De Oliveira et al. 2017; Candioti et al. 2016; Haad et al. 2014; Channing et al. 2012; Rödel et al. 2012; Haad et al. 2011; Lavilla & De Sá 2001; Altig & McDiarmid 1999; Haas & Richards 1998; Inger 1992; Cadle & Altig 1991).

Haas & Richards (1998) analyzed the correlations of cranial morphology, ecology and evolution in Australian suctorial tadpoles of the neobatrachid genera *Litoria* and *Nyctimystes* and concluded that the special morphological features of the cranial musculoskeleton, e.g. changes in muscular proportions and sizes as well as more massive and heavily condrified skeletal elements, are causally linked to the habitat types of the tadpoles. Positional shifts or changes in proportions are rather involved than structural novelties (Haas & Richards 1998).

Modified features of the cranium can be found in tadpoles of *A. occidentalis, N. corrugatus* and *T. robustus*, although the tadpole of *T. robstus* can be considered a suctorial tadpole based on the presence of a large oral sucker. We here interpret these features as adaption on the microhabitat and agree with the following features of Haas & Richards (1998) for *A. occidentalis, N. corrugatus* and *T. robustus* tadpoles examined in this study:

- The cornua trabecula is more robust and wide, and the trabeculae are fused along most of their length or completely fused.
- The lower jaw is more robust, but it does not change in form or shape.
- The cartilago labialis superior is wide and robust and forms a fused transversal plate.
- The palatoquadrate is robust and is connected to the neurocranium by a broad commissura quadratocranialis anterior and a broad processus oticus.
- The palatoquadrate bears a processus ventralis. This structure is a ventrad angled process and at the basis of the processus muscularis and is orientated posteriad.
- The ceratohyale is strong and wide and is larger compared to the branchial basket.
- The M. l. mandibulae anterior originates far posteriorly, at the capsula auditiva and the lateral alae of the parasphenoid.

Additionally, we add features mentioned by Haas & Richards (1998), but not integrated into their summary of common features of modified structures in lotic tadpoles:

- The processus muscularis is wide, robust and strongly chondrified.
- The M. orbitohyoideus is massive according to the wide and robust processus muscularis, and originates along the processus ventralis of the palatoquadrate.

Our data add further evidence that the cranial morphology of tadpoles is highly adaptive, depending on the (micro-)habitat. However, some modified structures such as a sucker disc, the fusion of the trabecular horns, a fused cartilago labialis superior and a massive hyobranchial skeleton can be present in lotic and bromeliad tadpoles living in completely different microhabitats. Also, some of these

characteristics are seen in carnivorous tadpoles. Therefore, such structures may have evolved independently in different functional tadpole guilds to stabilize the larval cranium due to strong selection pressures (waterflow, gravity, larval feeding strategies etc.).

Further investigations are necessary to answer this question more precisely. The main questions of this study therefore could be addressed more analytically in e.g. quantifying the stream velocities of each species or evaluating the cranial muscle relative to tadpole size. Also, the cranial morphology of *Leptodactylodon* and *Sctoplebs,* the closest relatives of the species investigated in this study, is of particular interest. More comparative data on lentic tadpoles may add further evidence to test the effect of different selection pressures in different (micro-) habitats.

Acknowledgements

We would like to thank Simon Loader and Michele Menegon for providing a tadpole of *Leptopelis parkeri*. We thank Annemarie Ohler for providing the tadpoles of *Astylosternus occidentalis* and *Trichobatrachus robustus*. We thank Egon Heiss and Benjamin Naumann for critically reading the manuscript. Funding was provided through a German Science Foundation (DFG) grant (MU2914/2-1).

References

Aguayo, R., Lavilla, E. O., Candioti M.F.V., Camacho, T. (2009). Living in Fast-Flowing Water: Morphology of the gastromyzophorous tadpole of the bufonid *Rhinella quechua* (*R. veraguensis* group). Journal of Morphology 270:1431–1442.

Altig, R., McDiarmid, R.W. (1999). Diversity. Familial and generic characterizations. In: Tadpoles. The Biology of Anuran Larvae, p. 295-337. Altig, R., McDiarmid, R.W., Eds, Chicago and London, University of Chicago Press.

Amiet J.-L. (1971). Le têtard d'*Astylosternus corrugatus* Boulenger (Amphibien Anoure). Annales de la Faculté des Sciences du Cameroun 6: 85–98

Baldo, D., Candioti, M.F.V., Haad, B., Kolenc, F., Borteiro, C., Pereyra, M. O., Zank, C., Colombo, P., Bornschein, M. R., Sis, F. N., Brusquetti, F., Conte, c. E., Nogueira-Costa, P., Almeida-Santos, P., Pie, M. R. (2014). Comparative morphology of pond, stream and phytotelm-dwelling tadpoles of the South American Redbelly Toads (Anura: Bufonidae: Melanophryniscus). Biological Journal of the Linnean Society, 1-25.

Barej, MF, Pfalzgraff T, Hirschfeld M, Liedtke HC, Penner J, Gonwouo NL, Dahmen M, Grözinger F, Schmitz A, Rödel MO (2015). The tadpoles of eight West and Central African Leptopelis species (Amphibia: Anura: Arthroleptidae). Amphibian and Reptile Conservation 9 (2) [Special Section]: 56–84.

Böck, P. (1989). Romeis Mikroskopische Technik. Urban & Schwarzenberg, München.

Boulenger, G. A. (1904). Descriptions of two new genera of frogs in the family Ranidae from Cameroon. Annals and Magazine of Natural History (Series 7) 13: 261–262. https://doi. org/10.1080/00222930409487067

Cadle, J. E., Altig, R. (1991). Two lotic tadpoles from the Andes of southern Peru: *Hyla armata* and *Bufo veraguensis*, with notes on the call of *Hyla armata* (Amphibia: Anura: Hylidae and Bufonidae), Studies on Neotropical Fauna and Environment, 26:1, 45-53.

Brucker, A. (2016). Larval morphology and ecology of leaf-folding treefrogs, genus *Afrixalus* (Anura: Hyperoliidae). Master thesis pp. 1-89.

Candioti, F.M.V., Haas, A., Altig, R., Peixoto, O. (2016). Cranial anatomy of the amazing bromeliad tadpoles of *Phyllodytes gyrinaethes* (Hylidae: Lophyohylini), with comments about other gastromyzophorous larvae. Zoomorphology. DOI 10.1007/s00435-016-0334-7

Channing, A. (2008). The mud dwelling tadpole of the long-toed tree frog, *Leptopelis xenodactylus* (Arthroleptidae). Herpetological Review 39: 288–290.

Channing, A., Rödel, M.-O., Channing, J. (2012). Tadpoles of Africa. The Biology and Identification of all known tadpoles of sub-Saharan Africa. Frankfurt Contributions of Natural History, Volume 35. Frankfurt-am-Main: Edition Chimaira. 402 pp.

De Oliveira, M.I.R.R., Weber, L.W., De Sá, R.O., Ferreira, J.S., Libório, A.E.C., Takazone, A.M.G. (2017). Chondrocranium and internal oral morphology of the tadpole of *Corythomantis greeningi* (Anura: Hylidae). Phyllomedusa 16(1):71–80.

De Jongh, H.J. (1968). Functional morphology of the jaw apparatus of larval and metamorphosing *Rana temporaria*. Netherlands Journal of Zoology 18:1–103.

De Sá, R.O. (1988). Chondrocranium and ossification sequence of *Hyla lanciformis*. Journal of Morphology 195:345–355.

Feng, Y. J., David C. Blackburn, D. C., Liang, D., Hillis, D. M., Wake, D. B., Cannatella; D. C., Zhang, P. (2017). Phylogenomics reveals rapid, simultaneous diversification of three major clades of Gondwanan frogs at the Cretaceous–Paleogene boundary. Proceedings of the National Academy of Sciences of the United States of America.

Frost, D. R. (2020). Amphibian Species of the World: An Online Reference. Version 6.1 (*Date of access*). Electronic Database accessible at https://amphibiansoftheworld.amnh.org/index.php. American Museum of Natural History, New York, USA.

Frost, D. R., Grant, T., Faivovich, J. N., Bain, R. H., Haas, A., Haddad, L. F. B., De Sa´, R.O, Channing, A., Wilkinson, M., Donellan, S. C., Raxworthy, C. J., Campbell, J. A., Blotto, B. L., Moler, P., Drewes, R. C., Nussbaum, R. A., Lynch, J. D., Green, D. M., Wheeler, W. C. (2006). The amphibian tree of life. Bulletin of the American Museum of Natural History Central Park West at 79th street, New York, ny 10024 number 297, 370 pp.

Gosner, Kenneth L. (1960). A simplified table for staging anuran embryos and larvae with notes on identification. Herpetologica. 16 (3): 183–190.

Gradwell, N. (1973). On the functional morphology of suction and gill irrigation in the tadpole of *Ascaphus*, and notes on hibernation. Herpetologica 29:84–93.

Griesbaum, F., Hirschfeld, M., Barej, M. F., Schmitz, A., Rohrmoser, M., Dahmen, M., Mühlberger, F., Liedtke, H. C., Gonwouo, N. L., Doumbia, J., Rödel, M.-O. (2019). Tadpoles of three western African frog genera: *Astylosternus* Werner, 1898, *Nyctibates* Boulenger, 1904, and *Scotobleps* Boulenger, 1900 (Amphibia, Anura, Arthroleptidae). Zoosystemtics and Evolution 95 (1): 133–160.

Haad, B., Candioti, M.F.V., Baldo, D. (2011). Shape variation in lentic and lotic tadpoles of *Melanophryniscus* (Anura: Bufonidae), Studies on Neotropical Fauna and Environment 46: 2, 91-99.

Haad, M. B., Candioti, M.F.V., Baldo, D. (2014). The stream tadpoles of *Rhinella rumbolli* (Anura: Bufonidae). Herpetologica 70(2): 184–197.

Haas, A. (1995). Cranial features of dendrobatid tadpoles (Amphibia: Anura: Dendrobatidae). Journal of Morphology 224: 241–264.

Haas, A. (1996). Das larvale Cranium von *Gastrotheca riobambae* und seine Metamorphose (Amphibia, Anura, Hylidae). Abhandlungen und Verhandlungen des Naturwissenschaftlichen Vereins in Hamburg 36:33–162.

Haas, A., Richards, S. J. (1998). Correlations of cranial morphology, ecology, andevolution in Australian suctorial tadpoles of the genera *Litoria* and *Nyctimystes* (Amphibia: Anura: Hylidae: Pelodryadinae). Journal of Morphology 238: 109-141.

Haas, A., Wolter, J., Hertwig, S. T., Das, I. (2009). Larval morphologies of three species of stream toads, genus *Ansonia* (Amphibia: Bufonidae) from East Malaysia (Borneo), with a key to known Bornean *Ansonia* tadpole. Zootaxa 2302: 1–18.

Inger, R. F. (1992): Variation of apomorphic characters in stream-dwelling tadpoles of the bufonid genus *Ansonia* (Amphibia: Anura). Zoological Journal of the Linnean Society 105: 225-237.

Lamotte, M., Lescure, J. (1988). Les caractéristiques biométriques du développement et de la métamorphose des têtards rhéophiles d'anoures. Bulletin de la Société zoologique de France 113: 21–30.

Lamotte, M., Lescure, J. (1989a). Les têtards rhéophiles et hygropétriques de l'ancien et du nouveau monde. Annales des Sciences naturelles, Zoologie Série 13 10: 111–122.

Lamotte, M., Lescure, J. (1989b). Les têtards rhéophiles et hygropétriques de l'ancien et du nouveau monde. Annales des Sciences naturelles, Zoologie Série 13 10: 125–144.

Lavilla, E. O., De Sá, R. (2001). Chondrocranium and visceral skeleton of *Atelopus tricolor* and *Atelophryniscus chrysophorus* tadpoles (Anura, Bufonidae). Amphibia-Reptilia 22: 167-177.

Lukas, P. (2021). Larval cranial anatomy of the Eastern Ghost Frog (*Heleophryne orientalis*). Acta Zoologica, 102(4): 452-466.

Nogueira-Costa, P., Wachlevski, M. (2015). The tadpoles of *Hylodes meridionalis* (Mertens, 1927), a lotic stream anura from the Atlantic Rainforest of Brazil. Zootaxa 4032 (2): 199-202.

Oberhummer, E., Barten, C., Schweizer, M., Das, I., Haas, A., Hertwig, S. T. (2014). Description of the tadpoles of three rare species of megophryid frogs (Amphibia: Anura: Megophryidae) from Gunung Mulu, Sarawak, Malaysia. Zootaxa 3835 (1): 059-079.

Perret, J.-L. (1966). Les Amphibiens du Cameroun. Zoologische Jahrbücher/ Abteilung für Systematik Band 8: 289-464.

Portik, D. M., Blackburn, D. (2016). The evolution of reproductive diversity in Afrobatrachia: A phylogenetic comparative analysis of an extensive radiation of African frogs. Evolution 70-9: 2017–2032.

Raj, P., Vasudevan, K., Deepak, V., Sharma, R., Singh, S., Aggarwal, R. K., Dutta, S. K. (2012). Larval morphology and ontogeny of *Nasikabatrachus sahyadrensis* Biju & Bossuyt, 2003 (Anura, Nasikabatrachidae) from Western Ghats, India. Zootaxa 3510: 65-76.

Rödel, M.-O. (2000). Herpetofauna of West Africa, Vol. I: Amphibians of the West African savanna. Edition Chimaira, Frankfurt am Main, 332 pp.

Rödel, M.-O., Barej, M. F., Hillers, A., Leaché, A.D., Kouamé, N. G., Ofori-Boateng, C., Assemian, N. E., Tohé, B., Penner, J., Hirschfeld, M., Doumbia, J., Gonwou, L. N., Nopper, J., Brede, C., Diaz, R., Fujita, M. K., Gil, M., Segniagbeto, G. H., Ernst, R., Sandberger, L. (2012). The genus *Astylosternus* in the Upper Guinea rainforests, West Africa, with the description of a new species (Ampibia: Anura: Arthroleptidae). Zootaxa 3245: 1-29.

Saidapur, S. K. (2001). Behavioural ecology of anuran tadpoles: The indian scenario. Proceedings of the Indian National Science Academy B67 No. 6 pp 311-322.

Satel, S. L., Wassersug, R. (1981). On the relative sizes of the buccal floor depressor and elevator musculature in tadpoles. Copeia 1981:129–137.

van der Westhuizen, C.M. (1961). The development of the chondrocranium of *Heleophryne purcelli* Sclater with special reference to the palatoquadrate and sound-conducting apparatus. Acta Zoolica (Stockholm) 42:1–72.

Wassersug, R. J., Hoff, K. (1979). A comparative study of the buccal pumping mechanism of tadpoles. Biological Journal of the Linnean Society 12:225–259.

Tables

Table 1: Specimen list. PMC, polymolybdenic acid; µCT, micro-computed tomography.

Species	Gosner stage	Total length [mm]	Head-body length [mm]	Tail length [mm]	technique	staining
Leptopelis parkeri	30	26.0	7.8	18.2	photo, µCT	1% PMA
Astylosternus occidentalis	25/26	44.6	16.3	28.3	photo, histology	Azan
Astylosternus occidentalis	26	45.3	16.8	28.5	clearing & staining	Alcian-Alizarin
Astylosternus occidentalis	35	73.8	26.5	47.3	µCT	1% PMA
Nyctibates corrugatus	26	52.9	22.3	30.6	photo, µCT	1% PMA
Trichobatrachus robustus	36/37	69.3	25.3	44.0	photo, µCT	1% PMA

Table 2: Description of origin and insertion of the larval cranial muscles in different species of Arthroleptids: *Leptopelis parkeri, Astylosternus occidentalis, Nyctibates corrugatus* and *Trichobatrachus robustus*. M.=Musculus, l.=levator.

Muscle group	Muscle	***Leptopelis parkeri* (present study) Fig. 10/15**	***Asytlosternus occidentalis* (present study) Fig. 11/15**	***Nyctibates corrugatus* (present study) Fig. 12/15**	***Trichobatrachus robustus* (present study) Fig. 13/15**
Mandibular group	**M. mandibulolabialis**	origin: ventromedial on cartilago meckeli; insertion: lower lip	origin: laterally on cartilago meckeli; insertion: lower lip	origin: anteroventral side of cartilago meckeli; insertion: lower lip	origin: laterally at the cartilago meckeli; insertion: lower lip
	M. intermandibularis anterior	attached along symphysis of cartilago labialis inferior	spans along ventral side of cartilago labialis inferior	spans along symphysis of cartilago labialis inferior	spans along ventral side of cartilago labialis inferior
	M. intermandibularis posterior	origin: medial raphe; insertion: medioventrally on cartilago meckeli	origin: median raphe; insertion: ventral part of cartilago meckeli	runs along ceratohyale	origin: medial raphe; insertion: ventral side of cartilago meckeli

M. l. mandibulae posterior superficialis	origin: anterior to capsula auditiva along processus oticus of palatoquadrate; insertion: dorsomedially on cartilago meckeli	origin: two-headed: on capsula auditiva; insertion: dorsomedial process of cartilago meckeli	origin: arcus suboccularis of palatoquadrate; insertion: dorsolateral part of cornu trabeculae	origin: lateral sidewall of the braincase; insertion: between dorsomedial process and processus retroarticularis of cartilago meckeli
M. l. mandibulae posterior profundus	origin: processus oticus, at posterior end of palatoquadrate; insertion: cartilago meckeli	origin: ventral part of capsula auditiva, close to lateral ala of parasphenoid; insertion: dorsolateral ala of cartilago labialis superior	origin: capsula auditiva; insertion: dorsal part of cartilago labialis inferior	origin: ventromedial side of capsula auditiva and posterior end of palatoquadrate; insertion: dorsomedial process of cartilago meckeli
M. l. mandibulae anterior	origin: anteroventrally on capsula auditiva; insertion: processus retroarticularis of cartilago meckeli; not seen in Fig. 13	origin: ventral part of capsula auditiva and lateral ala of parasphenoid; insertion: dorsal, lateral part of cartilago meckeli; not seen in Fig. 13	origin: ventrally on lateral alae of parasphenoid, posterior part of palatoquadrate and ventral side of capsula auditiva; insertion: between dorsomedial process and processus retroarticularis of cartilago meckeli; not seen in Fig. 13	origin: ventral part of capsula auditiva and lateral ala of parasphenoid; insertion: processus retroarticularis of cartilago meckeli; not seen in Fig. 13
M. l. mandibulae anterior articularis	not formed	not formed	origin: both tracts at processus muscularis of palatoquadrate; insertion: one tract at anterior part, second tract at posterior part of processus retroarticularis of cartilago meckeli; not seen in Fig. 13	not formed

	M. l. mandibulae externus	origin: internal wall of processus muscularis; insertion: laterally on cartilago labialis superior	origin: inner side of medial part of the processus muscularis; insertion: ventrolateral on cartilago labialis superior	origin: inner, lateral part of processus muscularis; insertion: lateral part of cartilago labialis superior	not formed
	M. l. mandibulae lateralis	not formed	not formed	origin: medial part of processus muscularis of palatoquadrate; insertion: medially along cartilago meckeli	not formed
Hyoid group	**M. hyoangularis**	origin: dorsolaterally on ceratohyale; insertion: on tip of processus retroarticularis of cartilago meckeli	origin: mediolateral part of ceratohyale; insertion: ventromedial process of palatoquadrate	origin: lateral part of ceratohyale; insertion: anteromedially on cartilago meckeli	origin: anteriorly on processus lateralis hyalis of ceratohyale; insertion: of processus retroarticularis of cartilago meckeli
	M. quadratoangularis	origin: on basis of processus muscularis; insertion: processus retroarticularis of cartilago meckeli	origin: inner ventrolateral part of processus muscularis; insertion: processus retroarticularis of cartilago meckeli	origin: ventrolateral part of processus muscularis; insertion: on ventromedial process of cartilago meckeli	origin: ventral side of processus muscularis; insertion: ventromedially on processus retroarticularis of palatoquadrate
	M. suspensorioangularis	origin: medioventrally on processus muscularis; insertion: anteroventrally on processus retroarticularis of cartilago meckeli	origin: inner lateral part of processus muscularis; insertion: processus retroarticularis of cartilago meckeli	origin: ventrolateral part of processus muscularis of palatoquadrate; insertion: anterior on dorsomedial process of cartilago meckeli	origin: postolateral margin of processus muscularis of and anterior part of arcus suboccularis; insertion: dorsal part of processus lateralis hyalis of ceratohyale

	M. orbitohyoideus	origin: along processus muscularis; insertion: on ventrolateral part of ceratohyale	origin: lateral surface of processus muscularis and processus ventralis of palatoquadrate; insertion: dorsolateral surface of ceratohyale	origin: lateral part of processus muscularis and processus ventralis; insertion: along lateral part of the ceratohyale and proc. hyoquadratis	consists of three layers; origin: lateral part of processus muscularis and processus ventralis; insertion: lateral part of ceratohyale
	M. suspensoriohyoideus	origin: cartilago meckeli, widens along processus muscularis of palatoquadrate; insertion: ventrally on ceratohyale	origin: ventrolateral on palatoquadrate; insertion: anterolateral on ceratohyale	origin: posteromedial part of palatoquadrate; insertion: mediolateral on ceratohyale	origin: ventrolateral on palatoquadrate; insertion: dorsolateral on ceratohyale
	M. interhyoideus	origin: both parts medially on raphe; insertion: lateral edge on ceratohyale	origin: medial raphe; insertion: mediolaterally on ceratohyale	origin: median raphe; insertion: ventrolateral part of ceratohyale	origin: medial raphe; insertion: ventrolateral margin of ceratohyale
Branchial group	**M. l. arcus branchialis I-IV**	I: originates mediolaterally along palatoquadrate, inserts dorsolaterally on ceratohyale; II: originates ventrolaterally on capsula auditiva, inserts on ceratobranchialia I and II; III and IV: originate ventrolaterally on capsula auditiva, insert on ceratobranchialia II and III; IV inserts medially on ceratobranchiale III	I: originates mediolaterally on arcus subocularis of palatoquadrate, inserts on dorsolateral margin of ceratobranchiale I; II: originates close to processus oticus of palatoquadrate, inserts on medial part of ceratobranchiale I; III: originates on processus oticus of palatoquadrate, inserts on ceratobranchiale I and II; IV: originates posterolateral on the capsula auditiva, inserts on ceratobranchiale II and III	I and II: originate at posteroventral part of capsula auditiva, insert dorsomedially on ceratobranchiale I; III: originates anteroventrally on capsula auditiva, inserts on ceratobranchiale I and II; IV: originates on posterior end of capsula auditiva, inserts on ceratobranchiale II and III	I: originates on posterolateral part of arcus subocularis of palatoquadrate, inserts on ceratobranchiale I and II; II: originates on posterolateral part of arcus subocularis of palatoquadrate, inserts on ceratobranchiale II and III; III and IV: originate on lateral side of capsula auditiva, insert on ceratobranchiale III and IV

M. constrictor branchialis I -IV	I: originates from ventral margin of ceratohyale, inserts on processus hyobranchialis of branchial basket; II: originates ventrally along processus hyobranchialis, inserts ventromedially on ceratobracnhiale I; III: originates at proximal end of ceratobranchiale II, inserts on ceratobranchialia II and III; IV: originates anteriorly on ceratobranchiale III, inserts medially on ceratobranchiale III	I: originates anteromedially on ceratobranchiale I, inserts on processus lateralis hyalis of ceratohyale; II: originates on anterior part of ceratobracnhiale II, inserts posteromedially on ceratobranchiale I; III: originates anteriorly on ceratobranchiale II, inserts on ceratobranchiale I and II; IV: originates on medial part of ceratobranchiale III, inserts on ceratobranchiale II and III	I: originates at basis of the ceratohyale, inserts medially on ceratobranchiale I; II: originates on anterior part of ceratobranchiale II, inserts on ceratobranchiale I and II; III: originates anteriorly on ceratobranchiale II, inserts on ceratobranchiale II and III; IV: originates on medial part of ceratobranchaile III, inserts on ceratobranchiale II and III	I: runs along ceratobranchiale I and II; II: originates on medial part of ceratobranchiale I, inserts on ceratobranchiale II and III; III: originates on medial part of ceratobranchiale, inserts on ceratobracnhiale III and IV; IV: originates on medial part of ceratobranchiale IV, inserts on ceratobranchiale IV
M. subarcularis rectus	origin: ceratohyale; insertion: ceratobranchiale IV	origin: on the ventral side of ceratohyale; insertion: anteriorly on ceratobranchiale III	I (dorsal head): originates on basis of the ceratohyale, inserts anterior on ceratobranchiale I; II (two ventral heads): originate on posteromedial part of ceratohyale, insert on anterior part of ceratobranchiale II; II – IV: originate on ceratobranchiale II, insert on anterior part of ceratobranchiale III	I (dorsal head): originates on medial part of ceratohyale, inserts on medial part of ceratobranchiale II; II (ventral head): originates mediolateral on ceratohyale and on medial part of ceratobranchiale II, inserts on anteromedial part of ceratobranchiale III; II-IV: originate on anteromedial part of ceratobranchiale III, insert on anteromedial part of ceratobranchiale IV

	M. subarcularis obliquus	origin: basihyale of hyobranchial skeleton; insertion: medioventral process of ceratobranchiale III	origin: anteriorly on planum hyobranchiale; insertion: anterior part of ceratobranchiale III	origin: planum hyobranchiale of hyobranchial apparatus; insertion: anterior part of ceratobranchiale III	origin: medially on planum hyobranchiale; insertion: anteromedial part of ceratobranchiale IV
Spinal group	**M. geniohyoideus**	origin: planum hypobrachiale of hyobranchial apparatus; insertion: ventromedially on cartilago labialis inferior	origin: on ventromedial part of planum hypobranchiale; insertion: posterior end of cartilago labialis inferior	origin: planum hypobrachiale of hyobranchial apparatus; insertion: ventrally on cartilago labialis inferior	origin: medially on hyobranchial plate; insertion: posterovenrtal side of cartilago labialis inferior
	M. rectus cervicis	origin: diaphragm; insertion: lateral margin of planum hypobranchiale, anterior to ceratobranchiale III	origin: diaphragm; insertion: between anterior end of ceratobranchiale I and II	origin: diaphragm; insertion: anteromedial part of ceratobranchiale III	origin: diaphragm; insertion: anteromedial part of ceratobranchiale IV

Table 3: Comparison of muscles of the larval cranium in different species of Arthroleptids: *Leptopelis parkeri*, *Astylosternus occidentalis*, *Nyctibates corrugatus* and *Trichobatrachus robustus*. Muscles that are not formed, are highlighted in orange. M.=Musculus, l.=levator, m.=mandibulae.

Species	*Leptopelis parkeri*	*Asytlosternus occidentalis*	*Nyctibates corrugatus*	*Trichobatrachus robustus*
Mandibular group	M. mandibulolabialis	M. mandibulolabialis	M. mandibulolabialis	M. mandibulolabialis
	M. intermandibularis anterior	M. intermandibularis anterior	M. intermandibularis anterior	M. intermandibularis anterior
	M. intermandibularis posterior	M. intermandibularis posterior	M. intermandibularis posterior	M. intermandibularis posterior
	M. l. m. posterior superficialis	M. l. m. posterior superficialis	M. l. m. posterior superficialis	M. l. m. posterior superficialis
	M. l. m. posterior profundus	M. l. m. posterior profundus	M. l. m. posterior profundus	M. l. m. posterior profundus
	M. l. m. anterior	M. l. m. anterior	M. l. m. anterior	M. l. m. anterior
	not formed	not formed	M. l. m. anterior articularis	not formed
	M. l. m. externus	M. l. m. externus	M. l. m. externus	not formed
	not formed	not formed	M. l. m. lateralis	not formed
Hyoid group	M. hyoangularis	M. hyoangularis	M. hyoangularis	M. hyoangularis
	M. quadratoangularis	M. quadratoangularis	M. quadratoangularis	M. quadratoangularis
	M. suspensorioangularis	M. suspensorioangularis	M. suspensorioangularis	M. suspensorioangularis
	M. orbitohyoideus	M. orbitohyoideus	M. orbitohyoideus	M. orbitohyoideus
	M. suspensoriohyoideus	M. suspensoriohyoideus	M. suspensoriohyoideus	M. suspensoriohyoideus
	M. interhyoideus	M. interhyoideus	M. interhyoideus	M. interhyoideus
Branchial group	M. l. arcus branchialis I-IV	M. l. arcus branchialis I -IV	M. l. arcus branchialis I IV	M. l. arcus branchialis I -IV
	M. constrictor branchialis I -IV	M. constrictor branchialis I -IV	M. constrictor branchialis I -IV	M. constrictor branchialis I-IV
	M. subarcularis rectus	M. subarcularis rectus	M. subarcularis rectus	M. subarcularis rectus
	M. subarcularis obliquus	M. subarcularis obliquus	M. subarcularis obliquus	M. subarcularis obliquus
Spinal group	M. geniohyoideus	M. geniohyoideus	M. geniohyoideus	M. geniohyoideus
	M. rectus cervicis	M. rectus cervicis	M. rectus cervicis	M. rectus cervicis

Figures

Figure 1: Habitat photos. **A:** *Leptopelis parkeri*, Nguru Mountains, Tanzania. Foto taken by Hendrik Müller in January 2008. **B:** Habitat of *Nyctibates corrugatus*, Ebo-Forest, Cameroon. Foto taken by Mark-Oliver Rödel in September 2010. **C:** Habitat of *Astylosternus occidentalis*, Krahn-Bassa National Forest, Liberia. Foto taken by Mark-Oliver Rödel in March 2018. **D:** Habitat of *Trichobatrachus robustus*, Obudu Plateau, Nigeria. Foto taken by Mark-Oliver Rödel in January 2007.

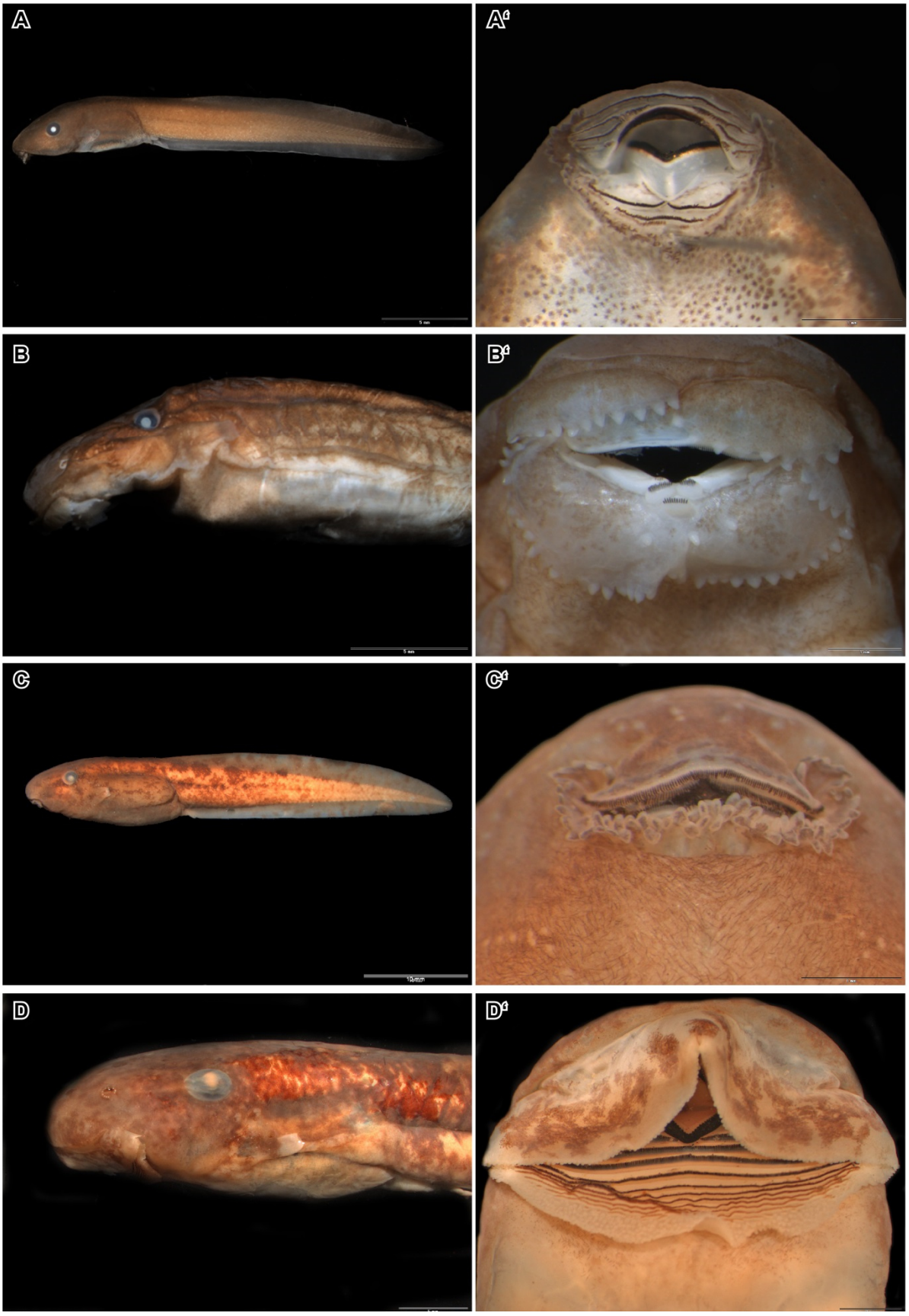

Figure 2: Photos of the tadpoles. **A and A':** *Leptopelis parkeri*, Gosner stage 30, habitus and mouthparts. **B and B':** *Astylosternus occidentalis*, Gosner stage 25/26, habitus and mouthparts. **C and C':** *Nyctibates corrugatus*, Gosner stage 26, head and mouthparts. **D and D':** *Trichobatrachus robustus*, Gosner stage 36/37, head and mouthparts.

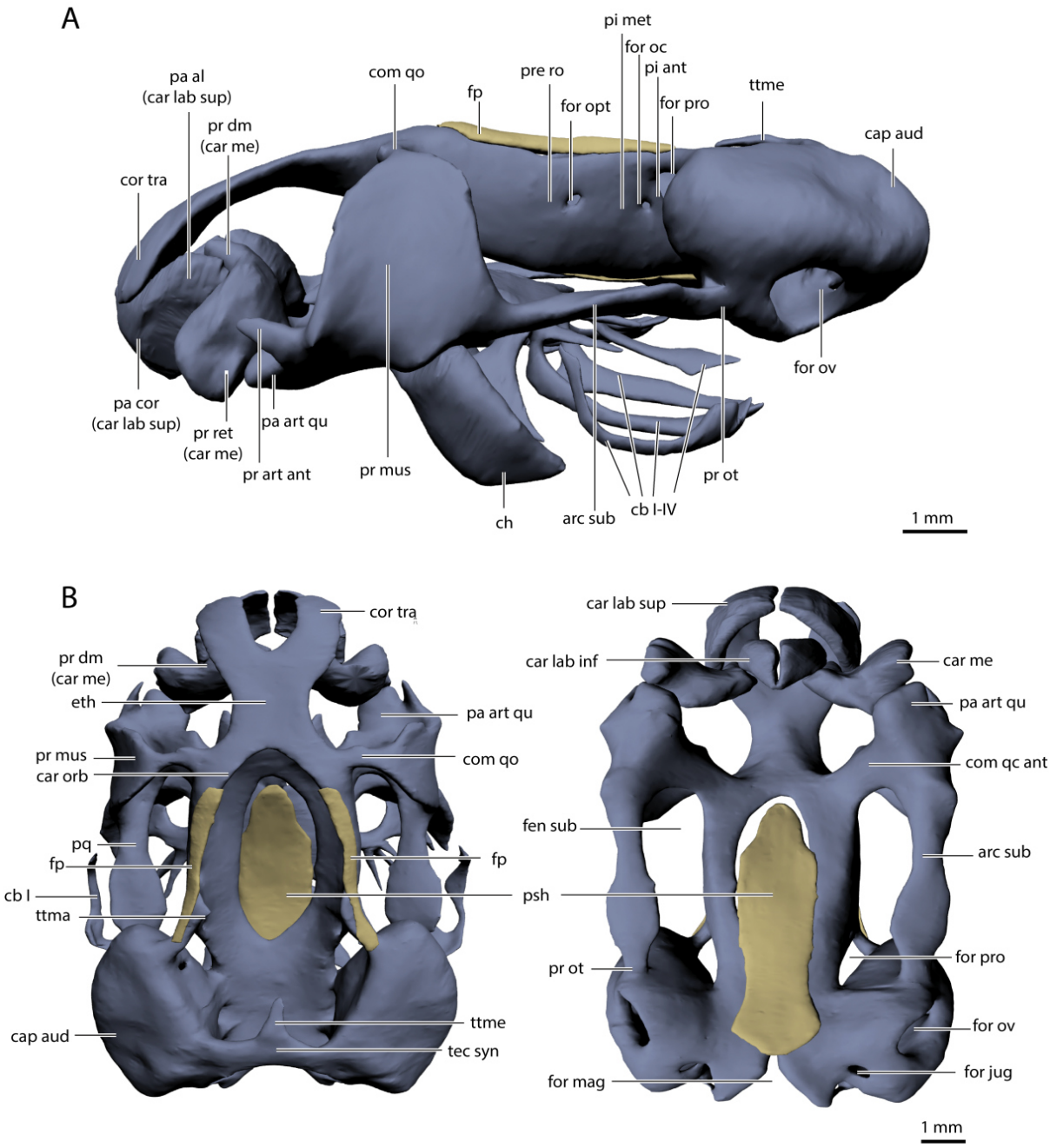

Figure 3: 3D reconstruction of a µCT scan of a tadpole of *L. parkeri* (Gosner stage 30) showing the skeletal morphology of the cranium. The different structures have been coloured as follows: cartilage, blue; bones, ochre; **A:** Lateral view. **B, left:** Dorsal view. **B, right:** Ventral view, hyobranchial skeleton not shown. See supplement for abbreviations.

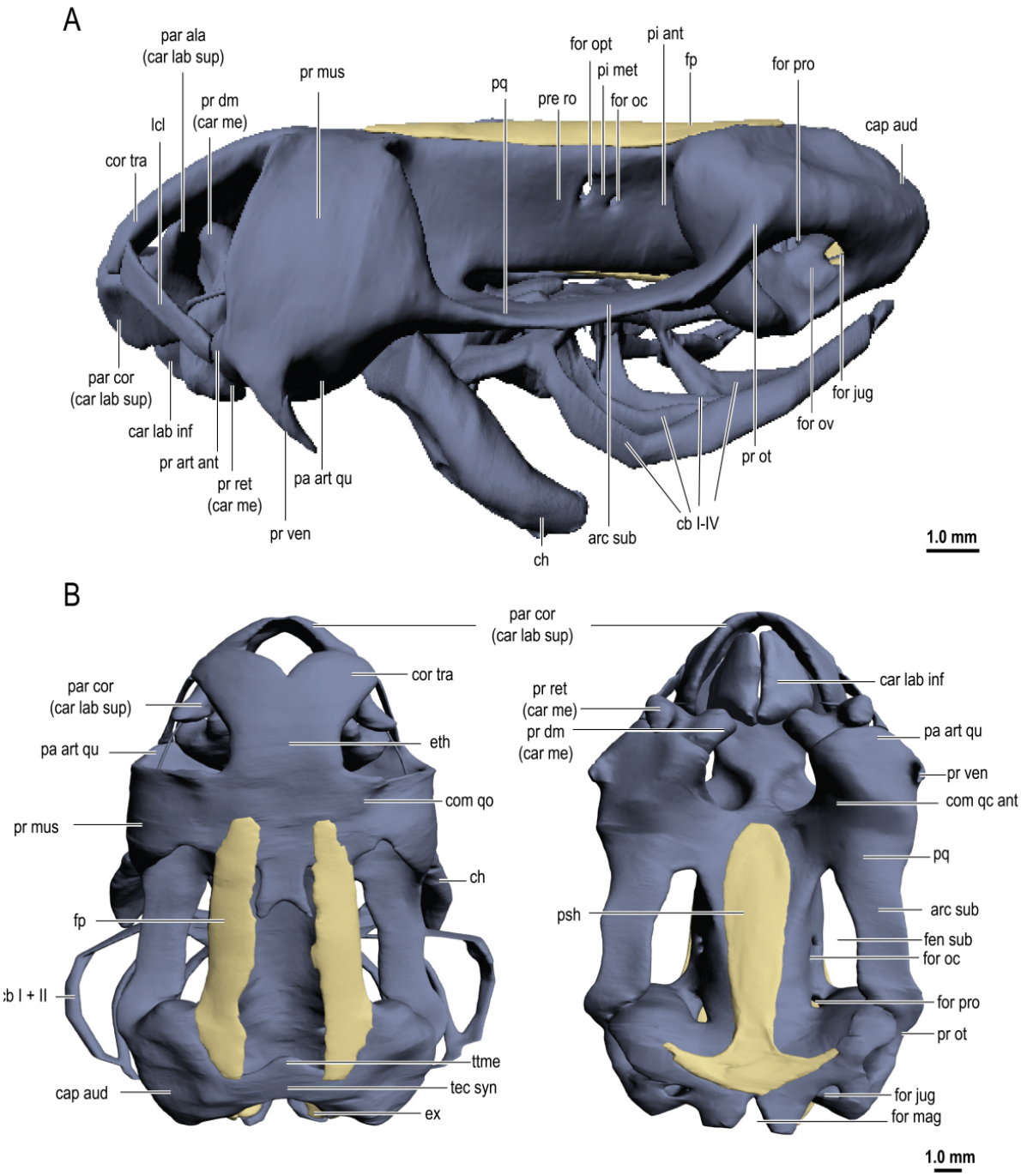

Figure 4: 3D reconstruction of a µCT scan of a tadpole of *A .occidentalis* (Gosner stage 25/26) showing the skeletal morphology of the cranium. The different structures have been coloured as follows: cartilage, blue; bones, ochre; **A:** Lateral view. **B, left**: Dorsal view, hyobranchial skeleton not shown. **B, right:** Ventral view. See supplement for abbreviations.

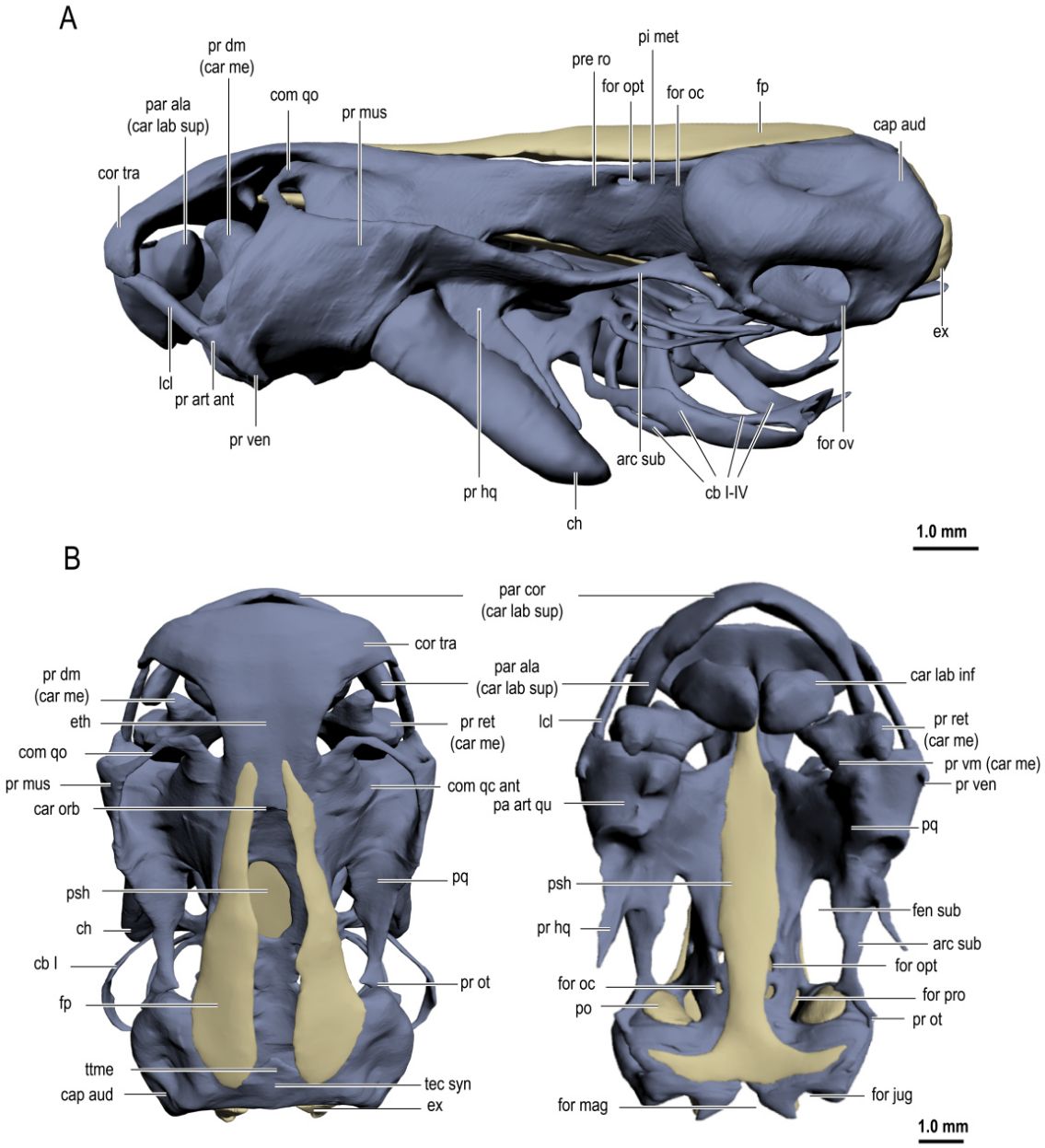

Figure 5: 3D reconstruction of a µCT scan of a tadpole of *N. corrugatus* (Gosner stage 26) showing the skeletal morphology of the cranium. The different structures have been coloured as follows: cartilage, blue; bones, ochre; **A:** Lateral view. **B, left:** Dorsal view, hyobranchial skeleton not shown. **B, right:** Ventral view. See supplement for abbreviations.

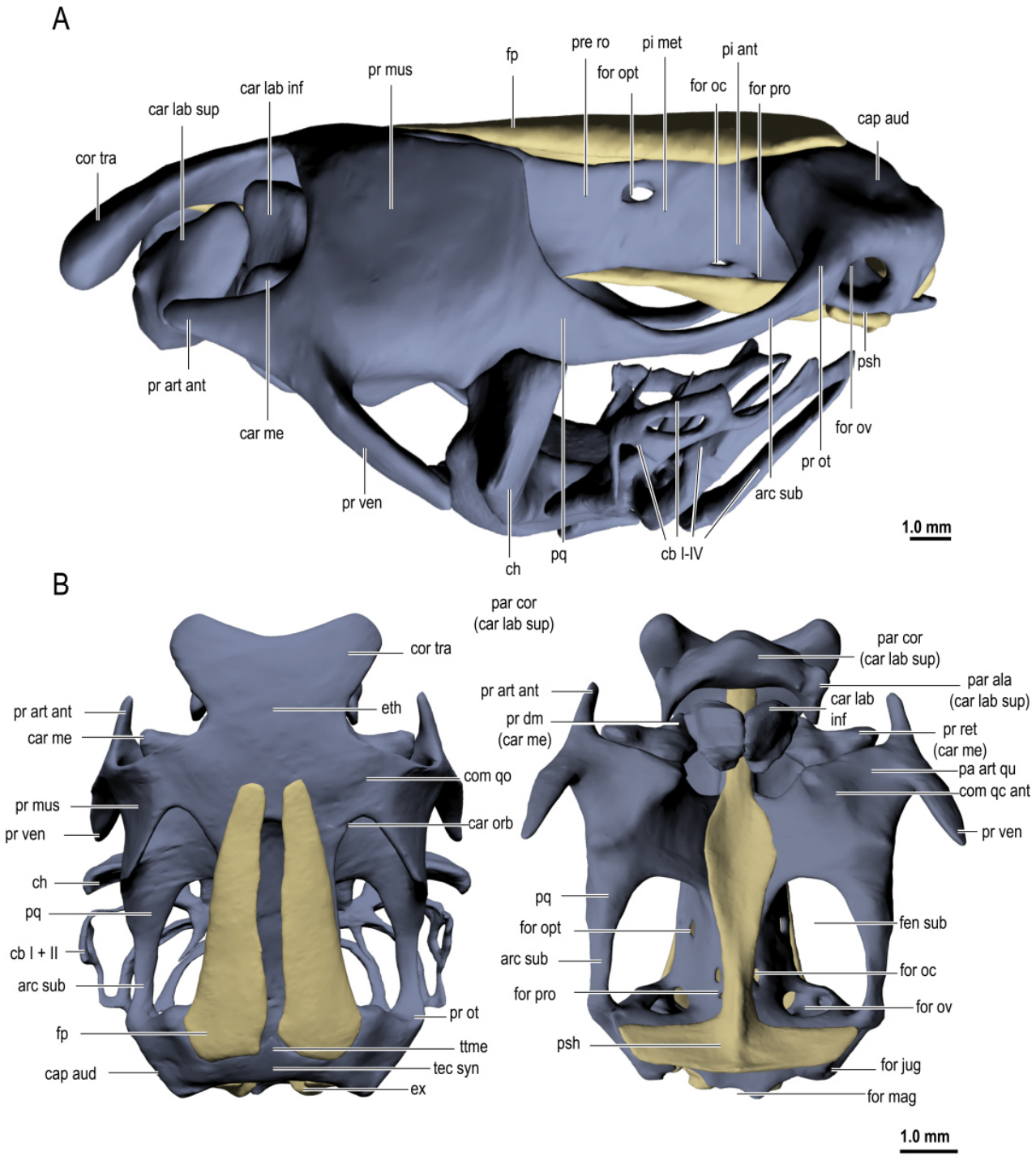

Figure 6: 3D reconstruction of a µCT scan of a tadpole of *T. robustus* (Gosner stage 36/37) showing the skeletal morphology of the cranium. The different structures have been coloured as follows: cartilage, blue; bones, ochre; **A:** Lateral view. **B, left:** Dorsal view, hyobranchial skeleton not shown. **B, right:** Ventral view. See supplement for abbreviations.

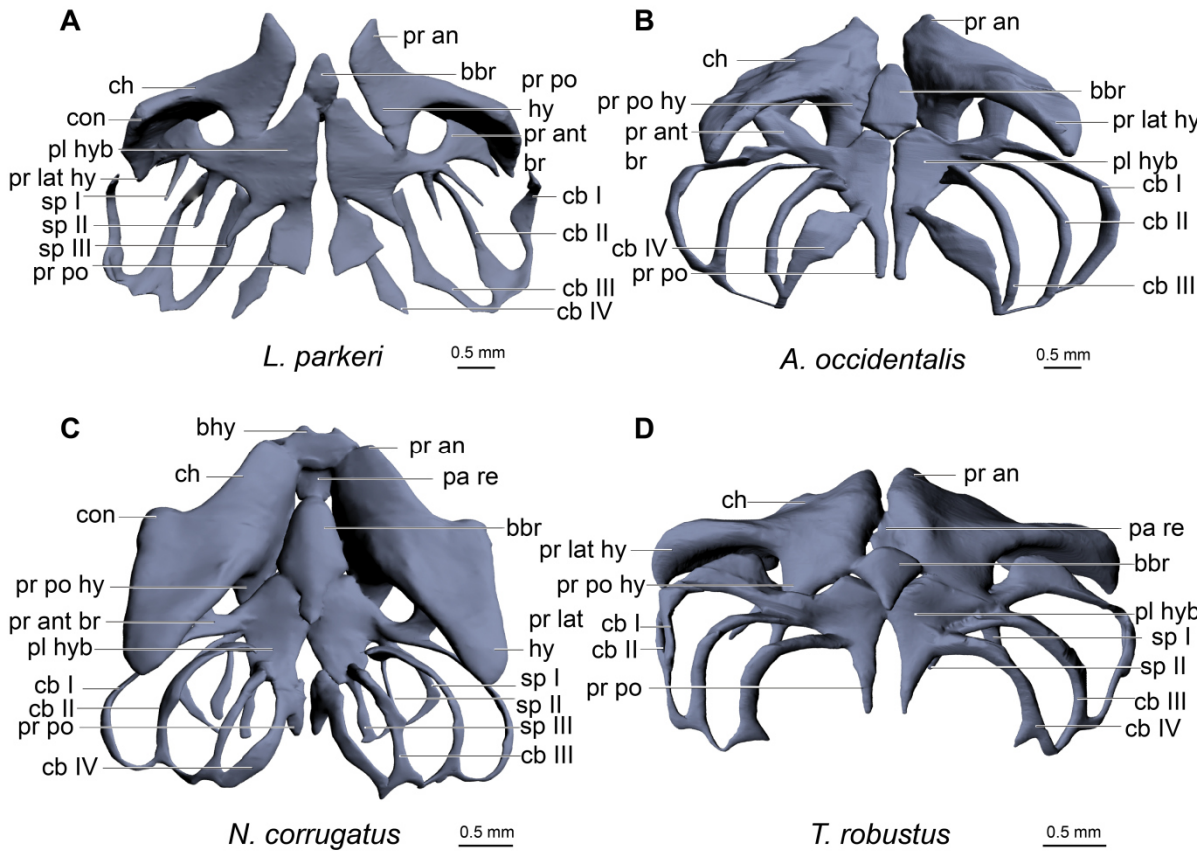

Figure 7: Hyobranchialskeleton of *L. parkeri* (Gosner stage 30), *A. occidentalis* (Gosner stage 25/26), *N. corrugatus* (Gosner stage 26) and *T. robustus* (Gosner stage 36/37) fom a ventral view. See supplement for abbreviations.

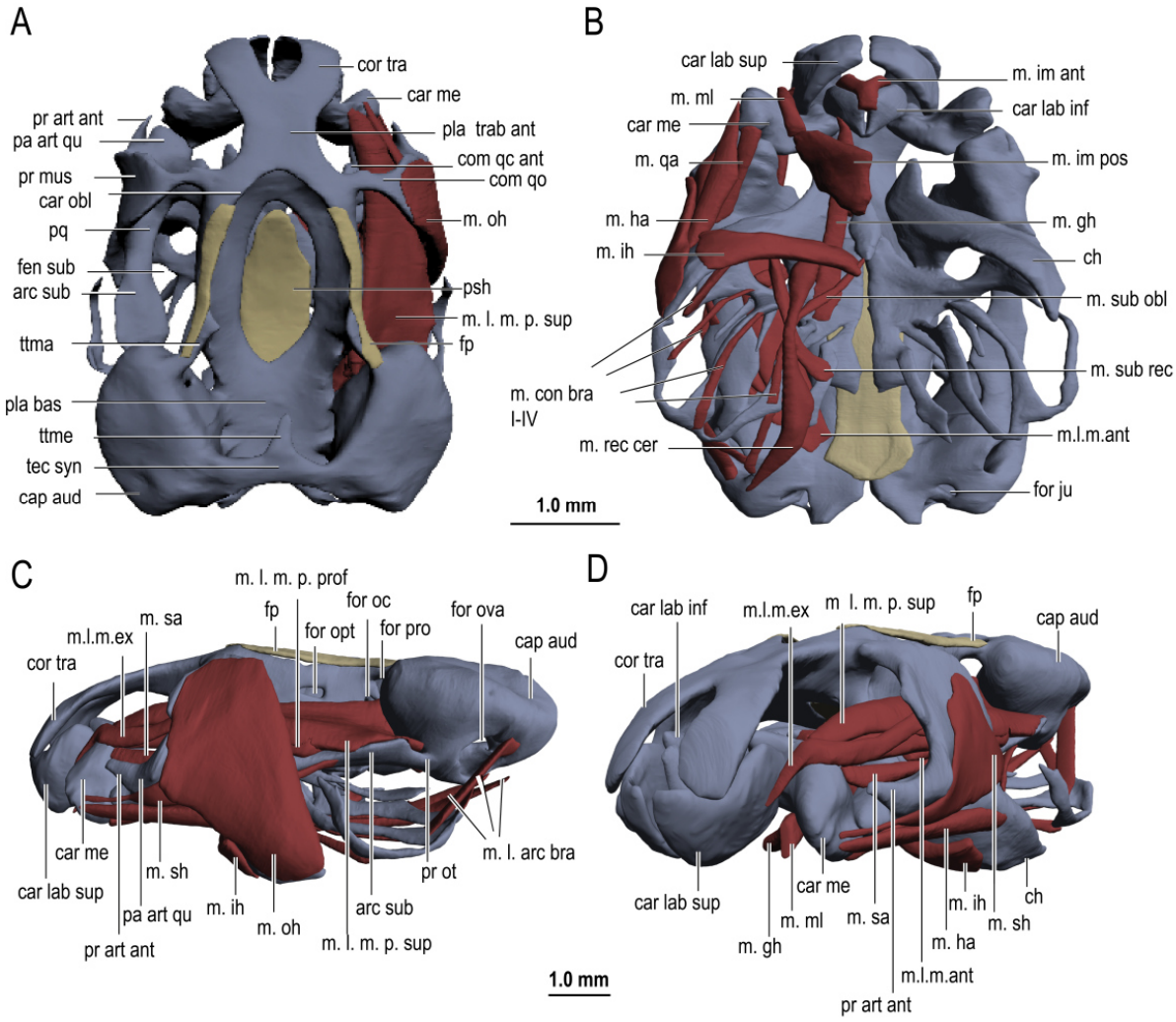

Figure 8: 3D reconstruction of a µCT scan of a tadpole of *L. parkeri* (Gosner stage 35) showing the muscoskeletal morphology of the cranium. The different structures have been coloured as follows: cartilage, blue; bones, ochre; muscles, red. **A:** Dorsal view. **B:** Ventral view. **C:** Lateral view. D: Frontolateral view. See supplement for abbreviations.

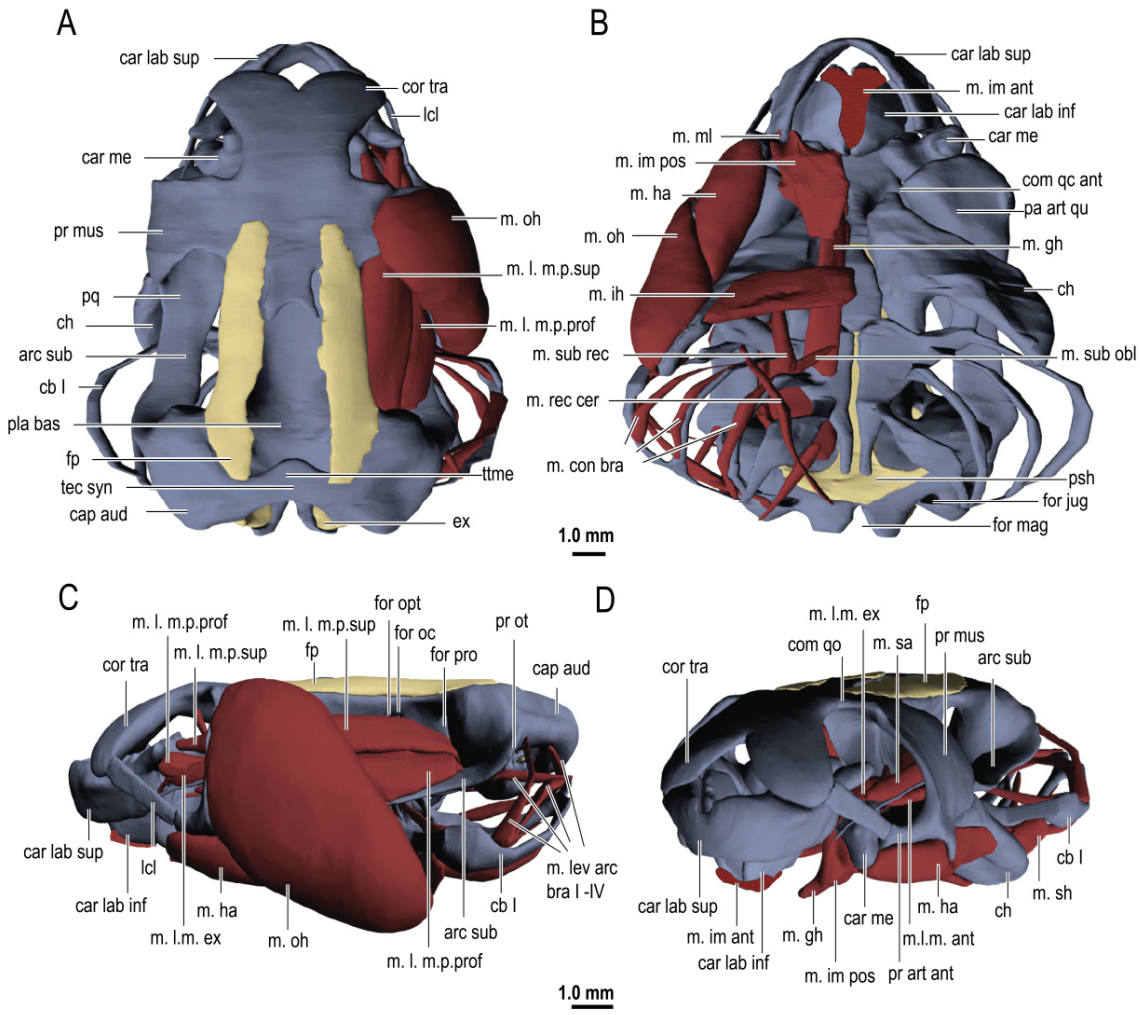

Figure 9: 3D reconstruction of a µCT scan of a tadpole of *A. occidentalis* (Gosner stage 25/26) showing the muscoskeletal morphology of the cranium. The different structures have been coloured as follows: cartilage, blue; bones, ochre; muscles, red. **A:** Dorsal view. **B:** Ventral view**. C:** Lateral view. D: Frontolateral view. See supplement for abbreviations.

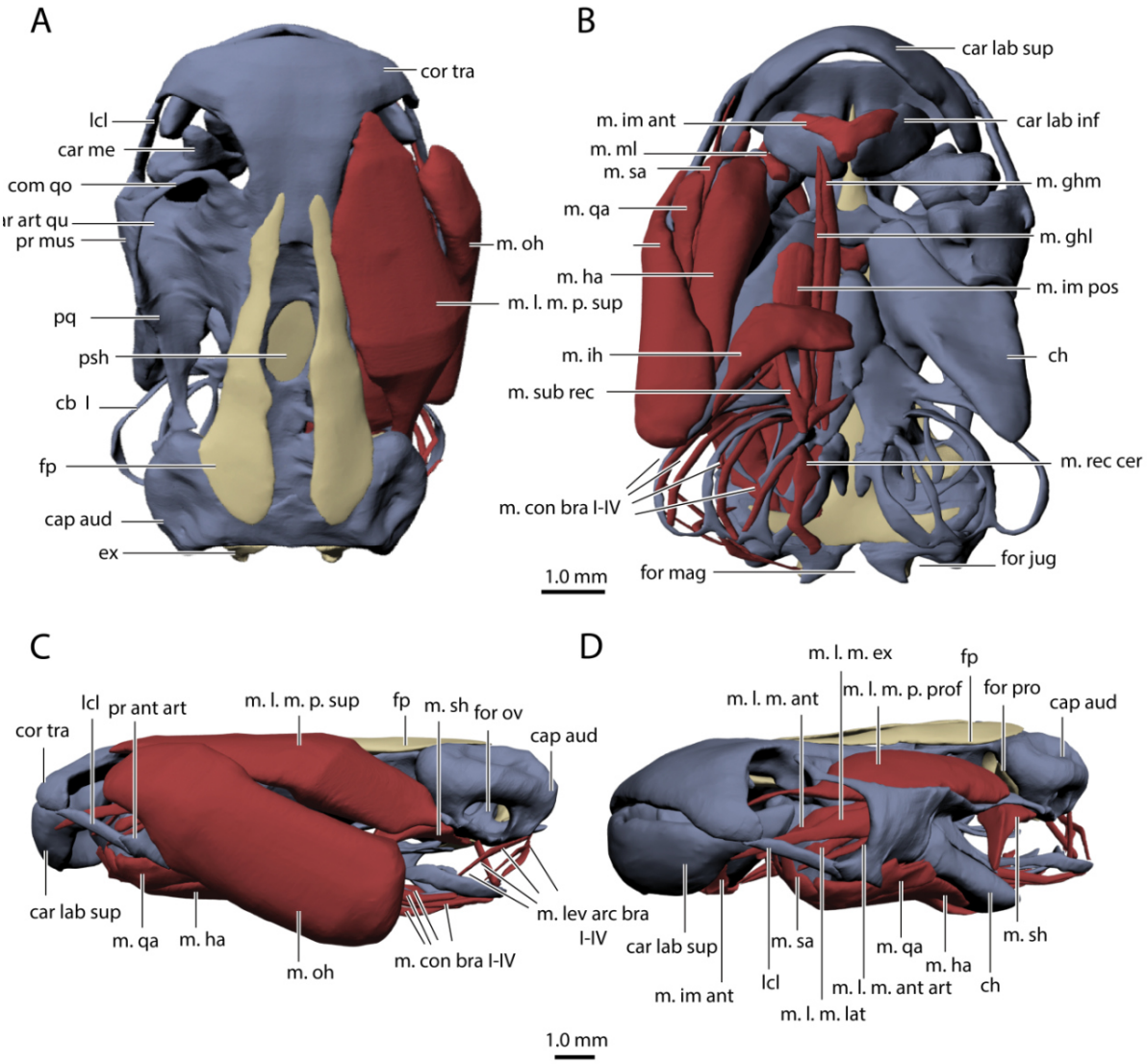

Figure 10: 3D reconstruction of a µCT scan of a tadpole of *N. corrugatus* (Gosner stage 26) showing the muscoskeletal morphology of the cranium. The different structures have been coloured as follows: cartilage, blue; bones, ochre; muscles, red. **A:** Dorsal view. **B:** Ventral view. **C:** Lateral view. **D:** Frontolateral view. See supplement for abbreviations.

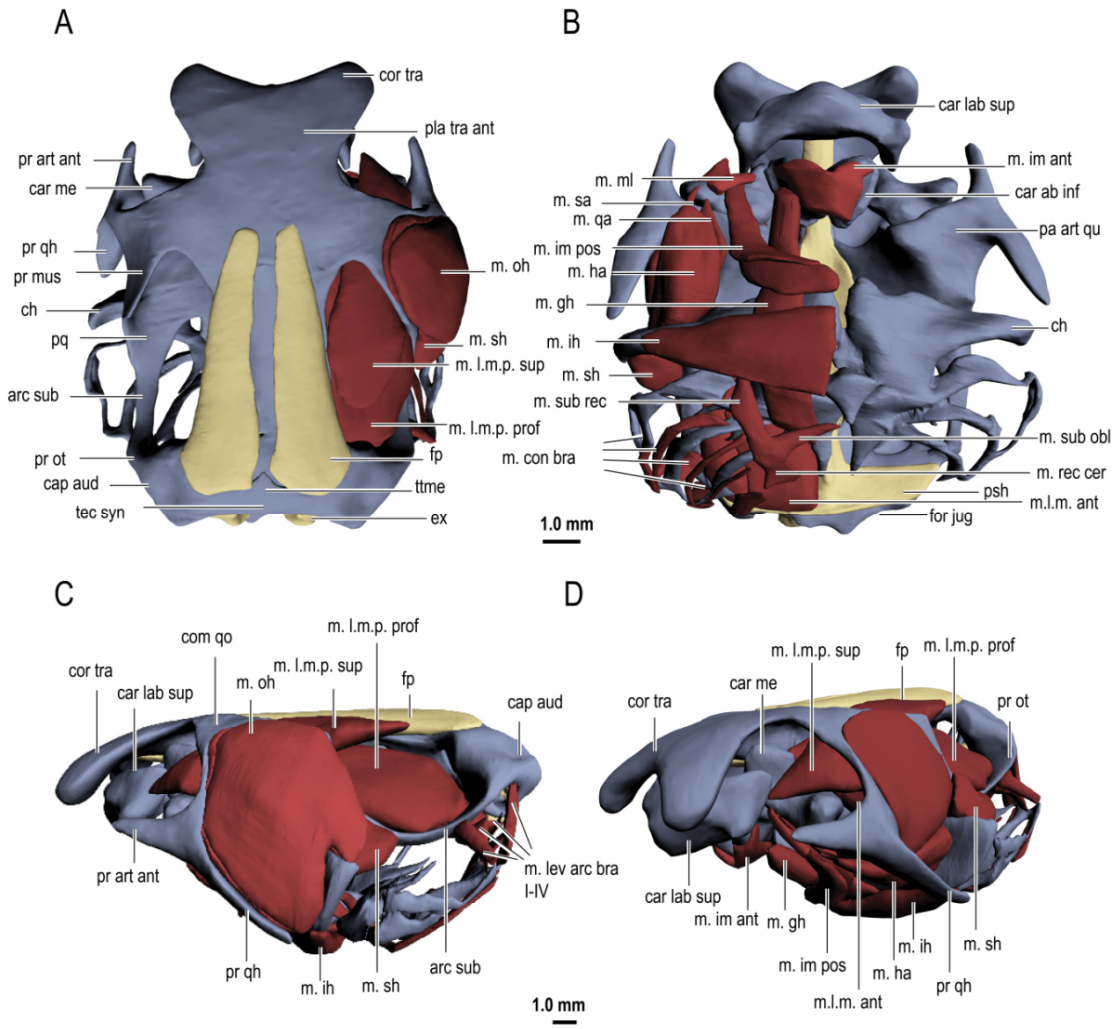

Figure 11: 3D reconstruction of a µCT scan of a tadpole of *T. robustus* (Gosner stage 26) showing the muscoskeletal morphology of the cranium. The different structures have been coloured as follows: cartilage, blue; bones, ochre; muscles, red. **A:** Dorsal view. **B:** Ventral view. **C:** Lateral view. **D:** Frontolateral view. See supplement for abbreviations.

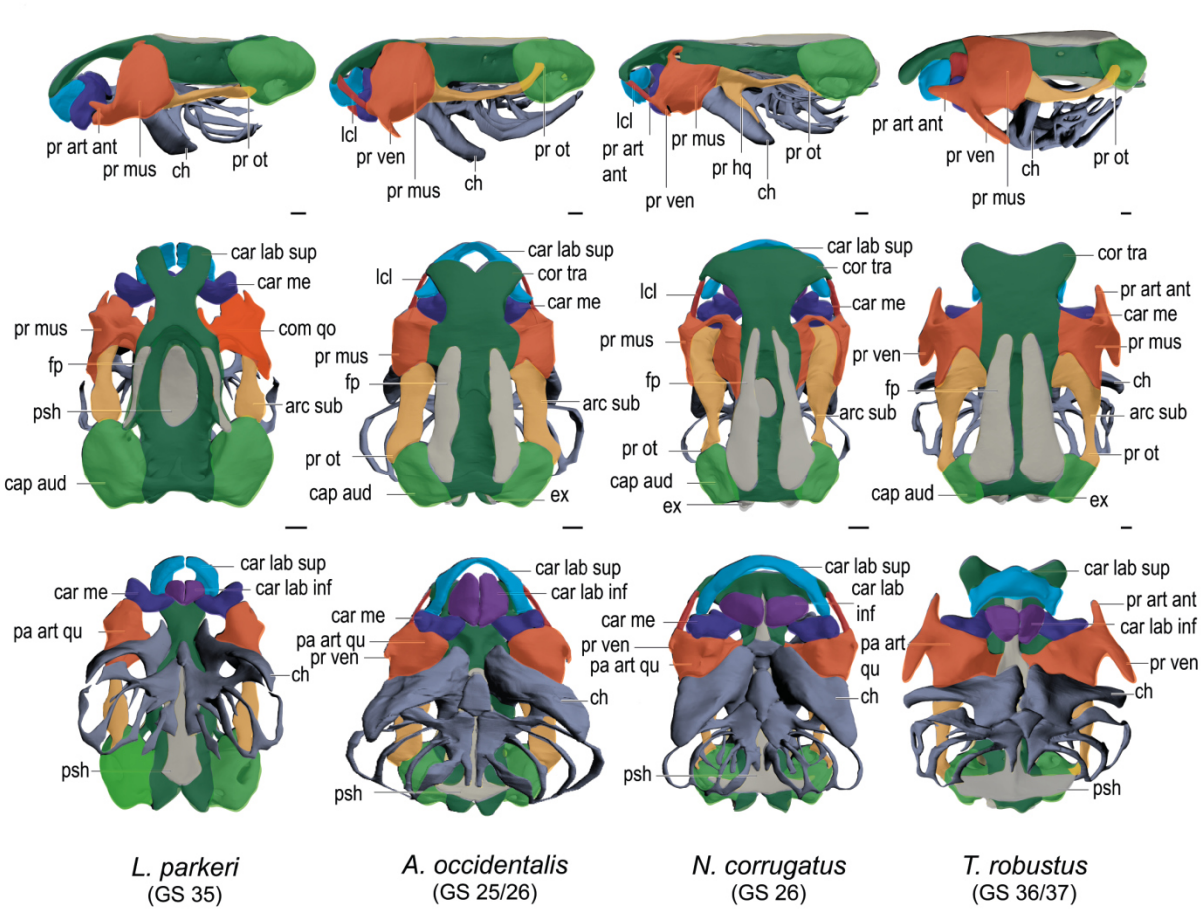

Figure 12: 3D reconstruction of µCT scan of tadpoles of *L. parkeri* (Gosner stage 35), *A. occidentalis* (Gosner stage 25/26), *N. corrugatus* (Gosner stage 26) and *T. robustus* (Gosner stage 36/37) showing the comparative morphology of the cranial skeleton. Homologous structures are depicted in the same color. See supplement for abbreviations. Scale bar 1.0 mm.

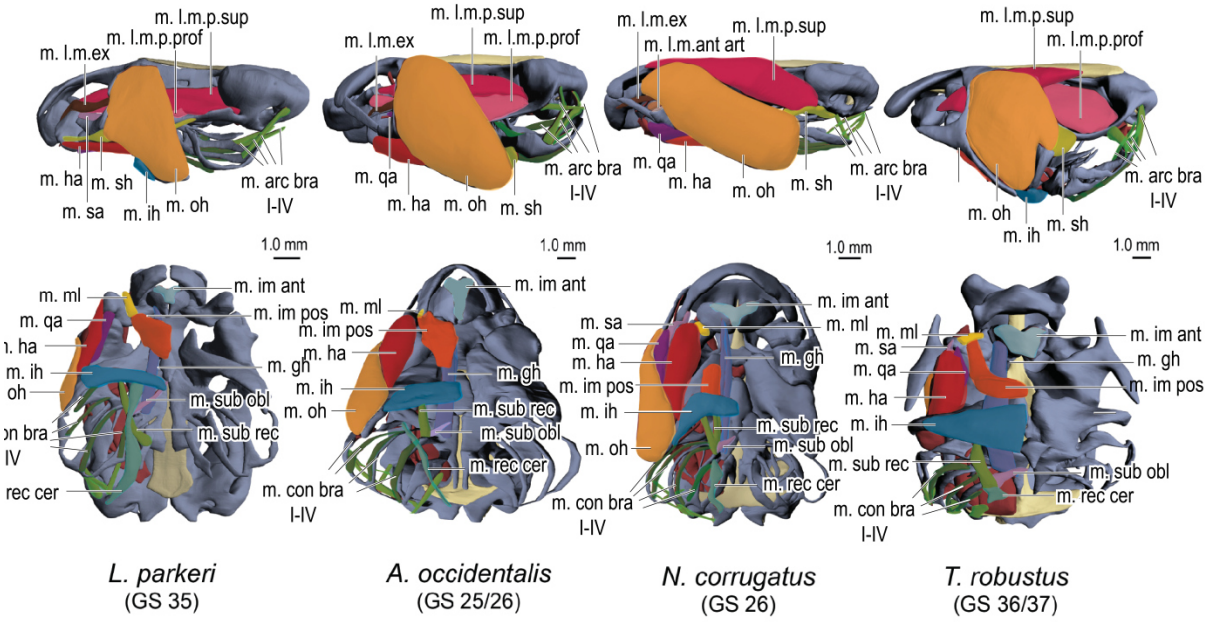

Figure 13: 3D reconstruction of µCT scan of tadpoles of *L. parkeri* (Gosner stage 35), *A. occidentalis* (Gosner stage 25/26), *N. corrugatus* (Gosner stage 26) and *T. robustus* (Gosner stage 36/37) showing the comparative morphology of the cranial muscles. Homologous muscles are depicted in the same color. See supplement for abbreviations.

Supplement

Abbreviations

arc sub	arcus subocularis
cap aud	capsula auditiva
car lab inf	cartilago labialis inferior
car lab sup	cartilago labialis superior
car me	cartilago meckeli
car orb	cartilago orbitalis
ch	ceratohyale
com qcq ant	commissura quadratocranialis anterior
com qo	commissura quadrato-orbitalis
cor tra	cornua trabeculae
fen sub	fenestra subocularis
for jug	foramen jugularis
for jug	formane jugulare
for mag	foramen magnum
for oc	foramen oculomotori
for opt	foramen opticum
for ov	foramen ovalis
for pro	foramen prooticum
fp	frontoparietale
lcl	lateral circumoral ligament
m. con bra	musculus constrictor branchialis
m. gh	musculus geniohyoideus
m. ha	musculus hyoangularis
m. ih	musculus interhyoideus
m. im ant	musculus intermandibularis anterior
m. im pos	musculus intermandibularis posterior
m. lev arc bra	m. lev arc bramusculus levator arcus branchialis
m. ml	musculus mandibulolabalis
m. oh	musculus orbitohyoideus
m. qa	musculus quadratoangularis
m. rec cer	musculus rectus cervicis
m. sh	musculus suspensoriohyoideus
m. sub obl	musclus subarcularis obliquus
m. sub rec	musculus subarcularis rectus
m.l.m.ex	musculus lavator mandibulae externus
m.l.m.p.sup	musculus levator mandibulae posterior superficialis
pa art qu	pars articularis quadrati
par ala (car lab sup)	pars alaris of the cartilago labialis superior
par cor (car lab sup)	pars corporis of the cartilago labialis superior
pi met	pila metoptica
pq	palatoquadrate
pr art ant	processus articularis anterior
pr dm (car me)	processus dorsomedialis of the cartilago meckeli
pr mus	processus muscularis
pr ot	processus oticus
pr ret (car me)	processus retroarticularis of the cartilago meckeli
psh	parasphenoid
tec syn	tectum synoticum
ttma	taenia tecti marginalis
ttme	taetia tecti medialis
pre ro	preoptic root
pi ant	pila antotica
eth	ethmoid
cb I-IV	ceratobranchiale I-IV

CHAPTER 5

Meristic and morphometric characters of *Leptopelis natalensis* tadpoles (Amphibia: Anura: Arthroleptidae) from Entumeni Forest reveal variation and inconsistencies with previous descriptions

Authors: **Schweiger, S.**, Harvey, J., Otremba, T. S., Weber, J., Müller, H.

Status: Published in Acta Herpetologica (2017) 12(2): 125-132

FORMULAR 1

Manuskript Nr.: 5

Titel des Manuskriptes: Meristic and morphometric characters of *Leptopelis natalensis* tadpoles (Amphibia: Anura: Arthroleptidae) from Entumeni Forest reveal variation and inconsistencies with previous descriptions

Autoren: Schweiger, Susan; Harvey, James; Otremba, Theresa. S.; Weber, Janina; Müller, Hendrik

Bibliographische Informationen: Published in Acta Herpetologica (2017) 12(2): 125-132

Der Kandidat / Die Kandidatin ist (bitte ankreuzen)

☒ Erstautor/-in, ☐ Ko-Erstautor/-in, ☐ Korresp. Autor/-in, ☐ Koautor/-in.

Anteile (in %) der Autoren / der Autorinnen an der Publikation (anzugeben ab 20%)

Autor/-in	Konzeptionell	Datenanalyse	Experimentell	Verfassen des Manuskriptes	Bereitstellung von Material
Schweiger, S.	80%	85%	60%	70%	33 %
Harvey, J.					33 %
Otremba, T.S.					
Weber, J.					
Müller, H.	20%			25%	33 %

December
2017
Vol. 12 – N. 2

Acta Herpetologica

ISSN 1827-9635

SOCIETAS HERPETOLOGICA ITALICA

Iscritto al Tribunale di Firenze con il n° 5450 del 03/11/2005
Poste Italiane S.p.A. - Spedizione in Abbonamento Postale 70% DCB Firenze

FIRENZE UNIVERSITY PRESS

Acta Herpetologica 12(2): 125-132, 2017
DOI: 10.13128/Acta_Herpetol-20740

Meristic and morphometric characters of *Leptopelis natalensis* tadpoles (Amphibia: Anura: Arthroleptidae) from Entumeni Forest reveal variation and inconsistencies with previous descriptions

Susan Schweiger[1], James Harvey[2], Theresa S. Otremba[1], Janina Weber[1], Hendrik Müller[1,*]

[1] *Institut für Spezielle Zoologie und Evolutionsbiologie mit Phyletischem Museum, Friedrich Schiller Universität Jena, Erbertstrasse 1, 07743 Jena, Germany. *Corresponding author.* E-mail: hendrik.mueller@uni-jena.de
[2] *41 Devonshire Avenue, Howick, 3290, South Africa*

Submitted on: 2017, 5th June; revised on: 2017, 31st August; accepted on: 2017, 3rd October
Editor: Rocco Tiberti

Abstract. The tadpole of *Leptopelis natalensis* is described based on a series of 32 specimens from Entumeni Forest, KwaZulu-Natal, South Africa. Previous descriptions are brief, lack morphometric data, or are based on specimens of imprecise origin. The tadpole resembles other *Leptopelis* tadpoles and is generally in agreement with existing accounts, although some differences exist. Some of these differences seem to fall within the range of natural variation. Others, such as the presence of a fifth anterior row of keratodonts, might be indicative of variation at the population level and should be considered in future taxonomic revisions. *Leptopelis natalensis* tadpoles seem to be most readily distinguished by their more narrowly keratinized beaks from the geographically overlapping or adjacent *L. mossambicus* and *L. xenodactylus*.

Keywords. South Africa, KwaZulu-Natal, Eastern Cape, taxonomy, buccal morphology, ontogenetic variation.

INTRODUCTION

The genus *Leptopelis* currently comprises 53 described species (Frost, 2017) of medium to large tree frogs that are distributed throughout most of Sub-Saharan Africa (Schiøtz, 1999). The most southerly distributed species of the genus is *L. natalensis*, which is found in a variety of habitats along the eastern region of the South African provinces of KwaZulu-Natal and part of Eastern Cape (Schiøtz, 1999; Bishop, 2004; Venter and Conradie, 2015). Although some, mostly brief, descriptions and illustrations of *L. natalensis* tadpoles have been published (Wager, 1930, 1965; van Dijk, 1966; Lambiris, 1988; Channing, 2001; du Preez and Carruthers, 2009; Channing et al., 2012), Channing (2001) considered none of the South African *Leptopelis* tadpoles to have been adequately described. The various descriptions furthermore differ in a number of diagnostic characters, such as labial keratodont formula. These differences in the existing descriptions could be the result of variation or population-specific differences that might be significant in future taxonomic revisions (Penske et al., 2015). To differentiate between these options, it is important to provide detailed locality information, which is lacking in some works providing information on tadpole morphology of *L. natalensis* (e.g., du Preez and Carruthers, 2009). While detailed, or at least limited, locality data are provided by Wager (1930, 1965, 1986), Pickersgill (2007) and Channing et al. (2012), these accounts provide mostly meristic data but few or no morphometric data that would help in assessing subtle differences that might exist between populations. We here provide a description and measurements of an ontogenetic series of tadpoles of *L. natalensis* based on a series collected at Entumeni Forest,

ISSN 1827-9635 (print)
ISSN 1827-9643 (online)

KwaZulu-Natal, assess variability and ontogenetic changes, and highlight differences between these and previous descriptions.

MATERIALS AND METHODS

A total of 32 tadpoles were collected at Entumeni Forest, KwaZulu-Natal, South Africa on 3 December 2014. The tadpoles were collected in a small forest stream (28.888334°S, 31.365928°E). Some tadpoles were preserved on the day of collection, while others were raised on a diet of commercial aquarium fish food and sampled in regular intervals to obtain different stages of development. Identification of the tadpoles was confirmed by raising some through metamorphosis. Specimens were euthanized in an aqueous solution of tricaine methanesulfonate (MS222; Fluka), fixed in 4% neutral buffered formalin, and transferred to 70% ethanol. Voucher specimens have been deposited in the herpetological collection of the Museum für Naturkunde Berlin, Germany (ZMB85717).

Staging followed Gosner (1960). Standard measurements and labial tooth row formula followed Altig and McDiarmid (1999) and description of buccopharyngeal morphology Wassersug (1976). Drawings were prepared with the aid of a camera lucida attached to a Zeiss SV12 stereomicroscope. For inspection of the buccopharyngeal morphology, one tadpole of stage 36 was dissected, postfixed with 1% osmium tetroxide, dehydrated and critical point dried in an Emitech K850 critical point dryer, sputter coated with gold-palladium using an Emitech K500 and investigated using a Phillips XL30 ESEM scanning electron microscope with a digital image capture system.

DESCRIPTION

Tadpole. The description is based on 32 tadpoles from Gosner (1960) stages 25 to 42 (see Table 1 for measurements and detailed information). The tadpole is slender overall, with a moderately elongated, slightly dorsoventrally flattened body (wider than deep) and a relatively long tail with low dorsal and ventral fins. The widest point of the body is just behind the eyes (Fig. 1). No nares are visible until stage 34. From stage 35 to 37, the nares are indicated as light coloured spots, but do not seem to be open until stage 38. When fully formed, the nares are positioned dorsolaterally, about twice as far from the eye than the tip of the snout in lateral view. The eyes are positioned dorsally. A small anlage of the developing eyelid is first visible at stage 40, anterior of the eye. The spiracle is sinistral, about as far from the snout as from the body-tail junction. The spiracular opening is an upright oval, slightly slanted forward; its largest diameter almost as large as the diameter of the eye lens. The spiracular tube is angled upwards at about 45°; the posterior end, including its inner wall, is free from the body. The tail is about 2.5 times as long as the body (see Table 1 for measurements) and very muscular. The myomeres are visible in the posterior half of the tail, but are otherwise indistinct or obscured by the dense pigmentation. The tailfins are very low, with the dorsal fin marginally deeper than the ventral fin. The dorsal fin has a low origin on the base of the tail, just behind the tail-body junction, and gradually rises towards the middle of the tail, where it reaches its maximum height. The ventral tailfin is very even, with the margin of the fin running more or less parallel to the ventral edge of the muscular tail. The overall deepest point of the tail is at about half its length. Tip of tail is pointed, with the muscular tail terminating some distance before the tail tip (Fig. 1B). The vent tube is attached to the right side of the ventral tailfin, with a very large opening forming a pointed arch. The coiled gut is well visible through the ventral body wall.

Oral Disc. The oral disc is positioned subterminally and is not visible in dorsal view. The oral disc is lightly emarginated and has a broad rostral gap. One row of globular marginal papillae is present anterolaterally and laterally; posteriorly, two rows of papillae are present. Papillae are largest anterolaterally and laterally, and smaller posteriorly. A few submarginal papillae are present laterally. Keratodont formula is 4(2-4)/3(1) in the majority of the examined specimens (see below for variation). Moving inwards, supralabial keratodont rows are progressively smaller (Fig. 1A), infralabial rows are of nearly equal length, with P3 being slightly shorter than P1 and P2. Interruption of P1, if present, is very narrow in some specimens (Fig. 1A) but more pronounced in others. Keratodonts are about equally sized in most rows, except in P3 where they get progressively smaller laterally. The individual keratodonts are spoon-shaped and have eight or nine cusps along their margins, with the apical cusps being larger than the more laterally positioned ones (see inset in Fig. 2A). The jaw sheaths are serrated but only narrowly keratinised (indicated by the dark pigmentation). By stage 42, the lower jaw sheath and all keratodonts are absent and the papillation is much reduced in extent.

Buccopharyngeal Morphology. The prenarial area of the buccal roof (Fig. 2A) is somewhat elongated and contains a few scattered pustules. In addition, a pair of short ridges is present and somewhat slanted laterally. The orientation of the choana is oblique to the midline (about 45 degrees) and both choanae form a forward-pointing angle of approximately 90 degrees. The jagged narial valves project deep into the buccal cavity and obscure the choanal openings. Anterolateral of each choana is a broad, flap-like papilla with a pustulate edge. Three to four thick, broad-based papillae are present posterolaterally to each

Table 1. Measurements of *Leptopelis natalensis*. All measurements in millimeters (arithmetic mean ± SD). * indicates a damaged tail in one of the specimens of the series, which was omitted from the calculations.

Gosner Stage	25 (n=3)	31 (n=1)	34 (n=1)	35 (n=2)	36 (n=14)	37 (n=2)	38 (n=2)	39 (n=1)	40 (n=1)	41 (n=1)	42 (n=4)
Total length	32.1 ± 2.3*	29.7	34.9	34.1 ± 1.2	36.5 ± 2.7*	35.3*	37.9 ± 0.8	41.7	39.1	37.2	36.2 ± 2.3
Body length	7.1 ± 0.6	8.2	9.5	9.2 ± 0.8	10.2 ± 0.8	10.7 ± 0.0	10.7 ± 0.8	11.8	11.2	11.0	10.9 ± 0.3
Body width	3.8 ± 0.2	4.0	4.9	4.5 ± 0.3	5.2 ± 0.6	5.9 ± 0.1	5.9 ± 0.1	6.0	6.1	5.5	4.3 ± 0.6
Body height	2.9 ± 0.1	3.6	4.2	3.4 ± 0.4	4.3 ± 0.4	4.8 ± 0.1	4.9 ± 0.1	5.3	4.4	5.0	4.2 ± 0.2
Tail length	16.7 ± 1.6*	21.2	25.2	24.9 ± 0.1	26.4 ± 2.3*	24.5*	27.1 ± 0.4	30.0	27.6	27.0	26.1 ± 1.8
Tail height	3.3 ± 0.3	3.6	4.2	4.1 ± 0.4	4.6 ± 0.3	4.4 ± 0.6	5.1 ± 0.4	5.0	4.9	5.0	4.1 ± 0.5
Tail muscle height	1.9 ± 0.3	2.3	3.0	2.8 ± 0.2	3.2 ± 0.4	3.2 ± 0.1	3.1 ± 0.1	3.5	3.0	2.9	2.8 ± 0.3
Width of oral disc	1.2 ± 0.2	1.4	1.6	1.6 ± 0.1	1.9 ± 0.2	1.9 ± 0.1	2.0 ± 0.1	2.4	2.2	2.0	1.6 ± 0.2
Interorbital distance	2.7 ± 0.3	3.3	3.9	3.5 ± 0.8	4.1 ± 0.3	4.4 ± 0.1	4.3 ± 0.1	4.6	4.3	4.7	4.7 ± 0.4
Internarial distance	-	-	-	-	-	-	1.9 ± 0.9	2.0	1.9	1.7	1.4 ± 0.2
Snout-naris distance	-	-	-	-	-	-	1.6 ± 0.1	1.6	1.7	1.6	1.2 ± 0.3
Snout-eye distance	2.5 ± 2.6	2.9	3.3	3.4 ± 0.1	3.3 ± 0.2	3.5 ± 0.2	3.4 ± 0.1	3.9	4.0	3.8	3.1 ± 0.1
Snout-spiracle distance	4.9 ± 0.5	5.4	6.1	6.3 ± 0.4	6.7 ± 0.4	27.1 ± 0.3	7.1 ± 0.2	8.1	7.4	7.2	-
Naris-eye distance	-	-	-	-	-	-	1.9 ± 0.1	2.1	2.0	2.1	2.2 ± 0.1
Eye diameter	0.6 ± 0.1	0.8	1.1	1.0 ± 0.0	1.2 ± 0.1	1.2 ± 0.1	1.2 ± 0.1	1.5	1.5	1.5	1.4 ± 0.1

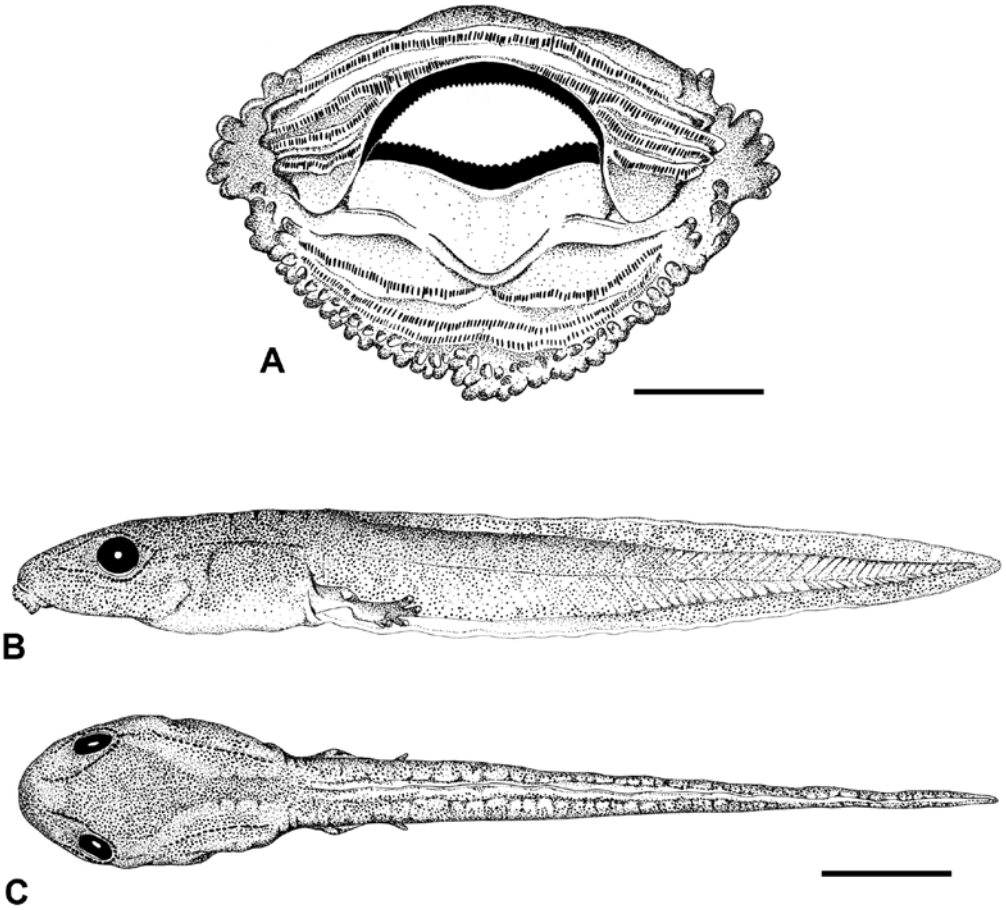

Fig. 1. Oral disc (A), lateral (B) and dorsal (C) view of a Gosner stage 36 tadpole of *Leptopelis natalensis* from Entumeni Forest, KwaZulu Natal, South Africa. Scale bar equals 0.5 mm in (A) and 5 mm in (B) and (C).

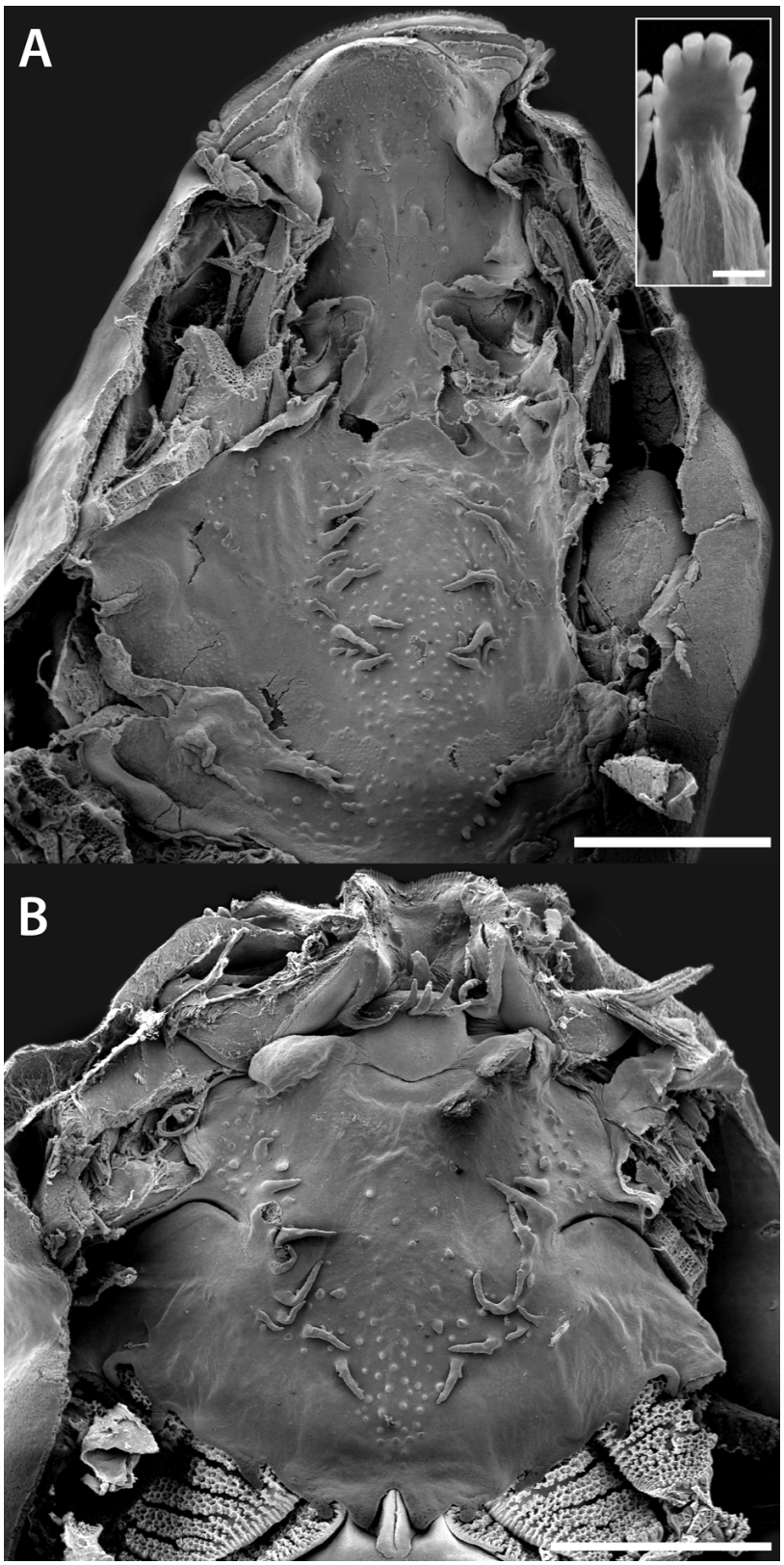

Fig. 2. Scanning electron microscope images of the (A) buccal roof and (B) buccal floor of a Gosner stage 36 tadpole of *Leptopelis natalensis*. Inset in (A) shows a close-up of a keratodont. Scale bars in (A) and (B) equal 1 mm, and 5 µm in the inset.

Table 2. Ontogenetic variation in labial keratodont formula. Number in brackets indicates number of specimens exhibiting the labial keratodont formula; asterisk (*) indicates asymmetry in the last (innermost) anterior keratodont row, with keratodonts present on one side only; keratodont data were only taken for 13 of the 14 investigated specimens of stage 36.

Stage	Labial keratodont formula
25	4(2-4)/3(1) [2]; 4(2-4*)/3 [1]
31	5(2-5)/3(1) [1]
34	5(2-5*)/3(1) [1]
35	4(2-4)/3(1) [2]
36	4(2-4)/3(1) [6]; 4(2-4)/3 [1]; 5(2-5*)/3(1) [1]; 5(2-5)/3(1) [5]
37	5(2-5)/3(1) [2]
38	4(2-4)/3(1) [2]
39	5(2-5)/3(1) [1]
40	5(2-5*)/3(1) [1]
41	5(2-5*)/3(1) [1]

choana, and about six small pustules are present in the area between them. The median ridge separating postnarial arena and buccal roof arena is very prominent and forms an almost semi-circular flap. The buccal roof arena is fringed by eight pairs of medium to large papillae of similar sizes as in the buccal floor arena. An additional three to four pairs of smaller papillae are present in second row towards the posterior part of the buccal roof arena. There is furthermore a group of three to four short lateral roof papillae at each side of the arena. Within the buccal roof arena and posterior to it are ca. 100 pustules. A well-defined glandular zone with numerous secretory pits is present; it is broader laterally and has a relatively narrow medial gap. The dorsal velum has a broad medial gap and number of smaller papillae and pustules along its edge and sides. Additional pustules are present posterior to the dorsal velum and within its median gap.

In the buccal floor (Fig. 2B), a pair of large, flap-like infralabial papillae, with smaller pustules along their margins, is present immediately inside the oral cavity on each side. An additional large, flap-like infralabial papilla is present medially just behind the lower jaw sheath. Four large lingual papillae are present on the tongue anlage. The area immediately behind the lingual papillae is marked by a transverse groove. To the left and right of this grove is a fairly large, bulbous structure. The buccal floor arena is fringed by nine to ten pairs of medium to large buccal floor papillae, all curved towards the buccal floor arena, except for the posteriormost pair of papillae, which point backwards (possibly an artefact of preservation). Around 60 pustules cover the posterior two thirds

Table 3. Summary of published information on *Leptopelis natalensis* tadpoles. EC – Eastern Cape Province, KZN – KwaZulu-Natal Province, G – Gosner (1960) stage.

Reference	Locality	Keratodont formula	Oral disc characters	Maximum length /tail length as multiple of body length
this study	Entumeni Forest (KZN)	4(2-4)/3(1) or 5(2-5)/3(1), rarely 4(2-4)/3	double row of marginal papillae posteriorly, single row of slightly larger papillae laterally; jaw sheaths delicate and narrowly keratinized; disc emarginated	42mm (G39)/2.5x
Wager (1930)	Port St. Johns (EC)	4(2-4)/3	double row of marginal papillae posteriorly, single row laterally; disc emarginated	51mm/2.5x
Wager (1965)	Port St. Johns (EC)	4(2-4)/3	double row of marginal papillae posteriorly, single row laterally; disc emarginated	49mm/2.75x
	Durban (KZN)	4(2-4)/3		35mm/2.5x
	Nkandla (KZN)	5(2-5)/3		50mm/2.3x
Lambiris (1988)	-	4(2-4)/3	double row of marginal papillae posteriorly, single row laterally	50mm (G38)/-
Pickersgill (2007)	Hillcrest (KZN)	4(2-4)/3, sometimes 4(2-4)/3(1)	double row of marginal papillae posteriorly, single row laterally; jaw sheaths narrowly keratinized; disc not emarginated	49mm (G37?)/2.5x
du Preez and Carruthers (2009)	-	4(2-4)/3, sometimes 4(2-4)/3(1)	double row of marginal papillae posteriorly, single row laterally; jaw sheaths delicate	50mm/2.6x (figured tadpole)
Channing et al. (2012)	KZN	4(2-4)/3	double row of marginal papillae posteriorly, single row of slightly larger papillae laterally; jaw sheaths delicate and keratinized along margins; disc emarginated	35mm/2.2x

of the buccal floor arena, as well as the area immediately posterior to it. In addition, ca. 15 pustules are present anterolaterally of the buccal floor arena, just in front of the buccal pockets. The buccal pockets are simple, narrow but deep, curved slits, with no associated papillae or pustules. It is unclear whether the buccal pockets are perforated to provide a bypass to the atrial chamber (Wassersug, 1976) or whether these end blind. The ventral velum is wide, with four marginal projections on each side, and a deep medial notch that exposes the glottis. The ventral velum contains secretory pits along its margin.

Coloration in life. A nearly uniform dark olive, with a scatter of iridiophores across the entire dorsal and lateral sides of body and tail. Ventral side more sparsely pigmented anteriorly, but skin above the abdominal cavity completely unpigmented and translucent in younger stages but becoming somewhat more opaque in older specimens.

Coloration in preservative. Dorsal body densely pigmented and overall homogenously dark brown in colour. Lateral line system very well visible as pigment-free spots in clearly defined lines along the body. Ventral body sparsely pigmented anteriorly but pigment-free above the abdominal cavity, with the coiled gut clearly visible. Pigmentation becomes somewhat less dense on tail and individual melanophores more easily discernible. Pigmentation on the dorsal tail-fin similar to the muscular tail, but distalmost edge pigment-free. Ventral fin free of pigment and translucent, with only some scattered melanophores present along the basal edge and towards the posterior end.

Variation. Overall, little variation is present within the examined material. Specimens differ slightly in the distribution of melanophores on the tail-fins, with some specimens having a ventral tailfin that is almost entirely free of pigmentation except for the very tip of the tail, whereas others show scattered pigment to a various extent within the posterior half of the fin. Pigmentation of the dorsal fin also slightly less or more dense in some specimens. The most variation is seen in the oral disc, in particular the number and arrangement of keratodont rows. Slightly more than half of the specimens (14 of 27; see Table 2) have four anterior rows of keratodonts, with the first always undivided, and the remainder divided. The rest of the specimens have an additional, innermost fifth keratodont row (A5). In all specimens, the last anterior row is usually rather short and in a number of specimens present on one side only (Table 2). The first posterior row is usually divided by a small gap of variable width, but undivided in two of the 27 specimens examined that have an oral apparatus.

DISCUSSION

Overall, the tadpole of *L. natalensis* resembles other *Leptopelis* tadpoles in general shape and appearance (see Channing et al., 2012, and Barej et al., 2015, for most recent and comprehensive treatments of the group). In South Africa, the range of *L. natalensis* is close to or overlaps with the ranges of *L. xenodactylus* and *L. mossambicus* (Channing, 2001; Minter et al., 2004). Based on the available information, the tadpole of *L. mossambicus* appears to be somewhat larger and proportionally shorter-tailed than that of *L. natalensis*, and overall darker in colouration, being more brown than olive (du Preez and Carruthers, 2009). *Leptopelis mossambicus* further appears to differ from *L. natalensis* by having slightly higher tailfins, a very broad rostral gap in the papillation of the oral disc that is almost as broad as the disc itself, and somewhat more robust jaw sheaths that are keratinized for about half their width (du Preez and Carruthers, 2009; Channing et al., 2012). The tadpole of *L. xenodactylus* is very similar to *L. natalensis* and these species appear to be indistinguishable by overall shape and colouration alone. However, in contrast to *L. natalensis*, *L. xenodactylus* tadpoles do seem to have a more robustly keratinized jaw (Channing, 2008; du Preez and Carruthers, 2009; Channing et al., 2012), which should help facilitate a correct identification. In addition there are differences in papillation, with more submarginal papillae being present in *L. xenodactyloides* and the posterior papillae differing in size (inner row of shorter, more globular papillae and outer row of relatively long papillae; Channing 2008). The two species have so far not been found in sympatry, although they occur in close proximity to each other in central KwaZulu-Natal.

A number of descriptions of the tadpole of *L. natalensis* have been provided before (summarized in Table 3), but most of them are brief, lack measurements, or do not provide precise locality information. All previous accounts and our observations agree on the overall shape and colouration of the tadpoles, but some differences especially in total length, oral disc morphology, and keratodont formula exist. While most accounts provide a maximum length of around 50 mm, Wager (1965) and Channing et al. (2012) reported 35 mm as total length, at least for some populations, but did not indicate what stage the examined specimens were at. Furthermore, there is some variation regarding the length of the tail, but all of this seems to be within the limit of normal variation, given that maximum length is largely dependent on condition. While most previous investigators reported or figured a slightly emarginated oral disc, which matches our own observations, Pickersgill (2007) illustrated a disc

that is not emarginated. Assuming all observations to be correct, this would indicate a more substantial difference between that population and others. Both van Dijk (1966) and du Preez and Carruthers (2009) reported the presence of an elygium in the eye of *L. natalensis* tadpoles, although van Dijk (1966) indicated that an ocular elygium might not generally be present and is not easily detected. In our specimens, an ocular elygium is not present, but dorsally the pigmented skin seems to somewhat extend onto the eyeball, which may represent an epidermal elygium (see Kruger et al., 2013).

Most previous descriptions gave the keratodont formula of *L. natalensis* tadpoles as 4(2-4)/3, indicating an undivided P1 (Wager, 1930, 1986; Lambiris, 1988; Pickersgill, 2007; du Preez and Carruthers, 2009; Channing et al., 2012), but Pickersgill (2007) and du Preez and Carruthers (2009) also stated that P1 can sometimes be divided. In our series, only two specimens had an undivided P1, the rest all had a divided P1 although the gap was very slight in some specimens. While this may be an indication of interpopulational variation, it seems possible that previous reports might have simply overlooked a narrow gap in P1. Similar variations in the presence of a divided vs. undivided P1 have been reported by Penske et al. (2015) for *Leptopelis* cf. *grandiceps*. Furthermore, only slightly more than half of the specimens (14, see Table 2) of our ontogenetic series of *L. natalensis* tadpoles had four anterior rows of keratodonts. Almost as many (13 specimens) had an additional, divided A5 and a resulting keratodont formula of 5(2-5)/3(1). Although also present in some younger specimens, the presence of an A5 seemed to be more pronounced in older tadpoles (Table 2).

Variation in the number of keratodont rows has been reported for a number of species, including *L. calcaratus*, *L. gramineus*, *L. vannutelli* and *L. yaldeni* (see Channing et al., 2012). An ontogenetic increase has further been reported for *L. aubryoides* (Barej et al., 2015), *L. calcaratus* (Lamotte and Perret, 1961) and *L. viridis* (Rödel 2000), and specimens with an additional A5 have been reported for *L. modestus*, *L. spiritusnoctis* and *L. rufus* (Barej et al., 2015). In many anuran tadpoles, anterior keratodont rows are added during ontogeny and the presence of an A5 in some *Leptopelis* might be related to overall tadpole size. It is therefore possible that previous investigations did not examine specimens of a sufficient age for an A5 to be expressed. At the same time, the maximum length of 50 mm reported by several authors for *L. natalensis* (e.g., Wager, 1930; Lambiris, 1988; see Table 2 for full list), which substantially exceeds the 42 mm of the largest specimen in our sample, would argue against this. Only Wager (1965) reported tadpoles with an A5 from Nkandla Forest, KwaZulu-Natal. Entumeni Forest, the origin of the specimens examined here and only other reported population of *L. natalensis* tadpoles with a fifth anterior row of keratodonts, is less than 30 km away from Nkandla Forest. Given the current state of knowledge, these two populations seem diagnosably different from other *L. natalensis* populations at the level of tadpole morphology. Future studies of phylogeography of *L. natalensis* should include these populations and investigate their degree of differentiation compared to others.

ACKNOWLEDGEMENTS

We would like to thank Ezemvelo KZN for issuing the necessary permits (OP4976/2013, OP635/2014) to undertake our research and in particular Adrian Armstrong and Sharon Louw for their generous advice and help facilitating our work. For help in the field we are grateful to Lars Möckel and Katrin Friedemann. Funding was provided through a German Science Foundation (DFG) grant to HM (MU2914/2-1).

REFERENCES

Altig, R., Mc Diarmid, R.W. (1999): Body plan – development and morphology. In: Tadpoles – the biology of anuran larvae, pp. 24-51. Mc Diarmid, R.W., Altig, R., Eds, Chicago University Press, Chicago.

Barej, M.F., Pfalzgraff, T., Hirschfeld, M., Liedtke, H.C., Gonwouo, N.L., Penner, J., Dahmen, M., Doherty-Bone, T., Schmitz, A., Rödel, M.O. (2015): The tadpoles of eight West and Central African *Leptopelis* species (Amphibia: Anura: Arthroleptidae). Amphib. Rept. Cons. **9**: 56-84.

Bishop, P.J. (2004): *Leptopelis natalensis* (Smith, 1849). In: Atlas and red data book of the frogs of South Africa, Lesotho and Swasiland, pp. 160-162. Minter, L.R., Burger, M., Harrison, J.A., Braack, H.H., Bishop, P.J., Kloepfer, D., Eds, Smithsonian Institution, Washington, D.C.

Channing, A. (2008): The mud dwelling tadpole of the long-toed tree frog, *Leptopelis xenodactylus* (Arthroleptidae). Herp. Rev. **39**: 288-290.

Channing, A. (2001): Amphibians of Central and Southern Africa. Comstock Publishing Associates, Cornell University Press, Ithaca.

Channing, A., Rödel, M.O., Channing, J. (2012): Tadpoles of Africa. Edition Chimaira, Frankfurt-am-Main.

du Preez, L., Carruthers, V. (2009): A complete guide to the frogs of Southern Africa. Struik Nature, Cape Town.

Frost, D.R. (2017): Amphibian Species of the World: an Online Reference. Version 6.0 (accessed 23 May 2017). Electronic Database accessible at http://research.amnh.org/herpetology/amphibia/index.html. American Museum of Natural History, New York.

Gosner, K.L. (1960): A simplified table for staging anuran embryos and larvae with notes on identification. Herpetologica **16**: 183-190.

Kruger, D.J.D., Weldon, C., Minter, L.R., du Preez, L.H. (2013): Morphology of the elygium and developing umbraculum in the eye of *Amietia vertebralis* tadpoles. J. Morphol. **274**: 551-556.

Lambiris, A.J.L. (1988): A review of the amphibians of Natal. Lammergeyer **39**: 1-212.

Lamotte, M., Perret, J.L. (1961): Contribution à l'étude des batraciens de l'Ouest africain XIII. Les formes larvaires de quelques espèces de *Leptopelis*: *L. aubryi*, *L. viridis*, *L. anchietae*, *L. ocellatus* et *L. calcaratus*. Bulletin de l'Institut Fondamental d'Afrique Noire, Serie A **3**: 855-885.

Minter, L.R., Burger, M., Harrison, J.A., Braack, H.H., Bishop, P.J., Kloepfer, D., Eds. (2004): Atlas and Red Data Book of the Frogs of South Africa, Lesotho and Swasiland. SI/MAB Series 9. Smithsonian Institution, Washington, D.C.

Penske, S., Gvoždík, V., Menegon, M., Loader, S.P., Müller, H. (2015): Description of the tadpole of *Leptopelis* cf. *grandiceps* (Amphibia: Anura: Arthroleptidae) from the Uluguru Mountains, Tanzania. Herpetol. J. **25**: 61-64.

Pickersgill, M. (2007): Frog search: results of expeditions to Southern and Eastern Africa. Edition Chimaira, Frankfurt-am-Main.

Rödel, M.O. (2000): Herpetofauna of West Africa. Volume I: Amphibians of the West African savanna. Edition Chimaira, Frankfurt-am-Main.

Schiøtz, A. (1999): Treefrogs of Africa. Edition Chimaira, Frankfurt-am-Main.

Van Dijk, D.E. (1966): Systematic and field keys to the families, genera and described species of South African anuran tadpoles. Ann. Natal. Mus. **18**: 231-286.

Venter, A.J., Conradie, W. (2015): A checklist of the reptiles and amphibians found in the protected areas along the South African Wild Coast, with notes on conservation implications. Koedoe **57**: 1-25

Wager, V.A. (1930): The breeding habits and life-histories of two rare South African Amphibia. I. *Hylambates natalensis* A. Smith. II. *Natalobatrachus bonebergi* Hewitt and Methuen (plates V-X). Trans. Roy. Soc. S. Afr. **19**: 79-91.

Wager, V.A. (1965): The frogs of South Africa. Purnell and Sons, Cape Town.

Wager, V.A. (1986): Frogs of South Africa: Their Fascinating Life Stories. Delta Books, Craighall.

Wassersug, R.J. (1976): Oral morphology of anuran larvae: terminology and general description. Occ. Pub. Mus. Nat. Hist. Univ. Kansas **48**: 1-23.

Discussion

Evolutionary scenarios on the origin of terrestrial development in Arthroleptidae (Afrobatrachia)

Amphibians are generally associated with a biphasic lifestyle depending on the availability of water. However, terrestrialization has taken place in many different amphibian lineages. We know little about the effects of highly modified reproductive strategies on amphibian embryonic development, especially how they differ from closely related species with the ancestral aquatic larva. The evolution of a complete terrestrial reproductive mode is not well understood and thus has resulted in much speculation.

Different degrees of terrestrialization have evolved in the African anuran taxon Afrobatrachia. What are the morphological consequences of terrestrialization for their embryonic development and how can the chapters in this study help understanding the evolution of terrestrialization in general?

Afrobatrachia range from fully aquatic biphasic development to direct development and also several 'intermediate' forms have evolved (***Figure 3***), offering the unique opportunity for a comparative approach not employed previously. Within Afrobatrachia, the family Arthroleptidae shows a wide range of developmental modes: The plesiomorphic biphasic development (aquatic eggs, aquatic tadpoles), a more terrestrial development (terrestrial eggs, aquatic tadpoles) and also direct development (terrestrial eggs, complete terrestrial development without a free-living larval stage) (***Figure 3***).

A fully aquatic, biphasic development is seen in *Nyctibates, Trichobatrachus* and *Astylosternus*. All members of these taxa live in streams of lowland or montane forests that differ in how fast the water flows in each of their (micro-) habitats (**Chapter 4**). The habitats of *Nyctibates* and *Trichobatrachus* can be characterized as the fastest flowing water systems inhabited by arthroleptid species. Their tadpoles show similar morphological adaptations to lotic habitats, i. e. wide and robust cranial cartilages of the jaws, a robust neurocranium with a broad processus muscularis of the palatoquadrate according to a strong muscularized cranium. The presence of such highly adapted cranial features has been reported for several stream-living species and has evolved several times independently (Griesbaum et al. 2019; De Oliveira et al. 2017; Candioti et al. 2016; Haad et al. 2014; Channing et al. 2012; Rödel et al. 2012; Haad et al. 2011; Haas et al. 2009; Lavilla & de Sá 2001; Haas & Richards 1998; Inger 1992; Cadle & Altig 1991; Goin & Goin 1962). The presence of different cranial features in closely related species presumably represent different ways in which the tadpoles of these species were adapted to different microhabitats (e.g. different flow velocities).

A more terrestrial mode of development has evolved in *Leptopelis* and is associated with water independent egg-deposition in moist, shallow soil. The tadpoles hatch

with the beginning of the rainy season and move actively towards the water where the larval development is completed (Barej et al. 2015). The detailed description of the tadpoles of *L. parkeri* (**Chapter 4**) and *L. natalensis* (**Chapter 5**) have shown that these resemble a 'normal-looking' tadpole. They mostly occur in water cavities of slow moving streams, where in most cases water flow velocity is so low that these tadpoles do not suffer from drift. The tadpoles exhibit a less robust chondrocranium in comparison to *Trichobatrachus* and *Nyctibates*.

Direct development within Arthroleptidae has only evolved in the genus *Arthroleptis* (***Figure 3***). Detailed descriptions and comparative data on the external morphology of direct development in *Arthrolpetis* are given in **Chapter 1.** In *Arthroleptis,* as well as other direct developing anurans (Goldberg et al. 2020, 2015, 2012; Anstis 2008; Anstis et al. 2007; Hanken et al. 2001; Callery et al. 2001; Callery & Elinson 2000; Hanken et al. 1997; Townsend & Stewart 1985), almost all larval features are absent during development. It is hypothesized that they have been reduced due to their loss of function (**Chapter 2**). It seems that the release from morphological constraints of forming necessary larval structures of the cranium during development is a characteristic of direct development. However, this does not mean that all larval features in general have been lost. The external morphology in direct developing anurans seems to be similar, but the detailed description of the internal morphology reveals variation among different taxa (**Chapter 2 and 3**). Thus, comparison of embryonic development of the skin and the cranial muscles, cartilages and bones of *Arthroleptis* shows that some larval traits are highly conserved whereas others, e.g. the presence or absence of the cartilago labialis superior or a processus muscularis of the palatoquadrate, vary between different direct developing species.

The evolution of terrestrial development, like direct development, has often been considered as one of the 'key innovations' leading to a high diversification rate in Lissamphibia (Meegaskumbura et al. 2015; Hedges et al. 2008; Bahir et al. 2005; Hanken et al. 1992). Contrary to this hypothesis, phylogenetic comparative analyses of puddle frogs (*Phrynobatrachus*) in relation to adaptation and diversification through time have shown that terrestrialization and the independence of water is not associated with higher rates of diversity (Zimkus et al. 2012). Studies on the rate dynamic and trait evolution of African bufonids likewise concluded that terrestrialization is not linked to higher species diversity and that lineage and trait diversification has been constant over time (Liedtke et al. 2016). Though terrestrial development may not be associated with species diversification, habitat quality can facilitate a spread into new ecological niches. This affects evolutionary changes in reproduction site and developmental processes. Many authors have discussed climate and environmental factors as well as ecological conditions that may have promoted the evolution of direct development in amphibians (Brink et al. 2020; Müller et al. 2013; Ernst et al. 2012; Poynton 1964; Goin & Goin 1962). In Arthroleptidae, for instance cold and streaming water habitats may have exert selection pressure on completely aquatic species in both evolutionary ways: First, highly specialized tadpoles have evolved in adaptation to different water flow velocities. And second, lotic habitats

may have favored a change towards a terrestrial breeding site where environmental and ecological conditions appear to be more suitable (Müller et al. 2013; Campbell & Duellman 2000; Alcala 1962; Goin & Goin 1962).

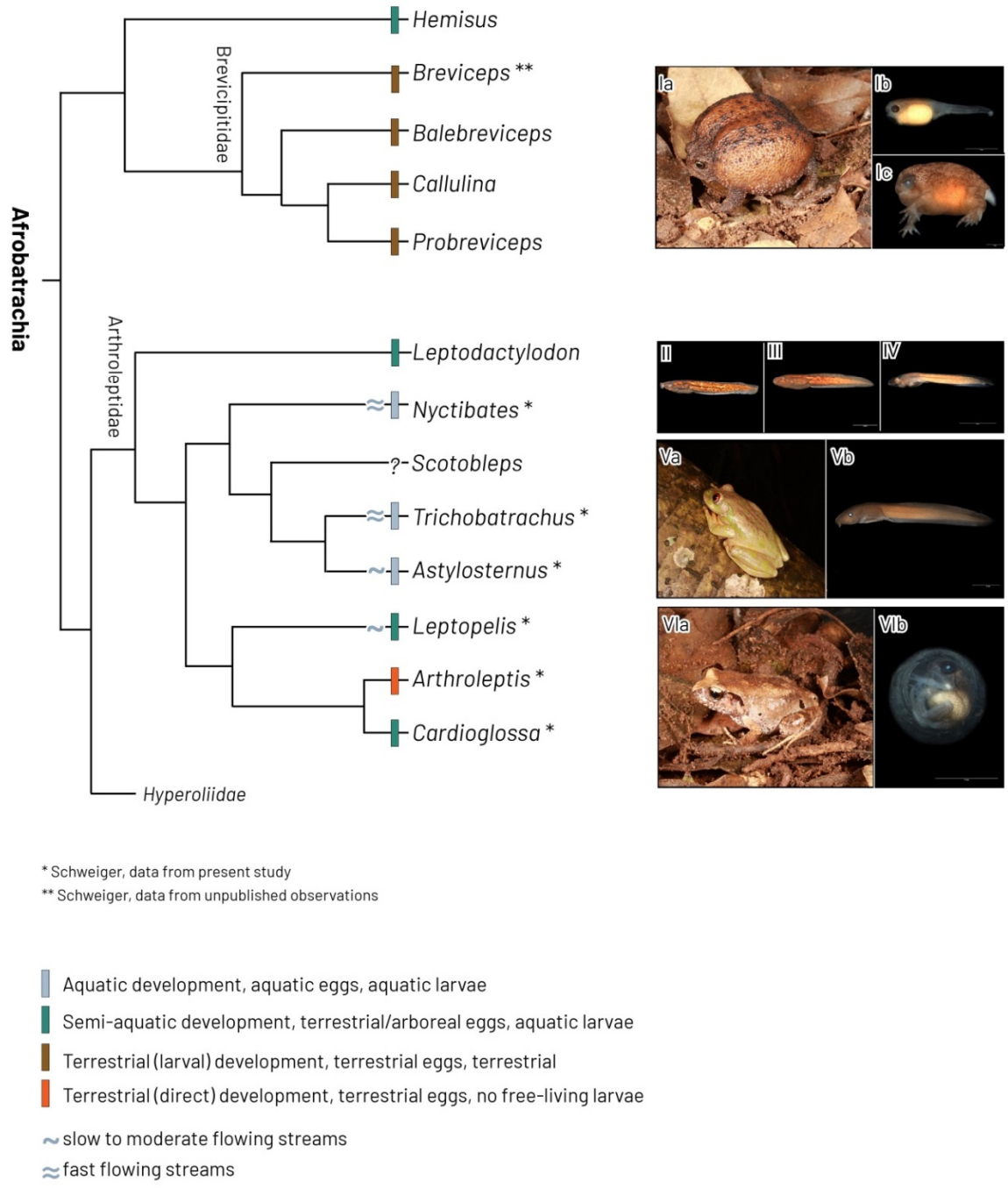

Figure 3: *Cladogramm showing the phylogeny of Arthroleptidae and Brevicipitidae (Afrobatrachia). Modes of reproduction (and habitat characters of the stream tadpoles) were mapped on the branches. Cladogramm modified after Portik & Blackburn (2016).* ***Ia*** *Adult of Breviceps verrucosus;* ***Ib*** *Terrestrial larva of Breviceps adspersus;* ***Ic*** *Metamorph of Breviceps adspersus.* ***II*** *Tadpole of Leptodactylodon mertensi, Gosner stage (GS) 25.* ***III*** *Tadpole of Astylosternus occidentalis, GS 25/26. Tadpole of Cardioglossa manengouba, GS 27.* ***Va*** *Adult of Leptopelis natalensis;* ***Vb*** *Tadpole of Leptopelis natalensis, GS 31.* ***VIa*** *Adult of Arthroleptis wahlbergii; VIb Egg with embryo of A. wahlbergii, Townsend & Stewart stage 14.*

Comparing the developmental mode of the 151 Arthroleptidae species - 50 species (*Arthroleptis*) exhibit direct development and 86 species (*Leptodactylodon, Leptopelis, Cardioglossa*) exhibit a semi-aquatic development. The tadpole of *Scotobleps* is described (Griesbaum et al. 2019), but oviposition sites (aquatic or terrestrial) remain unknown. The remaining 14 species are less diverse and develop fully aquatically in montane streams (***Table 1***).Thus, to a certain degree, terrestrial development in Arthroleptdiae seems to be evolutionarily more successful in terms of species numbers.

Table 1: *Distribution of species numbers of the family Arthroleptidae and first appearance along the geologic time scale.*

Genus	Species numbers	Mode of development	Habitat	Era (Portik&Blackburn 2016)
Leptodactylodon	15	biphasic/semi-aquatic	streams	Paleocene/Eocene (66 – 37.8 my)
Nyctibates	1	biphasic/aquatic	streams	
Scotobleps	1	Biphasic/?	streams	
Trichobatrachus	1	biphasic /aquatic	streams	
Astylosternus	12	biphasic /aquatic	streams	
Leptopelis	52	biphasic/semi-aquatic	streams	Miocene/Pleistocene (23.03 – 0.13 my)
Arthroleptis	50	direct/terrestrial	leaf litter	Oligocene/Miocene (33.9-7.25 my)
Cardioglossa	19	biphasic/semi-aquatic	streams	

Portik & Blackburn (2016) estimated the appearance of the most recent common ancestor of the family Arthroleptidae at approximately 54 my ago. Arthroleptids with a fully aquatic development first appear during the Paleocene/Eocene (Portik & Blackburn 2016). Early diversification events appear to be concentrated in the Late Oligocene and Early Miocene, an era where the semi-aquatic *Cardioglossa* and the direct developing *Arthroleptis* first appeared (Blackburn et al. 2021; Portik et al. 2019; Portik & Blackburn 2016). Divergence time analysis of Blackburn et al. (2021) revealed that montane lineages of *Cardioglossa* originated during the middle to late Miocene, when mountain building and volcano formation occurred. Further species divergence occurred during the Pleistocene, a period characterized by climatic change and diversification in many African anurans (Blackburn et al. 2021; Bell et al. 2017; Amiet 1975). On the basis of species diversity and their appearance during geological time scale, it seems that the evolutionary transition to a more terrestrial life-history provided a more suitable alternative for reproduction: Harsh environmental conditions present in montane areas might have exerted selective pressure on aquatic larvae and simultaneously played a role as evolutionary driver promoting a more terrestrial reproductive mode (Müller et al. 2013). Müller et al. (2013) also proposed that there is a correlation of terrestrial reproduction with montane environments and with forest habitats. These factors may have favored the evolution of arthroleptid species through a semi-aquatic and a completely terrestrial development.

But how can a more terrestrial reproductive mode evolve in an ancestral population of highly adapted stream-dwelling tadpoles? Brink et al. (2019) stated that metamorphosis may also be an evolutionary dead end in cases of high degradation of ecological conditions, ultimately leading to extinction rather than to the evolution of direct development. This would suggest that biphasic development with metamorphosis is highly conserved during evolution. Alternatively Brink et al. (2020) suggested that the evolution of direct development is associated with a high mutation rate and slow habitat degradation. Other factors proposed to drive the reproduction habitat to a more terrestrial breeding site are food resources, predation, humidity, the risk of desiccation of aquatic habitats and polyandry (Brink et al. 2020; Zamudio et al. 2016; Touchon & Worley 2015; da Silva et al. 2012; Gomez-Mestre et al. 2012; Ferrari & Chivers 2009; Wells 2007; Gomez-Mestre et al. 2006; Haddad & Prado 2005; Duellman & Trueb 1994; Noble 1931). For instance, direct development may be a more successful strategy when the intensity of aquatic predation is higher on free-living tadpoles than on direct developing frogs (Magnusson & Hero 1991; Duellman & Trueb 1986; Lutz 1948). Most terrestrially breeding frogs lay their eggs in humid, sheltered soil, between leaves or burrowed in the soil or in a subterranean chamber, likely to protect the eggs from predators and to minimize the risk of desiccation. Correspondingly, terrestrial development seems to depend on dense vegetation in forest habitats where climatic conditions are more stable (Poynton 1964). But there are also other examples: Terrestrial development in some species of *Breviceps* also occurs in arid habitats like deserts and savannahs (Minter 2004; Poynton 1964), though the subterranean nest provides a buffer for developing eggs from the arid environment above ground.

Collectively, possible evolutionary scenarios towards direct development in Afrobatrachia include: (1) Changes in reproductive behavior and habitat preference may lead to an increased independence of water. This may allow species to exist in a semi-terrestrial or even entirely terrestrial environment (Chipman 2002; Salthe & Duellman 1973; Lutz 1948). (2) Morphological changes in ontogeny, e.g. the increase of egg size, the near complete loss of tadpole-specific features like the larval jaw skeleton and its associated musculature, the cement glands, the lateral line system and the coiled intestine are some of the effects resulting of terrestrialization (present study, Hanken 2003; Hanken et al. 1997; Hanken 1992; Elinson 1990; Lutz 1948).

The developmental modes seen in hemisotids and brevicipitids, where a more terrestrial life-style has evolved, may be (explanatory) intermediate forms between a completely aquatic and a terrestrial direct development (Portik & Blackburn 2016; Crump 2015; Müller et al. 2007; Wells 2007). The phylogenetic model testing of Portik and Blackburn (2016) proposed that direct development has evolved from intermediate forms with subterranean or terrestrial egg deposition. Consequently, they suggested that these intermediate stages may have facilitated the evolution of direct development through a more terrestrial life-history ('intermediate stage hypothesis'). Alternatively, Pereira et al. (2015) and Gomez-Mestre et al. (2012) stated

that direct development in different lineages may has evolved from different starting points, either a fully aquatic or a more terrestrial mode of development. Descriptions of the cranial musculoskeleton of different developmental stages of *Breviceps adspersus* PETERS 1882 show, that larval features are present, such as the processus muscularis of the palatoqudrate, the typically shaped lower jaw with the short and strongly curved cartilago meckeli and the cartilago labialis inferior as well as the presence of larval levator muscles and a prominent musculus (m.) orbitohyoideus typical for the anuran tadpole (Schweiger, unpublished observations). In comparison to the direct developing *Arthroleptis,* there are more larval characters present. However, some other typical larval features like the cartilago labialis superior of the upper jaw are absent. Surprisingly, the form of the hyobranchial skeleton of *B. adspersus* is strikingly similar to the hyobranchial skeleton of the direct developing *Arthroleptis* and *Eleutherodactylus coqui*. Investigations on the development of *Breviceps* (***Figure 3 I a-c***) are in progress and will further contribute to our understanding of whether intermediate forms where precursors and have facilitated the evolution of direct development.

Direct development in frogs – parallel evolution driven by heterochronic shifts?

To understand the transition to direct development from an evolutionary and developmental point of view, heterochrony has often been discussed to be a key driver (Goldberg et al. 2012; Hanken et al. 1992; Hanken 1989; Raff & Wray 1989; Raff 1987). Experimental studies in *E. coqui* have shown that this species exhibits a mosaic pattern of heterochronic shifts for different morphological features (Schlosser 2008; Callery & Elinson 2000; Jennings & Hanken 1998; Hanken et al. 1997; Townsend & Stewart 1985; Hughes 1966; Lynn & Peadon 1955; Lynn 1948). This is similar to *Arthroleptis,* in which a mosaic of the presence, reduction and complete absence of tadpole-specific characters has been identified in this thesis (**Chapter 1-3**). The ontogeny is characterized by the short and incomplete development of few larval characters (*sensu* Hanken et al. 1992) and the appearance of most cartilaginous, skeletal and muscular elements in an already mid-metamorphic state (*sensu* Hanken et al. 1992) (**Chapter 1-3**). Tadpole-typical cartilages (the cartilago labialis inferior, the processus muscularis of the palatoquadrate, the processus oticus and the ceratobranchialia of the hyobranchial skeleton) are only present during the early developmental period until TS 10 (the 'larval period'). The patterning process of the skin and thyroid gland development in *Arthroleptis* (TS 5/6-12) is largely similar to that seen in *E. coqui* (Jennings & Hanken 1998; Townsend & Stewart 1985). Thus, comparative data have shown that direct development of these unrelated frog species is associated with a comparable heterochronic shift of thyroid gland maturation (**Chapter 3**).

However, larval elements that have not been observed in *Arthroleptis* comprise the cartilago labialis superior, the commissura quadratocranialis and the processus ascendens of the palatoquadrate. A processus ascendens is also not present in the

closest relatives showing a biphasic lifecycle (**Chapter 4**), indicating that the loss of this structure is not necessarily connected to the evolution of direct development in *Arthroleptis*. The absence of the cartilago labialis superior of the upper jaw from cranial ontogeny was also reported for *E. coqui* (Hanken et al. 1992). Finally, Kerney et al. (2010) investigated skeletal regulatory gene expression during early development in *E. coqui.* However they found that the anlagen of the cartilago labialis superior are transiently detectable (during TS 6/7), but these never develop into distinct cartilages. This indicates that this precursor also undergoes at least a recapitulation of the ancestral ontogeny (Kerney et al. 2010).

In comparison to biphasic anurans, the ossification sequence in direct developing taxa differs dramatically (**Chapter 2**). In biphasic species, bones supporting the dorsal and ventral cranium of the tadpoles form first (Moore & Townsend Jr. 2003; Trueb & Hanken 1992; Maglia & Púgener 1998; Wiens 1989; de Sa 1988; Gaudin 1978). In contrast, in *Arthroleptis* (**Chapter 2**) and *E. coqui* (Hanken et al. 1992), bones of the lower jaw and the suspensorium (angulosplenial and squamosal) ossify before hatching occurs.

Changes in the relative timing of development seem to be a common characteristic arising in all direct developing frogs investigated so far. Heterochrony therefore plays a major role in the evolution of direct development. In the last decade, several more investigations on direct development in frogs have been published and reveal that the extent to how features were expressed varies between different developing taxa (Goldberg et al. 2020, 2015, 2012; Narayan et al. 2010; Anstis 2008; Anstis et al. 2007; Kerney et al. 2007). The comparison of characteristic conditions in these taxa however, reveals differences in tempo and/or sequence of development of some features (e.g. early enlargement of the tail and the presence of an opercular fold), while other features (e.g. an egg tooth and a greatly enlarged tail fin) seem to be restricted to particular taxa and are indeed rather variable among different lineages (**Chapter 1**).

Besides heterochrony, heterotopy (spatial re-patterning or relative re-arrangement as defined by Haeckel 1866) may play another important role in the evolution of terrestrial development. Heterotopy is less widely common, but may be employed to explain changes in the location of morphological features leading to morphological novelties not present in metamorphosing species (Goldberg & Candioti 2015; Hanken 2015; Goldberg et al. 2012; Zelditch & Fink 1996). For example, the novel formation of structures like expanded tail fins enveloping nearly the whole embryo in the direct developing *Oreobates barituensis* VAIRA & FERRARI 2008 (Goldberg et al. 2012) and the closely related *Haddadus binotatus* SPIX 1824 (Goldberg & Candioti 2015) are understood as a cause of heterotopy. This characteristic has neither been observed in species of *Arthroleptis, E. coqui* or *Pseudophilautus* and therefore is presumably an apomorphic feature. It has been suggested that morphological repatterning, in form of *de novo* formation, plays an important role in the evolution of direct development (Hanken et al. 1992). This repatterning process is comparatively similar between *Arthroleptis* and *E. coqui* (**Chapter 2 and 3**). Further investigations on the evolution of

direct development in anurans regarding different species and 'intermediate' forms are needed to clarify these issues in more detail. Especially, the early ontogeny of terrestrial developing species is of particular interest, and additional techniques (e.g. gene expression techniques) are required to examine the role of anlagen in underlying developmental processes.

The evolution of metamorphosis, the 'tadpole hypotheses' and metamorphic changes in direct developing anurans

Within Lissamphibia, developmental changes and metamorphic patterns vary widely and there is no typical metamorphosis in general (Lynn 1961). Profound metamorphic transformation is present in most biphasic anurans and is associated with heterochrony, in terms of shifts in timing of developmental events, and caenogenesis, in terms of the formation of novel larval characteristics (Reiss 2002; Alberch 1989). Caenogenetic characteristics differentiating the tadpole from the larval stage of other lissamphibians include external features such as an oral disc, papillae and keratodonts as specific features of the mouth, cement glands and opercular folds (Wells 2007; Harris 1999; Thibaudeau & Altig 1999). Specific internal features not present in non-anuran lissamphibian larvae are the cartilagii labialis inferior et superior, the processus muscularis of the palatoquadrate, the cornuae trabeculae, the commissura quadratocranialis and the commissura terminalis of the hyobranchial skeleton (Altig & McDiarmid 1999; Cannatella 1999).

In Lissamphibia, common larva-specific traits may have evolved independently (Hanken 1999): The presence of gills, a finned tail and the basic structure of the hyobranchial skeleton with four ceratobranchialia. While the larval stage is thought to reduce intra-specific competition between different life history stages, the metamorphic process connecting the lissamphibian larva to its adult morphology is of a high risk (Brink et al. 2020; Wells 2007). A loss of the tadpole-stage and of the risky metamorphic transformation process might have been advantageous in habitats that were not suited for tadpoles. This evolutionary loss of the tadpole in direct developing anurans has left much room for speculation and different tadpole-hypotheses have been proposed. The near complete loss of larval characters in *E. coqui* has led to the hypothesis, that the tadpole represents a larval cassette that has been deleted from the ontogeny ('tadpole module hypothesis', ***Figure 4A***; Callery et al. 2001, Elinson 2001, Callery & Elinson 2000, Elinson 1990). If the tadpole-stage can be excised from development, this would suggest that all tadpole specific features and the TH-inducted metamorphosis are lost during evolution. The idea that the tadpole as a whole represents a module in evolution is controversial. Over time, more studies on other direct developing species were published showing that the degree of derived characters varies between species. In many cases, larval characters are retained or recapitulated revealing that the tadpole cannot easily be 'deleted' as a whole during evolution (Goldberg et al. 2020, 2015, 2012; Narayan et al. 2010; Anstis 2008; Anstis et al. 2007; Kerney et al. 2010, 2007). This challenges the hypothesis of the larva as an evolutionary module.

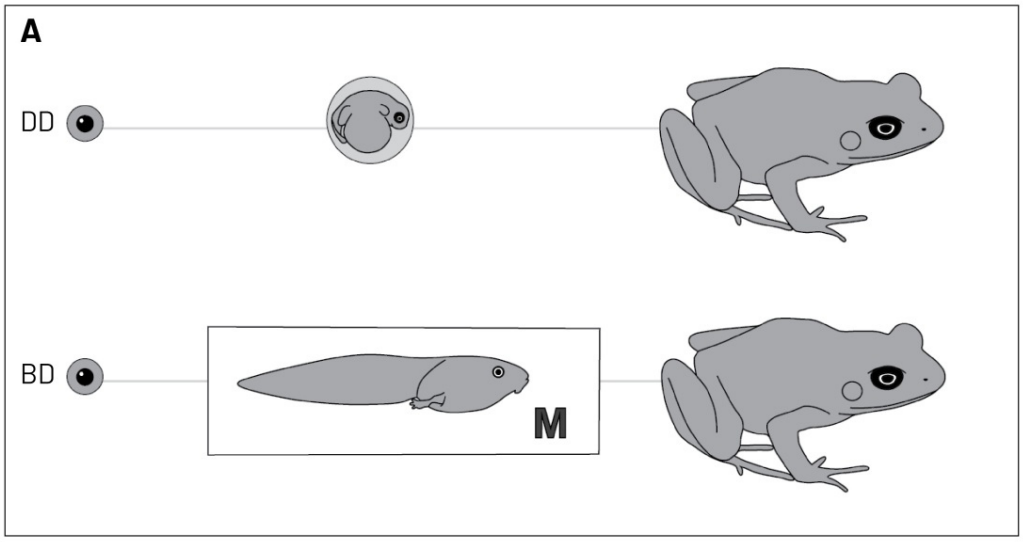
A
DD
BD
M

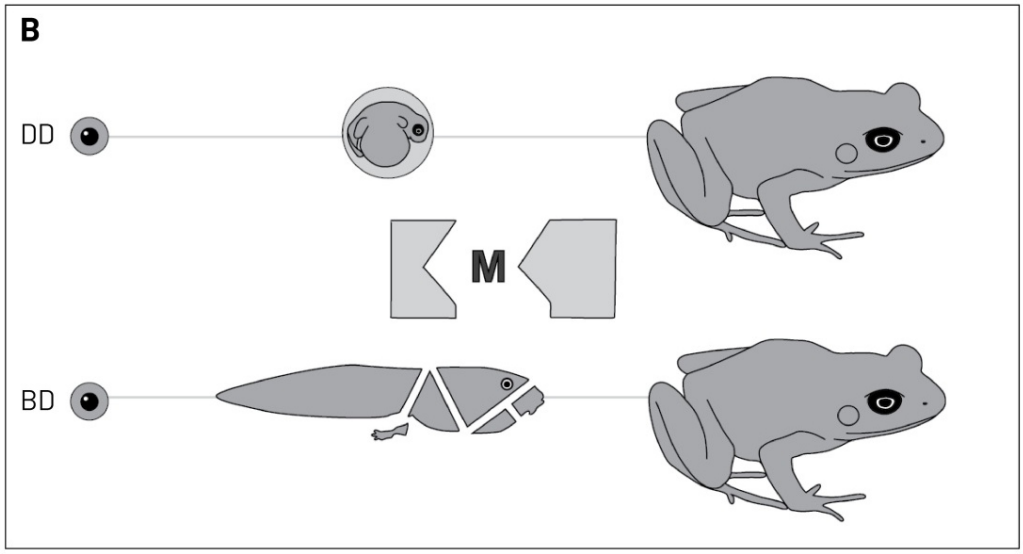
B
DD
M
BD

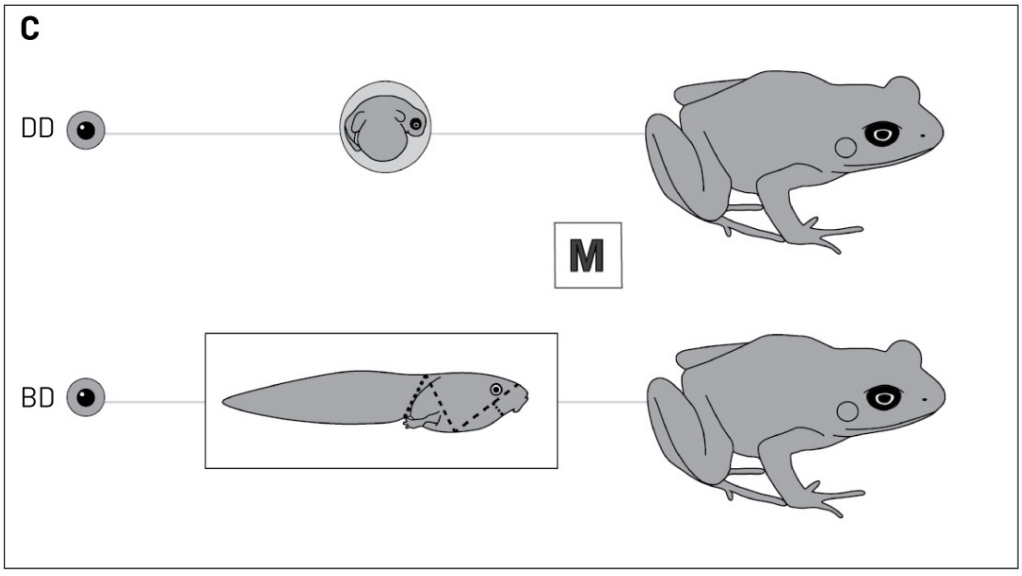
C
DD
M
BD

Figure 4: *Illustrations of the tadpole module hypotheses (previous page).* ***A:*** *Tadpole module hypothesis after Elinson (1990), Callery and Elinson (2000) and Elinson (2001): The tadpole stage (larva that undergoes metamorphosis) is a cassette that can be excised out of ontogeny in direct developing frogs.* ***B:*** *Tadpole module hypothesis after Schlosser (2005). The tadpole as a whole cannot be interpreted as an evolutionary module. Instead, the tadpole consists of several (larval) morphological modules and a TH-dependent metamorphosis module, together facilitating the evolution of direct development in frogs.* ***C:*** *Tadpole module hypothesis after Ziermann & Diogo (2014). The tadpole consists of morphological modules and the tadpole as a free-living larval stage is an evolutionary module disappearing during the evolution of direct developing frogs. TH-dependent metamorphosis is present as "cryptic metamorphosis" leading to the adult transformation.* ***Abbreviations:*** *DD, direct development. BD, biphasic development. M, metamorphosis.*

Schlosser (2005) proposed that the larva does not act as a module in amphibian development since not all larval characters were replaced, but rather remodeled during metamorphosis. According to Schlosser (2005) that would mean that the tadpole as a whole organism is not an evolutionary module, but that instead certain larval characters and metamorphosis itself might be viewed as distinct anatomical and/or functional modules (***Figure 4B***). Ziermann & Diogo (2014) also argued that the tadpole consists of particular morphological modules (like the head and limb development, as argued by Schlosser 2005) but state that the tadpole as a free-living larval stage is a life-history module (as proposed by Elinson 2001, Callery and Elinson 2000, Elinson 1990). This hypothesis implies that direct development could have evolved, because the morphological modules and the life-history module are uncoupled and independent from each other, facilitating the deletion of the life-history trait 'free-living aquatic larva' by retaining developmental processes (***Figure 4C***).

The results of this study support the arguments of Schlosser (2005) that the tadpole may consist of several morphological units and subunits, and that the larva as a whole cannot be excised from anuran ontogeny.

From an evolutionary and developmental point of view, the tadpole consists of 'larval features', typical for lissamphibian larvae, and 'typical tadpole features' only seen in anuran larvae. Few of these 'typical tadpole features' are only transiently present in some direct developing anurans (e.g. *E. coqui, Arthroleptis*), while others (e.g. *Pseudophilautus*) show a more larval related development (**Chapter 1 and 2**). Thus, direct developing anurans all develop a 'larval' hyobranchial skeleton with four ceratobranchialia. This is an evolutionary character uniting all lissamphibian larvae as a result of their shared ancestry with fishes (Carroll 2007). Carroll (2007) also stated that *Eusthenopteron* (a sarcopterygian known from the late Devon, 385 my ago), *Acanthostega* and the larvae of *Ambystoma* (a group of extant salamanders endemic to North America) show a similar configuration of the hyobranchial skeleton. This is also reported for many temnospondyls and microsaurs (Schoch 2009), indicating that the form of the hyobranchial skeleton is evolutionarily highly conserved in the ground pattern of amphibian larvae.

According to the definition of Alberch (1989), metamorphosis is a process of condensed morphological changes. However, it is difficult to interpret whether the ancestral condition was associated with a 'cryptic', gradual metamorphosis like seen in direct developing species, or if it has been as dramatic as seen in biphasic anurans.

The development of early amphibians is still poorly understood (Clack 2002; Ahlberg & Milner 1994; Fritzsch 1990), but morphological changes that may correlate with metamorphosis were found in Temnospondyli, a group of early amphibian-like tetrapods (Schoch & Fröbisch 2006; Schoch 2002; Boy 1974). Investigations of the development in larval temnospondyls have shown that some sort of metamorphic transformation has already been present in this group (Schoch 2001; Boy & Sues 2000; Alberch 1989; Boy 1974). For instance, the ossification sequence in branchiosaurids, a taxon of the Temnospondyli, is comparatively similar to the metamorphic pattern in salamanders, although it appears not as condensed (Schoch & Fröbisch 2006; Schoch & Carroll 2003; Schoch 2001; Schoch 1992; Boy 1974). A condensed morphological change (sensu Alberch 1989) evolved within the dissorophoids, which are considered to be the evolutionary origin of Lissamphibia (Schoch 2009; Clack 2002; Schoch 2001; Trueb & Cloutier 1991).

A metamorphic process is also present in direct developing anurans, demonstrating that the larval stage cannot easily be deleted from ontogeny. Several studies of *E. coqui* have shown that developmental events are coupled to TH-hormone activity and that development is incomplete if TH synthesis is inhibited (Singamsetty & Elinson 2010; Callery & Elinson 2000; Jennings & Hanken 1998; Hughes 1966; Lynn & Peadon 1956). This phase of TH-dependent developmental processes, occurring during direct development in *E. coqui,* is relatively short and not as obvious as seen in biphasic developing frogs ('cryptic metamorphosis', Elinson et al. 2001; Elinson & Callery 2000). This correlates with the results on the skin development in *Arthroleptis*: The skin develops in four major phases (embryonic, 'tadpole', metamorphic and adult) (**Chapter 2),** similar to many biphasic species (Robinson & Heintzelman 1987; Fox 1986). There are many similarities between *E. coqui* and *Arthroleptis* regarding metamorphic processes that correlate with increased TH activity such as tail regression, remodeling of the 'larval' into the adult hyobranchial apparatus, elongation of the jaw and cranial muscle development (Elinson 2001; Jennings & Hanken 1998; Hanken et al. 1997; Hanken & Summers 1988; **Chapter 1-3**). Most of these processes start slightly earlier in *Arthroleptis,* which correlates with an earlier appearance of the thyroid glands compared to *E. coqui* (**Chapter 3**). It seems that TH is a major regulator and also affects the ontogeny in direct developing anurans. The precocious TH-activation has already been invoked to explain the repeated occurrence of direct development in frogs (Schlosser 2005; Jennings & Hanken 1998; Hanken, Jennings, & Olsson 1997). Therefore, direct development depends on, and is possibly constrained by, the ancestral dependency on TH for adult development.

The presence of tadpole-like structures during ontogeny and the correlation of metamorphic changes with an increased thyroid gland activity indicate that the tadpole cannot be viewed as a holistic module that can either appear or disappear during evolution. But why do some larval features develop, whereas others are not present during direct development and why is direct development not as uniform as previously thought? According to the hypothesis of Schlosser (2005), the tadpole-modules

consist of coupled or uncoupled features that are present or absent in different direct developing species. Collectively, this may result in:

(1) External morphological similarities in direct developing species like early and simultaneous appearance of limb buds, the presence of a tail with a membranous fin used for respiration, the presence of a processus muscularis of the palatoquadrate with the related M. orbitohyoideus,

2) Different characteristics of the internal morphology between direct developing species like the presence or absence of larval features of the cranial musculoskeleton (cartilages of the jaw and larval levator muscles) and,

(3) TH-dependent metamorphosis that still plays a regulating role during the ontogeny of all the different direct developing species.

Chipman (2002) also stated that the modular arrangement in anuran embryogenesis forms the basis for a high degree of variation of developmental processes. Thus, some larval structures may have changed their function (e.g. the vascularized tail functioning as a respiratory organ) while others form in a mid-metamorphic state of development (Callery et al. 2001; Hanken et al. 1992; Townsend & Stewart 1989). According to Callery et al. (2001), it seems possible that the short-term presence or the formation in a mid-metamorphic shape of some tadpole-typical cranial cartilages may play an inductive role for further developmental processes which otherwise cannot reach the adult configuration. Furthermore, Callery et al. (2001) discussed that the retention of larval traits is possibly based on neutral selection and that more mutations were needed for a complete reduction of larval features during direct development. The idea of the meta-modul-hypothesis, together with several other factors like mutation rate and environmental selection pressures may lead to a complete terrestrial development and help for a better understanding of the evolution of a terrestrial development in anurans.

As mentioned in this thesis, the development of ‘intermediate’ forms is of particular interest. A future direction to improve our knowledge has to include a broader approach: It needs more detailed data from species closely related to direct developing taxa to understand the reproductional, developmental, morphological, genetic, evolutionary and ecological aspects of terrestrialization in amphibians.

Summary

During the last decades, the evolution of terrestrialization in amphibians received increased attention in evolutionary and developmental biology. That is not surprising, as amphibians are a group of tetrapod vertrebrates with a very high variety of life history strategies, as well as reproductive and developmental modes. Many of these modes have evolved several times independently within all three recent amphibian taxa; Anura, Urodela and Gymnophiona. Although the majority of frogs and toads reproduce in bodies of water, there are trends towards an increasingly terrestrial reproduction in several lineages including in the sub-Saharan frogs of the clade Afrobatrachia. Within this group, the family Arthroleptidae exhibits high ecological and reproductive diversity. This includes the plesiomorphic biphasic development, a more semiaquatic development and direct development. Biphasic, fully aquatic species of Arthroleptidae all inhabit streams showing a highly specialized and robust cranial skeleton very different from tadpoles of their semiaquatic relatives in this group. Direct development differs completely from these two developmental strategies as development is completed within the terrestrially laid egg. There is no free-living aquatic larva and most of the larval features are absent, whereas adult structures form early during development. With respect to species diversity among biphasic, semiaquatic and direct developing forms, it seems that terrestrialization in Arthroleptidae is a successful strategy as streaming water habitats may work as selective pressure leading to a more terrestrial development. To increase our knowledge on the evolution of terrestrial development in amphibians in general this study focuses on non-model organisms.

The central question is: To what extent and how have the ancestral larval developmental pathways been altered during the evolution of terrestrially breeding frogs? Generally, detailed investigations of direct development have only been conducted in the Puerto Rican coqui (*Eleutherodactlyus coqui*) and in lesser detail in only a few other species. Because direct development is associated with the loss of many typical larval features, it has been generally assumed that the tadpole was completely excised from the ontogeny of direct developing frogs. This idea is controversial and has led to different views about the tadpole as a developmental module, the role of metamorphosis and the evolutionary origin of the anuran larva. To help in a critical appraisal of these hypotheses, this study provides a detailed description of the direct developing African Squeaker frogs (*Arthroleptis wahlbergii* and *A. xenodactyloides,* Arthroleptidae, Afrobatrachia). The results are compared to closely related species exhibiting a more ancestral (e.g. biphasic) life history as well as to other non-related direct developing species. In this thesis it is shown that direct development is not invariably linked to a complete loss of larval features and that metamorphic changes correlate with thyroid gland activity. However, few larval elements that never develop in *Arthroleptis* are also not present in the closest relatives with biphasic development, indicating that the loss of these structures is not necessarily linked to the evolution of direct development.

In reflection of the 'tadpole module hypothesis' it is supposed that the tadpole cannot be viewed as a module that can either appear or disappear during evolutionary development. In contrast, the tadpole should be viewed as an evolutionary metamodule composed of many different developmental sub-modules. Different combinations of present and absent developmental sub-modules seem to underlie evolution of 'similar' direct developmental patterns in distantly related frogs. This indicates that a complete terrestrial development might have evolved in different ways. At last the evolution of anuran terrestrial development may be driven by an interaction of various environmental, genetic and developmental factors. However, there is still a need for more detailed studies to facilitate a comprehensive understanding of the evolution of terrestrialization in amphibians.

Zusammenfassung

Die Evolution der Terrestrialisierung bei Amphibien wurde in den vergangenen Jahrzehnten zu einem der herausfordernden Forschungsthemen der Evolutions- und Entwicklungsbiologie. Als eine Gruppe innerhalb der Tetrapoden (Landwirbeltiere) zeigen Amphibien eine enorm hohe Diversität an alternativen lebensgeschichtlichen Strategien (life history strategies) sowie verschiedenste Formen von Reproduktions- und Entwicklungsmodi. Viele dieser Modi sind mehrfach unabhängig voneinander in allen drei rezenten Gruppen (Frosch- und Schwanzlurche sowie Blindwühlen) evolviert. Obwohl die Mehrheit der Frösche und Kröten in ihrer Fortpflanzung und Entwicklung auf Gewässer angewiesen ist, ist ein Trend hin zur Terrestrialisierung erkennbar. Ein Beispiel dafür sind die Afrobatrachia, eine Gruppe subsaharischer Anuren. Innerhalb dieser Gruppe zeigt die Familie der Arthroleptidae eine hohe ökologische und reproduktive Diversität, ausgehend von biphasischer über semiaquatische bis hin zur direkten Entwicklung. Interessanterweise leben alle sich vollständig aquatisch entwickelnden Arten der Arthroleptidae in Gebirgsbächen. Womöglich als Adaptation an dieses Habitat, besitzen sie ein hochspezialisiertes und robustes Cranialskelett, welches sich deutlich von dem der Kaulquappen semiaquatischer Verwandter unterscheidet. Direktentwicklung unterscheidet sich ganz grundsätzlich von der aquatischen Entwicklung und findet vollständig terrestrisch, im an Land abgelegten Ei, statt. Eine freilebende, aquatische Larve ist in der Entwicklung nicht mehr vorhanden. Die meisten larvalen Strukturen sind evolutionär verloren gegangen, die Entwicklung ist stattdessen durch eine frühzeitige Ausbildung adulter Merkmale gekennzeichnet. Bezüglich der Artenzahl biphasischer, semiaquatischer und direktentwicklender Taxa scheint es, dass die Terrestrialisierung innerhalb der Arthroleptidae einen erfolgreichen evolutionären Trend darstellt. Davon ausgehend scheint es, dass strömende Gewässer als Habitate wohl einen Selektionsdruck hin zur terrestrischen Entwicklung ausüben. Um das Wissen über die Evolution der terrestrischen Entwicklung bei Amphibien im Allgemeinen zu fördern, wurden in dieser Studie insbesondere Nicht-Model-Organismen dahingehend untersucht. Im Fokus stand die Frage, in welcher Form ursprüngliche, larvale Entwicklungsmerkmale bei terrestrisch reproduzierenden Fröschen im Laufe der Evolution geändert wurden. Genauere Untersuchungen zur Direktentwicklung liegen bisher nur für den Coqui-Pfeifffrosch (*Eleutherodactlyus coqui*) vor. Für einige wenige andere Arten finden sich nur vereinzelte, unvollständige Berichte. Da Direktentwicklung mit dem Verlust einer Vielzahl von typischen Larvalmerkmalen einhergeht, wurde allgemein angenommen, dass die Kaulquappe bei direkt entwickelnden Fröschen aus der Ontogenese herausgeschnitten werden kann. Diese Sichtweise ist kontrovers und hat zu verschiedenen Ansichten über die Kaulquappen-Modul-Hypothese, die Rolle der Metamorphose und dem evolutionären Ursprung der Anuren-Larve geführt. Um einen kritischen Beitrag zur Auseinandersetzung mit diesen Hypothesen zu liefern, fokussiert sich diese Arbeit auf eine detaillierte Beschreibung der direkt entwickelnden afrikanischen Langfingerfrösche der Gattung *Arthroleptis* (*A. wahlbergii* and *A. xenodactyloides,* Arthroleptidae, Afrobatra-

chia) im Vergleich zu anderen nicht-verwandten Arten mit Direktentwicklung und nahe verwandten Arten ohne Direktentwicklung. Es konnte gezeigt werden, dass Direktentwicklung nicht ausnahmslos mit einer vollständigen Reduktion larvaler Merkmale einhergeht und metamorphe Umwandlungsprozesse vorhanden sind, die zudem mit der Aktivität der Thyroiddrüse korrelieren. Zudem fehlen in der Entwicklung einige wenige larvale Merkmale bei *Arthroleptis*, die ebenso wenig bei den nah verwandten, biphasischen Arten ausgebildet werden. Dies zeigt, dass der Verlust dieser Strukturen nicht automatisch mit der Evolution der Direktentwicklung zusammenhängt.

In Bezug auf die Kaulquappen-Modul-Hypothese wird angenommen, dass die Kaulquappe selbst nicht als Modul angesehen werden kann, welches während der evolutionären Entwicklung ohne weiteres in Erscheinung treten oder wieder verloren gehen kann. Wahrscheinlicher ist, dass die Kaulquappe als evolutionäres Meta-Modul fungiert, das seinerseits aus vielen verschiedenen Entwicklungsmodulen zusammengesetzt ist. Diese einzelnen Module wiederum bestehen ihrerseits aus verbundenen oder unverbundenen Entwicklungsmerkmalen, die bei verschiedenen direkt entwickelnden Arten vorhanden sind oder fehlen und somit eine terrestrische Entwicklung auf verschiedenen Wegen ermöglichen. Die Evolution der terrestrischen Entwicklung bei Anuren wird schließlich wohl durch das Zusammenspiel verschiedenster Faktoren (Umwelt, Genetik, Entwicklung) beeinflusst und es braucht insgesamt mehr detailliertere Untersuchungen für ein umfassenderes Verständnis der Terrestrialisierung bei Amphibien.

References

Ahlberg, E., Milner, A. R. (1994). The origin and early diversification of tetrapods. Nature 368: 507–514.

Alberch, P. (1989). Development and the evolution of amphibian metamorphosis. Fortschritte der Zoologie 35: 163-173.

Alcala, A. C. (1962). Breeding behavior and early development of frogs of Negros, Philippine Islands. Copeia: 679–726.

Altig, R., Mc Diarmid, R.W. (1999). Body plan– development and morphology. In: Tadpoles – the biology of anuran larvae. Edited by R. W. Mc Diarmid and R. Altig. Chicago University Press, USA, pp. 24–51.

AmphibiaWeb (2021). <https://amphibiaweb.org> University of California, Berkeley CA, USA. Accessed Nov 20, 2021.

Amiet, J.-L. (1975). Ecologie et distribution des Amphibiens Anoures de la region de Nkongsamba (Cameroun). Annales de la Faculté des Sciences de Yaoundé 20: 33–107.

Anstis, M. (2008). Direct development in the Australian myobatrachid frog Metacrinia nichollsi from Western Australia. Records of the Western Australian Museum 24: 133-150.

Anstis, M., Roberts, J.D., Altig, R. (2007). Direct development in two Myobatrachid Frogs, *Arenophryne rotunda* Tyler and *Myobatrachus gouldii* Gray, from Western Australia. Records of the Western Australian Museum 23: 259–271.

Atkinson, B.G. (1981). Biological Basis of Tissue Regression and Synthesis. In: Metamorphosis, edited by L.I Gilbert. and E. Frieden. Springer, Boston, MA.

Bahir, M.M., Meegaskumbura, M., Manamendra-Arachchi, K., Schneider C.J., Pethiyagoda, R. (2005). Reproduction and terrestrial direct development in Sri Lankan shrub frogs (Ranidae: Rhacophorinae: *Philautus*). Raffles Bulletin of ZoologySupplement 12: 339–350.

Barbour, T., Loveridge, A. (1928). A comparative study of the herpetological faunae of the Uluguru and Usambara Mountains, Tanganyika Territory, with descriptions of new species. Memoirs of the Museum of Comparative Zoology Harvard 50: 87-265.

Barej, M.F., Pfalzgraff, T., Hirschfeld, M., Liedtke, H.C., Gonwouo, N.L., Penner, J., Dahmen, M., DohertyBone, T., Schmitz, A., Rödel, M.O. (2015). The tadpoles of eight West and Central African *Leptopelis* species (Amphibia: Anura: Arthroleptidae). Amphibian and Reptile Conservation 9: 56-84.

Bell, R.C., Parra, J.L., Badjedjea, G., Barej, M.F., Blackburn, D.C., Burger, M.,Channing, A., Dehling, J.M., Greenbum, E., Gvoždík, V., Kielgast, J., Kusamba, C., Lötters, P.J., McLaughlin…Zamudio, K.R. (2017). Idiosyncratic responses to climate-driven forest fragmentation and marine incursions in reed frogs from

Central Africa and the Gulf of Guinea Islands. Molecular Ecology 26 (19): 5223–5224.

Blackburn, D.C, Nielsen, S.V., Ghose, S.L., Burger, M., Gonwouo, L.G., Greenbaum, E., Gvoždík, V., Hirschfeld, M., Kouete, M.T., Kusamba, C., Lawson, D., McLaughlin, P.J., Zassi-Boulou, A.-G., Rödel, M.-O. (2021). Phylogeny of African Long-Fingered Frogs (Arthroleptidae: *Cardioglossa*) Reveals Recent Allopatric Divergences in Coloration. Ichthyology & Herpetology 109 (3): 728–742.

Bogart, J.P. (1981). How many times has terrestrial breeding evolved in anuran amphibians? Monitore Zoologico Italiano Supplemento XV: 29–40.

Bonett, R.M., Steffen, M.A., Lambert, S.M., Wiens, J.J., Chippindale, P.T. (2013). Evolution of paedomorphosis in plethodontid salamanders: Ecological correlaes and re-evolution of metamorphosis. Evolution 68-2: 466-482.

Boy, J.A. (1974). Die Larven der rhachitomen Amphibien (Amphibia: Temnospondyli; Karbon – Trias). Paläontologische Zeitschrift 48: 236-282.

Boy, J.A., Sues, H.-D. (2000). Branchiosaurs: Larvae, metamorphosis, and heterochrony in temnospondyls and seymouriamorphs. In: Amphibian Biology, Vol. 4, Palaeontology. Edited by H. Heatwole and R.L. Carroll. Chipping Norton, New South Wales, Australia, Surrey Beatty and Sons, pp. 1150–1197.

Brink, H.t., Onstein, R.E., de Roos, A.M. (2020). Habitat deterioration promotes the evolution of direct development in metamorphosing species. Evolution 74 (8): 1826-1850.

Brink, H.t., de Roos, A.M., Dieckmann, U. (2019). The Evolutionary Ecology of Metamorphosis. The American Naturalist 193 (5): E116-E131.

Brown, W.C., Alcala, A.C. (1970). Population ecology of the frog *Rana erythraea* in southern Negros, Philippines. Copeia, 611–22.

Brown, D.D., Cai, L. (2007). Amphibian metamorphosis. Developmental Biology 306 (1): 20.

Cadle, J.E., Altig, R. (1991). Two lotic tadpoles from the Andes of southern Peru: *Hyla armata* and *Bufo veraguensis*, with notes on the call of *Hyla armata* (Amphibia: Anura: Hylidae and Bufonidae). Studies on Neotropical Fauna and Environment 26 (1): 45-53.

Callery, E.M., Elinson, R.P. (2000a). Thyroid hormone-dependent metamorphosis in a direct developing frog. Proceedings of the National Academy of Sciences 97 (6): 2615-2620.

Callery, E.M., Elinson, R.P. (2000b). Opercular development and ontogenetic reorganization in a direct-developing frog. Development, Genes and Evolution 210: 377–381.

Callery, E.M., Fang, H., Elinson, R.P. (2001). Frogs without polliwogs: evolution of anuran direct development. BioEssays 23: 233–241.

Campbell, J.A., Duellman, W.E. (2000). New species of stream-breeding hylid frogs from the northern versant of the highlands of Oaxaca, Mexico. Scientific Papers (National History Museum, the University of Kansas) 16: 1–28.

Cannatella, D. (1999). Architecture - Cranial and Axial Musculoskeleton. In: Tadpoles – the biology of anuran larvae. Edited by R. W. Mc Diarmid and R. Altig. Chicago University Press, USA, pp. 24–51.

Candioti, F.V., Haas, A., Altig, R., Peixoto, O. (2016). Cranial anatomy of the amazing bromeliad tadpoles of *Phyllodytes gyrinaethes* (Hylidae: Lophyohylini), with comments about other gastromyzophorous larvae. Zoomorphology 136.

Carroll, R.L. (2000a). The fossil record and large-scale patterns of amphibian evolution. In: Amphibian Biology, Vol. 4, Palaeontology. Edited by H. Heatwole and R. L. Carroll. Chipping Norton, New South Wales, Australia: Surrey Beatty and Sons, pp. 973–78.

Carroll, R.L. (2007). The Palaeozoic Ancestry of Salamanders, Frogs and Caecilians. Zoological Journal of the Linnean Society 150 (1): 1–140.

Castroviejo-Fisher, S., Padial, J.M., De La Riva, I., Pombal, J.P., Da Silva, H.R., Rojas-Runjaic, F.J.M., Medina-Méndez, E., Frost, D.R. (2015). Phylogenetic systematics of egg-brooding frogs (Anura: Hemiphractidae) and the evolution of direct development. Zootaxa 4004 (1): 001–075.

Channing, A. (2008): The mud dwelling tadpole of the long-toed tree frog, *Leptopelis xenodactylus* (Arthroleptidae). Herpetological Review 39: 288-290.

Channing, A., Rödel, M.-O., Channing, J. (2012). Tadpoles of Africa, the biology and identification of all known tadpoles in sub-Saharan Africa. Chimaira, Frankfurt a.M., 402 pp.

Chipman, A.D. (2002). Variation, plasticity and modularity in anuran development. Zoology 105: 97–104.

Chippindale, P. T. (2000). Species boundaries and species diversity in the Central Texas hemidactyliine plethodontid salamanders, genus *Eurycea*. In: The Biology of Plethodontid Salamanders. Edited by R. C. Bruce, R. G. Jaeger, and L. D. Houck. New York, Kluwer Academic/Plenum, pp.149–65.

Chippindale, P.T., Bonett, R.M., Baldwin, A.S., Wiens, J.J. (2004). Phylogenetic evidence for a major reversal of life-history evolution in plethodontid salamanders. Evolution 58: 2809–2822.

Clack, J. A. (2002). Gaining Ground. The Origin and Evolution of Tetrapods. Bloomington, Indianapolis, Indiana, 369 pp.

Crump, M.L. (2015). Anuran reproductive modes: evolving perspectives. Journal of Herpetology 49: 1–16.

Da Silva, F.R., Almeida-Neto, M., Prado, V.H.M., Haddad, C.F.B., Rossa-Feres, D.C. (2012). Humidity levels drive reproductive modes and phylogenetic diversity of

amphibians in the Brazilian Atlantic Forest. Journal of Biogeography 39: 1720–1732.

De Oliveira, M.I.R.R., Weber, L.N., de Sá, R.O., Ferreira, J.S., Libório, A.E.C, Takazone, A.M.G. (2017). Chondrocranium and internal oral morphology of the tadpole of *Corythomantis greeningi* (Anura: Hylidae). Phyllomedusa 16 (1): 71–80.

De Sa, R.O. (1988). Chondrocranium and ossification sequence of *Hyla lanciformis*. Journal of Morphology 195 (3): 345-355.

Denver, R.J. (2013). Neuroendocrinology of Amphibian Metamorphosis. In: Current Topics in Developmental Biology, Vol. 103. Academic Press, Eslevier, pp. 195-227.

Dolinay, M., Nečas, T., Zimkus, B.M., Schmitz, A., Fokam, E.B., Lemmon, E.M., Lemmon, A.R., Gvoždík, V. (2021). Gene flow in phylogenomics: sequence capture resolves species limits and biogeography of Afromontane forest endemic frogs from the Cameroon Highlands. Molecular Phylogenetics and Evolution 163: 107258.

Drewes, R.C. (1984). A Phylogenetic Analysis of the Hyperoliidae (Anura): Treefrogs of Africa, Madagascar, and the Seychelles Islands. Occasional Papers of the California Academy of Sciences 139, 70 pp.

Duellman, W.E. (1989). Alternative life-history styles in anuran amphibians: Evolutionary and ecological implications. In: Alternatice life-history styles in animals. Edited by M.N. Bruton. Dordrecht, Kluwer Academic Publishing, pp. 101-126.

Duellman, W.E., Trueb L. (1986). Biology of Amphibians. London: Johns Hopkins University Press.

Duellman, W.E., Waxson, L.R., Jesiolowski, C.A. (1988). Evolution of marsupial frogs (Hylidae: Hemiphractinae): Immunological evidence. Copeia: 527–543.

Elinson, R.P. (1990). Direct development in frogs: wiping the recapitulationist slate clean. Seminars in Cell and Developmental Biology 1: 263-270.

Elinson, R.P. (2001). Direct Development: An Alternative Way to Make a Frog. Genesis 29: 91–95.

Elinson, R.P., Beckham, Y. (2002). Development in frogs with large eggs and the origin of amniotes. Zoology 105: 105–117.

Elinson, R., Fang, H. (1998). Secondary coverage of the yolk by the body wall in the direct developing frog, *Eleutherodactylus coqui*: An unusual process for amphibian embryos. Development, Genes and Evolution 208 (8): 457-466.

Ernst, R., Keller, A., Landburg, G., Grafe, T.U., Linsenmair, K.E., Rödel, M.-O., Dziock, F. (2012). Common ancestry or environmental trait filters: cross-continental comparisons of trait–habitat relationships in tropical anuran amphibian assemblages. Global Ecology and Biogeography 21: 704–715.

Ernst, R., Nienguesso, A.B.T., Lautenschläger, T., Barej, M.F., Schmitz, A., Hölting, M. (2014). Relicts of a forested past: Southernmost distribution of the hairy frog

genus *Trichobatrachus* Boulenger, 1900 (Anura: Arthroleptidae) in the Serra do Pingano region of Angola with comments on its taxonomic status. Zootaxa 3779 (2): 297–300.

Etkin, W. (1935). The mechanisms of anuran metamorphosis. I. Thyroxine concentrations and the metamorphic pattern. Journal of Experimental Zoology 71: 317–340.

Fang, H., Elinson, R.P. (1996). Patterns of distal-less gene expression and inductive interactions in the head of the direct developing frog *Eleutherodactylus coqui*. Developmental Biology 179 (1): 160-172.

Feng, Y.J., Blackburn, D.C., Liang, D., Hillis, D.M., Wake, D.B., Cannatella, D.C., Zhang, P. (2017). Phylogenomics reveals rapid, simultaneous diversification of three major clades of Gondwanan frogs at the Cretaceous–Paleogene boundary. Proceedings of the National Academy of Sciences 114: E5864–E5870.

Ferrari, M.C.O., Chivers, D.P. (2009). Sophisticated early life lessons: threat-sensitive generalization of predator recognition by embryonic amphibians. Behavior and Ecology 20: 1295–1298.

Fox, H. (1986). The skin of amphibia. Biology of the Integument, Vertebrates 2: 78-148.

Fritzsch, B. (1990): The Evolution of Metamorphosis in Amphibians. Journal of Neurobiology 21 (7): 1011-1021.

Frost, D.R., Grant, T., Faivovich, Bain, R.H., Haas A., Haddad, C.F.B., De Sá, R.O., Channing, A. Wilkinson, M., Donnellan, S.C., Raxworthy, C.J., Campbell, J.A., Blotto, Moler, B.L. P., Drewes, R.C., Nussbaum, R.A., Lynch, J.D., Green D.M., Wheeler, W.C. (2006). The amphibian tree of life. Bulletin of the American Museum of National History 297:1–370.

Gaudin, A. J. (1978). The sequence of cranial ossification in the California toad, *Bufo boreas* (Amphibia, Anura, Bufonidae). Journal of Herpetology 12 (3): 309-318.

Goin, O. B., Goin, C.J. (1962). Amphibian eggs and the montane environment. Evolution 16: 364–71.

Goldberg, J., Candioti, F. (2015). A Tale of a Tail: Variation during the Early Ontogeny of *Haddadus binotatus* (Brachycephaloidea: Craugastoridae) as Compared with Other Direct Developers. Journal of Herpetology 49 (3): 479-484.

Goldberg, J., Candioti, F.V., Akmentins, M.S. (2012). Direct-developing frogs: ontogeny of *Oreobates barituensis* (Anura: Terrarana) and the development of a novel trait. AmphibiaReptilia 33 (2): 239-250.

Goldberg, J., Taucce, P.P., Quinzio, S.I., Haddad, C.F., Candioti, F.V. (2020). Increasing our knowledge on direct-developing frogs: The ontogeny of *Ischnocnema henselii* (Anura: Brachycephalidae). Zoologischer Anzeiger 284: 78-87.

Gomez-Mestre, I., Pyron, R.A., Wiens, J.J., (2012). Phyogenetic analyses reveal unexpected patterns in the evolution of reproductive modes in frogs. Evolution 66: 3687–3700.

Griesbaum, F., Hirschfeld, M., Barej, M.F., Schmitz, A., Rohrmoser, M., Dahmen, M., Mühlberger, F., Liedtke, H.C., Gonwouo, N.L., Doumbia, J., Rödel, M.-O. (2019). Tadpoles of three western African frog genera: *Astylosternus* Werner, 1898, *Nyctibates* Boulenger, 1904, and *Scotobleps* Boulenger, 1900 (Amphibia, Anura, Arthroleptidae). Zoosystematics and Evolution 95 (1): 133–160.

Haad, B., Candioti, V.F., Baldo, D. (2011). Shape variation in lentic and lotic tadpoles of *Melanophryniscus* (Anura: Bufonidae). Studies on Neotropical Fauna and Environment 46 (2): 91-99.

Haad, M. B., Candioti, V.F., Baldo, D. (2014). The stream tadpoles of *Rhinella rumbolli* (Anura: Bufonidae). Herpetologica 70 (2): 184–197.

Haas, A., Richards, S.J. (1998). Correlations of cranial morphology, ecology, and evolution in Australian suctorial tadpoles of the genera *Litoria* and *Nyctimystes* (Amphibia: Anura: Hylidae: Pelodryadinae). Journal of Morphology 238: 109-141.

Haas, A., Wolter, J., Hertwig, S.T., Das, I. (2009). Larval morphologies of three species of stream toads, genus *Ansonia* (Amphibia: Bufonidae) from East Malaysia (Borneo), with a key to known Bornean *Ansonia* tadpoles. Zootaxa 2302: 1–18.

Haeckel, E. (1866). Generelle Morphologie der Organismen: Allgemeine Grundzüge der organischen Formen-Wissenschaft, mechanisch begründet durch die von Charkes Darwin reformierte Descendenz-Theorie. Reimer, Berlin.

Haddad, C.F.B., Prado, C.P.A. (2005). Reproductive modes in frogs and their unexpected diversity in the Atlantic Forest of Brazil. BioScience 55: 207–17.

Haldane, J. B. S. (1932). The time of action of genes and its bearing on some evolutionary problems. American Naturalist 66: 5-24.

Hanken, J. (1989): Development and Evolution in Amphibians. American Scientist 77 (4): 336-343.

Hanken, J. (1992). Life history and morphological evolution. Journal of Evolutionary Biology 5: 549-557.

Hanken, J. (1999). Larvae in amphibian development and evolution. In: The Origin and Evolution of Larval Forms. Edited by B. K. Hall and M. H. Wake. San Diego, Academic Press, pp. 61–108.

Hanken, J. (2003): Direct development. In: Keywords and Concepts in Evolutionary Developmental Biology. Edited by B.K. Hall and W.M Olson. Cambridge, Harvard University Press, pp. 97-102.

Hanken, J. (2015). Is Heterochrony Still an Effective Paradigm for Contemporary Studies of Evo-devo? In: Conceptual Change in Biology, Boston Studies in the Phi-

losophy and History of Science. Edited by A.C. Love. Springer Science+Business Media Dordrecht, 307 pp.

Hanken J., Carl, T.F., Richardson, M.K., Olsson, L., Schlosser, G., Osautey, C.K., Klymkowski, M.W. (2001). Limb development in a "nonmodel" vertebrate, the direct *Eleutherodactylus coqui*. Journal of Experimental Zoology 291 (4) :375-388.

Hanken, J., Klymkowsky, M.W., Alley, K.E., Jennings, D.H. (1997). Jaw muscle development as evidence for embryonic repatterning in direct-developing frogs. Proceedings in Biological Sciences: 1349-1354.

Hanken, J., Klymkowsky, M.W., Summers, C.H., Seufert, D.W., Ingebrigtsen, N. (1992). Cranial ontogeny in the direct-developing frog, *Eleutherodactylus coqui* (Anura: Leptodactylidae), analyzed using whole mount immunohistochemistry. Journal of Morphology 211: 95–118.

Hanken, J., Summers, C.H. (1988). Skull development during anuran metamorphosis: III. Role of thyroid hormone in chondrogenesis. Journal of Experimental Zoology 246: 156–170.

Harris, R.N. (1999). The anuran tadpole - Evolution and Maintenance.In: Tadpoles – The Biology of Anuran Larvae. Editet by R.W. Mc Diarmid and R. Altig. The University of Chicago Press.

Hayes, T.B. (1997). Amphibian Metamorphosis: An Integrative Approach. American Zoologist 37: 121-123.

Hedges, S.B., Duellman, W.E., Heinicke, M.P. (2008). New World direct-developing frogs (Anura: Terrarana): Molecular phylogeny, classification, biogeography, and conservation. Zootaxa 1737: 1–182.

Hime, P.M., Lemmon, A.R., Moriarty Lemmon, E.C, Prendini, E., Brown, J.M., Thomson, R.C., Kratovil, J.D., Noonan, B.P., Pyron, A., Peloso, P.L.V., Michelle, L.K., Keogh, J.S., Donnellan, S.C., Lockridge Mueller, R., Raxworthy, C.J., Kunte, K., Ron, S.R., Das, S., Gaitonde, N., Green, D.M., Labisko, J., Che, J., Weisrock, D.W. (2021). Phylogenomics Reveals Ancient Gene Tree Discordance in the Amphibian Tree of Life. Systematic Biology, Volume 70 (1): 49–66.

Hirschfeld, M., Barej, M.F, Gonwouo, N.L., Rödel, M.-O. (2012). Tadpole descriptions of three *Cardioglossa* species from southwestern Cameroon (Amphibia: Anura: Arthroleptidae). Salamandra 48(3): 147-156.

Hughes, A. (1966). The thyroid and the development of the nervous system in *Eleutherodactylus martinicensis*: an experimental study. Journal of Embryology and Experimental Morphology 16: 401–430.

Inger, R.F. (1992): Variation of apomorphic characters in stream-dwelling tadpoles of the bufonid genus *Ansonia* (Amphibia: Anura). Zoological Journal of the Linnean Society 105: 225-237.

Jennings, D.H., Hanken, J. (1998). Mechanistic basis of life history evolution in anuran amphibians: Thyroid gland development in the direct-developing frog, *Eleutherodactylus coqui*. General Comparative Endocrinology 111 (2): 225-232.

Just, J.J., Kraus-Just J., Check, D.A. (1981). Survey of Chordate Metamorphosis. In: Metamorphosis. Edited by L.I. Gilbert and E. Frieden. Springer, Boston, MA.

Kaminsky, S.K., Linsenmair, K.E., Grafe, T.U. (1999). Reproductive Timing, Nest Construction and Tadpole Guidance in the African Pig-Nosed Frog, *Hemisus marmoratus*. Journal of Herpetology 33 (1): 119-123.

Kaye, N.W. (1961). Interrelationships of the thyroid and pituitary in embryonic and premetamorphic stages of the frog, *Rana pipiens*. General and Comparative Endocrinology 1: 1–19.

Kerney, R., Gross, J.B., Hanken, J. (2010). Early cranial patterning in the direct *Eleutherodactylus coqui* revealed through gene expression. Evolution & Development 12 (4): 373-382.

Kerney, R., Meegaskumbura, M., Manamendra-Arachchi, K., Hanken, J. (2007). Cranial ontogeny in *Philautus silus* (Anura: Ranidae: Rhacophorinae) reveals few similarities with other directdeveloping anurans. Journal of Morphology 268: 715–725.

Kollros, J.L. (1961). Mechanisms of Amphibian Metamorphosis: Hormones. American Zoologist 1: 107–114.

Lamotte, M. J., Lescure, J. (1977). Tendances adaptatives a l'affranchissement du milieu aquatique chez les amphibiens anoures. Terre et Vie 31: 225–311.

Laslo, M., Denver, R.J., Hanken, J. (2019). Evolutionary conservation of thyroid hormone receptor and deiodinase expression dynamics in ovo in a direct-developing frog, *Eleutherodactylus coqui*. Frontiers in Endocrinology 10: 307.

Laurin, M., Reisz, R.R. (1997). A new perspective on tetrapod phylogeny. In: Amniote Origins. Edited by S. Sumida and K.L.M. Martin. Academic Press, San Diego, pp. 9–59.

Lavilla, E.O., De Sá, R. (2001). Chondrocranium and visceral skeleton of *Atelopus tricolor* and *Atelophryniscus chrysophorus* tadpoles (Anura, Bufonidae). Amphibia-Reptilia 22: 167-177.

Lutz, B. (1947). Trends towards Non-Aquatic and Direct Development in Frogs. Copeia 4: 242-252.

Lutz, B. (1948). Ontogenetic evolution in frogs. Evolution 2: 29–39.

Lynn, W.G. (1961). Types of amphibian metamorphosis. American Zoologist 1: 151–161.

Lynn, W.G., Peadon, A.M. (1955). The role of the thyroid gland in direct development in the anuran, *Eleutherodactylus martinicensis*. Growth 19: 263–286.

Maglia, A. M., Púgener, L. A. (1998). Skeletal development and adult osteology of *Bombina orientalis* (Anura: Bombinatoridae). Herpetologica: 344-363.

Magnusson, W.E., Hero, J.-M. (1991). Predation and the evolution of complex oviposition behavior in Amazon rainforest frogs. Oecologia 86: 310–318.

Mapouyat, L., Hirschfeld, M., Rödel, M.-O., Liedtke, H.C., Loader, S.P., Gonwouo, L.N., Dahmen, M., Doherty-Bone, T.M., Barej, M.F. (2014). The tadpoles of nine Cameroonian *Leptodactylodon* species (Amphibia, Anura, Arthroleptidae). Zootaxa 3765 (1): 29–53.

Meegaskumbura, M., Senevirathne, G., Biju, S.D., Garg, S., Meegaskumbura, S., Pethiyagoda, R., Hanken, J., Schneider, C.J. (2015). Patterns of reproductive-mode evolution in Old World tree frogs (Anura, Rhacophoridae). Zoologica Scripta 44: 509–522.

Mercurio, V., Böhne, W., Streit, B. (2009). Reproductive diversity of Malawian anurans. Herpetology Notes 2: 175-183.

Moore, M.K., Townsend Jr, V.R. (2003). Intraspecific variation in cranial ossification in the tailed frog, *Ascaphus truei*. Journal of Herpetology 37 (4): 714-717.

Mueller, R.L., Macey, J.R., Jaekel, M., Wake, D.B., Boore, J.L. (2004). Morphological homoplasy, life history evolution, and historica biogeography of plethodontid salamanders inferred from complete mitochondrial genomes. Proceedings of the National Academy of Science USA 101: 13820–13825.

Müller, H., Liedtke, H.C., Menegon, M., Beck, J., Balesteros, L., Nagel, P., Loader, S.P. (2013). Forests as promoters of terrestrial life-history strategies in East African amphibians. Biology Letters 9: 20121146.

Müller, H., Loader, S.P., Ngalason, W., Howell, K.M., Gower, D.J. (2007). Reproduction in Brevicipitid Frogs (Amphibia: Anura: Brevicipitidae)—Evidence from *Probreviceps m. macrodactylus*. Copeia: 726–733.

Minter, L. R. (2004). Genus Breviceps Merrem, 1820 (Family Microhylidae). In: Atlas and Red Data Book of the Frogs of South Africa, Lesotho and Swaziland. Edited by L. R. Minter, M. Burger, J. A. Harrison, H. H. Braack, P. J. Bishop, and D. Kloepfer. SI/MAB Series #9. Smithsonian Institution, Washington, D.C: 168–170.

Narayan, E.J., Hero, J.-M., Christi, K.S., Morley, C.G. (2010). Early developmental biology of *Platymantis vitiana* including supportive evidence of structural specialization unique to the Ceratobatrachidae. Journal of Zoology 284: 68–75.

Noble, G.K. (1925). An outline of the relation of ontogeny to phylogeny within the Amphibia. American Museum Novitates 165: 1-17.

Noble, G.K. (1929). The adaptive modifications of the arboreal tadpoles of *Hoplophryne* and the torrent tadpoles of *Staurois*. Bulletin of the American Museum of National History 83: 201–336.

Noble, G.K. (1931). The biology of the Amphibia. McGraw-Hill. 577 pp.

Nunes-de-Almeida, C.H.L., Haddad, C.F.B., Toledo, L.F. (2021). A revised classification of the amphibian reproductive modes. Salamandra 57(3): 413–427.

Oldham, R.S. (1977). Terrestrial locomotion in two species of amphibian larva. Journal of Zoology 181 (3): 285-295.

Olsson, L., Moury, D.J., Carl, T.F., Håstad, O., Hanken, J. (2002). Cranial neural crest-cell migration in the direct-developing frog, *Eleutherodactylus coqui*: Molecular heterogeneity within and among migratory streams. Zoology 105 (1): 3-13.

Orton, G.L. (1953). The systematics of vertebrate larvae. Systematic Zoology 2: 63-75.

Packard, M.J., Seymour, R.S. (1997). Evolution of the amniote egg. In: Amniote Origins: Completing the transition to land. Edited by S.S. Sumida and K.L.M. Martin. Academic Press, pp. 265–90.

Perret, J.-L. (1962). La biologie d'*Acanthixalus spinosus* (Amphibia, Salientia). Recherches Scientifiques du Cameroun 1: 90–101.

Pereira, E.B., Collevatti, R.G., de Carvalho Kokubum, M.N., de Oliveira Miranda, N.E., Maciel, N.M. (2015). Ancestral reconstruction of reproductive traits shows no tendency toward terrestriality in Leptodactyline frogs. BMC Evolutionary Biology 15: 1–12.

Portik, D.M., Blackburn, D.C. (2016). The evolution of reproductive diversity in Afrobatrachia: a phylogenetic comparative analysis of an extensive radiation of African frogs. Evolution 70: 2017–2032.

Portik, D.M., Bell, R.C., Blackburn, D.C., Bauer, A.M., Barratt, C.D., Branch, W.R., Burger, M., Channing, A., Colston, T.J., Conradie, W., Dehling, J.M., Drewes, R.C., Ernst, R., Greenbaum, E. ... McGuire, J. A. (2019). Sexual dichromatism drives diversification within a major radiation of African amphibians. Systematic Biology 68: 859–875.

Poynton, J. (1964). Relationship between habitat and terrestrial breeding in amphibians. Evolution 18: 131.

Pyron, R.A., Wiens, J.J. (2011). A large-scale phylogeny of Amphibia including over 2,800 species, and a revised classification of extant frogs, salamanders, and caecilians. Molecular Phylogenetics and Evolution 61: 543–583.

Raff, R.A. (1987). Constraint, flexibility, and phylogenetic history in the evolution of direct development in sea urchins. Developmental Biology 119: 6–19.

Raff, R.A. (1996). The shape of life; genes, development and the evolution of animal form. University of Chicago Press, Chicago. 544 pp.

Raff, R.A., Wray, G.A. (1989). Heterochrony - Developmental mechanisms and evolutionary results. Journal of Evolutionary Biology 2: 409-434.

Reiss, J.O. (2002). The phylogeny of amphibian metamorphosis. Zoology 105: 85–96.

Robinson, D.H., Heintzelman, M.B. (1987). Morphology of ventral epidermis of *Rana catesbeiana* during metamorphosis. The Anatomical Record 217(3): 305-317.

Rödel, M.-O. (2000). Herpetofauna of West Africa. Vol. 1. The Amphibians of the West African Savanna. Chimaira, Frankfurt am Maim, Germany.

Rödel, M.-O., Spieler, M., Grabow, K., Böckheler, C. (1995). *Hemisus marmoratus* (Peters, 1854) (Anura: Hemisotidae), Fortpflanzungsstrategien eines Savannenfrosches. Bonner Zoologische Beiträge Bd. 45: 191-207.

Rödel, M.-O., Barej, M.F., Hillers, A., Leaché, A.D., Kouamé, N.G., Ofori-Boateng, C., Assemian, N.E., Blayda Tohé, B., Penner, J., Hirschfeld,M., Doumbia, J., Gonwouo, L.N., Nopper, J., Brede, C., Diaz, R., Fujita, M.K., Gil, M., Segniagbeto G.H., Ernst, E., Sandberger, L. (2012). The genus *Astylosternus* in the Upper Guinea rainforests, West Africa, with the description of a new species (Amphibia: Anura: Arthroleptidae). Zootaxa 3245: 1–29.

Roelants, K.; Haas, A.; Bossuyt, F. (2011). Anuran radiations and the evolution of tadpole Morphospace. PNAS 108 (21): 8731-8736.

Rose, C. S. (1999). Hormonal control in larval development and evolution. In: Amphibians - The origin and evolution of larval forms. Edited by B. K. Hall and M. H. Wake. San Diego, Academic Press, pp. 167–216.

Salthe, S.N., Duellman, W.E., (1973). Quantitative constraints associated with reproductive modes in Anurans. In: Evolutionary Biology of the Anurans. Edited by J.L. Vial, University of Missouri Press, Columbia, pp. 229–249.

Schiøtz, A. (1999). Treefrogs of Africa. Frankfurt am Main, Germany: Edition Chimaira, 350 pp.

Siu-Ting, K., Torres-Sánchez, M., San Mauro, D., Wilcockson, D., Wilkinson, M., Pisani, D., O'Connell, M.J., Creevey, C.J. (2019). Inadvertent Paralog Inclusion Drives Artifactual Topologies and Timetree Estimates in Phylogenomics. Molecular Biology and Evolution 36 (6): 1344–1356.

Schlosser, G. (2005). Amphibian Variations: The Role of Modules in Mosaic Evolution. In: Modularity: Understanding the Development and Evolution of Natural Complex Systems. Edited by W. Callebaut and D. Rasskin–Gutman. The Vienna Series in Theoretical Biology, pp. 143-179.

Schlosser, G. (2008). Development of the retinotectal system in the direct-developing frog *Eleutherodactylus coqui* in comparison with other anurans. Frontiers in Zoology 5:9.

Schlosser, G., Kintner, C., Northcutt, R.G. (1999). Loss of ectodermal competence for lateral line placode formation in the direct developing frog *Eleutherodactylus coqui*. Developmental Biology 213 (2): 354-369.

Schlosser, G., Roth, G. (1997a). Evolution of Nerve Development in Frogs. Brain, Behavior and Evolution 50 (2): 94-112.

Schlosser, G., Roth, G. (1997b). Development of the retina is altered in the directly developing frog *Eleutherodactylus coqui* (Leptodactylidae). Neuroscience Letters 224 (3): 153-156.

Schoch, R. R. (1995). Heterochrony and the development of the amphibian head. In: Heterochrongy and Evolutionary Change. Edited by K. J. McNamara. Wiley, Chichester, pp. 107–124.

Schoch, R. (2009). Evolution of Life Cycles in Early Amphibians. Annual Review of Earth and Planetary Sciences 37: 15.1–15.28

Schoch, R.R., Carroll, R.L. (2003). Ontogenetic evidence for the Paleozoic ancestry of Slamanders. Evolution & Development 5 (3): 314–324.

Schoch, R.R., Fröbisch, N.B. (2006). Metamorphosis and neoteny: Alternative pathways in an extinct amphibian clade. Evolution, 60 (7): 1467–1475.

Sherratt, E.; Anstis, M.; Keogh, J.S. (2018). Ecomorphological diversity of Australian tadpoles. Ecology and Evolution 8: 12929–12939.

Szarski, H. (1957). The origin of the larva and metamorphosis in Amphibia. The American Naturalist 91: 283–301.

Tata, J.R. (2006). Amphibian metamorphosis as a model for the developmental actions of thyroid hormone. Molecular and Cellular Endocrinology 246 (1-2): 10-20.

Thibaudeau, G., Altig, R. (1999). Endotrophic anurans, development and evolution. In Tadpoles - The Biology of Anuran Larvae. Edited by R.W. McDiarmid and R. Altig. University of Chicago Press, p 170–188.

Touchon, J.C., Worley, J.L. (2015). Oviposition site choice under conflicting risks demonstrates that aquatic predators drive terrestrial egg-laying. Proceedings of the Royal Society B 282: 20150376.

Townsend, D.S., Stewart, M.M. (1985). Direct development in *Eleutherodactylus coqui* (Anura: Leptodactylidae): A staging table. Copeia 1985: 423–436.

Trueb, L., Cloutier, R. (1991). A phylogenetic investigation of the inter- and intrarelationships of the Lissamphibia (Amphibia: Temnospondyli). In: Origins of the Higher Groups of Tetrapods, Edited by H.-P. Schultze and L. Trueb. Thaca, Cornell University Press, pp. 175-188.

Trueb, L., Hanken, J. (1992). Skeletal Development in *Xenopus laevis* (Anura: Pipidae). Journal of Morphology 214: 1–4.

Wager, V.A. (1930). The breeding habits and life-histories of two rare South African Amphibia. I. *Hylambates natalensis* A. Smith. II. *Natalobatrachus bonebergi* Hewitt and Methuen (plates V-X). Transactions of the Royal Society of South Africa 19: 79-91.

Wagner, G.P. 1996. Homologues, natural kinds and the evolution of modularity. American Zoologist 36: 36–43.

Wassersug, R.J. (1975). The adaptive significance of the tadpole stage with comments on the maintenance of complex life cycles in anurans.American Zoologist 15: 405-417.

Wassersug, R.J., Duelman, W.E. (1984). Oral structures and their development in egg-brooding hylid frog embryos and larvae: Evolutionary and ecological implications. Journal of Morphology 182: 1-37.

Wassersug, R.J., Frogner, K.J., Inger, R.F. (1981). Adaptations for life in tree holes by rhacophorid tadpoles from Thailand. Journal of Herpetology 15: 41–52.

Wassersug, R.J., Hoff, K. (1982). Developmental changes in the orientation of the anuran jaw suspension. A preliminary exploration into the evolution of anuran metamorphosis. In Evolutionary Biology, Vol. 15. Edited by M. Hecht, B. Waiiace, and G. Prace. New York, Plenum, pp. 223-246.

Wake, D.B. (2012). Taxonomy of Salamanders of the Family Plethodontidae (Amphibia: Caudata). Zootaxa 3484: 75–82.

Wake, M.H. (1976). The reproductive biology of caecilians: An evolutionary perspective. In: The Reproductive Biology of Amphibians. Edited by D.H. Taylor and S.I. Guttman. Plenum Press, New York and London, pp. 73-101.

Wake, D.B., Hanken, J. (1996). Direct development in the lungless salamanders: What are the consequences for developmental biology, evolution and phylogenesis? The International Journal of Developmental Biology 40: 859-869.

Wells, K.D. (2007). The Ecology & Behavior of Amphibians. University of Chicago Press, 1427 East 60th Street, Chicago, Ilinois 60637. 1148 pages.

Werner, E.E. (1986). Ambibia metamorphosis: Growth rate, predation risk, and the optimal size at transformation. The American Naturalist 128 (3): 319-341.

White, B. A., & Nicoll, C. S. (1981). Hormonal control of amphibian metamorphosis. In: Metamorphosis: A problem in developmental biology. Edited by L. I. Gilbert and E. Frieden (Eds.), New York: Plenum, pp. 363-396.

Wiens, J. J. (1989). Ontogeny of the skeleton of Spea bombifrons (Anura: Pelobatidae). Journal of Morphology 202 (1): 29-51.

Zamudio, K.R., Bell, R.C., Nali, R.C., Haddad, C.F.B., Prado, C.P.A. (2016). Polyandry, Predation, and the Evolution of Frog Reproductive Modes. American Naturalist 188, pp. S000–S000.

Zelditch, M.L., Fink, W.L. (1996). Heterochrony and heterotopy: Stability and innovation in the evolution of form. Paleobiology 22: 242–254.

Zhang, P., Zhou, Chen, Y—Q., Liu, Y.-F., Qu, L.-H. (2005). Mitogenomic Perspectives on the Origin and Phylogeny of Living Amphibians. Systematic Biologists 54 (3): 391–400.

Ziermann, J.M. (2019). Diversity of Heads, Jaws, and Cephalic Muscles in Amphibians. In: Heads, Jaws, and Muscles. Fascinating Life Sciences. Edited by J. Ziermann, Jr R. Diaz and R. Diogo. Springer, pp 143-170.

Ziermann, J.M., Diogo, R. (2014). Cranial Muscle Development in Frogs with Different Developmental Modes: Direct Development versus Biphasic Development. Journal of Morphology 275: 398–413.

Zimkus, B.M., Lawson, L., Loader, S.P., Hanken, J. (2012). Terrestrialization, Miniaturization and Rates of Diversification in African Puddle Frogs (Anura: Phrynobatrachidae) PLoS ONE 7 (4): 1-11.

Ehrenwörtliche Erklärung / Statement of authorship

Ich erkläre hiermit, dass mir die geltende Promotionsordnung der Fakultät für Biowissenschaften der Friedrich-Schiller-Universität Jena bekannt ist. Die vorliegende Dissertationsschrift wurde von mir selbstständig angefertigt. Dabei wurden keine Textabschnitte einer/-s Dritten oder eigene Prüfungsarbeiten ohne Kennzeichnung übernommen. Alle von mir benutzten Hilfsmittel, persönliche Mitteilungen und Quellen sind in der Arbeit angegeben. Alle Personen, die Beiträge zum Material, zu dessen Auswertung oder zur Herstellung der Manuskripte geleistet haben, sind jeweils als Autoren aufgeführt:

PD Dr. Hendrik Müller[1], PD Dr. Mark-Oliver Rödel[2], Dr. Benjamin Naumann[3], Dr. Jörg U. Hammel[4], James Harvey[5], Lars Möckel[6], Theresa S. Otremba[7], Janina Weber[7]

[1]Zentralmagazin Naturwissenschaftlicher Sammlungen, Martin-Luther-Universität Halle-Wittenberg, Halle, Germany

[2]Museum für Naturkunde, Leibniz-Institut für Evolutions- und Biodiversitätsforschung, Berlin, Germany

[3]Institut für Biowissenschaften, Abteilung Allgemeine und Spezielle Zoologie, Universität Rostock, Germany

[4]Röntgenbildgebung mit Synchrotronstrahlung, Hereon-Außenstelle am DESY in Hamburg, Hamburg, Germany

[5]41 Devonshire Avenue, Howick, 3290, South Africa

[6]Kernbergstraße 38, 07749 Jena, Germany

[7]Institut für Zoologie und Evolutionsforschung, Friedrich-Schiller-Universität, Jena, Germany

Die Hilfe einer kommerziellen Promotionsvermittlung wurde nicht in Anspruch genommen und Dritte haben weder unmittelbar, noch mittelbar geldwerte Leistungen von mir für Arbeiten erhalten, die im Zusammenhang mit dem Inhalt der vorgelegten Dissertation stehen. Die Dissertation wurde noch nicht als Prüfungsarbeit für eine staatliche oder andere wissenschaftliche Prüfung eingereicht. Eine gleiche, eine in wesentlichen Teilen ähnliche oder eine andere Abhandlung wurde nicht als Dissertation bei einer anderen Hochschule oder anderen Fakultät eingereicht.

Jena, 01.02.2022

Susan Schweiger

Acknowledgements

Throughout the writing of this dissertation, I cannot be thankful enough for the support that I have received during the last years. I am deeply grateful to the people who accompanied me on this journey and encouraged me to complete this project despite all the personal difficulties I had to go through.

I am very grateful to my doctoral adviser Prof. Dr. Lennart Olsson for providing me with knowledge, giving me the opportunity to work on all aspects of my thesis and supporting me calmly with professional advice and helping criticism.

This project would not have been possible without PD Dr. Hendrik Müller. My deepest thanks to you for all the years of support, guidance, advice, joint field trips, inspiring discussions and encouragement.

I am very grateful to Prof. Dr. Martin Fischer for financial support at the beginning of my dissertation, for his critical advice and challenging discussions.

I also want to thank Prof. Dr. Ryan Kerney (Gettysburg) for agreeing to external review this dissertation.

I would like to thank all the people helping during the fieldwork and for sharing unforgettable moments. Special thanks to Dr. Benjamin Naumann (Rostock), Lars Möckel (Jena) and Dr. Katrin Friedemann (Koblenz). Thanks to Adrian Armstrong and Sharon Louw from KZN Wildlife. I also thank Dr. Les Minter (Barrydale) for introducing me into the world of Breviceps, and Prof. Dr. Alan Channing (Stellenbosch) for providing his knowledge about frogging in South Africa. Thank you to Jane Chanells for your warm hospitality and making South Africa feel like a second home.

Thank you to my colleagues and friends, Dr. Peter Konstantinidis (Corvallis) and Dr. Peter Warth (Stuttgart). I would also like to thank my co-authors and international colleagues for advices and support. Special thanks to PD Dr. Mark-Oliver Rödel (Berlin), Dr. Rayna C. Bell (Berkeley), Dr. H. Christoph Liedtke (Seville), Dr. Egon Heiss (Berlin) and Dr. Jörg U. Hammel (Hamburg).

I thank Prof. Dr. Rolf G. Beutel (Jena) for helpful advices in general, PD Dr. Hans Pohl (Jena) for invaluable advice regarding the work on illustrations and Dr. Benjamin Wipfler (Bonn) and David Neubert (Halbertstadt) for helping in the field of 3D reconstructions.

Katja Felbel, thank you for all your support, in the lab, and as a friend. I also would like to thank for good discussions and a relaxed and inspiring working atmosphere: Sandra Penske, Theresa Otremba, Janina Weber, Paul Lukas, Sandra Rüdiger and many others.

The deepest thanks to my family and friends, who have always supported me and endured my complaining with patience and love. Max, I need a lot more space to write down all the ways you supported me over the years. I am more than grateful. Thank you.

Appendix

FORMULAR 2

Manuskript Nr.: 1

Kurzreferenz: Schweiger et al. (2017), Org Div Evol

Beitrag des Doktoranden / der Doktorandin:

Beitrag des Doktoranden / der Doktorandin zu Abbildungen, die experimentelle Daten wiedergeben (nur für Originalartikel):

Abbildung(en) 1-6	☒	100% (die in dieser Abbildung wiedergegebenen Daten entstammen vollständig experimentellen Arbeiten, die der Kandidat/die Kandidatin durchgeführt hat)
	☐	0% (die in dieser Abbildung wiedergegebenen Daten basieren ausschließlich auf Arbeiten anderer Koautoren)
	☐	Etwaiger Beitrag des Doktoranden / der Doktorandin zur Abbildung: _____% Kurzbeschreibung des Beitrages: *(z. B. „Abbildungsteile a, d und f" oder „Auswertung der Daten" etc)*

FORMULAR 2

Manuskript Nr.: 2

Kurzreferenz: In Vorbereitung (drafted manuscript)

Beitrag des Doktoranden / der Doktorandin

Beitrag des Doktoranden / der Doktorandin zu Abbildungen, die experimentelle Daten wiedergeben (nur für Originalartikel):

Abbildung(en) 1, 3, 4, 6, 7,	☒	100% (die in dieser Abbildung wiedergegebenen Daten entstammen vollständig experimentellen Arbeiten, die der Kandidat/die Kandidatin durchgeführt hat)
	☐	0% (die in dieser Abbildung wiedergegebenen Daten basieren ausschließlich auf Arbeiten anderer Koautoren)
	☐	Etwaiger Beitrag des Doktoranden / der Doktorandin zur Abbildung: _____% Kurzbeschreibung des Beitrages:

Abbildung(en) 2, 5, 8, 9	☐	100% (die in dieser Abbildung wiedergegebenen Daten entstammen vollständig experimentellen Arbeiten, die der Kandidat/die Kandidatin durchgeführt hat)
	☐	0% (die in dieser Abbildung wiedergegebenen Daten basieren ausschließlich auf Arbeiten anderer Koautoren)
	☒	Etwaiger Beitrag des Doktoranden / der Doktorandin zur Abbildung: __60___% Kurzbeschreibung des Beitrages: *(Auswahl der Daten (Entwicklungsstadien), Auswertung und Visualisierung der Daten)*

FORMULAR 2

Manuskript Nr.: 3

Kurzreferenz: Naumann et al. (2021), Dev Dyn

Beitrag des Doktoranden / der Doktorandin

Beitrag des Doktoranden / der Doktorandin zu Abbildungen, die experimentelle Daten wiedergeben (nur für Originalartikel):

Abbildung(en) 3-5, 7	☐	100% (die in dieser Abbildung wiedergegebenen Daten entstammen vollständig experimentellen Arbeiten, die der Kandidat/die Kandidatin durchgeführt hat)
	☒	0% (die in dieser Abbildung wiedergegebenen Daten basieren ausschließlich auf Arbeiten anderer Koautoren)
	☐	Etwaiger Beitrag des Doktoranden / der Doktorandin zur Abbildung: _____% Kurzbeschreibung des Beitrages: *(z. B. „Abbildungsteile a, d und f" oder „Auswertung der Daten" etc.)*

Abbildung(en) 1, 2, 6, 8, 9	☐	100% (die in dieser Abbildung wiedergegebenen Daten entstammen vollständig experimentellen Arbeiten, die der Kandidat/die Kandidatin durchgeführt hat)
	☐	0% (die in dieser Abbildung wiedergegebenen Daten basieren ausschließlich auf Arbeiten anderer Koautoren)
	☒	Etwaiger Beitrag des Doktoranden / der Doktorandin zur Abbildung: __50___% Kurzbeschreibung des Beitrages: *(Erstellung von Aufnahmen und Rekonstruktionen, Auswertung und Visualisierung der Daten)*

FORMULAR 2

Manuskript Nr.: 4

Kurzreferenz In Vorbereitung (drafted manuscript)

Beitrag des Doktoranden / der Doktorandin

Beitrag des Doktoranden / der Doktorandin zu Abbildungen, die experimentelle Daten wiedergeben (nur für Originalartikel):

Abbildung(en): 1	☐	100% (die in dieser Abbildung wiedergegebenen Daten entstammen vollständig experimentellen Arbeiten, die der Kandidat/die Kandidatin durchgeführt hat)
	☐	0% (die in dieser Abbildung wiedergegebenen Daten basieren ausschließlich auf Arbeiten anderer Koautoren)
	☒	Etwaiger Beitrag des Doktoranden / der Doktorandin zur Abbildung: __40___% Kurzbeschreibung des Beitrages: *(Abbildungstafel erstellen (Aufnahmen der Fotos während der Feldarbeiten durch Koautoren))*

Abbildung(en): 2-13	☒	100% (die in dieser Abbildung wiedergegebenen Daten entstammen vollständig experimentellen Arbeiten, die der Kandidat/die Kandidatin durchgeführt hat)
	☐	0% (die in dieser Abbildung wiedergegebenen Daten basieren ausschließlich auf Arbeiten anderer Koautoren)
	☐	Etwaiger Beitrag des Doktoranden / der Doktorandin zur Abbildung: _____% Kurzbeschreibung des Beitrages: *(z. B. „Abbildungsteile a, d und f" oder „Auswertung der Daten" etc.)*

FORMULAR 2

Manuskript Nr.: 5

Kurzreferenz: Schweiger et al. (2017), Acta Herp

Beitrag des Doktoranden / der Doktorandin

Beitrag des Doktoranden / der Doktorandin zu Abbildungen, die experimentelle Daten wiedergeben (nur für Originalartikel):

Abbildung(en) 1	☒	100% (die in dieser Abbildung wiedergegebenen Daten entstammen vollständig experimentellen Arbeiten, die der Kandidat/die Kandidatin durchgeführt hat)
	☐	0% (die in dieser Abbildung wiedergegebenen Daten basieren ausschließlich auf Arbeiten anderer Koautoren)
	☐	Etwaiger Beitrag des Doktoranden / der Doktorandin zur Abbildung: _____% Kurzbeschreibung des Beitrages: *(z. B. „Abbildungsteile a, d und f" oder „Auswertung der Daten" etc.)*

Abbildung(en) 2	☐	100% (die in dieser Abbildung wiedergegebenen Daten entstammen vollständig experimentellen Arbeiten, die der Kandidat/die Kandidatin durchgeführt hat)
	☐	0% (die in dieser Abbildung wiedergegebenen Daten basieren ausschließlich auf Arbeiten anderer Koautoren)
	☒	Etwaiger Beitrag des Doktoranden / der Doktorandin zur Abbildung: __25___% Kurzbeschreibung des Beitrages: *(Auswertung und Visualisierung)*